Plasticity of winter wheat architecture modulated by sowing date and plant population density and its effect on Septoria tritici epidemics

Rim Baccar

ParisTech
INSTITUT DES SCIENCES ET TECHNOLOGIES
PARIS INSTITUTE OF TECHNOLOGY

AgroParisTech
INSTITUT DES SCIENCES ET INDUSTRIES DU VIVANT ET DE L'ENVIRONNEMENT
PARIS INSTITUTE OF TECHNOLOGY FOR LIFE, FOOD AND ENVIRONMENTAL SCIENCES

Ecole Doctorale ABIES
Agriculture Agriculture Alimentation Food Biologie Biology Environnement Environment Santé Health

Doctorat ParisTech

T H È S E

pour obtenir le grade de docteur délivré par

L'Institut des Sciences et Industries du Vivant et de l'Environnement

(AgroParisTech)

présentée et soutenue publiquement par

Rim Baccar

Le 06 juin 2011

Plasticité de l'architecture du blé d'hiver modulée par la densité et la date de semis et son effet sur les épidémies de *Septoria tritici*

Directeur de thèse : **Bruno Andrieu**
Co-directeur de thèse : **Corinne Robert**

Jury

M. Jan Vos,	Associate Professor, Université de Wageningen	Rapporteur
M. Michael Dingkuhn,	Directeur de recherche, CIRAD	Rapporteur
M. Bertrand Ney,	Professeur, SIAFFE, AgroParisTech	Examinateur
M. David Gouache,	Ingénieur, ARVALIS	Examinateur
M. Neil Paveley,	Senior Principal Researcher, ADAS, UK	Examinateur
M. Bruno Andrieu,	Directeur de recherche, INRA Grignon	Directeur de thèse
Mme. Corinne Robert,	Chargé de recherche, INRA Grignon	Co-Directeur

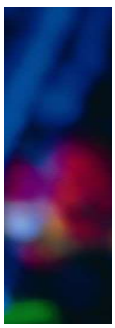

AgroParisTech
Institut National de la Recherche Agronomique
Unité Environnement et Grandes Cultures
78850 Thiverval Grignon

ParisTech
INSTITUT DES SCIENCES ET TECHNOLOGIES
PARIS INSTITUTE OF TECHNOLOGY

AgroParisTech
INSTITUT DES SCIENCES ET INDUSTRIES DU VIVANT ET DE L'ENVIRONNEMENT
PARIS INSTITUTE OF TECHNOLOGY FOR LIFE, FOOD AND ENVIRONMENTAL SCIENCES

Ecole Doctorale ABIES
Agriculture Agriculture Alimentation Food Biologie Biology Environnement Environment Santé Health

Doctorat ParisTech

T H È S E

pour obtenir le grade de docteur délivré par

L'Institut des Sciences et Industries du Vivant et de l'Environnement

(AgroParisTech)

présentée et soutenue publiquement par

Rim Baccar

Le 06 juin 2011

Plasticity of winter wheat architecture modulated by sowing date and plant population density and its effect on *Septoria tritici* epidemics

Directeur de thèse : **Bruno Andrieu**
Co-directeur de thèse : **Corinne Robert**

Jury

M. Jan Vos,	Associate Professor, Université de Wageningen	Rapporteur
M. Michael Dingkuhn,	Directeur de recherche, CIRAD	Rapporteur
M. Bertrand Ney,	Professeur, SIAFFE, AgroParisTech	Examinateur
M. David Gouache,	Ingénieur, ARVALIS	Examinateur
M. Neil Paveley,	Senior Principal Researcher, ADAS, UK	Examinateur
M. Bruno Andrieu,	Directeur de recherche, INRA Grignon	Directeur de thèse
Mme. Corinne Robert,	Chargé de recherche, INRA Grignon	Co-Directeur

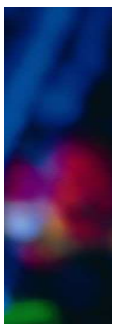

AgroParisTech
Institut National de la Recherche Agronomique
Unité Environnement et Grandes Cultures
78850 Thiverval Grignon

Dédicaces

Aux êtres qui me sont le plus cher au monde :

Mes parents bien-aimés Saida et Mekki qui ont toujours cru en moi et toujours soutenue,

Mon adorable grand-mère Cherifa qui m'a beaucoup gâtée et aimée,

Mon cher frère Karim,

J'espère qu'ils trouveront dans ce travail toute ma reconnaissance et tout mon amour.

Rim

Remerciements

Le travail de thèse présenté dans ce mémoire a été réalisé au sein de l'UMR "Environnement et Grandes Cultures" et a été co-financé par le Département INRA "Environnement et Agronomie" et "Arvalis-Institut du Végétal". Je remercie l'Unité Expérimentale de Grignon qui a veillé au bon déroulement des expérimentations au champ pendant deux années. Je remercie aussi les membres de mon jury, en particulier, Jan Vos et Michael Dingkuhn pour avoir accepté d'être rapporteur de ce travail.

Je tiens évidemment à remercier chaleureusement mon directeur de thèse Bruno Andrieu, qui m'a accompagnée quotidiennement dans la réalisation de ce travail. Je salue sa disponibilité permanente, sa générosité et ses qualités scientifiques et humaines. J'ai beaucoup appris à ses côtés et espère continuer à le faire.

Merci également à mon co-directeur de thèse Corinne Robert, qui m'a permis de compléter ma formation par ses connaissances en pathologie végétale. Son soutien moral et sa présence à mes cotés pendant le travail de simulation et de rédaction m'ont rassurée et m'ont permis de mieux avancer.

Je suis reconnaissante à mon cher ami et collègue Tino Dornbusch pour tout ce qu'il m'a apporté pendant deux ans et demi. Je n'oublierai jamais tous les moments de travail, de discussions fructueuses mais aussi de complicité et de bonne humeur qu'on a partagé. Vielen Dank Tino !

Je remercie également Christian Fournier, sans qui le travail de modélisation n'aurait pas été possible. Malgré ses occupations, il a toujours répondu présent quand j'avais besoin de son aide ; merci pour tous les allers-retours entre Grignon et Montpellier pour accomplir ce travail.

Merci aussi à Mariem Abichou, avec qui j'ai collaboré d'abord en tant que stagiaire et ensuite en tant qu'ingénieur. Son dynamisme, son autonomie et sa gentillesse sont autant de qualités qui nous ont rapprochées professionnellement et personnellement.

Un merci collectif à cette mini équipe (Bruno, Corinne, Tino, Christian et Mariem) dans laquelle j'ai évolué pendant plus de trois ans. Grâce à vous je ne me suis jamais sentie seule.

Je remercie également toute l'équipe technique de l'équipe plante et en particulier Emmanuel Fovart et Fabrice Duhamel pour leur aide technique dans l'énorme travail de manipulations au champ et en laboratoire ; Maxime Marques pour son aide au prélèvement et dépouillement des plantes ; Florence Lafouge pour son aide à réaliser les analyses d'azote mais aussi pour sa gentillesse et les longues discussions qu'on a pu avoir ; Alain Fortineau pour son aide à installer et comprendre le fonctionnement des centrales d'acquisition de données ; Pierre Belluomo pour les programmes OPTIMAS qu'il a développé et adapté pour répondre à mes besoins. Je tiens à dire un grand merci à Valérie Bontemps, ingénieur, pour sa grande implication et son sérieux dans la réalisation des mesures de septoriose. Avec elle, j'ai partagé de

longues et fastidieuses mesures au champ mais aussi de bons moments de fous rires et complicité.

Je remercie sincèrement tous les membres de mon comité de pilotage et notamment Bertrand Ney, Delphine Luquet, Abraham Escobar, Philippe Gate et David Gouache pour les conseils prodigués au cours de nos réunions.

Mes remerciements s'adressent également à Claudine Lauransot et Marina Pavlidès pour leur aide efficace et rapide dans mes recherches bibliographiques, à Christine Tual pour sa bonne humeur et sa gestion de tous les événements qui animent la vie au sein de l'unité et qui ont permis de nous réunir à plusieurs occasions. Je remercie vivement notre directeur d'unité Enrique Barriuso ainsi que tout le service de secrétariat de notre unité : Catherine Richard, Christine Lepennec, Annie Meurisse et Fabrice Goffin qui assurent la gestion de tous les aspects administratifs et nous procurent les bonnes conditions de travail. Merci à tous les chercheurs de l'équipe Plante et de l'équipe Atmosphère avec qui j'ai pu discuter, solliciter des conseils ou simplement partager de bons moments à l'unité.

Je n'oublie pas de remercier mes amis et colocataires Juliette et Pietro pour tous les moments agréables qu'on a partagé. Votre soutien et votre écoute m'ont permis de moins appréhender les derniers jours de la thèse et je vous en remercie. Merci à tous mes amis : Inès, Rym, Amir, Karim, Christophe, Nicolas, Marc, Sylvia, Emna, Camille et Karine pour les bons moments que nous avons partagé ensemble.

Sommaire

RESUME EN FRANÇAIS 8
I. CONTEXTE ET OBJECTIFS DE LA THESE : 9
II. APPROCHE 10
1. 1. Expérimentation 10
2. 2. Modélisation 11
III. RESULTATS 11
IV. DISCUSSION ET CONCLUSION 17

GENERAL INTRODUCTION 18
I. GENERAL CONTEXT OF PLANT DISEASES 19
II. GENERAL MODELS VS. VIRTUAL PLANT MODELS 20
1. Approaches to modelling crop diseases 20
2. Virtual plant modelling 21
3. The virtual plant as a tool to simulate disease 21
III. GENERAL OBJECTIVES OF THIS WORK 22
IV. THE PATHOSYSTEM STUDIED: WHEAT-SEPTORIA TRITICI 22
4. Presentation of the wheat plant 22
1.1. Structure of wheat 22
1.2. Growth and development 23
5. Presentation of Septoria tritici 24
2.1. Life cycle and ways of propagation 25
2.2. Infection cycle 26
6. Interactions between plant architecture and S. tritici epidemic 27
V. SEPTO3D: PRESENTATION, STRUCTURE AND LIMITS 28
7. Model presentation 28
8. Limits of the model 29
VI. OBJECTIVES AND RATIONALE OF THIS THESIS 29
VII. ORGANISATION OF THE MANUSCRIPT 31
REFERENCES 33

CHAPTER 1 37
Phyllochron of winter wheat (*Triticum aestivum* L.) for a range of densities and sowing dates
ABSTRACT 38
INTRODUCTION 39
MATERIALS AND METHODS 40
9. Overview 40
10. Experimental design and treatments 40
11. Plant measurement 41
3.1. Leaf emergence 41
3.2. Leaf initiation 42
12. Meteorological measurements 42
13. Data analysis 42
5.1. Calculation of thermal time 42
5.2. Calculation of phyllochron and plastochron 43
14. Statistical analysis 43
RESULTS 44
During winter, time course assuming a non-linear response to temperature differed from time course calculated assuming a linear response. 44
The rate of HS progress varied between density treatments only when these treatments differed in the final leaf number 45
Compensated thermal time provided consistent results of HS progress between sowing treatments and growing seasons 46
Two phases with two different rates described the HS progress of a wheat tiller 47
Change in the rate of HS progress coincided with the initiation of the flag leaf 50
The duration of the period from HSbreak to the appearance of the flag leaf ligule was independent of Nleaf 51

For each phase, the duration of the phase and the phyllochron were correlated to the photoperiod at seedling emergence ... 52
The progress of HS in primary tillers showed a similar trend to that of the main stem ... 54
DISCUSSION ... 55
When expressed in Γc, results were consistent between sowing dates and contrasted climate conditions ... 55
The progress of Haun Stage was described by two phases ... 55
The moment of shift in the rate of Haun Stage progress was related to the moment of flag leaf initiation ... 56
Both the values of phyllochron of each phase and their corresponding durations varied linearly with photoperiod at seedling emergence ... 57
During phase II, phyllochron varied according to final leaf number for a wheat tiller ... 57
ACKNOWLEDGMENTS ... 58
REFERENCES ... 61

CHAPTER 2 ... 64
Pasticity of winter wheat modulated by sowing date and plant population density
ABSTRACT ... 65
INTRODUCTION ... 66
MATERIALS AND METHODS ... 68
1. Overview ... 68
2. Experimental design and treatments ... 68
3. Measurements and sampling procedure ... 68
3.1. Plant population density and date of seedling emergence ... 68
3.2. Organ dimensions ... 69
3.3. Leaf senescence ... 71
3.4. Leaf area index ... 71
3.5. Ground cover ... 72
4. Data processing and presentation of results ... 73
RESULTS ... 74
I. ARCHITECTURE AT PLANT SCALE ... 74
1. Final leaf number for main stem and tillers ... 74
Main stem final leaf number varied between density and sowing date treatments ... 74
Tillers final leaf number followed the same pattern as the main stem ... 76
2. Organ dimensions ... 78
General pattern in the vertical profiles of length of blades, sheaths and internodes ... 78
Within a same treatment, plants with higher leaf number had smaller juvenile leaves, but larger adult leaves and higher stature. ... 80
Lower sowing density resulted in longer blades and sheaths and higher area of adult leaves ... 80
Main stem showed different profiles of length of blades, sheaths and internodes between the two sowing dates ... 84
Length of adult leaf blades, sheaths and internodes was almost identical between the main stem and axillary tillers of the same rank counted from the shoot top ... 85
3. Senescence ... 88
Senescence at leaf scale ... 88
Senescence at the shoot scale ... 88
4. Tillering dynamics ... 90
II. ARCHITECTURE AT CANOPY SCALE ... 91
1. Number of tillers per square meter ... 91
2. Ground cover and leaf area index ... 91
DISCUSSION ... 94
I. GENERAL PATTERN OF ORGAN DIMENSIONS AND MAIN DIFFERENCES BETWEEN TREATMENTS, PLANTS AND TILLERS ... 94
A general pattern describes organ dimensions for a given cultivar and under similar conditions ... 94
Architecture differences between sowing dates ... 95
Architecture differences between plant population densities ... 96
Variability of architecture between plants differing in the final leaf number ... 97
Differences between main stem and axillary tillers ... 98
II. ABILITY TO REPRODUCE WHEAT ARCHITECTURE WITH A 3D MODEL USING THE COLLECTED DATA ... 99
The rate of leaf appearance and senescence for each axis ... 99
The tillering dynamic of the plant ... 99
Dimensions of mature organs ... 100
Geometry of organs ... 100
Difficulties and improvements of the sampling protocol ... 100
REFERENCES ... 102

CHAPTER 3 106
Modelling the effect of wheat canopy as affected by sowing density on *Septoria tritici* epidemics using a coupled epidemic-virtual plant model
ABSTRACT 107
INTRODUCTION 108
MATERIALS AND METHODS 109
1. Overview 109
2. Modelling 110
2.1. Model description 110
2.2. Epidemic model parameterisation 112
2.3. Reconstruction of individual plant architecture 112
2.4. Canopy reconstruction with different levels of plant variability 113
3. Field experiment 114
3.1. Treatments and experimental design 114
3.2. Field measurements 114
3.3. Data analysis 115
4. Disease simulations and test of Septo3D 116
RESULTS 116
1. Effect of density on plant architecture and development 116
1.1 Comparison between treated and non-treated plants 116
1.2. Final leaf number and phyllochron 117
1.3. Organ dimensions 117
1.4. Tillering dynamics 118
2. Plant-to-plant variability of development 119
3. Disease development 119
3.1. Pattern of total necrosis development 119
3.2. Effect of density treatment on lesion development 120
4. Disease simulations 122
4.1. Simulations of lesion development with the reference scenario Sref 122
4.2. Effect of the canopy reconstruction scenarios on the disease simulation 125
DISCUSSION 125
Originalities of the field experimental design 125
Density effect on architecture 126
Density effect on epidemics 126
Modelling canopy variability and its effect on epidemics 127
New parameterisation of initial infection conditions improved triggering the disease 127
Capacity of the model to simulate S. tritici epidemics 127
Difficulties of validation of coupled architecture-epidemic models 128
ACKNOWLEDGEMENTS 128
REFERENCES 129

CHAPTER 4 133
I. SUMMARY OF MAIN RESULTS 134
II. EFFECT OF DIFFERENCES IN ARCHITECTURAL VARIABLES DUE TO SOWING DATE AND SOWING DENSITY ON DISEASE DEVELOPMENT 137
1. Septoria epidemic and possible interactions with canopy architecture 137
1.1. Epidemic parameters influenced by canopy architecture 137
1.2. Architectural variables that could influence Septoria epidemic development 137
2. A grid of architecture-epidemic interactions during wheat growth cycle 138
3. Expected effects of architecture modified by density and sowing date on Septoria tritici development 141
III. IMPROVEMENTS BROUGHT TO SEPTO3D 143
1. Initialisation of the disease 143
2. Modelling canopy variability and its effect on epidemic simulations 144
IV. CRITICAL ASSESSMENT OF SEPTO3D 145
V. PERSPECTIVES AND POSSIBLE APPLICATIONS OF THE APPROACH OF COUPLED VIRTUAL PLANT-DISEASE MODELS 147
1. Possible applications of the approach using Septo3D 147
1.1. Quantification of the effects of density and sowing date on disease development for different climate scenarios 147
1.2. Identification of the key architectural features for disease propagation 149
REFERENCES 151

APPENDIXES **154**
APPENDIX I 155
APPENDIX II 159
APPENDIX III 161
APPENDIX IV 167
LIST OF PUBLICATIONS……..177

Résumé en français

I. Contexte et objectifs de la thèse :

L'utilisation intensive de produits phytosanitaires durant les dernières décennies a engendré l'apparition de problèmes liés l'impact environnemental de ces produits mais également liés à la baisse d'efficacité de certaines molécules chimiques suite à l'apparition de souches pathogènes résistantes. Ainsi, la lutte contre les maladies basée exclusivement sur la lutte chimique n'est plus possible. Pour pallier à ces problèmes, la politique agricole actuelle est en train d'évoluer vers une utilisation raisonnée des pesticides et la promotion de moyens de lutte alternatifs et plus écologiques comme le recours à la sélection variétal ou encore la maitrise des bio-agresseurs par l'optimisation des techniques culturales.

Des pratiques culturales comme la fertilisation, le travail du sol, la date et densité de semis peuvent entraîner des modifications de l'architecture des plantes et du couvert végétal ce qui a pour conséquence de moduler le développement des épidémies. Cependant l'effet de ces pratiques est souvent irrégulier entre années, aussi bien en termes d'intensité que de direction ; et les mécanismes mis en jeu dans l'interaction entre l'architecture et la maladie sont complexes. La modélisation apparaît comme un outil qui peut nous aider à mieux comprendre ces effets. Les modèles de "Plante Virtuelle" semblent particulièrement convenir à l'étude des interactions architecture-maladie. Ces modèles, connus encore sous le nom de modèles "Structure-Fonction", permettent la description de façon explicite du développement au cours du temps de l'architecture et des fonctions des organes de la plante dans une représentation tri-dimensionnelle (3D). L'intérêt de ce type de modèle réside dans le fait que:

(i) d'une part, ils permettent une représentation précise des processus physiques et biologiques à une échelle fine de la plante : l'organe,

(ii) d'autre part, ce type de modèle tient compte de l'effet de l'architecture de la plante et du couvert dans les simulations du développement épidémique.

Cette approche de modélisation a commencé à se développer dans les années 1990 et est donc relativement récente. A ce jour, il existe peu d'exemples de modèles "Plante Virtuelle" appliqués à l'étude des interactions entre architecture et épidémies. Par conséquent, il y a un manque de validation de l'approche et un besoin de démontrer son efficacité sur des cas d'études réels.

La motivation générale de notre étude a été de combler ce manque de validation en s'appuyant sur l'exemple du pathosystème blé-septoriose. La septoriose est une maladie foliaire du blé, causée par *Mycosphaerella graminicola*. Les symptômes apparaissent d'abord sous forme de chloroses qui se transforment en nécroses contenant des pycnidiospores (forme asexuée). Les pycnidiospores sont adaptées à la dissémination à courte distance, principalement par les éclaboussures produites pendant un événement pluvieux. Les pycnidiospores sont ainsi transportées d'une feuille malade en bas de la plante vers une feuille jeune du haut de la même plante ou d'une plante voisine. La maladie progresse par infections successives jusqu'à la feuille drapeau. Deux autres moyens de dispersion peuvent assurer la transmission de la maladie : la dissémination sur de longues distances de la forme sexuée : les ascospores, ou la transmission par simple contact entre feuilles malades et feuilles saines.

L'objectif général de ce travail a consisté à étudier l'effet de l'architecture de la plante de blé sur le développement épidémique de la septoriose en utilisant un modèle couplé blé-septoriose. Cet objectif a été décliné en sous-objectifs :

- Décrire de façon détaillée la plasticité de l'architecture du blé pour des conditions environnementales contrastées.
- Evaluer l'effet de cette plasticité sur le développement épidémique de la septoriose.
- Evaluer la capacité d'un modèle couplé blé-septoriose à prédire les dynamiques de la maladie à l'échelle de la feuille individuelle.

II. Approche

L'approche choisie a été de combiner la modélisation et l'expérimentation. L'expérimentation a permis de créer et de décrire des architectures de blé contrastées et de suivre le développement épidémique sur ces mêmes couverts. Les différents couverts ont été obtenus en faisant varier les densités et dates de semis. En effet, plusieurs études rapportent que ces deux techniques culturales modulent le développement des épidémies à travers, entre autres, la modification de l'architecture du couvert. La modélisation a permis d'apporter des améliorations au module de reconstruction du couvert du modèle utilisé (Septo3D) et à confronter les simulations avec les observations.

1. 1. Expérimentation

La variété de blé d'hiver Soissons a été semée au champ pendant deux années consécutives : 2007/2008 (Y1) et 2008/2009 (Y2) à Grignon. L'expérimentation a comporté six traitements, constitués par le croisement de deux dates de semis : un semis précoce (S1) et un semis tardif (S2) et de trois densités de semis : faible (D1), moyenne (D2) et élevée (D3). Cette expérimentation a été originale par le caractère détaillé du suivi des variables d'architecture (les deux années) et de septoriose (la deuxième année sur le semis tardif). L'expérimentation a permis de collecter les données nécessaires à :

- L'analyse des effets de la densité et la date de semis sur l'architecture,
- Le calage et l'évaluation du modèle couplé blé-septoriose.

Le suivi du **rythme de développement du blé** a consisté à :

- Mesurer les Haun Stage (HS, qui est une mesure décimale du nombre de feuilles ligulées sur un axe ; Haun, 1973) du maître brin et des talles primaires des plantes tout le long du cycle de culture sur toutes les modalités.
- Suivre le rythme d'initiation des feuilles grâce à des dissections d'apex sous vidéo microscope en 2008/2009.

Le suivi de la **plasticité du blé** a consisté à :

- Mesurer les variables d'architecture à *l'échelle de la plante* de blé (dimensions des organes, nombre de talles, surface foliaire). La collecte de ces données a été réalisée grâce à des prélèvements périodiques d'échantillons de plantes suivis par des opérations de scans d'organes et d'analyse d'images.

- Mesurer les variables d'architecture à *l'échelle du peuplement* : par exemple, des photos aériennes du couvert ont été réalisées tout le long du cycle de la culture pour estimer le taux de couverture.

Le suivi du **développement de la septoriose** a consisté à :

- Suivre finement par des mesures au champ une à deux fois par semaine (en moyenne tous les 100 °Cd) le développement des lésions de septoriose sur les feuilles du maître brin.

2. 2. Modélisation

Le modèle utilisé a été spécialement développé pour étudier les interactions entre l'architecture du blé et la septoriose. Il s'agit du modèle Septo3D (Robert et al., 2008). Septo3D résulte du couplage entre un modèle de description de l'architecture du blé en 3D (ADEL-Wheat, Fournier et al., 2003) et un modèle de développement épidémique de la septoriose. Initialisé à partir d'un niveau d'infection des trois premières feuilles, le modèle simule le développement de l'épidémie à partir des feuilles basales infectées vers les feuilles saines du haut du couvert. Septo3D procède itérativement en faisant intervenir à chaque pas de temps (un jour) trois modules : (i) développement du blé, (ii) cycle infectieux et (iii) dispersion.

Le modèle rend compte de quatre effets de la structure du couvert sur les épidémies :

- La quantité de surface foliaire influence le développement des lésions
- La densité de végétation influence la pénétration de la pluie et la redistribution des gouttelettes après éclaboussement.
- Les distances entre tissus infectés et sains fixent la distance à parcourir par une goutte infectieuse
- La sénescence des feuilles tue les lésions en incubation.

Ce modèle présente un certain nombre de limites :

- Le couvert reconstruit dans le modèle, est constitué de la répétition d'une seule plante moyenne et donc ne considère pas la variabilité entre plantes ;
- La durée de latence est un paramètre du modèle et ne varie pas selon les conditions environnementales ;
- Le seul moyen de propagation considéré dans le modèle est la propagation par éclaboussure de pluie ;
- Enfin, à ce jour les simulations n'ont pas été confrontées à des observations réelles.

Le travail de modélisation a consisté à (i) améliorer le réalisme des couverts reconstruits par le modèle et à (ii) comparer le développement épidémique simulé aux observations.

III. Résultats

Chapitre 1 : Variations du phyllochron en fonction de la densité et de la date de semis

Le phyllochrone est un paramètre important dans les modèles de culture et qui joue un rôle crucial sur la dynamique de propagation de la septoriose (Lovell et al., 1997, Robert et al., 2008). Nous avons étudié les variations du phyllochrone au cours du cycle de développement du blé et entre traitements de densité et date de semis. Quatre méthodes de calcul du temps thermique ont été comparées pour définir l'échelle de temps la plus appropriée pour le calcul du phyllochrone. La relation entre le phyllochrone du brin-maître et des talles primaires a également été étudiée.

L'utilisation du temps thermique compensé (calculé en utilisant une réponse non linéaire à la température) pour représenter l'évolution du Haun Stage a permis d'obtenir des résultats homogènes et consistants entre années et entre traitements.

Pour les deux dates de semis, l'évolution du Haun Stage en fonction du temps thermique compensée a présenté deux phases linéaires caractérisées par des rythmes différents: le phyllochrone de la phase 1 était dépendant de la date de semis, et le phyllochrone de la phase 2 était dépendant à la fois de la date de semis et du nombre final de feuilles. Le moment de changement de pente entre les deux phases était indépendant du nombre final de feuilles: il était le même pour une date de semis donné. La comparaison de ce moment avec le rythme d'initiation des primordia a révélé que le changement de pente a coïncidé avec le moment d'initiation de la feuille drapeau, ce qui suggère que c'est un événement lié à l'ontogénie de la plante. Nos résultats suggèrent qu'une partie de la variation du phyllochrone d'un axe de blé entre densités et dates de semis peut être expliquée par la photopériode à l'émergence des plantes d'une part, et d'autre part, la variation à une date donnée peut être expliquée par la variation du nombre final de feuilles.

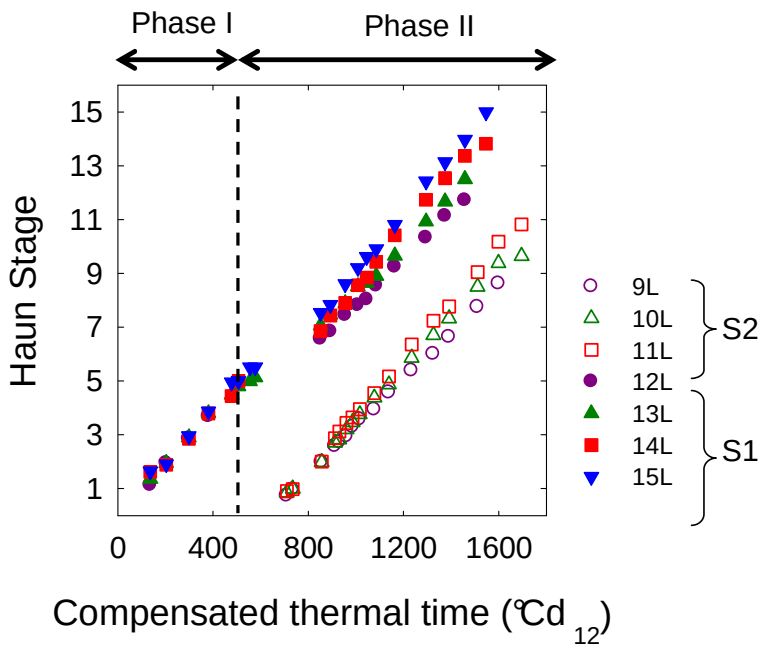

Figure 1. Evolution du Haun Stage (HS) en fonction du temps thermique compensé pour le brin maître des plantes du blé d'hiver Cv. Soissons cultivé à Grignon en 2008/2009 à deux dates de semis : un semis précoce (S1, début septembre) et un semis tardif (S2, mi novembre). Les symboles correspondent à la valeur médiane de HS pour un groupe de plantes ayant le même nombre final de feuilles.

Aussi bien pour le semis précoce que pour le semis tardif, l'évolution du HS en fonction du temps thermique compensé présente deux phases linéaires successives avec des pentes différentes. La pente de la phase I est indépendante du nombre final de feuilles produites alors que la pente de la phase II varie en fonction du nombre final de feuilles. Les pentes des deux phases varient en fonction de la date de semis.

Ce comportement nous a permis de construire un modèle descriptif du phyllochrone qui a été validé pour le brin-maître et les talles primaires. La variation du phyllochrone a été de l'ordre de 15-30% entre les phases 1 et 2 et de 7-16%, en phase 2, entre les groupes de plantes qui diffèrent par le nombre final de feuilles. Le phyllochrone était jusqu'à 30% plus court en semis tardif par rapport au semis précoce. Ces variations se trouvent dans une gamme qui est susceptible d'avoir une influence sur le développement de la septoriose.

Les paramètres du modèle de phyllochrone ont été implémentés dans le modèle Septo3D pour calculer les dates d'émergence des feuilles et le taux d'extension de la tige.

Les résultats obtenus dans ce premier chapitre de la thèse ont été soumis au journal *European Journal of Agronomy* sous forme d'un article scientifique intitulé "Phyllochron of winter wheat (*Triticum aestivum* L.) for a range of densities and sowing dates". Cet article est actuellement en cours de révision.

Chapitre 2 : Plasticité de l'architecture du blé en fonction de la densité et la date de semis

La densité et la date de semis sont des pratiques agronomiques connues pour avoir un effet sur l'architecture des plantes. Notre objectif a été à la fois de faire une description détaillée de la variation de l'architecture à l'échelle de la plante et du couvert et, de produire une base de données décrivant les variables d'architecture du blé pour les traitements étudiés dans l'intention de l'utiliser pour la reconstruction 3D des peuplements correspondants à nos expérimentations. Cela a donc nécessité une caractérisation détaillée des variables d'architecture au niveau de chaque phytomère pour le brin-maître et les talles primaires. Les profils verticaux de dimensions des organes ont été comparés entre traitements de date de semis et de densité et, au sein de chaque traitement, entre les groupes de plantes qui diffèrent par le nombre final de feuilles. Une caractérisation des variables d'architecture à l'échelle du couvert (comme l'indice de surface foliaire et la couverture du sol) a été également réalisée.

Les profils verticaux des dimensions de limbes, gaines et entrenœuds correspondaient à ceux habituellement décrits pour le blé d'hiver, mais ces profils variaient entre traitements.

Pour les phytomères juvéniles (développés avant le début d'extension de la tige), il n'y avait pas de différence de dimensions des organes entre traitements de densité. Par contre, des différences existaient pour les phytomères adultes (développés après le début d'extension de la tige) : la taille des organes était plus importante pour les plantes issues de la faible densité. A l'échelle du couvert, bien que le nombre de talles produit par plante était plus grand pour la faible densité, les taux d'évolution de l'indice foliaire (LAI) et du taux de couverture du sol étaient plus faibles pour la faible densité que pour les densités moyenne et forte.

Des différences dans le nombre et les dimensions des phytomères juvéniles ont été observées entre plantes issues de dates de semis différentes. Le semis précoce a conduit à la production de plantes avec un plus grand nombre de phytomères juvéniles et des feuilles plus grandes que celles du semis tardif. Pour les phytomères adultes, le nombre et les dimensions des organes étaient presque identiques entre semis précoce et semis tardif, probablement parce que l'élongation de la tige a été quasi simultanée pour les plantes des deux semis et que les phytomères adultes ont été soumis aux mêmes conditions environnementales. Par ailleurs, le nombre de tiges par mètre carré ainsi que les taux d'évolution du LAI et de la couverture du sol ont été plus élevés dans le semis précoce.

Une variabilité du nombre final de feuilles a été observée entre traitements et au sein d'un même traitement. Le nombre final de feuilles était plus élevé pour la faible densité et le semis précoce. Au sein d'un traitement donné, le nombre final de feuilles produit par un axe a varié allant de deux à quatre valeurs différentes. Des différences de dimensions des organes du brin-maître, ont également été observées entre plantes à nombre final de feuilles différent. Les plantes ayant produit un plus grand nombre de feuilles avaient des tailles d'organes plus petites pour les phytomères juvéniles (compté du bas vers le haut) et des tailles d'organes plus grandes pour les phytomers adultes (compté du haut vers le bas). Nous supposons que les variations observées du nombre de feuilles et des dimensions d'organes qui l'accompagnent ont pour origine les variations locales de densité et donc la quantité et qualité de lumière.

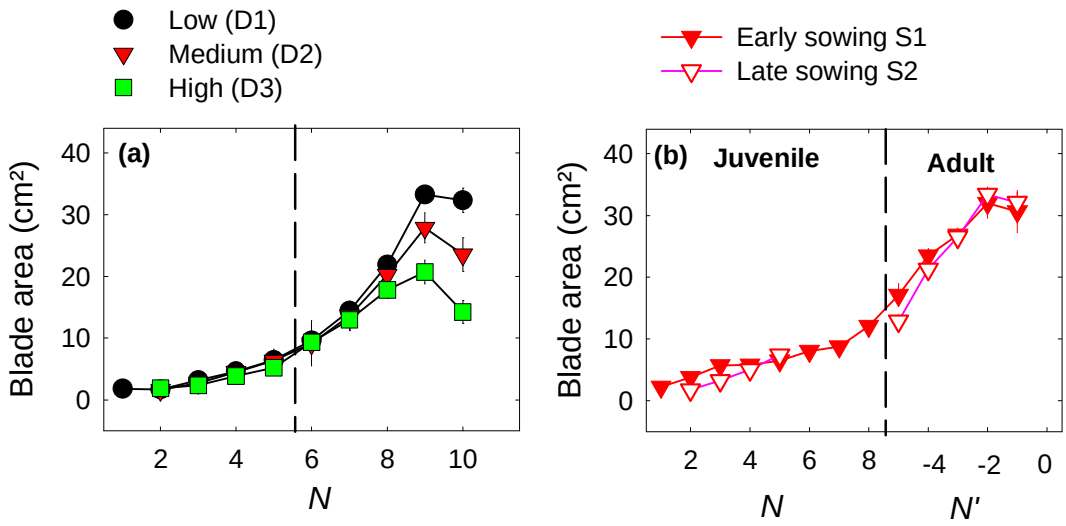

Figure 2. Surface foliaire en fonction du rang du phytomère **(a)** numéroté depuis la base de la tige principale pour des plantes ayant le même nombre final de feuilles (10) cultivées en 2008/2009 à une date de semis tardif (S2) à trois densités de semis : D1, D2 et D3 **(b)** numéroté depuis la base de la tige pour les phytomères juvéniles (développés avant l'extension de la tige) et depuis le haut de la tige pour les phytomères adultes (développés après l'extension de la tige) pour les plantes ayant le nombre final de feuilles le plus fréquent cultivés à deux dates de semis : précoce (S1, 13 feuilles) et tardif (S2, 9 feuilles) à une densité moyenne (D2). Les données correspondent au blé d'hiver Cv. Soissons cultivé à Grignon. S1 : fin septembre, S2 : mi novembre. D1 : 77, D2 : 228, D3 : 514 plantes. m^{-2}

La surface des feuilles des phytomères juvéniles était indépendante de la densité alors que pour les phytomères adultes, en particulier les trois derniers, la surface foliaire était plus importante pour les plantes issues de la faible densité.

Le semis précoce a produit des plantes avec un plus grand nombre de phytomères juvéniles mais le même nombre de phytomères adultes. Les feuilles développées sur les phytomères adultes des deux dates de semis avaient des surfaces foliaires presque identiques.

La comparaison des profils verticaux des dimensions d'organes et des hauteurs de tiges entre le maitre brin et les talles primaires confirment que la similarité des profils de dimensions d'organes entre la tige principale et les talles primaires a été maintenue pour la gamme de densités étudiée. La correspondance dans les profils verticaux de dimensions d'organes peut être simplement exprimée en considérant la position des phytomères compté à partir du haut de la tige.

Les résultats concernant la plasticité de l'architecture du blé issus des expérimentations réalisées au cours de ce projet (Cv. Soissons, deux années d'étude pour deux dates de semis et trois densités) ont été complétés par les résultats issus d'autres études faisant intervenir d'autres variétés et différents traitements de fertilisation. L'ensemble des données a permis de réaliser une étude plus large sur la plasticité de l'architecture du blé en réponse à différents facteurs. Les résultats de cette étude ont été publiés sous forme d'un article scientifique : "Dimensions and size of leaf blades, sheaths and internodes in relation to their position on a stem. *Field Crops Research*, 121, 1, 116-124."

Chapitre 3 : Simulation de l'effet des différences d'architecture du blé d'hiver modulées par la densité sur le développement épidémique de la septoriose

Au terme de l'expérimentation réalisée au cours de ce projet, une base de données complète de l'architecture du blé et du développement épidémique de la septoriose a été obtenue pour les trois densités du semis tardif en 2008/2009 (Y2S2). Ces données ont permis

de paramétrer le modèle de reconstruction du blé dans Septo3D et de confronter les simulations d'épidémie aux observations. Cependant, étant donné que les mesures épidémiques réalisées au champ ne correspondaient pas exactement aux sorties du modèle, nous avons défini une nouvelle variable épidémique pour permettre la comparaison entre simulations et observations. Cette variable est la proportion de lésions de septoriose dans la partie verte de la feuille. Elle est calculée à partir de la quantité de surface sénescente apicale et de la proportion de nécroses dues aux lésions de septoriose dans toute la feuille. Cette nouvelle variable a été utile puisqu'elle a permis une caractérisation détaillée des premiers stades de progression de la maladie à l'échelle de chaque feuille individuelle. Par ailleurs, le suivi de l'architecture des plantes a permis de déterminer la variabilité de développement entre plantes et la variabilité du nombre final de feuilles au sein de chaque traitement. Ces deux sources de variabilité ont été utilisées pour définir trois scénarii de simulations qui diffèrent par le degré de description du couvert :

- Scanario 1 (S_1): aucune source de variabilité n'est considérée. Il s'agit du scénario le plus simple
- Scénario 2 (S_2): on tient compte seulement de la variabilité du nombre final de feuilles dans chaque traitement
- Scénario 3 ou scénario de référence (S_{ref}): on tient compte des deux sources de variabilité.

Malgré les structures contrastées du couvert végétal des trois traitements de densités, il y a eut peu de différences dans le développement de la septoriose. Seule la faible densité a connu un développement légèrement plus rapide de la maladie par rapport aux deux autres densités qui ont montré le même niveau d'infection. Les prédictions du modèle, réalisées avec le scénario de référence (S_{ref}), étaient conformes aux mesures de terrain (faibles écarts entre simulations et observations). Cependant, des divergences par rapport aux observations ont été relevées. Parmi ces points, on a noté :

- Une sous-estimation de la vitesse de progression de la maladie pour les feuilles du bas du couvert pour toutes les densités (cf. Fig. 3);
- Une sous-estimation de la vitesse de progression de l'épidémie pour tous les rangs foliaires pour la faible densité (cf. Fig. 3);
- Sur certains étages foliaires, le modèle a simulé l'apparition précoce de faibles lésions de septoriose alors que les observations sur terrain n'ont pas montré ce type de lésions.

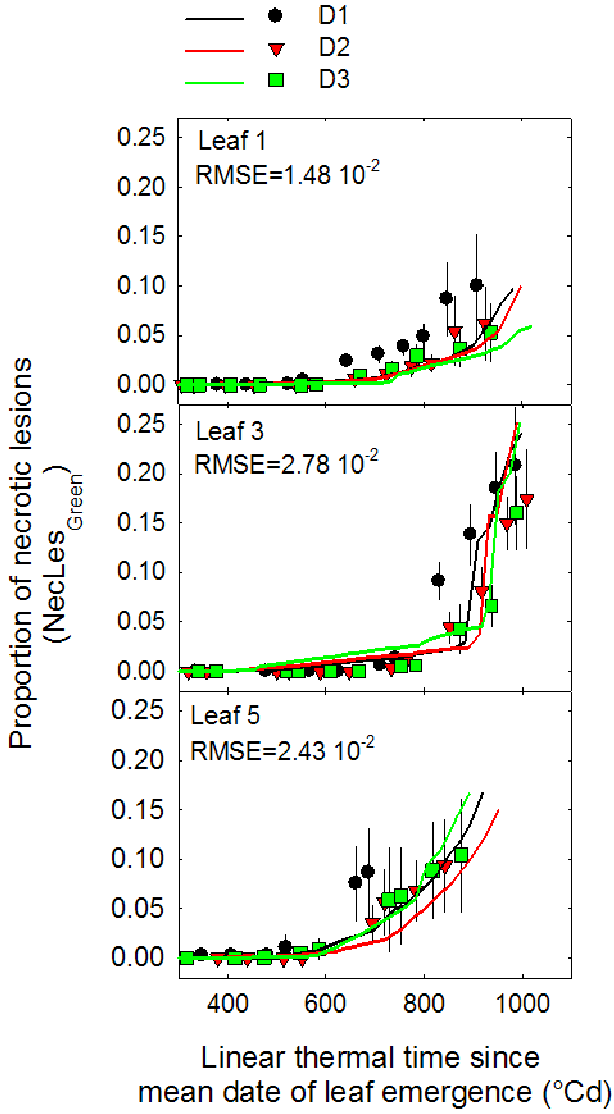

Figure 3. Dynamique des lésions nécrotiques de septoriose observées (symboles) et prédites avec Septo3D (lignes) en fonction du temps thermique linéaire calculé depuis la date moyenne d'émergence des feuilles pour les feuilles 1, 3 et 5, numérotées depuis le haut du couvert. Les données correspondent au blé d'hiver Cv. Soissons cultivé à Grignon en 2008/2009 à une date de semis tardif (mi novembre), à trois densités : D1 : 77, D2 : 228, D3 : 514 plantes. m^{-2}. Les segments verticaux représentent les intervalles de confiance à 95%. Les simulations sont réalisées avec le scénario qui tient compte de la variabilité de développement et du nombre final de feuilles des plantes (S_{ref}).

Le développement épidémique de la septoriose mesuré sur les différents étages foliaires a été très proche pour les plantes issues des densités moyenne et élevée (D2 et D3), et légèrement plus rapide pour la densité faible (D1). Les prédictions du modèle réalisées avec le scénario S_{ref} étaient proches des observations avec des écarts faibles entre simulations et observations. Cependant, le modèle a sous-estimé le développement épidémique de la maladie pour les feuilles du bas du couvert pour les trois densités, et pour tous les étages foliaires pour la faible densité.

Ces observations ont mis en évidence certaines limites du modèles ce qui a remis en question certaines hypothèses du modèle. Parmi les hypothèses avancées pour expliquer les points faibles du modèle :

- L'absence des autres moyens de dispersion de la maladie dans Septo3D, à savoir, la propagation par les ascospores et par contact peut être à l'origine de la sous-estimation notée sur les feuilles basales. L'introduction de ces deux types de moyens de propagation pourrait améliorer les prédictions du modèle.
- La sous-estimation des niveaux d'infection pour les feuilles basales a probablement conduit à la production d'une quantité d'inoculum limitant pour la faible densité. Etant donné le mode de propagation de la septoriose, de feuille en feuille, ce manque d'inoculum se serait répercuté sur les simulations des feuilles du haut de la tige.
- Le paramétrage d'une durée de latence fixe dans le modèle est probablement à l'origine de l'apparition précoce de lésions de septoriose dans les simulations. Changer le paramétrage de la durée de latence dans le modèle de façon à ce qu'elle soit une fonction qui dépend de la température et de l'humidité relative peut corriger ce problème.

La comparaison des simulations effectuées avec les trois scénarii a montré que le scénario dans lequel on tient compte de la variabilité entre plantes (S_{ref}) a produit les simulations les

plus proches des observations. En revanche, les simulations réalisées avec le scénario S_1 (sans variabilité) ont produit des courbes en forme d'escalier ce qui traduit une réponse simultanée de toutes les plantes à un même événement pluvieux. Ces courbes ont considérablement divergé des observations. Ces résultats démontrent l'importance de tenir compte de la variabilité entre plantes pour les simulations de septoriose.

Les résultats obtenus dans cette partie du projet a fait l'objet d'un article scientifique intitulée "Modelling the effect of wheat canopy architecture as affected by sowing density on *Septoria tritici* epidemics using a coupled epidemic-virtual plant model" qui est paru en ligne le 01/07/2011 dans le journal *Annals of botany*. (*doi:10.1093/aob/mcr126*)

IV. Discussion et conclusion

Ce travail a permis de :

- Identifier les principales variables d'architecture du blé modulées par la densité et la date de semis susceptibles de jouer un rôle dans la propagation de la septoriose.
- En nous aidant de données bibliographiques, établir une grille d'analyse de l'effet des variables d'architecture identifiées dans notre étude sur le développement de la septoriose. Cette grille a été décomposée en trois phases qui diffèrent par le mode de propagation de la maladie et le stade de développement du blé.
- Apporter des améliorations au modèle utilisé (Septo3D) notamment pour le module d'initialisation de la maladie et la prise en compte de la variabilité entre plantes pour la reconstruction du couvert.
- Apporter une analyse critique du modèle suite aux simulations réalisées. Cette analyse a permis d'identifier les limites qu'il faut adresser dans le modèle et de proposer des améliorations sur le court et le long terme.
- Proposer des applications pour ce type de modèle, comme par exemple :
    - Faire des études de prospection pour quantifier l'effet de la densité sur le développement épidémique pour une large gamme de conditions climatiques.
    - Analyser le rôle spécifique de variables d'architecture sur la maladie.

General introduction

I. General context of plant diseases

In the decades after the Second World War, a worldwide initiative, the Green Revolution aimed at increasing global food production. The initiative involved increased use of various technologies such as pesticides, herbicides and fertilizers as well as new breeds of high yield crops. Since this period and up to now, disease control has been mainly based on the use of chemicals and on breeding for resistant varieties. Breeding by itself results only occasionally in fully resistant breeds to a given pathogen, moreover when this is the case, their short life cycle and high genetic diversity allow pathogens to select biotypes able to circumvent plant resistance genes. As a consequence, the use of chemicals is generally the solution adopted to ensure disease-free crops. Nowadays, this strategy is questioned for many reasons. In response to the use of chemicals, pathogens select various mechanisms of resistance. Therefore, products become inefficient against new emerging pathogen biotypes (Leroux et al., 2006a, Leroux et al., 2006b). This process, known as "erosion" of pesticide efficiency results in a race in which we must continually find novel molecules to circumvent the ongoing selection of resistant pathogen races. Besides, sooner or later after their application, chemicals or derived molecules migrate to various environmental compartments. They can be washed by rain, volatilized in the atmosphere or simply degraded before penetrating the leaves (Willis and McDowell, 1987). The fraction that does penetrate plant tissues may ultimately be found in harvested products or, for most of it, be incorporated in the soil with crop residues. The environmental impact of these products or derived molecules raises growing concerns relative to the functioning of ecological systems and to human health.

The agricultural context is currently changing to promote sustainable practices that would avoid raising ecological issues. The new European guidelines ("Framework for Community Action to achieve a sustainable use of pesticides", 13th Jan. 2009, Strasbourg; Grenelle Environment Round Table, 2009[1]; Ecophyto, 2018) encourage developing agro-ecological means of disease control focusing for instance on varietal selection for resistant or tolerant breeds and optimisation of agronomic practices that limit disease pressure. Rather than growing disease-free crops one may accept some amount of disease development if it is kept to a level allowing sufficient yield while requiring no or few use of chemicals.

Multiple canopy features do influence disease development: level of resistance to pathogens, morphology and physiological status of organs and, plant and canopy architecture (Ando et al., 2007). In this work, we want to contribute to rationalising the use of canopy architecture as a tool to limit disease development. It is recognized that architectural traits can facilitate disease escape by limiting pathogen contact with the host, creating an unfavourable environment for pathogen growth or hampering the ability of the pathogen to trigger the infection process. Modifications of canopy structure appear as an interesting means since architecture can be partially controlled by varietal selection and by the use of agronomic practices. Agronomic practices (e.g., nitrogen fertilization, sowing density and date of sowing) are known to influence disease development in many ways including the modification of canopy architecture (Subedi et al., 2007, Gladders et al., 2001, Armour et al., 2004, Leitch and Jenkins, 1995, Tompkins et al., 1993, Broscious et al., 1985, Pfleeger and Mundt, 1998). However, these effects are irregular between years in terms of intensity and direction and the mechanisms likely involved are complex and difficult to disentangle. This is specially the case because genotypes differing in plant architecture generally differ also in

[1] www.legrenelle-environnement.fr

their intrinsic resistance to pathogens and, different crop architectures result in differences in microclimate and the physiological status of plant organs. This is where the modelling approach particularly, the coupled virtual plant-disease models come in. By changing values of parameters or input variables, models allow to analyse the influence of specific factors on predicted variables. Virtual plant modelling is a modelling approach in which the three-dimensional (3D) structure of the plants is explicitly described, thus providing the means to better reflect the effect of the plant architecture on the epidemic development. The modelling approach using this type of coupled models appears as a promising tool to investigate architecture-disease interactions.

II. General models vs. virtual plant models

1. Approaches to modelling crop diseases

The first plant disease simulators were designed in late 1960s. Later, in 1980s, models with descriptive mathematical equation were constructed. The approach was to find analytical functions able to represent the disease progress curve, which is a simplified representation of the epidemic (Teng et al., 1980). Single equation models have been used to describe disease population dynamics and the main two curves were the exponential growth and the logistic growth. This was a first step in quantitative epidemiology but the approach was limited because used equations did not have a sufficient biological basis. Equation parameters could be estimated *a posteriori* by fitting models on observation but could not be estimated in advance so as to predict the epidemic dynamics that a given set of conditions may produce. In parallel, some mechanistic models, which attempt to explain disease development through detailed representation of its component processes, have been developed (Zadoks, 1971, Rapilly, 1979). Determination of the disease development requires quantitative knowledge of the interactions between the host and the pathogen as well as the effects of environmental variables on this interaction. Some disease models attempted to account for the host crop by including it as a substrate for the pathogen (Teng et al., 1980, Bruhn and Fry, 1981).

In parallel, in agricultural sciences, many studies have been devoted to modelling the growth of crops and plants in relation to environmental conditions leading to the development of crop growth models or "process-based models" (PBM). This modelling approach simulates physiological processes and gives an account of crop growth in terms of mass variables per unit area of soil; growth is derived from light interception (Marcelis et al., 1998). PBM are based mainly on two approximations: first, the geometric structure of plants is assimilated to a continuous, homogeneous medium used to compute mass and energy transfers; second, organs are represented as a set of non-spatialized compartments to render biological functions and internal transfers within plants (Andrieu et al., 2006). Many models that express crop and disease growth dynamically have thus been developed based on the PBM approximations. (Johnson and Teng, 1990, O'Callaghan et al., 1994, Rossi et al., 1997). In many cases, the aim of these models was to support decision making in fungicide application (O'Callaghan et al., 1994, Moreau and Maraite, 1999, Audsley et al., 2005). Such models did not aim to understand the mechanisms of canopy-disease interactions, but rather at having a good prediction capacity of potential risks. In most of these models, a representation of potential disease dynamics, independent of the crop characteristics, was integrated to a process-based model of crop growth: the disease effects that may affect crop growth and yield are simulated either by a direct effect on functions that calculate the rate of variables within the crop, or by an indirect effect through reducing the energy inputs at the crop canopy. However, most of

these models ignore the interactions that take place between the host plant, the disease and the environment at the organ scale.

2. Virtual plant modelling

From the 1960s, a formalism for the simulation of plant structure and its dynamics (Lindenmayer, 1968a, 1968b) has been developed which led to the foundation of "functional-structural plant modelling" (FSPM) or "virtual plant modelling" (Room et al., 1996). Virtual plant modelling is a modelling approach in which the three-dimensional (3D) structure of the plant is explicitly described (Prusinkiewicz, 2004, Room et al., 1996). All the organs a plant is composed of (leaves, internodes, flowers, fruits, etc) can be represented in 3D. In this way, the geometry (e.g., leaf shape, leaf curvature, branching angles) and the topology (sequence and connections between organs) of the plants are described in detail. Since the early 1990s, virtual plant modelling increasingly aroused interest. The first reason is related to the fact that more and more research groups become aware of the advantages of using explicit 3D description of a plant. The second reason is that since the 1990s, desktop computers have become sufficiently powerful to support this kind of modelling. FSPM were subsequently extended to many plants (herbaceous and trees) and to both microscopic and macroscopic scales of plant processes (Godin and Sinoquet, 2005, Hanan and Prusinkiewicz, 2008).

In comparison to classical process-based models, FSPM take explicitly into account the spatial distribution of plant organs which allows dealing with environmental and biological processes at the organ level. Moreover, as stated by Vos et al. (2010) in this approach, "organs of individual plants are the primary objects" rather than compartments and thus individual growth of each organ needs to be modelled whereas in PBM, mainly leaf blades are considered (Andrieu et al., 2006).

3. The virtual plant as a tool to simulate disease

Room (1996) was the first to invoke the potential of virtual plant models, as a tool of comprehension, on plant pathology research. The author proposed that "by handling 3D information on the development and growth of individual plant organs and the activity of the organisms which live on them, these models should represent in depth the interactions between the plant architecture and the pathogen".

- By superimposing disease development on a dynamic growth model for a plant, FSPM offer a "one-step process" in modelling disease and host growth which is more interesting than the deterministic and mathematical modelling approaches which require integration with crop growth models (Wilson and Chakraborty, 1998).
- Physical and biological processes computed at the organ scale are more accurate expressing thereby the possible variability of microclimate within the canopy. This can have an important consequence on disease development, often linked to microclimatic conditions.
- The detailed description of organ morphology and their spatial distribution, should improve simulations of disease propagation which is known to be influenced by plant and canopy architecture.

However, few examples exist where virtual plant models have been used to investigate the interactions between plants and diseases. Wilson and Chakraborty (1998) used a virtual plant model to quantify the impact of anthracnose on the branching of a pasture legume. More recently, virtual plant models have been coupled to plant diseases; examples include grape and powdery mildew (Calonnec et al., 2008), wheat and *Septoria tritici* (Robert et al., 2008) and a pasture legume with *Colletotrichum gloeosporioides* under elevated CO_2 (Pangaa et al., 2011) .

III. General objectives of this work

For all the above-mentioned reasons, using Virtual Plant Modelling appears as an interesting tool to study pathogen growth in interaction with its host. However, this approach has been developed only in the few last years and there is still little validation. At the moment we are not yet able to confirm whether it can render the services expected or not. Consequently, the general objectives of our work were to advance the approach of using Virtual Plant models in understanding the interaction canopy-disease and to evaluate it. We aimed also at checking whether we can model architecture sufficiently well so as to draw information on its impact on epidemics. To achieve these goals, we chose the pathosystem wheat-*Septoria tritici*, which is the model system to investigate the interactions plant-pathogen-climate in the INRA research unit "EGC", where this work has been carried out. Several reasons are behind this choice:

- Wheat (*Triticum aestivum* L.) is the most widely cultivated Gramineae in the world and *Septoria tritici* is a major wheat disease in many parts of the world, particularly in the Mediterranean seacoast (Eyal, 1981a, 1981b, Ben Mohamed et al., 2000) and European countries. *S. tritici* is one of the most damaging foliar diseases on wheat crops. In France, it can lead to yield losses of 50 q/ha in the most critical situations (Gouache et al., 2009).
- An increase of importance of this disease has been observed in the last decades due to the rapid replacement over large areas of local cultivars by the high-yielding, early-maturing, short cultivars that are susceptible to the pathogen and also to changes in agronomic practices (Eyal, 1981a, 1981b). In the last years, *S. tritici* has developed resistance to many fungicides (Leroux et al., 2006a, 2006b) which further emphasize the need for alternative solutions for disease reduction.
- *S. tritici* is a splash-dispersed disease i.e., the main way of propagation is the transport of spores from leaf to leaf by rain drops. Yield losses occur when the top two or three leaves, which are important contributors to grain filling, become infected (Shaw and Royle, 1989). Thus, *Septoria* is largely influenced by plant and canopy architecture (Lovell et al., 1997).

A recent development in the unit has been the coupling of a virtual wheat plant Adel-wheat (Fournier et al., 2003) with a dynamic model of *S. Tritici.* This model, called "Septo3D" (Robert et al., 2008) was used in our study to investigate wheat-*Septoria* interactions.

IV. The pathosystem studied: wheat-Septoria tritici

4. Presentation of the wheat plant

1.1. Structure of wheat

A wheat plant consists of a set of axes (tillers) which comprise a vegetative part, the stem bearing leaves, and a reproductive part, the ear, and a root system (Fig. 1a). The first formed axis is called main stem and the other axes may be primary tillers, that are ramifications of the main stem or higher order tillers, which are ramifications of ramifications. An axis presents a modular structure and is formed by a set of morphological units: the phytomers. A phytomer consists of several botanical entities that are, from bottom to top: a node bearing an axillary bud, an internode, a sheath and a blade (Fig. 1b). The blade and the sheath, separated by the ligule, form the entire leaf. Only the four or five upper internodes elongate to form the stem. The lower internodes remain short and the base of the stem is formed by a stack of nodes from which nodal roots develop. The bud present at each node can

develop into a tiller that emerges from the sheath of the lower phytomer. For wheat plants grown in the field only buds from the lower- non elongated internodes – may develop. Some of the tillers regress, so that in a crop sown at standard density, a plant has usually 2 to 3 tillers at flowering.

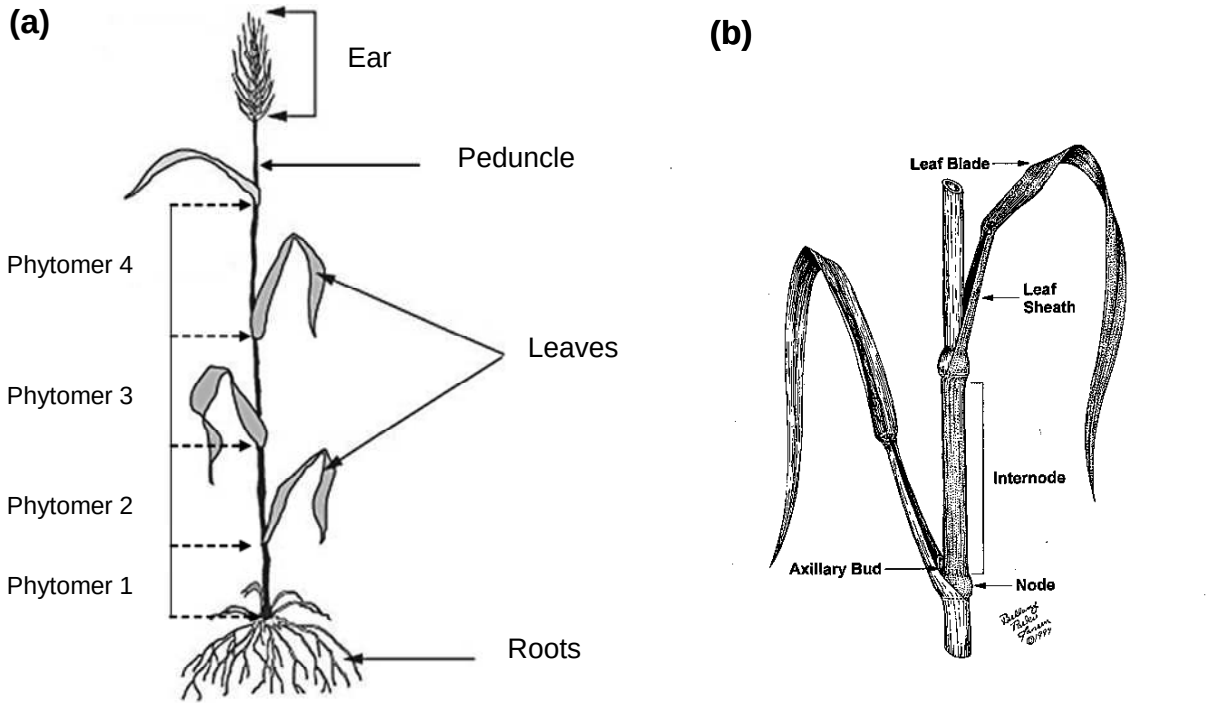

Figure 1. (a) An example of a wheat tiller with its components from bottom to top: roots, the successive phytomers, the peduncle and the ear on the top **(b)** An example of a typical Gramineae phytomer and its components: internode, node, tiller bud, leaf sheath and leaf blade (Moore and Moser, 1995).

1.2. Growth and development

The growth cycle of wheat is usually divided in four phases (Gate, 1995) as illustrated in figure 2. Following Simmons et al. (2011), the main features of each phase are:

- *Germination and seedling emergence.* When a kernel is sown in a moist soil, the germination process begins. The radicle and seminal roots first extend, followed by the coleoptile. As the coleoptile emerges from the soil, its growth stops and the first true leaf pushes through the tip.

- *Tillering and head differentiation.* When the main stem has 3 to 4 leaves, the first tiller emerges from the bud situated at the axil of the first true leaf: it is the first primary tiller. During tillering, the main stem produces primary tillers from its axillary buds; and primary tillers give rise to secondary tillers, etc. Tiller appearance is closely coordinated with the appearance of leaves on the main stem (Masle-Meynard and Sebillotte, 1981). A variable number of tillers may emerge during that phase, depending on plant population density and water and nutriments are availability. During the time that tillering occurs, the initiation of heads on the main stem and tillers takes place. Although the head at this time is microscopic, the parts that will become the floral structures and kernels are already being formed.

- *Stem elongation, head growth and flowering.* When head formation is complete, the plant stops producing new tillers and the stems begin elongating; tillers that have produced more than three leaves and have initiated their own root system are more likely to elongate (Masle-Meynard, 1981); while less developed tillers will regress then die. Stem elongation results from the sequential extension of the last formed internodes and the associated leaves gain height. Stem elongation coincides with rapid head growth in which the individual florets become prepared to pollinate. When the flag leaf sheath encloses the growing head, this is called the "boot" stage. As the stem continues to elongate, the head is pushed out of the flag leaf sheath, a stage referred to as "heading". Within a few days after heading, flowering (pollination) begins in the head.

- *Kernel growth and maturity*. Growth progresses in three distinct phases spanning about four weeks under usual conditions. In the first phase, the "watery ripe" and "milk" stages, the number of cells in the endosperm (the major starch and protein storage portion of the kernel) is established. Not much weight is accumulated during this phase. Then 1 to 2 weeks after pollination, the kernel begins accumulating starch and protein rapidly and its dry weight increases in a nearly linear manner. This is when most of the final mass of the kernel is accumulated: carbon principally comes from the current leaf photosynthesis, while nitrogen mainly originates from the remobilisation of the Rubisco stored in the leaves. Finally, growth rate of the kernel declines as kernel mass approaches a maximum attained at physiological maturity.

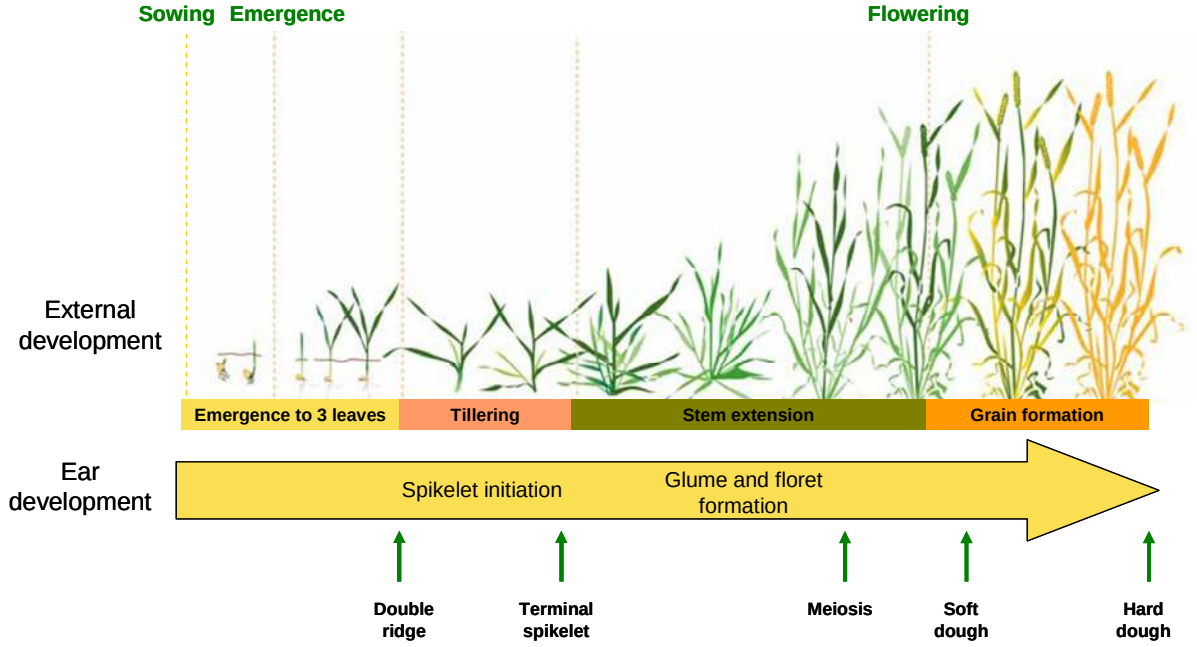

Figure 2. Principle phases of external development of a wheat plant and of ear development (Slafer and Rawson, 1994)

5. Presentation of *Septoria tritici*

Septoria leaf blotch of wheat, caused by *Septoria tritici* Rob. ex Desm. (anamorph of *Mycosphaerella graminicola* (Fuckel) Schroeter), develops mainly on wheat, but also occasionally on rye, triticale and some grass species. *S. tritici* is a hemibiotroph fungus: after an initial phase where the infection occurs without host tissue damage, there is a necrotrophic phase where colonized tissues begin to die. The initial symptoms are small yellow spots on

the leaves. These lesions often become light tan as they age, and the fungal fruiting bodies can be seen embedded in the lesions on the awns. Lesions are irregularly shaped and range from elliptical to long and narrow (Figure 1). Lesions contain small, round, black speckles that are the fruiting bodies of the fungus called pycnidia (Figure 3).

Figure 3. Symptoms of *Septoria tritici* include light brown lesions. Lesions are often elongated, and may merge, resulting in large sections of dead leaf tissue (De Wolf, 2008).

2.1. Life cycle and ways of propagation

Septoria tritici survives through the summer on residues of a previous wheat crop and initiates primary infections in automn. Primary infection can originate from local source from ascospores (sexual form) or pycnidiospores (asexual form) borne by crop debris in the field. It can also occur by long distance spread of air-borne ascospores, (Shaw and Royle, 1989, Hunter et al., 1999). Pycnidiospores are transported mainly by rain-splash from residues or lower infected leaves to newly emerging leaves. During the winter, most of pathogen spread consists of vertical movement of spore-containing droplets called also "Dispersal Units" (Rapilly and Jolivet, 1976). Therefore, the disease progresses from the bottom to the top of the plant by successive infection cycles, hence the qualification of polycyclic disease. In wet conditions, direct contact between leaves could also result in spore dispersal (Lovell et al., 2004b). A second possible period of ascospore release coincides with the emergence of the upper two leaves (Lovell et al., 1997) which leads to the possibility of some infection of the upper leaves without rainfall.

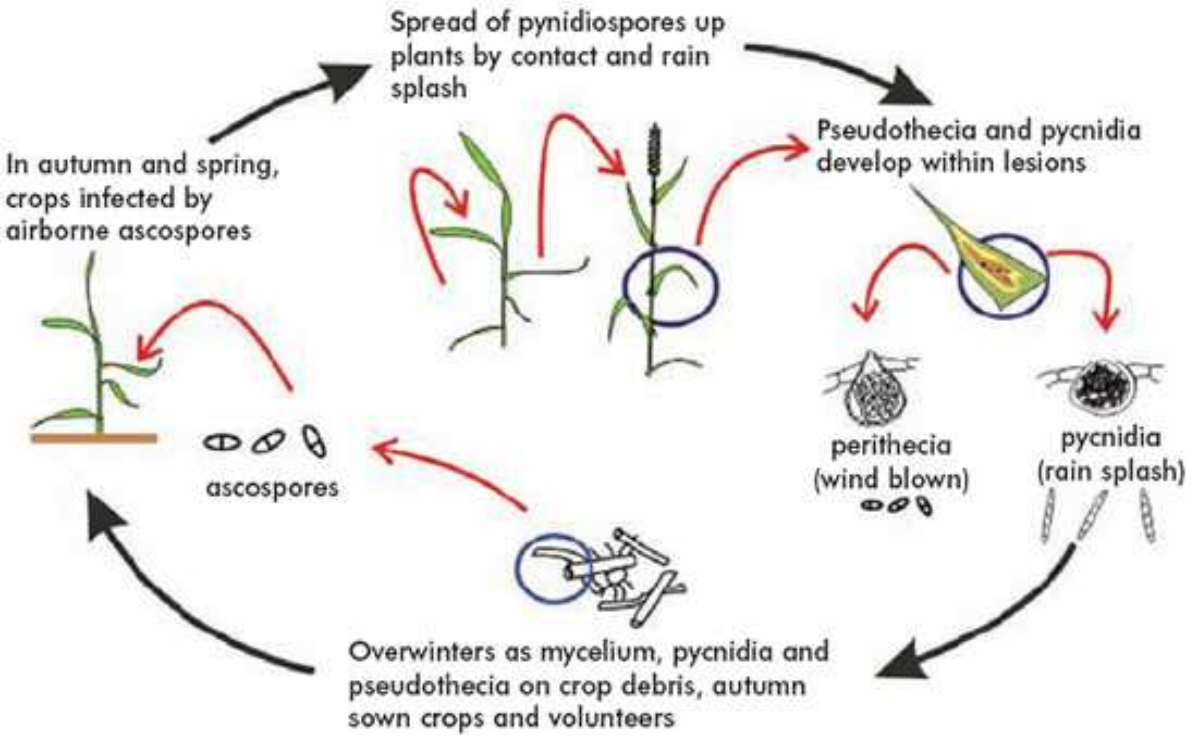

Figure 4. Representation of the life cycle of *Septoria tritici* (caused by *M. graminicola*) on a wheat plant. Disease progress occurs mainly by ascospores (sexual form) in autumn and pycnidiospores (asexual form) in winter and spring[1]

2.2. Infection cycle

The infection cycle of *S. tritici* can be divided in four phases:

Infection: spore germination and stomatal penetration into the leaf occurs when conditions of high humidity and moderately high temperatures (between 10 and 25°C) are met during 15 to 20 hours (Magboul et al., 1992).

Latency period: this phase spreads from the initial infection to the formation of the first visible sporulating structures; no external symptoms can be seen but a slow and non destructive mycelial growth takes place in the intercellular spaces (**biotrophic phase**); this is also called incubation. For S. tritici, the latency period lasts 270 to 500 °Cd depending on environmental conditions (Lovell et al., 2004a).

Sporulation: the end of the latency period corresponds to the beginning of the **necrotrophic phase**. The pathogen development intensifies and leads to the destruction of cell walls (Keon et al., 2007). This leads to the sporulation, which consists in the emission of pycnidiospores (filiform spores of 50-80 µm length and less than 5 µm diameter). Pycnidiospores are produced by pycnidia that develop within lesions and are exuded in sticky masses the "cyrrhus".

Dispersion: pycnidiospores represent the main form responsible for disease propagation and are dispersed mainly by rain splashes. During a rain event, drops that hit a sporulating lesion are splashed away carrying spores to upper leaves of the same or another plant. Features of the canopy structure e.g., density of leaves, distance between leaves and rate of leaf emergence can thus influence the disease propagation by enhancing or reducing the probabilities of contact and the proximity between organs (Lovell et al., 2004b).

[1] http://www.hgca.com

6. Interactions between plant architecture and *S. tritici* epidemic

Due to its main way of propagation, i.e., splash dispersal, *Septoria* is a disease that is highly influenced by plant and canopy structure. Several studies have been performed to identify and quantify architectural features that impact *S. tritici* development. They revealed that many variables interact with *Septoria* epidemic involving complex and dynamic processes. These variables are often correlated which further complicate their comprehension.

- Ground cover and leaf area index impact *S. tritici* epidemics by influencing rain penetration and raindrop distribution. On the one hand, crops characterised by a low and late canopy closure allow more raindrops to penetrate the canopy and more splashes to occur in agreement with Eyal (1981a) who reported that raindrop splashing effect was increased in less dense crops leading to a sooner and faster pathogen progress. On the other hand, in dense crops dispersal units that reach the upper leaves are likely to have more surface area available which enhance disease progress (Pielaat et al., 2002). Other variables that influence LAI could indirectly contribute to impact the disease, such as leaf blade area and number of axes per m². Increased number of tillers may also promote the proximity and the horizontal contact between leaves (Broscious et al., 1985).

- Leaf senescence: increased rate of monocarpic senescence could limit disease progress by decreasing the probability for a dispersal unit to hit green tissue and by hampering incubating lesions to develop. Conversely, Lovell et al. (1997) found that for the upper four leaves *S. tritici* was responsible for most of the senescence recorded. Given the difficulty to distinguish between monocarpic and induced senescence, it is thus difficult to assess senescence effect on *Septoria* development.

- Vertical distance between leaves and plant height: the vertical progress of the pathogen, called the "ladder effect" (Bahat et al., 1980), depends on the distance between the successive leaves of an axis. Indeed, the close proximity of the leaves (e.g., in dwarf cultivars) allows upper leaves to be more readily exposed to splashed pycnidiospores as distance can be covered even by low energetic droplets (Lovell et al., 1997). Shaw (1987) calculated that there is a fivefold reduction in the number of spores transported vertically by splash with each increase in height of 10 cm. There may even be in direct contact with infected lower leaves making infection possible in the absence of rain. Consequently, many studies reported that tall plants are less attacked by *S. tritici* (Tavella, 1978, Danon et al., 1982, Camacho-Casas et al., 1995, Simon et al., 2005). Leaf posture also influences the proximity between sources and receptors of the pathogen. For instance, when leaves have an erected posture, the newly emerging leaves have greater risk to overlap with tips of old infected leaves for longer zone and period than when leaves have a bent posture (Lovell et al., 1997).

- Rate of stem extension in relation to phyllochron: during stem extension, new emerging leaves gain height in the canopy which increases the distance between them and the basal infected leaves (Lovell et al., 1997). Thus, by elongating, the plant can outgrow the disease. The top three leaves of winter wheat commonly emerge at a height below leaves that are fully developed and that may be diseased. Internode extension is closely coordinated with leaf extension so that the phyllochron determines the period of overlap of successive leaves. Otherwise, by varying phyllochron values, Robert et al. (2008) reported that simulated *S. tritici* epidemics were reduced for reduced phyllochron (i.e., increased rate of stem extension).

V. Septo3D: presentation, structure and limits

7. Model presentation

The model Septo3D (Robert et al., 2008) was specifically designed for studying the interaction between canopy architecture and epidemic development. Septo3D combines a dynamic architectural model of wheat, ADEL-Wheat (Fournier et al., 2003) with a dynamic model of *S. tritici* epidemic based on Rapilly and Jolivet (1976). Starting from a given initial state of infection, the model simulates the lesion development and propagation from the infected lower leaves to the healthy upper leaves in a canopy. Epidemics result from repeated successions of lesion development resulting in spore production and spore dispersal. The model includes three modules, which deal respectively with canopy development, lesion development and spore dispersal.

Canopy development Canopy simulation is based on a simplified version of the model ADEL-Wheat, a virtual plant model of winter wheat (Fournier et al., 2003), that was also adapted to spring wheat (Evers et al., 2005). ADEL-Wheat simulates in 3D the dynamics of appearance and extension of all vegetative organs of a wheat canopy. To have a good description of green area dynamics, the model was completed with a parameterisation of the progress of natural senescence and of tiller dynamics (Robert et al., 2008).

Lesion development This module simulates the development of a lesion after deposition of a spore-containing droplet on the leaf. Four stages are considered: infection (spore germination and penetration in the leaf), incubation, appearance and extension of chloroses, and maturation of chloroses into sporulating necrotic tissue. Infection and incubation are assumed to occur only on green tissue. In Septo3D, each leaf blade is divided into small regions called sectors in which we keep track of disease development. At each time step, the model computes in each leaf sector the area allocated to each stage of the infection cycle: incubating, chlorotic, and sporulating.

Spore dispersal In the model, spore dispersal occurs during rain events. Sporulating lesions are considered empty after occurrence of three rain events. For the simulation of spore dispersal the canopy is represented as a horizontal homogenous turbid medium where droplets transport is simulated between layers of the vegetation as a function of the distance to the source. The properties of the turbid medium are derived from the 3D representation of the canopy. The 3D representation allows to calculate the density and orientation of leaves within each layer for emission and interception of droplets and to allocate intercepted droplets to the sectors of leaves located in each layer. The amount of infectious droplets per layer results from the net balance of production, deposition and loss due to washing.

To summarize, in the model, plant development and the resulting canopy architecture influence epidemic development by four effects:

- They determine the distance between the sources of spores (lesions) and the receptors (green leaf tissues);
- They influence rain penetration and spore distribution in the canopy;
- They determine, via the progression and green leaf tissues, the quantity of leaf area available for lesion development;
- The progression of leaf senescence kills incubating lesions.

The model was used in a sensitivity analysis in which architectural variables were varied artificially (increased or decreased by 30%). This analysis revealed that the

phyllochron and the leaf size are two key variables in disease development (Robert et al., 2008).

8. Limits of the model

Septo3D is a promising tool to assess the influence of wheat architecture on *Septoria* epidemic development, yet the current version (i) has not been validated against detailed epidemic data and (ii) presents several simplifications that may hamper the realism of simulations:

- Choice of the initial conditions: epidemics are initiated by assuming that the first three leaves are similarly infected. Thus, the variability of initial infections resulting from interactions between initial inoculum, climate and canopy development is not taken into account.
- Simplifications in the canopy model lead to some unrealistic features of the canopy. For instance, the crop is represented by cloning a single plant which induces an unrealistic periodicity across the canopy. Besides, leaf blades are modelled as straight "flame-shaped" surfaces assuming that leaf angle is invariant during leaf growth, whereas, it is known that leaf angle and posture depends on leaf age, cultivar and density of plants. These simplifications could induce errors in the disease simulations.
- In the model, the duration of the latency period is a user-defined parameter, whereas, in reality, the rate of progress of incubation and thus the duration of the latency period may vary with temperature and humidity (Shaw, 1990, Lovell et al., 2004a).
- Many empirical rules are used in the modules of lesion development and of spore dispersal, e.g., the fraction of splashed dispersal units is parameterised following Rapilly and Jolivet (1976) without particular model analysis for the current model; parameter values for splashed droplets were obtained using data representing splash in liquid water (Pietravalle et al., 2001) but were not validated in the case of real canopy. An evaluation of such empirical assumptions is necessary to investigate their importance in disease simulations.
- Disease propagation is based only on spore dispersal by splashes. Two mechanisms of dispersion are thus missing: ascospore transport by wind (Shaw and Royle, 1989) and contact between leaves (Lovell et al., 2004b).

While including approximations is part of the essence of modelling, obviously this also implies that the model should be validated against experimental data. Up to now, a quantitative validation of Septo3D had not been performed.

VI. Objectives and rationale of this thesis

In order to reach our general goal: examining the effect of plant architecture on disease development using a virtual plant modelling approach, and given the specificities of the pathosystem studied and the model Septo3D, our specific objectives during this work were:

- To provide a comprehensive description of varied wheat architectures intended to better understand wheat plasticity and to accurately parameterize the canopy model ;
- To assess the effect of these changes on Septoria development ;
- To bring improvements to the current version of Septo3D and validate it by comparing simulated epidemics to observed epidemics in the field ;

- To investigate the effect of the degree of detail with which canopy architecture parameterisation influence disease prediction.

In order to create a wide range of wheat architectures, we chose to grow wheat for contrasted densities and sowing dates. First, there are many reports in the literature that these agronomic practices influence disease epidemics via their effect on canopy architecture (Shaw and Royle, 1993, Broscious et al., 1985). Thus, understanding how they can influence diseases is interesting in the current context. In addition, experiments carried out through collaboration between INRA and ARVALIS-Institut du Végétal to test the effect of sowing date and density on *Septoria* disease epidemics on wheat, revealed that these practices present a potential for crops to partly escape *Septoria* epidemic. Therefore, we used an approach that combines experiment and modelling.

The experiment was designed so as:

- To provide measurements of architectural variables (i) at the plant level: the number and dimensions of phytomers at maturity, topology of phytomers and tillers, etc., and (ii) at the canopy scale: leaf area index, ground cover, number of tillers/m².
- To monitor frequently the progress of *Septoria* epidemic in the field through detailed measurements on individual leaves of diseased plants. Measurements were performed on the true leaf rank i.e., on leaves counted from the base and not from the top of the plant as usually done in epidemic studies.

The modelling required the following steps:

- The parameterisation of the canopy model considering realistic plant variability derived form experimental measurements.
- The calculation of a specific epidemic variable to compare accurately simulated kinetics of the disease at the level of each leaf layer.

Initial outlines

Several steps were defined to achieve our objectives:

1) Study of the plasticity of winter wheat in response to contrasted densities and sowing dates with a trial to understand and quantify some regulatory mechanisms involved in the observed variations; in particular we aimed at understanding regulations of tillering dynamics and at implementing it in the current version of the model.

2) Parameterisation of the canopy model of Septo3D using the obtained architectures from field experiment.

3) Evaluation of Septo3D for its capacity to simulate detailed epidemic progress at different leaf layers by comparing simulated epidemics to observed ones and identification of the important architectural features influencing the disease.

4) Using the data set of wheat architecture for different sowing date and densities, performing a risk analysis which allows providing new insights into the effect of the studied agronomic practices on the disease progress for various climatic conditions.

Adaptation of objectives during the work

Response to temperature and phyllochron study

Measurements of the rate of leaf emergence were performed during two growing seasons 2007/2008 and 2008/2009 which experienced different climatic conditions. Analysis of these measurements revealed contrasted results of phyllochron between the two years when expressed in linear thermal time, which is usually used to account for temperature effect on plant development. Thus we undertook a deeper analysis, including comparing several alternatives to linear thermal time. This allowed comparing the rate of leaf emergence for the different treatments investigated and developing a phyllochron model. Presentation of the model and analyses of the effect of sowing date and density on phyllochron are presented in Chapter 1.

A comprehensive description of wheat plasticity instead of analysis of its mechanisms

The objective of studying wheat plasticity initially included understanding the processes involved in the regulation of tillering. This was finally abandoned and the experiment was not designed in this particular purpose. A detailed and comprehensive description of the architectural variables at the plant and the canopy level is presented, but without aiming at a mechanistic modelling of the behaviour.

Lack of time to perform the risk analysis

Several complications led to spend more time than expected in the analysis of disease data and the parameterisation of the canopy model. This left insufficient time at the end of the thesis to perform the risk analysis under different climatic conditions. Only a preliminary analysis could be made and presented in the general discussion of the thesis.

VII. Organisation of the manuscript

Chapter 1

The effect of both sowing date and density on the phyllochron of winter wheat, grown under field conditions, is presented in this chapter. The variations of phyllochron during the crop cycle are discussed in terms of a two phase model determined by photoperiod at seedling emergence and final leaf number. Here, the advantage of a non-linear response of temperature to compute thermal time is presented. This model allowed estimating the phyllochron for each investigated treatment with accuracy. The estimated parameters were also used to parameterise the rate of organ appearance in the canopy model in Septo3D.

Chapter 2

In this chapter we present a comprehensive description of the plasticity of winter wheat at the plant scale– expressed as the organ dimensions of main stem and axillary tillers in relation to their position on a stem– and at the canopy scale for the investigated density and sowing date treatments. The collected architecture data are then discussed for their adequacy for the model parameterisation. Part of these data were completed were used as inputs to parameterise canopy model.

Chapter 3

In this chapter, a brief description of the canopy model parameterisation is given. Here, we test the capacity of the model Septo3D to simulate *Septoria tritici* progress on the different leaf layers for three density treatments by comparing simulated to observed

epidemics. In this study, we draw attention to the importance of taking into account interplant variability in disease simulations and the limits of this approach.

Chapter 4

In the general discussion, we give a summary of the main results reported in this work and a critical assessment of the model with regards to our findings. Based on the architecture differences observed between sowing date and density treatments, we present a general overview of their possible effects on *Septoria* development and finally we give an outlook on future applications of the model.

Appendixes

Meteorological data such as air and plant temperatures, change in daylength and rain quantity and intensity are presented in Appendix I.

Agronomic interventions as well as dates, doses and product names of the different applied chemicals are summarized in Appendix II.

Appendix III presents supplementary figures of the vertical profiles of organ dimensions for the investigated treatments.

Architecture data from our work was complemented by other studies with variable genotypes and fertilization treatments as part of a study that gives a wider view on wheat plasticity. This published study in *Field Crops Research* (Dornbusch et al., 2010) is presented in Appendix IV.

References

Ando K, Grumet R, Terpstra K, Kelly JD. 2007. Manipulation of plant architecture to enhance crop disease control. *CAB Reviews: Perspectives in Agriculture, Veterinary Science, Nutrition and Natural Resources,* **2**: 8 pp.

Andrieu B, Lecoeur J, Lemaire G, Ney B. 2006. Le peuplement végétal cultivé. In: (T.Doré MLB, P. Martin, B. Ney, J. Roger-Estrade, Coord.) ed. *L'agronomie aujourd'hui.* Versailles, Editions Quae.

Armour T, Viljanen-Rollinson SLH, Chng S, Butler RC, Jamieson PD, Zyskowski RF. 2004. Examining the latent period of Septoria tritici blotch in a field trial of winter wheat. *New Zealand Plant Protection, Volume 57, 2004. Proceedings of a conference, Hamilton, New Zealand, 10-12 August 2004.*

Audsley E, Milne A, Paveley N. 2005. A foliar disease model for use in wheat disease management decision support systems. *Annals of Applied Biology,* **147**: 161-172.

Bahat A, Gelernter I, Brown MB, Eyal Z. 1980. Factors affecting the vertical progression of Septoria leaf blotch in short-statured wheats. *Phytopathology,* **70**: 179-184.

Ben Mohamed L, Rouaissi M, Sebei A, Hamza S, Harrabi M. 2000. Effect of genotype, sowing date, nitrogen and potassium fertilisation and fungicides on the development of Septoria tritici. *Durum wheat improvement in the Mediterranean region: new challenges. Proceedings of a seminar, Zaragoza, Spain, 12-14 April, 2000.*

Broscious SC, Frank JA, Frederick JR. 1985. Influence of winter wheat management practices on the severity of powdery mildew and Septoria blotch in Pennsylvania. *Phytopathology,* **75**: 538-542.

Bruhn JA, Fry WE. 1981. Analysis of potato late blight epidemiology by simulation modelling. *Phytopathology,* **71**: 612-616.

Calonnec A, Cartolaro P, Naulin JM, Bailey D, Langlais M. 2008. A host-pathogen simulation model: powdery mildew of grapevine. *Plant Pathology,* **57**: 493-508.

Camacho-Casas MA, Kronstad WE, Scharen AL. 1995. Septoria tritici resistance and associations with agronomic traits in a wheat cross. *Crop Science,* **35**: 971-976.

Danon T, Sacks JM, Eyal Z. 1982. The relationships among plant stature, maturity class, and susceptibility to Septoria leaf blotch of wheat. *Phytopathology,* **72**: 1037-1042.

De Wolf E. 2008. Septoria Tritici Blotch. *Kansas State University.*

Dornbusch T, Baccar R, Watt J, Hillier J, Bertheloot J, Fournier C, Andrieu B. 2010. Plasticity of winter wheat modulated by sowing date, plant population density and nitrogen fertilisation: Dimensions and size of leaf blades, sheaths and internodes in relation to their position on a stem. *Field Crops Research,* **(accepted for publication 2.12.2011)**.

Evers JB, Vos J, Fournier C, Andrieu B, Chelle M, Struik PC. 2005. Towards a generic architectural model of tillering in Gramineae, as exemplified by spring wheat (Triticum aestivum). *New Phytologist,* **166**: 801-812.

Eyal Z. 1981a. Integrated control of Septoria diseases of wheat. *Plant Disease,* **65**: 763-768.

Eyal Z. 1981b. Research on Septoria leaf blotch: recent advances. *EPPO Bulletin,* **11**: 53-57.

Fournier C, Andrieu B, Ljutovac S, Saint-Jean S. 2003. ADEL-wheat: A 3D architectural model of wheat development. In: Hu B-G, Jaeger M eds. *Proceedings of International Symposium of Plant Growth Modeling and Applications.* Beijing, China. 2003 Tsinghua University Press - Springer Verlag.

Gate P. 1995. *Ecophysiologie du blé,* Doc./Lavoisier, (eds), p. 423.

Gladders P, Paveley ND, Barrie IA, Hardwick NV, Hims MJ, Langton S, Taylor MC. 2001. Agronomic and meteorological factors affecting the severity of leaf blotch caused by Mycosphaerella graminicola in commercial wheat crops in England. *Annals of Applied Biology,* **138**: 301-311.

Godin C, Sinoquet H. 2005. Functional-structural plant modelling. *New Phytologist,* **166**: 705-708.

Gouache D, Gate P, Robert C, Fournier C. 2009. Sowing date, disease pressure and yield potential: from understanding to recommendations. *Association Francaise de Protection des Plantes, 9eme conference international sur les maladies des plantes, Tours, France, 8 et 9 Decembre 2009.*

Hanan J, Prusinkiewicz P. 2008. Foreword: Studying plants with functional-structural models. *Functional Plant Biology,* **35**: I-iii.

Hunter T, Coker RR, Royle DJ. 1999. The teleomorph stage, Mycosphaerella graminicola, in epidemics of Septoria tritici blotch on winter wheat in the UK. *Plant Pathology*, **48**: 51-57.

Johnson KB, Teng PS. 1990. Coupling a disease progress model for early blight to a model of potato growth. *Phytopathology,* **80**: 416-425.

Keon J, Antoniw J, Carzaniga R, Deller S, Ward JL, Baker JM, Beale MH, Hammond-Kosack K, Rudd JJ. 2007. Transcriptional adaptation of Mycosphaerella graminicola to programmed cell death (PCD) of its susceptible wheat host. *Molecular Plant-Microbe Interactions* **20**: 178-193.

Leitch MH, Jenkins PD. 1995. Influence of nitrogen on the development of Septoria epidemics in winter wheat. *Journal of Agricultural Science,* **124**: 361-368.

Leroux O, Walker AS, Albertini C, Gredt M. 2006a. Resistance to fungicides in French populations of Septoria tritici, the causal agent of wheat leaf blotch. *Aspects of Applied Biology*: 153-162.

Leroux P, Gredt M, Albertini C, Walker AS. 2006b. Resistance to fungicides in Septoria tritici, the causal agent of wheat leaf blotch: from genes to fields *8eme Conference Internationale sur les Maladies des Plantes, Tours, France, 5 et 6 Decembre, 2006. 564-573.*

Lindenmayer A. 1968a. Mathematical models for cellular interactions in development. I. Filaments with one-side inputs. *Journal of Thoretical Biology,* **18**: 280-299.

Lindenmayer A. 1968b. Mathematical models for cellular interactions in development. II. Simple and branching filaments with two-sided inputs. *Journal of Thoretical Biology,* **18**: 300-315.

Lovell DJ, Hunter T, Powers SJ, Parker SR, Bosch Fvd. 2004a. Effect of temperature on latent period of septoria leaf blotch on winter wheat under outdoor conditions. *Plant Pathology*, **53**: 170-181.

Lovell DJ, Parker SR, Hunter T, Royle DJ, Coker RR. 1997. Influence of crop growth and structure on the risk of epidemics by Mycosphaerella graminicola (Septoria tritici) in winter wheat. *Plant Pathology,* **46**: 126-138.

Lovell DJ, Parker SR, Hunter T, Welham SJ, Nichols AR. 2004b. Position of inoculum in the canopy affects the risk of septoria tritici blotch epidemics in winter wheat. *Plant Pathology*, **53**: 11-21.

Magboul AM, Geng S, Gilchrist DG, Jackson LF. 1992. Environmental influence on the infection of wheat by *Mycosphaerella graminicola*. *Phytopathology,* **82**: 1407-1413.

Marcelis LFM, Heuvelink E, Goudriaan J. 1998. Modelling biomass production and yield of horticultural crops: a review. *Scientia Horticulturae,* **74**: 83.

Masle-Meynard J. 1981. Elaboration of ear number in a population of winter wheat subjected to competition for nitrogen. I. Evidence of a critical state for elongation of a tiller. *Agronomie,* **1**: 623-631.

Masle-Meynard J, Sebillotte M. 1981. Study of the heterogeneity of a winter wheat stand. II. Origin of the different sorts of individuals in the stand; factors allowing description of its structure. *Agronomie,* **1**: 217-223.

Moore KJ, Moser LE. 1995. Quantifying developmental morphology of perennial grasses. *Crop Science,* **35**: 37-43.

Moreau JM, Maraite H. 1999. Integration of knowledge on wheat phenology and Septoria tritici epidemiology into a disease risk simulation model validated in Belgium. *Information technology for crop protection, 23 September 1999, Harpenden, UK.*

O'Callaghan JR, Dahab MH, Hossain AHMS, Wyseure GCL. 1994. Simulation of *Septoria tritici*-winter wheat interactions. *Computers and Electronics in Agriculture,* **11**: 309-321.

Pangaa IB, Hanan J, Chakraborty S. 2011. Pathogen dynamics in a crop canopy and their evolution under changing climate. *Plant Pathology,* **60**: 70-81.

Pfleeger TG, Mundt CC. 1998. Wheat leaf rust severity as affected by plant density and species proportion in simple communities of wheat and wild oats. *Phytopathology,* **88**: 708-714.

Pielaat A, Bosch Fvd, Fitt. BDL, Jeger MJ. 2002. Simulation of vertical spread of plant diseases in a crop canopy by stem extension and splash dispersal. *Ecological Modelling,* **151**: 195-212.

Pietravalle S, Van den Bosch F, Welham SJ, Parker SR, Lovell DJ. 2001. modelling of rain splash trajectories and prediction of rain splash heigth. *agricultural and Forest Meteorology,* **109**: 171-185.

Prusinkiewicz P. 2004. Modeling plant growth and development. *Current Opinin in Plant Biology,* **7**: 79-83.

Rapilly F. 1979. Simulation of an epidemic of Septoria nodorum Berk. on wheat in relation to the possibility of horizontal resistance. *EPPO Bulletin,* **9**: 243-250.

Rapilly F, Jolivet E. 1976. Construction d'un modèle (episept) permettant la simulation d'une épidémie de Septoria nodorum BERK sur blé. *Revue de statistiques appliquées,* **3**: 31-60.

Robert C, Fournier C, Andrieu B, Ney B. 2008. Coupling a 3D virtual wheat (Triticum aestivum) plant model with a Septoria tritici epidemic model (Septo3D): a new approach to investigate plant-pathogen interactions linked to canopy architecture. *Functional Plant Biology,* **35**: 997-1013.

Room P, Hanan J, Prusinkiewicz P. 1996. Virtual plants: new perspectives for ecologists, pathologists and agricultural scientists. *Trends in Plant Science,* **1**: 33-39.

Rossi V, Racca P, Pancaldi D, Alberti I. 1997. A simulation model for the development of brown rust epidemics in winter wheat. *European Journal of Plant Pathology,* **103**: 453-465.

Shaw MW. 1987. Assessment of upward movement of rain splash using a fluorescent tracer method and its application to the epidemiology of cereal pathogens. *Plant Pathology,* **36**: 201-213.

Shaw MW. 1990. Effects of temperature, leaf wetness and cultivar on the latent period of Mycosphaerella graminicola on winter wheat. *Plant Pathology,* **39**: 255-268.

Shaw MW, Royle DJ. 1989. Airborne inoculum as a major source of Septoria tritici (Mycosphaerella graminicola) infections in winter wheat crops in the UK. *Plant Pathology,* **38**: 35-43.

Shaw MW, Royle DJ. 1993. Factors determining the severity of epidemics of *Mycosphaerella graminicola* (*Septoria tritici*) on winter wheat in the UK *Plant Pathology*, **42**: 882-899.

Simmons SR, Oelke EA, Anderson PM. 2011. Grwoth and development guide for spring wheat. *University of Minnesota Extension.* University of Minnesota. p.9.

Simon MR, Perello AE, Cordo CA, Larran S, Putten PELvd, Struik PC. 2005. Association between Septoria tritici blotch, plant height, and heading date in wheat. *Agronomy Journal*, **97**: 1072-1081.

Slafer GA, Rawson HM. 1994. Sensitivity of wheat phasic development to major environmental factors: a re-examination of some assumptions made by physiologists and modellers. *Australian Journal of Plant Physiology*, **21**: 393-426.

Subedi KD, Ma BL, Xue AG. 2007. Planting date and nitrogen effects on Fusarium head blight and leaf spotting diseases in spring wheat. *Agronomy Journal*, **99**: 113-121.

Tavella CM. 1978. Date of heading and plant height of wheat varieties, as related to Septoria leaf blotch damage. *Euphytica*, **27**: 577-580.

Teng PS, Blackie MJ, Close RC. 1980. Simulation of the barley leaf rust (Puccinia hordei) epidemic: structure and validation of BARSIM-I. *Agricultural Systems*, **5**: 85-104.

Tompkins DK, Fowler DB, Wright AT. 1993. Influence of agronomic practices on canopy microclimate and Septoria development in no-till winter wheat produced in the Parkland region of Saskatchewan. *Canadian Journal of Plant Science*, **73**: 331-344.

Vos J, Evers JB, Buck-Sorlin GH, Andrieu B, Chelle M, de Visser PHB. 2010. Functional-structural plant modelling: a new versatile tool in crop science. *Journal of Experimental Botany*, **61**: 2101-2115.

Willis GH, McDowell LL. 1987. Pesticide persistence on foliage. *Reviews of Environmental Contamination and Toxicology*, **100**: 23-73.

Wilson PA, Chakraborty S. 1998. The virtual plant: a new tool for the study and management of plant diseases. *Crop Protection*, **17**: 231-239.

Zadoks JC. 1971. Systems analysis and the dynamics of epidemics. *Phytopathology*, **61**: 600-610.

Chapter 1

Phyllochron of winter wheat (*Triticum aestivum* L.) for a range of densities and sowing dates

European Journal of Agronomy (to be submitted after revision)

Phyllochron of winter wheat (*Triticum aestivum* L.) for a range of densities and sowing dates

Rim Baccar [1,2], Tino Dornbusch [1,2], Mariem Abichou [1,2], Jessica Bertheloot [1,2,3], Philippe Gate [4], Bruno Andrieu [1,2*]

[1] INRA, UMR 1091 EGC, F-78850 Thiverval-Grignon, France.
[2] AgroParisTech, UMR 1091 EGC, F-78850 Thiverval-Grignon, France.
[3] INRA, UMR 0462 SAGAH, F-49071 Beaucouzé Cedex
[4]ARVALIS-Institut du végétal, 3 rue Joseph et Marie Hackin 75116, France

[*] *Corresponding author. Email: bruno.andrieu@grignon.inra.fr*

Abstract

Phyllochron is an important parameter in crop models. For wheat, it is generally approximated as constant during crop development, and is expressed in thermal time. However, several studies reported ontogenic changes during the growing season. A number of authors observed that phyllochron varied according to sowing date but other proposed that these changes may include artefact due to the difference between the temperature of the air and that of the growing zones. In this paper, we investigate the phyllochron of winter wheat under field conditions for contrasted sowing dates and population densities. We seek to parameterize possible changes in phyllochron throughout crop development and for the different tillers.

Triticum aestivum 'Soissons' was grown during two years, at three densities and two sowing dates. Apex temperature was calculated based on soil temperature before stem extension and then on air temperature. Haun stage was monitored weekly and linear and non-linear rate responses to temperature were compared to calculate thermal time. A descriptive model was adjusted and parameter values were compared between treatments.

The use of compensated thermal time (Γ_c) assuming a non-linear response to temperature allowed a high reproducibility of time course of leaf emergence between years. The Haun Stage showed two successive linear phases over the growth cycle: rate in phase I differed between sowing dates, rate in phase II differed depending both on sowing date and on final leaf number. The duration of each phase was correlated to the photoperiod at seedling emergence and, for a given sowing date, was independent of the total leaf number. Thus plants of different density treatments differed in phyllochron only if they differed by the total number of leaves.

Much of the variation in the phyllochron of a wheat tiller with density and sowing date can be ascribed to the photoperiod at seedling emergence and the total number of leaves on the tiller.

Key words: winter wheat, *Triticum aestivum*, phyllochron, sowing date, density, photoperiod, final leaf number, phyllochron model, leaf emergence rate, Haun Stage progress

Introduction

Phyllochron, that is the time interval between similar developmental stages—often appearance or ligulation—of two successive leaves on the culm (Wilhelm and McMaster, 1995) is an important parameter that regulates the time course of leaf area establishment and stem extension and thus resource capture as well as the ability to suppress weeds and escape fungal diseases (Robert et al., 2007, 2008). The few studies that have examined changes of phyllochron with sowing density have found little (Kirby and Faris, 1972) or no effect (Masle et al., 1989). On the other hand it has been well established that the phyllochron varies in function of sowing date (Baker et al., 1980, Kirby et al., 1982, Kirby and Perry, 1987, 1985). Many studies have been carried out to better characterize these effects but they produced conflicting finding interpretations.

It is widely accepted that temperature is the main factor regulating phyllochron (Baker et al., 1986, Cao and Moss, 1989b, 1994). Effects of temperature are usually taken into account by expressing the phyllochron in thermal time (°Cd). However in winter wheat, the phyllochron expressed in thermal time has been found to change with sowing date: the later the sowing, the shorter the phyllochron (Kirby et al., 1982, 1985). A number of authors agree upon this change and have accounted for it by invoking either a preconditioning effect of the day length (Cao and Moss, 1989a, 1989b, 1991) or the rate of change in daylength (Baker et al., 1980, Kirby and Perry, 1987) around plant emergence. Otherwise, a direct and continuous effect of daylength during development has been suggested (Masle et al., 1989, Miralles and Richards, 2000), which can be accounted for by the use of photothermal time instead of thermal time. On the other hand, Jamieson et al. (1995) proposed that correlations with daylength may at least partly reflect bias in the calculation of thermal time.

Thermal time is usually computed based on air temperature measured at 2m high; assuming that this represents the temperature the plant receives. However, at the early stages of development, the shoot apical meristem (SAM) is under the soil surface so that it is under the influence of soil temperature. For maize (a summer annual crop), several authors (Brooking and McPherson, 1989, Cellier et al., 1993, Guilioni et al., 2000) have shown that soil temperature differs substantially from air temperature especially when the canopy is sparse. For winter wheat, the difference between soil and air temperature was generally found to be small (Gallagher, 1979, Ljutovac, 2002). However, using a data set of eight wheat cultivars sown in New Zealand at dates ranging from March to September, Jamieson et al. (1995) have shown that near surface soil temperature provided a better prediction of leaf appearance than air temperature.

The use of thermal time implies that a linear relationship exists between leaf appearance rate and temperature. Although widely used, this approximation is also problematic. Non-linear growth responses to temperatures have been evaluated for a range of species, including wheat (Kemp and Blacklow, 1982, Xue et al., 2004), maize, rice, and *Arabidopsis* (Parent, 2009). According to these studies, it allowed a more accurate prediction of leaf appearance than the assumption of linear responses.

It is often assumed that phyllochron in wheat is constant during plant development (Baker et al., 1980, Kirby et al., 1985, Cao and Moss, 1989a, 1989b). However, several authors have observed that the first six to eight leaves emerged faster than the later ones (Calderini et al., 1996, Miralles and Richards, 2000, Miralles et al., 2001). Boone et al. (1990) provided evidence that such change in the rate of leaf appearance may mark the occurrence of an early event related to the floral transition of the SAM—perhaps the single ridge stage. On the other hand later changes in the phyllochron, taking place around the developmental stage

of double ridge have also been reported (Cao and Moss, 1991). Likely, some of the changes reported may have resulted from a change in temperature regime when the growing zone emerges above soil surface due to stem extension.

Finally, we are still lacking a clear picture of the conditions under which phyllochron changes throughout the plant cycle. The phyllochron is a required parameter in crop models such as CERES-Wheat (Ritchie and NeSmith, 1991), CERES-Maize (Kiniry, 1991), SIRIUS (Jamieson et al., 1998) and in virtual plant models such as ADEL-Maize (Fournier and Andrieu, 1998), ADEL-Wheat (Fournier et al., 2003), GRAAL (Drouet and Pages, 2003). The latter approach provides 3D representations of plant architecture which allow detailed simulation of competition for light (Fournier and Andrieu, 1999) and disease escape (Robert et al., 2008). In this study, we focus on wheat phyllochron in the perspective of deriving an appropriate parameterisation for the virtual plant approach. With this in mind we investigated possible changes in phyllochron throughout crop development and between tillers, considering a range of density and sowing dates.

Materials and methods

9. Overview

The Haun Stage progress of main stems and first order tillers was monitored for different densities and sowing dates for winter wheat (*Triticum aestivum* 'Soissons') grown under field conditions. Air and soil temperatures were monitored. Thermal time was calculated using soil temperature before stem extension and air temperature after. Four methods to calculate thermal time were compared, assuming either a linear or a non-linear response to temperature and including or not photoperiod (photothermal time). Descriptive models of phyllochron were adjusted and the changes in the value of their parameters with sowing date and final number of leaves were investigated.

10. Experimental design and treatments

The experiment was conducted on the INRA experimental fields at Thiverval-Grignon, France (48°51N, 1°58E, 70m) on a silty loam soil. *T. aestivum* 'Soissons' was grown in two seasons, 2007/2008 (Y1) and 2008/2009 (Y2). Six treatments were carried out. There was an early (S1, late September) and a late (S2, mid November) sowing date and three sowing densities: 77, 228, 514 plants m^{-2}. Density treatments will be referred to as low density (D1), intermediate density (D2) and high density (D3). Actual population densities were measured when plants had one liguled leaf and were lower than sowing densities (Table 1). In Y1, all treatments were used; in Y2, treatment S1D2 was excluded to alleviate measurements.

Table 1
Dates of sowing and seedling emergence; and plant population densities of winter wheat Cv. 'Soissons' sown in late September (S1) and mid November (S2) at three densities:D1, D2, D3 in 2007/2008 (Y1) and 2008/2009 (Y2) D1 : 77, D2 : 228, D3 : 514 plants m^{-2}.

		Y1		Y2	
		S1	**S2**	**S1**	**S2**
Date of sowing		25/09/2007	12/11/2007	30/09/2008	17/11/2008
Date of emergence		01/10/2007	01/12/2007	08/10/2008	18/12/2008
Population density (plants m^{-2})	**D1**	77	53	55	59
	D2	211	168	180	160
	D3	483	394	374	406

Each treatment was carried out in three parallel plots, at least 30 m in length and spaced 0.2 m from each other. Each plot consisted of nine rows of plants with an inter-row distance of 0.175 m. Measurements were done in the central plot only. The space between plots was used as an access path, so the two external rows on each side of the plot were considered as borders and not used for measurements.

For both experimental years of experiments the previous crop was *Vicia faba*. The soil nitrogen content was measured at the end of January, to adjust fertilization following recommendation for high yielding crops. The amount of nitrogen in soil was around 70 kg ha^{-1} at the end of January, thus depending on density, 130 to 200 kg ha^{-1} ammonium nitrate were provided overall, divided into two applications. An irrigation system was installed to complement natural rainfall when needed. Weeds were controlled by herbicide application at sowing and during the crop cycle. Recommended fungicides and insecticides were applied to prevent diseases and insect damage. In Y2, a growth regulator (Moddus 0.5 $l.ha^{-1}$) was used for the early sowings at high density. No growth regulator was used in Y1.

Data from another field experiment were also used. This experiment was carried out in 2005/2006 (Y') at the same location, using Cv. 'Soissons'. The sowing date was 27th October 2005 (referred to S_{int}). Sowing density was 250 plants m^{-2}, and there were two nitrogen fertilization treatments: without N application (0N) and with optimal fertilisation (N+).

11. Plant measurement

3.1. Leaf emergence

When plants had two fully expanded leaves, 20 median plants were tagged in each treatment. These plants were used to monitor leaf appearance and ligulation on the main stem and on the primary tillers. Tags were further placed on upper leaves to allow accurate notation of leaf and tiller ranks. Once or twice weekly, depending on temperature, the rank and the length of the youngest liguled leaf and the length of the new growing leaves were measured. These measurements were used to calculate the Haun Stage (HS; Haun, 1973) of each tiller. Leaves were counted acropetally, number one being for the first true leaf (the coleoptile was not taken into account). The main stem will be referred to as T_0 and the axillary tillers as T_k (k = 1, 2…) starting with k = 1 for the tiller that emerges at the axil of the first true leaf. The coleoptile tiller rarely emerged and thus was not considered in data processing.

3.2. Leaf initiation

Plants were dissected during Y2 to monitor leaf primordia initiation. Measurements began at HS = 5.9 for S1 and at HS = 2.0 for S2. For each treatment, ten plants were sampled randomly once or twice weekly, depending on temperature. The number of main stem primordia (N_{prim}) was counted under a video microscope (Hirox KH 1000, Microelectronique S.A, France) (maximum magnification 300x), taking into account only primordia larger than 30µm. Dissections were stopped when 32 primordia had been initiated.

12. Meteorological measurements

Air temperature at 2 m was recorded over growing seasons at a weather station 500 m from the field. Soil temperature at 3 cm deep was measured from sowing until the start of fast internode elongation. These measurements were taken in two treatments in Y1 (S1D2 and S2D2) and in four treatments in Y2 (S1D1, S1D3, S2D1, and S2D3). Two sets of four thermocouples were lined up within one row of a plot for each treatment and were connected to a data logger. Data was recorded every 30 seconds to compute an average hourly value. Measurements of soil temperature at various density treatments showed negligible differences, and were thus averaged regardless of the density. Malfunctioning of the data logger meant that a few values of soil temperature went missing. In such a case, a relationship between soil and air temperature was used to estimate the missing data. It was fitted using temperature measurements taken a few days before and after the malfunction. Daylength was calculated as the duration between sunrise and sunset, using the classical astronomical formulas.

13. Data analysis

5.1. Calculation of thermal time

a. Linear thermal time

In most studies, thermal time (Γ) is computed assuming a linear response to temperature, which leads to the temperature sum expressed in units of degree days (°Cd):

$$\Gamma = \frac{1}{24}\sum_{i} \max(0, T_{\mathrm{i}} - T_{\mathrm{b}}) \tag{1}$$

where i is the number of hours elapsed after seedling emergence, T_{i} is the hourly-averaged temperature and T_{b} is the base temperature. For wheat, T_{b} = 0°C was chosen as it is widely accepted (Baker et al., 1986, Baker et al., 1980, Gallagher, 1979).

b. Compensated thermal time

Alternatively, Johnson and Lewin (1946) proposed a model based on a modified Arrhenius equation to describe a non-linear response of biological processes to temperature:

$$F(T) = \frac{kT \exp\left(\frac{-E_a}{RT}\right)}{1 + \exp\left(\frac{\Delta S}{R} - \frac{\Delta H}{RT}\right)} \tag{2}$$

where $F(T)$ is the given temperature response rate, k is a proportionality constant, E_{a} is the average activation energy for the considered process, R is the gas constant, ΔH is the enthalpy, and ΔS is the entropy of the reactions. Parent (2009) demonstrated the applicability of this equation to the rate of growth and development in rice, maize, and *Arabidopsis*. He

proposed the use of a reference temperature T_{ref} (which can be chosen arbitrarily), and defined a temperature compensated rate, $J_{Tref}(T_i)$, as the ratio $F(T_i)/F(T_{ref})$. For a process following Eq. (2), a period of time D at a temperature T_i results in the same progress as a period of time $D \cdot J_{Tref}(T_i)$ at the temperature T_{ref}. Using this concept, Parent (2009) defined the temperature-compensated time in term of "hours at T_{ref}". Here we followed this logic but we have chosen to express the duration in temperature-compensated thermal time (Γ_c). To this end, we determined that a period D at temperature T_{ref} represents $T_{ref} \cdot D \cdot J_{Tref}(T_i)$ "degree.days T_{ref}" ($°Cd_{Tref}$). Following this, the temperature-compensated thermal time is calculated as:

$$\Gamma_c = \frac{T_{ref}}{24} \sum_{i=1} \frac{F(T_i)}{F(T_{ref})} \tag{3}$$

where T_{ref} is the reference temperature. We chose T_{ref} = 12°C, which is close to the average temperature during the wheat growing season, because as can be seen from Eq. (3), when temperature is around T_{ref}, the compensated thermal time progresses similarly to the usual thermal time.

c. Linear photothermal time

On the other side, Masle et al. (1989) proposed to account for both temperature and photoperiod by computing a photothermal time ($^P\Gamma$) expressed in °Cd. In this basis, temperatures (above T_b) are accumulated during the light period only:

$$^P\Gamma = \frac{1}{12} \sum_i \delta_i \max(0, T_i - T_b) \tag{4}$$

where δ_i is the fraction of hour i situated in the light period.

d. Compensated photothermal time

Using the two concepts: non-linear response to temperature and integration of photoperiod in the calculation of thermal time, we computed a compensated photothermal time ($^P\Gamma_c$) expressed in $°Cd_{12}$ as follows:

$$^P\Gamma_c = \frac{T_{ref}}{12} \sum_{i=1} \delta_i \frac{F(T_i)}{F(T_{ref})} \tag{5}$$

5.2. Calculation of phyllochron and plastochron

The stages of wheat development were quantified using a decimal index for the number of liguled leaves, the Haun Stage (HS; Haun, 1973), even if our calculation differed slightly from Haun (1973):

$$HS = n + L/L' \tag{6}$$

where n is the number of liguled leaves at a given time, L is the exposed length of the laminae of leaf n+1.

The trends in HS and N_{prim} *vs.* compensated thermal time were modelled so that they would reflect the two linear phases observed. Then the phyllochron and the plastochron (i.e., the difference in thermal time between the initiation of two successive leaf primordia on the SAM) were calculated for each phase as the inverse of the slopes of the fitted models.

14. Statistical analysis

In order to characterize the behaviour of the most frequent individual plant, representative values for HS and N_{prim} at each sampling date were calculated as the medians

of measurements on individual plants having the same final number of leaves (N_{leaf}). Model parameters were estimated using either the least squares fitting methods in Matlab (function nlinfit) or Excel 2003 (Solver). The significance of differences in the number of final leaves and in phyllochron between density treatments were tested using the non-parametric Kruskall & Wallis and Mann & Whitney tests (Georgin and Gouet, 2000) and correlations between phase durations, phyllochron values, and photoperiod were established using the Spearman test (Georgin and Gouet, 2000). As a measure for the deviation from a 1:1 line between measured and predicted values, we used the root mean squared error (RMSE).

Results

During winter, time course assuming a non-linear response to temperature differed from time course calculated assuming a linear response.

To evaluate the model of Johnson and Lewin (1946) for wheat, we used the data of leaf extension of *T. aestivum* Cv. 'Gamenya' published by Kemp and Blacklow (1982). Original data are for leaf four and five, which have different maximum growth rates. We normalized them to a maximum extension rate of one before pooling data together. Then we estimated the parameters in Eq. (2) by fitting the function to this data set. Figure 1 illustrates that the model allowed an excellent fit with a low root mean squared error (RMSE = 0.047). The calculated parameters (Table 2) were then used to compute Γ_c with Eq. (3).

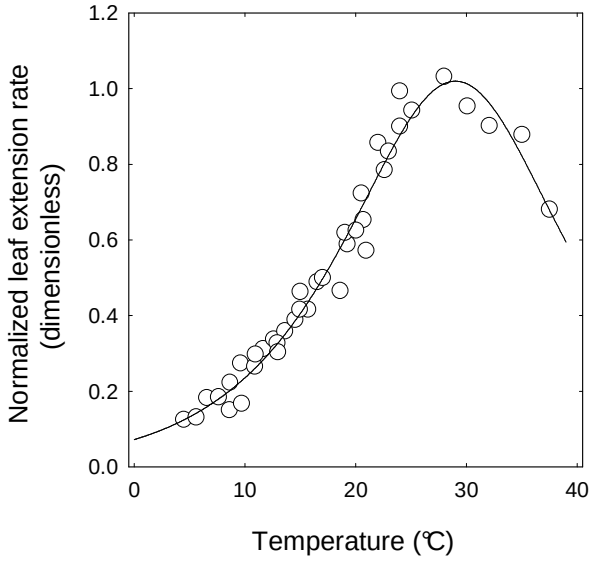

Figure 1. Normalized extension rate of winter wheat leaves (Cv.'Gamenya') as a function of growth temperature. (○) represent data from Kemp and Blacklow (1982). The solid line was computed with Johnson and Lewin's model (1946).

Table 2
Parameter values of Johnson and Lewin's (1946) model fitted to Kemp and Blacklow's data (1982) for winter wheat leaf extension (*Triticum aestivum* Cv. 'Gamenya')

Parameter	Description	Units	Value
K	Proportionality constant	dimensionless	$3.8088\ 10^{10}$
Ea/R	Average activation energy divided by the gas constant	°K	8899.6
ΔS/R	Entropy divided by the gas constant	dimensionless	68
ΔH/R	Enthalpy divided by the gas constant	°K	20736

The rate of HS progress varied between density treatments only when these treatments differed in the final leaf number

The final number of leaves of tillers varied with sowing date and density. As expected, S1 typically resulted in 13 to 14 leaves on the main stem, whereas S2 typically resulted in 9 to 11 main stem leaves. The median main stem N_{leaf} was approximately one less at D3 compared to D1. However, for Y1S2, all density treatments resulted in the same median main stem N_{leaf}. The main stem N_{leaf} also varied among plants of the same treatment. Generally, the most frequent value for N_{leaf} represented 50 to 90% of the plants, and one or two other less frequent values could be found (Table 3). However, in Y1S2, where variability in the main stem N_{leaf} between density treatments was small; there was also little variability between plants within a same treatment.

Regardless of time scale considered, the rate of HS progress varied between density treatments (data not shown) but these differences nearly vanished when plants with the same N_{leaf} were compared (see Fig. 2 using Γ_c). In Y1S2, when the three density treatments resulted in the same, median value for N_{leaf}, HS progressed at the same rate in all treatments (Fig. 2).

Table 3
Total number of leaves formed on a main stem. Data are for winter wheat Cv. 'Soissons' sown Grignon in late September (S1) and mid November (S2) at three densities: D1, D2, D3 in 2007/2008 (Y1) and 2008/2009 (Y2). D1 : 77, D2 : 228, D3 : 514 plants m^{-2}. Numbers in bold represent the most frequent value for each density. Numbers between brackets correspond to the total number of used plants.

			Main stem final leaf number							
Experiment	**Sowing**	**Density**	**8**	**9**	**10**	**11**	**12**	**13**	**14**	**15**
Y1	**S1**	**D1** (7)						0.14	**0.86**	
		D2 (15)						**0.80**	0.20	
		D3 (11)					0.36	**0.64**		
	S2	**D1** (17)			**0.94**	0.06				
		D2 (19)			**0.79**	0.21				
		D3 (20)			**0.95**	0.05				
Y2	**S1**	**D1** (15)						0.20	**0.67**	0.13
		D2 (-)								
		D3 (16)					0.12	**0.88**		
	S2	**D1** (13)			**0.54**	0.38	0.08			
		D2 (18)		0.17	**0.72**	0.11				
		D3 (14)	0.07	**0.79**	0.14					

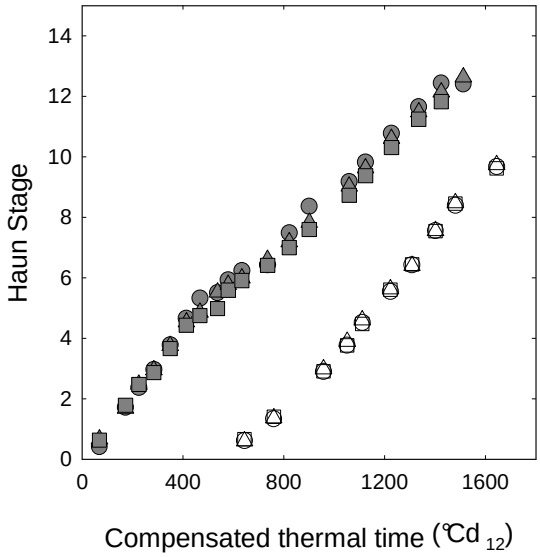

Figure 2. Haun Stage *vs.* compensated thermal time (Γ_c) for main stem of winter wheat Cv. 'Soissons' grown in Grignon in 2007/2008 (Y1) at three densities: D1 (○), D2 (Δ), and D3 (□). Data are median values for plants with 13 final leaves (gray symbols) sown in late September (S1) and for plants with 10 final leaves (open symbols) sown in mid November (S2). D1: 77, D2: 228, D3: 514 plants m^{-2}.

Compensated thermal time provided consistent results of HS progress between sowing treatments and growing seasons

Because, for a given sowing date, the main source of variability for the progress of HS was the N_{leaf}, we analysed the HS progress of main stems separately according to their N_{leaf}, while pooling together density treatments. Analyses were performed in parallel using the four time scales: linear thermal time (Γ), compensated thermal time (Γ_c), linear photothermal time ($^P\Gamma$) and compensated photothermal time ($^P\Gamma_c$).

The plot of HS for the median main stem from each sowing (i.e., main stem with 13 N_{leaf} for S1 and 10 N_{leaf} for S2) diverged between the two growing seasons (cf. supplementary figure S1, p.52) when expressed in Γ and $^P\Gamma_c$ (RMSE respectively 0.64 and 0.58 leaves). Contrariwise, results from the two years were well unified when expressed in Γ_c and $^P\Gamma$ (RMSE respectively 0.28 and 0.26 leaves).

To give an overall impression of the consistency of HS data over sowing treatments and growing seasons, all the data were normalized to a maximum of one and plotted against the different types of time courses (cf. supplementary figure S2, p.53). The normalization of HS data by the final number of leaves allowed to group data per sowing date treatment. However, the dispersion of points varied according to the time scale used. The plot with Γ showed the highest dispersion (RMSE = 3.47 10^{-2}) mainly because of the lower consistency of data between the two years for S2. PΓ allowed to unify data of each sowing to the best (RMSE = 2.34 10^{-2}). However, the use of photothermal time did not result in a calculated phyllochron constant during ontogeny, but rather a progressive decrease in leaf emergence rate. Moreover, the duration of the cycle for the intermediate sowing date was not intermediate between that for the early and late sowing date.

Overall, the compensated thermal time resulted in a good reproducibility between Y1 and Y2, with the intermediate sowing behaving intermediate between the early and late

sowing. It showed a pattern consisting of either one phase (for S_2 and S_{int}, as usually reported for Soissons) or two linear phases (for S_1) similar to that described by Boone (1990) for experiment in constant photoperiod.

Since leaf extension rate in wheat showed a non-linear response to temperature that was well represented by Johnson and Lewin's model (1946) and given the consistency of results obtained when using the compensated thermal time, only results expressed as a function of Γ_c are presented in detail thereafter.

Two phases with two different rates described the HS progress of a wheat tiller

The plot of normalized HS of all the data against Γ_c (Fig. 3) displayed two main groups: the first group consisted of points from the early sowing S1 (typically plants with 12-14 leaves) and showed two phases with two distinct rates; the second group consisted of points from the late and the intermediate sowings (typically plants with 10-12 leaves) that showed a linear trend along the growing season, but the rate of normalized HS progress in S2 was slightly higher than that in S_{int}. However, when HS was plotted against Γ_c separately for each growing season (Fig. 4), two phases were clearly distinguishable for both S1 and S2, and a little less for S_{int}. Phase I displayed a linear trend with a rate of HS progress independent of N_{leaf} for plants of a given sowing date; phase II showed different rates for the progress of HS, depending on N_{leaf}: the higher the N_{leaf}, the faster the rate of HS progress. Between the two phases, there was a marked difference in the rate of HS progress for S1 and S2: this rate decreased in phase II for S1, whereas, it rather increased for S2. Conversely, for S_{int}, there was almost no change in the rate of HS progress.

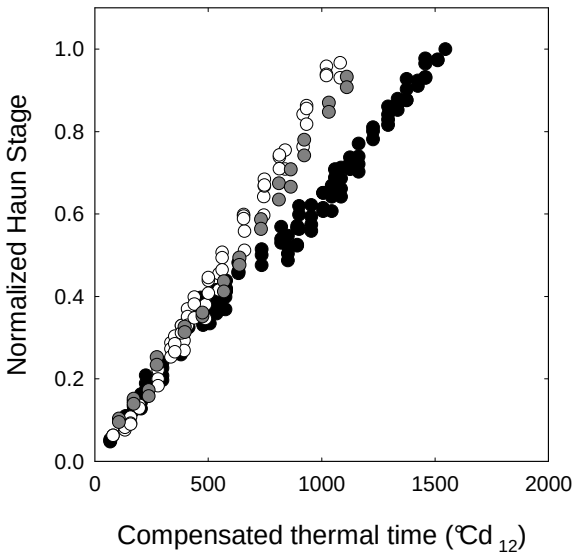

Figure 3. Normalized Haun Stage *vs.* compensated thermal time (Γ_c) for the main stem of winter wheat Cv. 'Soissons' sown in Grignon in late September (S1,●) and in mid November (S2, ○) in 2007/2008 (Y1) and 2008/2009 (Y2) at three densities: D1, D2, D3 and in late October (S_{int}, ●) in 2005/2006 (Y') at density D2. D1: 77, D2: 22, and D3: 514 plants m^{-2}.

A model consisting of two linear phases, with a break point at a developmental stage (HS_{break}) was therefore constructed to reflect the observations. In the case of S1, in which plants had 13 final leaves or more, the HS progress in phase II deviated somewhat from a linear trend, the rate just after HS_{break} being lower than that for the last leaves. We adjusted a

linear model to phase I using leaves up until HS_{break} and a linear model for phase II using only the last five upper leaves on the main stem in order to obtain an accurate estimation of the phyllochron of these leaves (P_{II}^{end}), which is important if we are to compare the development of the plant with the development of fungal diseases. This also allows an accurate estimation of the time of flag leaf ligulation. The proposed model has four parameters (Table 4) and is given by Eq. (7).

$$\left.\begin{aligned} \mathrm{HS}(\Gamma_c) &= \frac{1}{P_{\mathrm{I}}}\Gamma_c, \qquad \text{if } \mathrm{HS} < \mathrm{HS}_{\mathrm{break}} \\ \mathrm{HS}(\Gamma_c) &= \frac{1}{P_{\mathrm{II}}^{\mathrm{end}}}\Gamma_c + b, \text{ if } \mathrm{HS} > N_{\mathrm{leaf}} - 5 \end{aligned}\right\} \tag{7}$$

where Γ_c is the compensated thermal time, P_I the phyllochron in phase I, P_{II}^{end} the phyllochron in phase II, b the offset of the linear model of the last five leaves.

When attempting to estimate simultaneously all parameter values in Eq. (7) from experimental data, the procedure converged only in some of the cases. We therefore estimated firstly the value of HS_{break}, as explained below; then, P_I and P_{II}^{end} were estimated. Finally, the time of flag leaf ligulation, the duration of each phase, and the mean phyllochron in phase II (P_{II}^{mean}) were calculated.

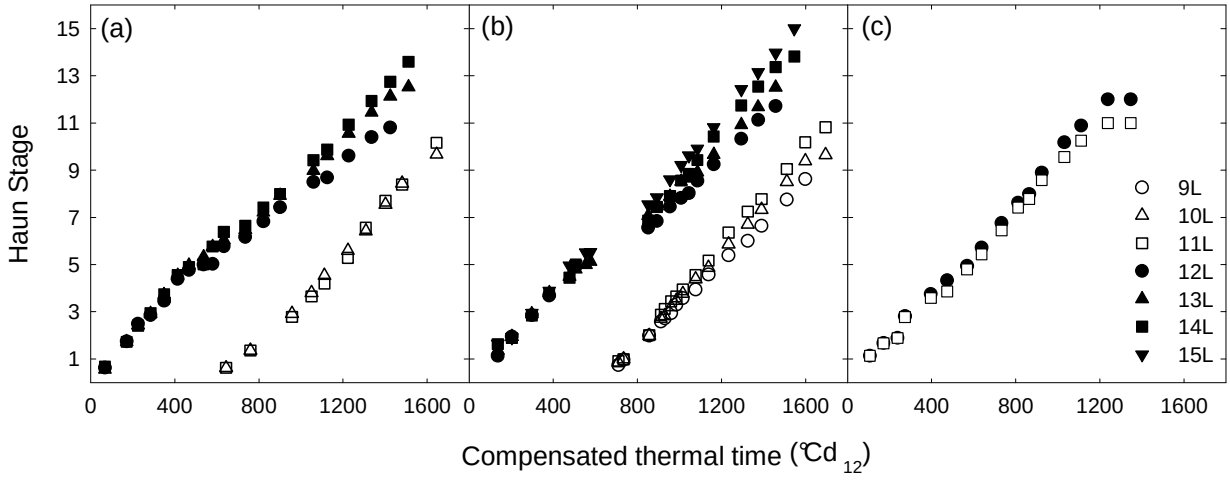

Figure 4. Haun Stage *vs.* compensated thermal time (Γ_c), for main stem of winter wheat Cv. 'Soissons' sown in Grignon in late September (S1, filled symbols) and mid November (S2, open symbols) at three densities: D1, D2, D3 in **(a)** 2007/2008 (Y1), and **(b)** 2008/2009 (Y2) and **(c)** in late October (S_{int}) at density D2 in Y05/06 (Y'). Symbols show the median values calculated for plants with a final leaf number of 9 (○), 10 (Δ), 11(□), 12 (●), 13 (▲), 14 (■), and 15 (▼).D1: 77, D2: 228, D3: 514 plants m^{-2}.

Table 4
Parameter values and RMSE of the adjusted models to HS progress of main stem of winter wheat Cv. 'Soissons' sown in Grignon in late September (S1) and mid November (S2) at three densities: D1, D2, D3 in 2007/2008 (Y1), and 2008/2009 (Y2) and in late October (S_{int}) at density D2 in Y05/06 (Y') at two fertilization regimes: without (0N) and with (N+) fertilization. D1: 77, D2: 228, D3: 514 plants m^{-2}.

Experiment	Sowing	Fertilization	FLN	Number of plants	P_1 (°Cd_{12})	P_{II}^{end} (°Cd_{12})	*b*	Time at flag leaf ligulation (°Cd_{12})	RMSE	
									Parameters fitted on the same year	Parameters fitted on the other year
Y1	S1	N+	12	4	100	147	1.22	1581	0.16	0.28
			13	20	95	117	0.03	1527	0.09	0.29
			14	8	94	109	-0.37	1562	0.08	0.29
	S2	N+	10	50	136	90	-1.80	1062	0.05	0.23
			11	4	134	84	-1.35	1154	0.10	0.91
Y2	S1	N+	12	2	105	113	-1.12	1478	0.08	0.26
			13	17	105	107	-1.10	1513	0.10	0.31
			14	10	104	96	-1.83	1514	0.13	0.32
			15	2	98	94	-1.53	1548	0.13	-
	S2	N+	9	13	134	117	-0.26	1087	0.13	-
			10	23	131	106	-0.22	1087	0.14	0.19
			11	7	128	98	-0.30	1112	0.54	0.47
	S_{int}	0N	11	-	103	107	-0.30	1206	0.14	
			12	-	99	97	-0.65	1226	0.12	
		N+	11	-	107	110	-0.04	1209	0.19	
			12	-	106	94	-1.00	1224	0.18	

According to figure 4, the break point is both the time of the shift in the rate of HS progress and the time when differences in phyllochron exist depending on N_{leaf}. The latter criterion was the most evident when there was a sufficient variability in N_{leaf}. In these cases, plants from the same sowing that presented at least a difference of two in their N_{leaf} (a difference of one was considered for S_{int} because this was the maximum variability) were grouped and, a linear model was fitted to the HS data plotted against Γ_c from seedling emergence and following the progression of sampling dates, one after the other. We considered that HS_{break} was reached when the addition of a new sampling date increased the RMSE of the model above a given threshold (here 0.15). HS_{break} was then calculated as the mean between the value just before the threshold and the value just after. In Y1S2, where nearly all plants had the same N_{leaf} independently of density, HS_{break} could be estimated as a parameter in the model with two linear phases when the fitting procedure converges. The obtained values of HS_{break} were 5, 3.5, and 3 respectively for early, intermediate and late sowings.

The model of HS progress was adjusted separately for each year, sowing date and group of plants with the same N_{leaf}. This procedure provided an accurate adjustment to the experimental data (RMSE values below 0.54 leaves). Besides, the model adjusted on one year estimated accurately the HS progress of the other year (with the exception of one value, RMSE values were below 0.47 leaves). Detailed results are presented in Table 4.

Change in the rate of HS progress coincided with the initiation of the flag leaf

The number of initiated leaf primordia (N_{prim}) on the main stem was monitored during Y2. For all treatments, N_{prim} as a function of Γ_c was described by a model consisting of two linear phases (Eq. (8)), consistent with results reported in previous works (Kirby, 1990).

$$\left.\begin{aligned} N_{prim}(\Gamma_c) &= \frac{1}{P_I'}\Gamma_c + b', && \text{if } \Gamma_c < \Gamma_c' \\ N_{prim}(\Gamma_c) &= \frac{1}{P_{II}'}(\Gamma_c - \Gamma_c') + (\frac{1}{P_I'}\Gamma_c' + b'), && \text{if } \Gamma_c > \Gamma_c' \end{aligned}\right\} \quad (8)$$

where N_{prim} is the number of initiated primordia, P_I' the plastochron during the first phase P_{II}' the plastochron during the second phase, Γ_c' the thermal time of transition between the two phases of plastochron and b' the number of primordia at plant emergence. Adjusted parameter values in the model are given in Table 5.

Table 5
Parameter values and RMSE of the adjusted model to the number of initiated primordia initiation. Data are for main stem of winter wheat Cv. 'Soissons' sown in Grignon in late September (S1) and mid November (S2) at three densities: D1, D2, D3 in 2008/2009 (Y2). D1: 77, D2: 228, D3: 514 plants m^{-2}.

	S1		**S2**		
	D1	**D3**	**D1**	**D2**	**D3**
$\boldsymbol{P'_I}$	67	76	35	34	38
$\boldsymbol{P'_{II}}$	17	15	18	18	24
$\boldsymbol{b'}$	6.5	6.8	0.8	0.5	1.2
$\boldsymbol{\Gamma'_c}$	880	920	400	399	387
RMSE	0.423	0.144	0.545	0.709	0.576

The parameter *b'* should be larger than the number of primordia in the embryo, usually three (Friend et al., 1962). Here, *b'* was estimated around 1 in S2, which reflects a lack of measurements for the early stages of primordia initiation. However the low RMSE (around 0,6 primordia) indicates that the model is appropriate to estimate the number of primordia in the range for which data where collected.

The time of HS_{break} was estimated with Eq. (7) and then the number of primordia initiated at HS_{break} was estimated with Eq. (8). This number was linearly correlated to the mean final leaf number of the main stem (Fig. 5, $R^2 = 0.97$, $^{**}P < 0.01$): independently of sowing date and density, HS_{break} occurred around one plastochron after the flag leaf was initiated.

The value of HS_{break} increased linearly with increasing N_{leaf} (Fig. 5). A linear relation ($R^2 = 0.99$; $^{*}P < 0.05$) was fitted to our dataset completed by data from Boone et al. (1990).

$$HS_{break} = 0.62 \cdot N_{leaf} - 3.2 \qquad (9)$$

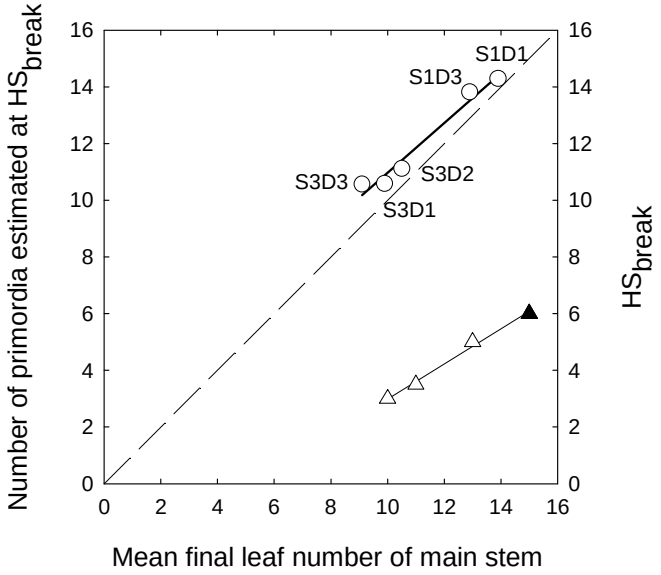

Figure 5. Estimated number of primordia at the time of HS_{break} (○) in 2008/2009 (Y2) and estimated values of HS_{break} (Δ) as a function of the mean final leaf number of main stem. Data are for winter wheat Cv. 'Soissons' sown in Grignon in late September (S1) and mid November (S2) at three densities: D1, D2, D3 in 2007/2008 (Y1), and 2008/2009 (Y2) (▲) corresponds to data from Boone et al. (1991). D1: 77, D2: 228, D3: 514 plants m^{-2}. The dashed 1:1 line is shown.

The duration of the period from HSbreak to the appearance of the flag leaf ligule was independent of Nleaf

The time of flag leaf ligulation was estimated with Eq. (7). Plants sown at a same time but differing in N_{leaf} were nearly synchronous in the date of flag leaf ligulation (Table 4) with a mean increase of only 17 °Cd_{12} per additional main stem leaf. Consistently, the duration of phase II —estimated as the difference between Γ_c when $HS = HS_{break}$ and Γ_c when $HS = N_{leaf}$— was also approximately independent of N_{leaf} (Fig. 6). Yet, this duration varied between sowing dates, being shorter for later sowings (1000-1100 °Cd_{12} for S1, 850 °Cd_{12} for S_{int}, and 650-700°Cd_{12} for S2). For each year and sowing date, values for P_{II}^{mean} were calculated by dividing the estimated duration of phase II by the number of leaves emerged during this phase. P_{II}^{mean} was close to P_{II}^{end} but systematically higher when N_{leaf} was larger than 12, that is to say, in S1 (Fig. 7). As a consequence of the stable duration of phase II for a given sowing date,

P_{II}^{mean} and P_{II}^{end} decreased with increasing N_{leaf}, thus they were generally shorter in low density than in high density treatments.

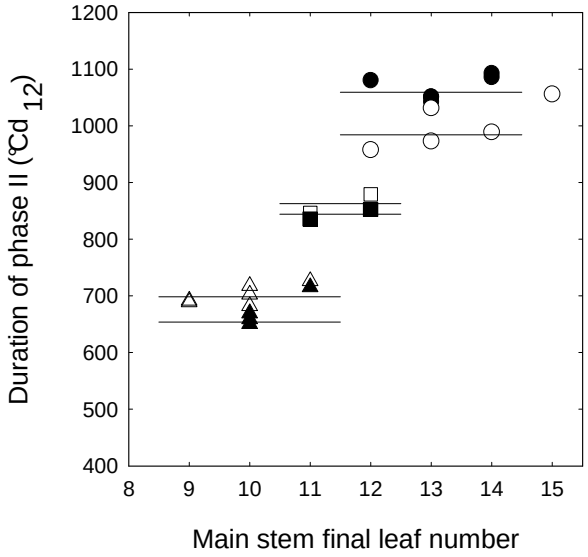

Figure 6. Duration of phase II of Haun Stage progress expressed in compensated thermal time (Γ_c) *vs.* final leaf number of main stem for winter wheat Cv. 'Soissons' sown in Grignon in late September (S1, ○,●) and mid November (S2, ▲,Δ) at three densities: D1, D2, D3 in 2007/2008 (Y1, filled symbols) and 2008/2009 (Y2, empty symbols); and in late October (S_{int}) at density D2 in 2005/2006 (Y') with (■) and without (□) nitrogen fertilization. Horizontal lines correspond to the weighted average of the duration of phase II for each treatment. See text for definition of phase II.

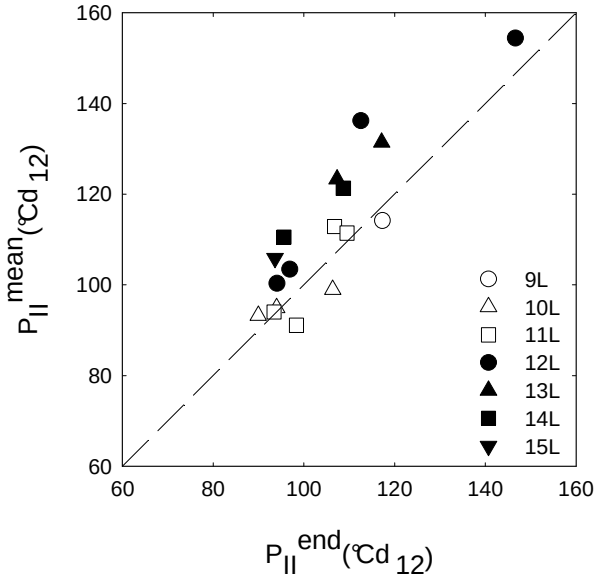

Figure 7. Mean phyllochron of phase II (P_{II}^{mean}) *vs.* phyllochron of the five last leaves (P_{II}^{end}) expressed in compensated thermal time (Γ_c) for the main stem of winter wheat Cv. 'Soissons' sown in Grignon in late September (S1) and mid November (S2) at three densities: D1, D2, D3 in 2007/2008 (Y1) and 2008/2009 (Y2). Data are for plants with a final leaf number of 9 (○), 10 (Δ), 11(□), 12 (●), 13 (▲), 14 (■), and 15 (▼). D1: 77, D2: 228, D3: 514 plants m^{-2}. See text for definition of phase II.

For each phase, the duration of the phase and the phyllochron were correlated to the photoperiod at seedling emergence

The durations of phases I and II (calculated for each year, sowing date, and N_{leaf}) were plotted against the photoperiod at seedling emergence (Fig. 8a). As photoperiod decreased from around 11.5 hours at S1 to 8 hours at S2, the duration of phase I decreased from 530 to 350 °Cd_{12} and that of phase II from 1090 to 650 °Cd_{12}. The duration of phase II was highly correlated to the photoperiod at seedling emergence (R^2 = 0.96, $^{**}P < 0.01$), whereas the

correlation was lower for the duration of phase I ($R^2 = 0.61$, $^{**}P < 0.01$). This may be because the relationship with photoperiod is not linear for this phase; alternatively, the reason may be that the terms of calculation of HS_{break}—at least a 2-leaf difference— were not met in the case of the growing season Y' for which there was a low variability in N_{leaf}. The linear models adjusted to the relationship between durations of each phase and the photoperiods are:

$$\Delta_I = 34.38\ PP - 98.72, \quad (10a)$$

$$\Delta_{II} = 120.26\ PP - 309.23, \quad (10b)$$

where Δ_I and Δ_{II} are the durations of phase I and II, and PP the photoperiod at seedling emergence expressed in hours.

To characterize the behaviour at the crop level, the phyllochron in each phase was calculated as the weighted average of P_I and of P_{II}^{mean} of plants of different N_{leaf}. P_I and P_{II}^{mean} were linearly correlated to the photoperiod at seedling emergence (Fig. 8b; $R^2 = 0.89$, $^{*}P < 0.05$ and $R^2 = 0.86$, $^{*}P < 0.05$ respectively for P_I and P_{II}^{mean}). P_I decreased and P_{II}^{mean} increased when the photoperiod increased.

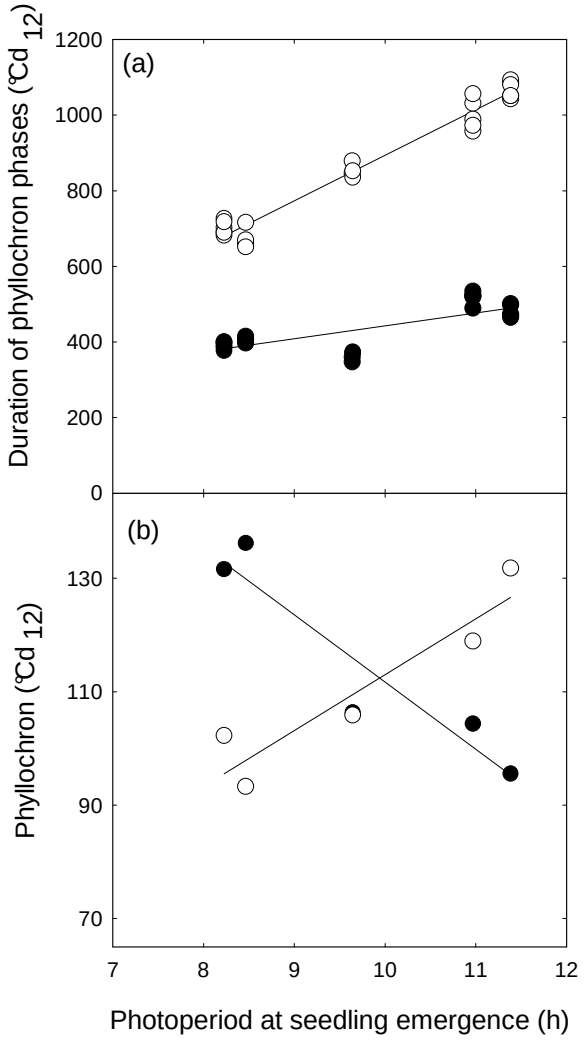

Figure 8. (a) Durations and **(b)** mean phyllochrons (P_I and P_{II}^{mean}) expressed in compensated thermal time (Γ_c) during phase I (●) and phase II (○) plotted against the photoperiod at seedling emergence. Data are for the main stem of winter wheat Cv. 'Soissons' sown in Grignon in late September (S1) and mid November (S2) at three densities: D1, D2, D3 in 2007/2008 (Y1) and 2008/2009 (Y2) and in late October (S_{int}) in 2005/2006 (Y') at density D2. D1: 77, D2: 228, D3: 514 plants m^{-2}. See text for definition of phase I and phase II.

.

The progress of HS in primary tillers showed a similar trend to that of the main stem

When plotted against Γ_c, the HS progress of the primary tillers T_1 to T_5 showed the same pattern as T_0 i.e., their phyllochron was described by a two-linear phase model: rate in phase I being the same independently of plant-to-plant variability in N_{leaf} and rate in phase II showing differences according to N_{leaf} (Fig. 9). Phase I was shorter for T_2 than for T_1 and could not be identified for the following tillers. We did not attempt to numerically estimate HS_{break} of T_1 and T_2 in each treatment, but visual inspection of the graphs showed that it always occurred for the primary tillers almost at the same time as for T_0, and thus likely both denotes the same change, occurring at the whole plant scale.

Similarly to T_0, the date of flag leaf ligulation was synchronous for a given tiller rank independently of its N_{leaf} (data not shown). Moreover, the duration between seedling emergence and flag leaf ligulation was linearly correlated to the tiller rank for S1 ($R^2 = 0.81$, $*P < 0.05$) and S2 ($R^2 = 0.62$, $P < 0.1$) (Fig. 10). This is expressed in equation (11):

$$\Gamma_{lig}(k) = \Gamma_{lig}(0) + \alpha k \qquad (11)$$

where k is the tiller rank, $\Gamma_{lig}(k)$ is the compensated thermal time at flag leaf ligulation for the tiller of rank k, $\Gamma_{lig}(0)$ being for T_0, and α the difference in Γ_{lig} between successive tillers. Estimated values for α were respectively 21.4 and 17.7 °Cd12 for S1 and S2.

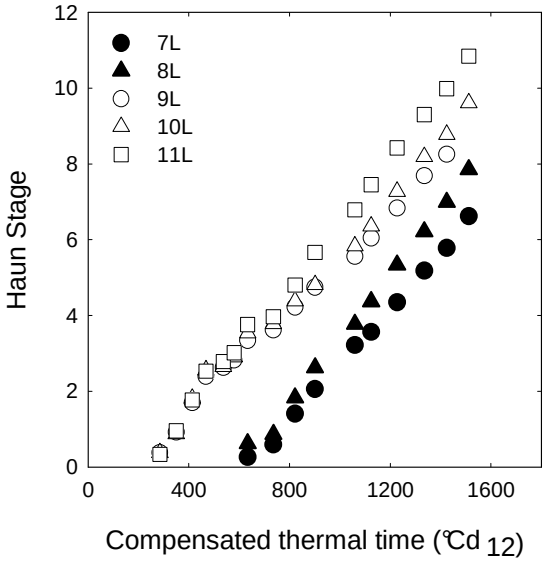

Figure 9. Haun Stage *vs.* compensated thermal time (Γ_c), for tillers T_1 (open symbols) and T_4 (filled symbols) of winter wheat Cv. 'Soissons' sown in late September (S1) at three densities: D1, D2, D3 in 2007/2008 (Y1). Symbols show the median values calculated for tillers with a final leaf number of 7 (●), 8 (▲), 9 (○), 10 (Δ), and 11 (□). D1: 77, D2: 228, D3: 514 plants m^{-2}.

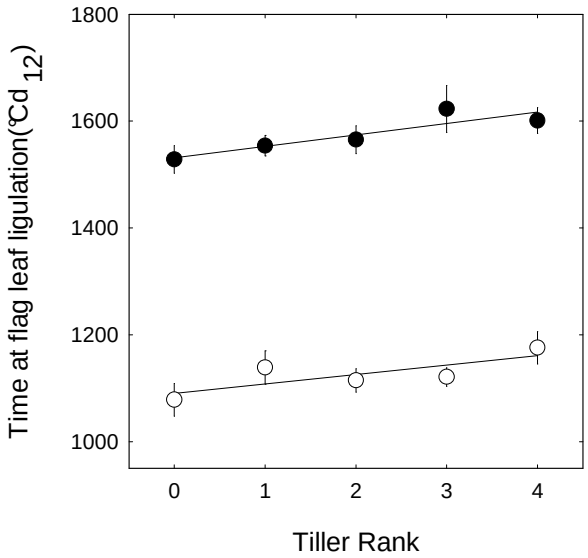

Figure 10. Compensated thermal time (Γ_c) at flag leaf ligulation *vs.* tiller rank (k) for winter wheat Cv. 'Soissons' sown in late September (S1, ●) and mid November (S2, ○) in Grignon at three densities: D1, D2, D3. Data correspond to weighted average values of two years: 2007/2008 (Y1) and 2008/2009 (Y2). D1: 77, D2: 228, D3: 514 plants m^{-2}. Error bars mark the 95% confidence intervals. Solid lines correspond to linear regressions for:

S1: $Y=1531 + 21.42.k$, $R^2=0.81$ and for

S2: $Y= 1090 + 17.67.k$, $R^2=0.62$.

Discussion

When expressed in Γc, results were consistent between sowing dates and contrasted climate conditions

The contrasted densities and sowing dates tested in our study resulted in negligible differences in soil temperatures before stem extension for Y1 and Y2; therefore, soil temperature could have been monitored for only one treatment. Moreover, the differences between cumulated soil temperature and cumulated air temperature remained quite small, consistently with previous results (Gallagher, 1979, Ljutovac, 2002). This suggests that using soil surface temperature to calculate thermal time before stem extension, under north-western European conditions, is not enough to explain differences in phyllochron between sowing dates as put forward by Jamieson et al. (1995). Besides, in our study phyllochron variability between sowings was found even when plant temperature (soil then air temperature) was used to compute thermal time. This is not to say that the small differences between soil and air temperatures should be ignored, especially since it is quite simple to estimate soil temperature either by direct measurements or by estimation with models (Cellier et al., 1993, Guilioni et al., 2000).

Masle et al. (1989) reported that including photoperiod in the calculation of thermal time (i.e., using linear photothermal time) allowed removing the variations in the rate of leaf appearance between sowing dates. However this was not the case in our experiments.

Here, the non-linear function proposed by Johnson and Lewin (1946) to describe the response of growth and development processes to temperature was adjusted to leaf extension rates of winter wheat from the data of Kemp and Blacklow (1982) and yielded a good fitting (RMSE = 0.047). This generalizes the results of Parent (2009) on maize and *Arabidopsis* and brings added proof, given the wide range of temperatures provided by Kemp and Blacklow (1982). Differences between linear (Γ and PΓ) and non-linear (Γ_c and ${}^{P}\Gamma_c$) responses to temperature were exhibited when plants experienced cold temperatures (i.e., $T_p \leq 0$). This was particularly true for Y2S2 treatment where there was a cold winter episode at the first stages of wheat development. Thus, we observed a higher divergence between linear and non-linear responses to temperature (18% at flowering) and a higher inconsistency between years for S2 when we used linear thermal time (RMSE=5.06 10-2). Using the non-linear photothermal time did not bring further improve of the rate of HS progress and it displayed the same discrepancies as the linear photothermal time concerning the order of sowings. Consequently, in our study, the non-linear response proved to be the most conclusive time course that made it possible to homogenize results within and between sowings and between contrasted climate conditions.

Xue et al. (2004) compared three leaf-appearance predicting models. Their findings showed that the model based on a beta response function to temperature accurately predicted leaf appearance rate (RMSE = 0.42 to 0.82 leaf) in comparison to two other models based on linear response function (RMSE = 0.42 to 1.24). Therefore, taking into account non-linear responses better reflects the behaviour of phyllochron under our conditions. This should have an importance for crop models and prediction of developmental stages.

The progress of Haun Stage was described by two phases

For all sowing dates investigated here, the HS progress expressed in Γ_c reflected a pattern involving two phases. During phase I, the HS progress was linear, with a rate independent of N_{leaf}. During phase II, the rate varied according to N_{leaf}: it was slower for lower N_{leaf}, and there was some departure from linearity for plants with $N_{leaf} \geq 13$ i.e., for early sowings. A change in the rate of leaf emergence has been reported for wheat: most often a

decrease (Cao and Moss, 1991, Calderini et al., 1996, Miralles et al., 2001, Slafer and Rawson, 1997, Miralles and Richards, 2000, Baker et al., 1986, Boone et al., 1990, Hay and Delecolle, 1989) and less frequently an increase (Cao and Moss, 1991); and also for dicotyledons (Villalobos and Ritchie, 1992). However, from some of our data (i.e., S_{int}) an from many reports in the literature (Kirby et al., 1982, Baker et al., 1980, Masle-Meynard and Sebillotte, 1981), this departure from linearity is not systematic and a linear constant phyllochron could be found.

The moment of shift in the rate of Haun Stage progress was related to the moment of flag leaf initiation

In our study, the time of the shift in phyllochron did not occur at the same developmental stage for all sowing dates but, it coincided with the time of flag leaf initiation. Changes in rate of leaf appearance in wheat have been previously related to change in ontogeny, more precisely to time of double ridge formation (Baker et al., 1986, Cao and Moss, 1991), and thus later than estimated here. However, our results are consistent with Boone et al. (1990) who situated the timing of shift in phyllochron at single ridge formation, that is precisely the moment of completion of the flag leaf primordium and the beginning of formation of the first spikelet (Klepper et al., 1983). In addition, HS_{break} was linearly correlated to N_{leaf}. Linear relationships between the number of leaves visible at floral initiation and the final number of leaves were reported for maize (Tollenaar and Hunter, 1983), clover and winter cereals (Aitken, 1971), wheat (Kirby, 1990) and sunflower (Sadras and Villalobos, 1993). Boone et al. (1990) found that the timing of the shift in phyllochron for eight treatments was exactly parallel to the timing of the identifiable reproductive stages (double ridge, heading, and anthesis), further proof that it is linked to plant ontogeny. Cao and Moss (1991) supported the concept that there are at least two periods when phyllochron is sensitive to the environment, one at seedling emergence and another at the time of double ridge formation, the second being responsible for the shift in phyllochron, but it seems that the second period of sensitivity does not always occur. Contrariwise, Slafer and Rawson (1997) proposed that the changes in rate of leaf appearance, observed under natural conditions, could be reflecting a response to photoperiod or vernalization rather than a change due to ontogeny.

The positioning of HS_{break} one plastochron after the flag leaf initiation, and coinciding with the initiation of the first spikelet, backs the idea that the fate of the primordium that will become the flag leaf —and that of the primordium which will become the first spikelet—are determined as soon as they are initiated although at that moment, neither the morphology of the apex and the primordium, nor the rate of primordium initiation make it possible to identify these distinct fates. Indeed, it has often been proposed that the fate between leaf and spikelet primordia is not determined until many plastochrons after the primordium of the future flag leaf have been initiated (Brooking et al., 1995). The lower spikelet primordia would therefore result from a conversion of leaf primordia into reproductive organs. However, the occurrence of HS_{break} at this moment backs the hypothesis of a much earlier differentiation. A study in which wheat plants were reciprocally transferred between 12 and 18h photoperiod regimes at several occasions between seedling emergence and terminal spikelet appearance (Slafer and Rawson, 1995) showed that plants produced significantly different final leaf number only when they were transferred before 25 days after seedling emergence (which according to the authors probably coincides with floral initiation). Later, final leaf number was entirely insensitive to photoperiod, meaning that this number was determined earlier.

Both the values of phyllochron of each phase and their corresponding durations varied linearly with photoperiod at seedling emergence

In our study, the phyllochron in both observed phases depended on the photoperiod at seedling emergence and trends in it were distinctly different between the two phases (increasing in phase I and decreasing in phase II) (Fig. 8b), thus changes in phyllochron of each phase according to sowing date would be significantly higher than that of the "mean phyllochron" calculated for the whole growing cycle. For instance phyllochron during stem extension decreased from 110-120 °Cd_{12} in S1 to 80-90 °Cd_{12} in S2. This is important because phyllochron during stem elongation is related both to LAI establishment and to its vertical development and the range of variation found here is highly significant in disease escape (Robert et al., 2008) and crop weed competition. Another implication of the opposite behaviour of the phyllochron in both phases is that, the values differ for either early or late sowing, whereas for usual sowing dates, the phyllochron is very similar in both phases, so that the two phases can hardly be distinguished. In this work, we analyzed the change in phyllochron in relation to photoperiod at seedling emergence. This does not imply that seedling emergence is exactly the time when a value for the phyllochron of both phases is determined. Kirby et al. (1985) testing a wide range of varieties and sowing dates, proposed that the rate of leaf emergence is correlated to the rate of change of photoperiod at the time of plant emergence, rather than to the absolute value of the photoperiod.

The durations of the two phases of phyllochron increased linearly with increasing photoperiod at seedling emergence. Experiments with controlled variation of the photoperiod have demonstrated a historic effect of photoperiod during early plant development on the duration of later stages (Slafer and Rawson, 1994, Slafer and Rawson, 1995, Miralles and Richards, 2000). However, in our case, correlation under field conditions did not permit us to make such an analysis. Taking into account seedling emergence was sufficient to obtain a good fit of linear models for phyllochron-photoperiod relationships.

During phase II, phyllochron varied according to final leaf number for a wheat tiller

The phyllochron of phase II and the mean phyllochron increased (i.e., the rate of leaf emergence decreased) with increasing densities. A similar result was observed on barley (Kirby and Faris, 1972) whereas Masle et al. (1989) reported no density effect on wheat over a range of densities. Plant population density affects the rate of leaf appearance mainly through two mechanisms: changes of light intensity and light signals. First, high density results in a severely reduced photosynthetically active radiation (PAR) (Evers et al., 2006) which is associated to long phyllochron (Bos and Neuteboom, 1998). Second, increase in density is associated with a low red: far-red ratio (R:FR) (Evers et al., 2006) caused by a selective absorption of red and reflection of far-red by green leaves (Casal and Smith, 1989, Davis and Simmons, 1994). Decline in R:FR has been shown to act as an early signal for plant to avoid competition (Ballaré and Casal, 2000). In response to this signal, plants adapt their morphology, it is the "shade avoidance syndrome", including by changing their rate of development (Smith and Whitelam, 1997).

We also observed a decrease in the mean N_{leaf} with increasing densities. Although most plants of a given density treatment had a similar leaf number, there were almost always a few plants with one more or one less leaf (Brooking et al., 1995). Interestingly, when there was no difference of N_{leaf} between density treatments (Y1S2), we did not observe any density effect on the phyllochron. Besides, when we considered plants from different density treatments that produced the same N_{leaf}, we noticed that the phyllochron was almost the same. On the contrary, plants of the same density with increased N_{leaf} had lower phyllochron. These results demonstrate that the phyllochron of the second phase is correlated to N_{leaf}. A similar

trend of phyllochron change with final leaf number was observed on rice (Jaffuel and Dauzat, 2005). To explain this dependency relationship, one could speculate that variations of light quantity and quality in relation to local variations of density are responsible for the observed variation of N_{leaf} and thus of phyllochron.

As the date of flag leaf ligulation was the same, independently of the number of leaves formed, the phyllochron of phase II was systematically shorter when the final leaf number was higher (Fig. 7). Thus, the stable date of flag leaf ligulation and the variation in N_{leaf} due to density might be the key variables of the process by which phyllochron of phase II is determined.

Our results support the approach of using a non-linear response to temperature to improve the description of the wheat behaviour in winter. They bring some light on the conflicting finding about stability against ontogenic changes in wheat phyllochron, as both behaviours could be observed in our experiment, for a same variety depending on the sowing date. They also clarify the variability in phyllochron between plants or between axes.

Acknowledgments

This work was funded by INRA, Department of Environnement et Agronomie and by ARVALIS, Institut du végétal. Crops were grown by the Unité Expérimentale of INRA, Versailles-Grignon. The authors gratefully acknowledge Emmanuel Fovart, Fabrice Duhamel and Maxime Marques for their excellent technical assistance. They thank S. Tanis-Plant for thorough editorial advice in English.

Supplementary figures

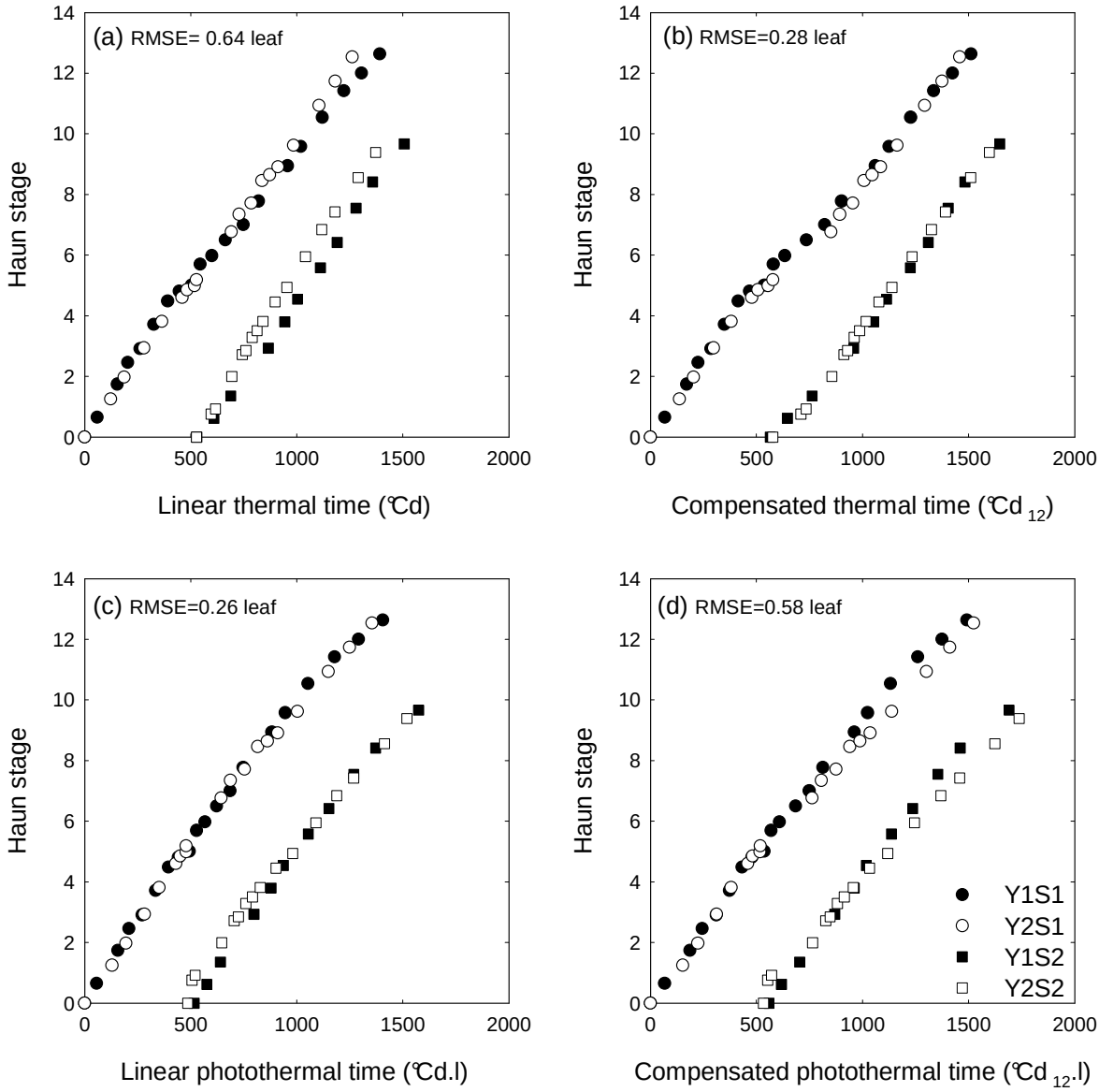

Figure S1. Haun Stage of main stems with the median final leaf number from plants sown in late September (S1, ●,○) and mid November (S2, □,■) at three densities: D1, D2, D3 in 2007/2008 (Y1, filled symbols) and 2008/2009 (Y2, empty symbols) *vs.* **(a)** linear thermal time (Γ), **(b)** compensated thermal time (Γ_c), **(c)** linear photothermal time ($^P\Gamma$), and **(d)** compensated photothermal time ($^P\Gamma_c$). Data are for main stems of winter wheat Cv. 'Soissons' with the most frequent final leaf number (13 for S1 and 10 for S2). D1: 77, D2: 228, D3: 514 plants m^{-2}.

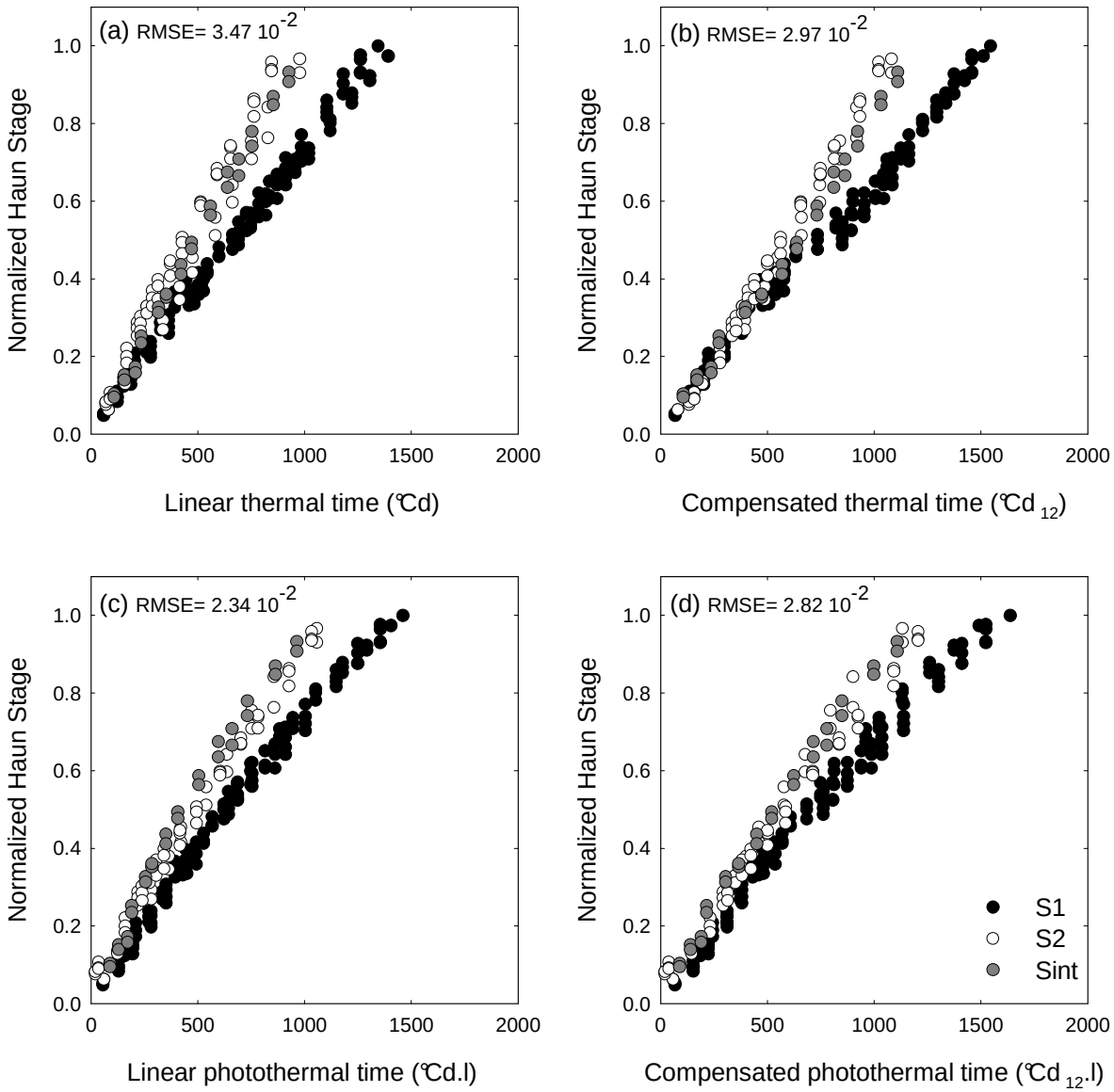

Figure S2. Normalized Haun Stage for the main stem of winter wheat Cv. 'Soissons' sown in Grignon in late September (S1, ●) and in mid November (S2,○) in 2007/2008 (Y1) and 2008/2009 (Y2) at three densities: D1, D2, D3 and in late October (S_{int}, ●) in 2005/2006 (Y') at density D2. Data are plotted against **(a)** linear thermal time (Γ), **(b)** compensated thermal time (Γ_c), **(c)** linear photothermal time ($^P\Gamma$), and **(d)** compensated photothermal time ($^P\Gamma_c$). D1: 77, D2: 228, D3: 514 plants m^{-2}.

References

Aitken Y. 1971. Non-destructive methods for estimation of flower initiation in subterranean clover and cereals. *J. Aust. Inst. Agric. Sci.,* **37**: 57-60.

Baker CK, Gallagher JN, Monteith JL. 1980. Daylength change and leaf appearance in winter wheat. *Plant, Cell and Environment,* **3**: 285-287.

Baker JT, Pinter PJ, Jr., Reginato RJ, Kanemasu ET. 1986. Effects of temperature on leaf appearance in spring and winter wheat cultivars. *Agronomy Journal,* **78**: 605-613.

Ballaré CL, Casal JJ. 2000. Light signals perceived by crop and weed plants. *Field Crops Research,* **67**: 149-160.

Boone MYL, Rickman RW, Whisler FD. 1990. Leaf appearance rates of two winter wheat cultivars under high carbon dioxide conditions. *Agronomy Journal,* **82**: 718-724.

Bos HJ, Neuteboom JH. 1998. Morphological analysis of leaf and tiller number dynamics of wheat (Triticum aestivum L.): responses to temperature and light intensity. *Annals of Botany,* **81**: 131-139.

Brooking IR, Jamieson PD, Porter JR. 1995. The influence of daylength on final leaf number in spring wheat. *Field Crops Research,* **41**: 155-165.

Brooking IR, McPherson HG. 1989. Sweet corn as a processing crop in the Manawatu. *Proceeding of Agronomy Society* New Zeland.

Calderini DF, Miralles DJ, Sadras VO. 1996. Appearance and growth of individual leaves as affected by semidwarfism in isogenic lines of wheat. *Annals of Botany,* **77**: 583-589.

Cao WX, Moss DN. 1989a. Temperature and daylength interaction on phyllochron in wheat and barley. *Crop Science,* **29**: 1046-1048.

Cao WX, Moss DN. 1989b. Temperature effect on leaf emergence and phyllochron in wheat and barley. *Crop Science,* **29**: 1018-1021.

Cao WX, Moss DN. 1991. Phyllochron change in winter wheat with planting date and environmental changes. *Agronomy Journal,* **83**: 396-401.

Cao WX, Moss DN. 1994. Sensitivity of winter wheat phyllochron to environmental changes. *Agronomy Journal,* **86**: 63-66.

Casal JJ, Smith H. 1989. The function, action, and adaptive significance of phytochrome in light-grown plants. *Plant, Cell and Environment,* **12**: 855-862.

Cellier P, Ruget F, Chartier M, Bonhomme R. 1993. Estimating the temperature of a maize apex during early growth stages. *Agricultural and Forest Meteorology,* **63**: 35-54.

Davis MH, Simmons SR. 1994. Tillering response of barley to shifts in light quality caused by neighbouring plants. *Crop Science,* **34**: 1604-1610.

Drouet J-L, Pages L. 2003. GRAAL: a model of GRowth, Architecture and carbon ALlocation during the vegetative phase of the whole maize plant: Model description and parameterisation. *Ecological Modelling,* **165**: 147-173.

Evers JB, Vos J, Andrieu B, Struik PC. 2006. Cessation of tillering in spring wheat in relation to light interception and red:far-red ratio. *Annals of Botany,* **97**: 649-658.

Fournier C, Andrieu B. 1998. A 3D architectural and process-based model of maize development. *Annals of Botany,* **81**: 233-250.

Fournier C, Andrieu B. 1999. ADEL-maize: an L-system based model for the integration of growth processes from the organ to the canopy. Application to regulation of morphogenesis by light availability. *Agronomie,* **19**: 313-327.

Fournier C, Andrieu B, Ljutovac S, Saint-Jean S. 2003. ADEL-wheat: A 3D architectural model of wheat development. In: Hu B-G, Jaeger M eds. *Proceedings of International Symposium of Plant Growth Modeling and Applications.* Beijing, China. 2003 Tsinghua University Press - Springer Verlag.

Gallagher JN. 1979. Field studies of cereal leaf growth. I. Initiation and expansion in relation to temperature and ontogeny. *Journal of Experimental Botany,* **30**: 625-636.

Georgin P, Gouet M. 2000. *Statistiques avec Excel 2000,* Paris, Eyrolles.

Guilioni L, Cellier P, Ruget F, Nicoullaud B, Bonhomme R. 2000. A model to estimate the temperature of a maize apex from meteorological data. *Agricultural and Forest Meteorology,* **100**: 213-230.

Hay RKM, Delecolle R. 1989. The setting of rates of development of wheat plants at crop emergence: influence of the environment on rates of leaf appearance. *Annals of Applied Biology,* **115**: 333-341.

Jaffuel S, Dauzat J. 2005. Synchronism of leaf and tiller emergence relative to position and to main stem development stage in a rice cultivar. *Annals of Botany,* **95**: 401-412.

Jamieson PD, Brooking IR, Porter JR, Wilson DR. 1995. Prediction of leaf appearance in wheat: a question of temperature. *Field Crops Research,* **41**: 35-44.

Jamieson PD, Semenov MA, Brooking IR, Francis GS. 1998. SIRIUS: a mechanistic model of wheat response to environmental variation. *European Journal of Agronomy,* **8**: 161-179.

Johnson FH, Lewin I. 1946. The growth rate of *E.coli* in relation to temperature, quinine, and coenzyme. *Journal of Cellular and Comparative Physiology,* **28**: 239 - 251.

Kemp DR, Blacklow WM. 1982. The responsiveness to temperature of the extension rates of leaves of wheat growing in the field under different levels of nitrogen fertilizer. *Journal of Experimental Botany,* **33**: 29-36.

Kiniry JR. 1991. Maize phasic development. In: Hanks RJ, Ritchie JT eds. *Modelling Plant and Soil Systems.* American Society of Agronomy, Madison (USA).

Kirby EJM. 1990. Co-ordination of leaf emergence and leaf and spikelet primordium initiation in wheat. *Field Crops Research,* **25**: 253-264.

Kirby EJM, Appleyard M, Fellowes G. 1982. Effect of sowing date on the temperature response of leaf emergence and leaf size in barley. *Plant Cell and Environment,* **5**: 477-484.

Kirby EJM, Appleyard M, Fellowes G. 1985. Effect of sowing date and variety on main shoot leaf emergence and number of leaves of barley and wheat. *Agronomie,* **5**: 117-125.

Kirby EJM, Faris DG. 1972. The effect of plant density on tiller growth and morphology in barley. *Journal of Agricultural Science, Cambridge,* **78**: 281-288.

Kirby EJM, Perry MW. 1987. Leaf emergence rates of wheat in a mediterranean environment. *Australian Journal of Agricultural Research,* **38**: 455-464.

Klepper B, Tucker TW, Dunbar BD. 1983. A numerical index to assess early inflorescence development in wheat. *Crop Science,* **23**: 206-208.

Ljutovac S. 2002. *Coordination dans l'extension des organes aériens et conséquences pour les relations entre les dimensions finales des organes chez le blé,* PhD thesis, Institut National Agronomique Paris-Grignon, Paris, France.

Masle-Meynard J, Sebillotte M. 1981. Study of the heterogeneity of a winter wheat stand. II. Origin of the different sorts of individuals in the stand; factors allowing description of its structure. *Agronomie,* **1**: 217-223.

Masle J, Doussinault G, Farquhar GD, Sun B. 1989. Foliar stage in wheat correlates better to photothermal time than to thermal time. *Plant Cell and Environment,* **12**: 235-247.

Miralles DJ, Ferro BC, Slafer GA. 2001. Developmental responses to sowing date in wheat, barley and rapeseed. *Field Crops Research,* **71**: 211-223.

Miralles DJ, Richards RA. 2000. Responses of leaf and tiller emergence and primordium initiation in wheat and barley to interchanged photoperiod. *Annals of Botany,* **85**: 655-663.

Parent B. 2009. *Leaf development in rice and maize: framework of analysis, compared responses to temperature and growth regulation under water deficit.*, PhD degree, Montpellier Supagro, Montpellier, France.

Ritchie JY, NeSmith DS. 1991. Temperature and crop development. In: Ritchie JHaJT ed. *Modelling Plant and Soil Systems.* Madison (USA), American Society of Agronomy.

Robert C, Fournier C, Andrieu B, Ney B. 2007. Coupling 3D virtual plant and foliar epidemic models: a new modelling approach to investigate plant-pathogen interactions linked to architecture. *5th international workshop on functional structural plant modelling.* Napier, New Zealand.

Robert C, Fournier C, Andrieu B, Ney B. 2008. Coupling a 3D virtual wheat (Triticum aestivum) plant model with a Septoria tritici epidemic model (Septo3D): a new approach to investigate plant-pathogen interactions linked to canopy architecture. *Functional Plant Biology,* **35**: 997-1013.

Sadras VO, Villalobos FJ. 1993. Foliar initiation, leaf initiation and leaf appearance in sunflower. *Field Crops Research,* **33**: 449-457.

Slafer GA, Rawson HM. 1994. Does temperature affect final numbers of primordia in wheat? *Field Crops Research,* **39**: 111-117.

Slafer GA, Rawson HM. 1995. Development in wheat as affected by timing and length of exposure to long photoperiod. *Journal of Experimental Botany,* **46**: 1877-1886.

Slafer GA, Rawson HM. 1997. Phyllochron in wheat as affected by photoperiod under two temperature regimes. *Australian Journal of Plant Physiology,* **24**: 151-158.

Smith H, Whitelam GC. 1997. The shade avoidance syndrome: multiple responses mediated by multiple phytochromes. *Plant Cell and Environment,* **20**: 840-844.

Tollenaar M, Hunter RB. 1983. A photoperiod and temperature sensitive period for leaf number of maize. *Crop Science,* **23**: 457-460.

Villalobos FJ, Ritchie JT. 1992. The effect of temperature on leaf emergence rates of sunflower genotypes. *Field Crops Research,* **29**: 37-46.

Wilhelm WW, McMaster GS. 1995. Importance of the phyllochron in studying development and growth in grasses. *Crop Science,* **35**: 1-3.

Xue QW, Weiss A, Baenziger PS. 2004. Predicting leaf appearance in field-grown winter wheat: evaluating linear and non-linear models. *Ecological Modelling,* **175**: 261-270.

Chapter 2

Plasticity of winter wheat architecture modulated by sowing date and plant population density

Abstract

Plants respond to their environment by adapting their growth and development. In cereals, modulation of the rate of organ extension, number of shoots, number and size of organs and time of phase change in response to environmental factors reflects the high degree of adaptability of plants. The underlying mechanisms involved in these adaptive responses are complex and interconnected and not fully understood. Consequently, no mechanistic models are able to describe cereal plasticity. Up to now, architectural plant models are largely descriptive and parameters need to be estimated for each species, cultivar and environment. Hence investigating morphological patterns and their modulation as a response to environmental conditions may help to complement current knowledge. In this chapter we describe the plasticity of winter wheat at the plant scale– expressed as the organ dimensions of main stem and axillary tillers in relation to their position on a stem– and at the canopy scale– expressed as number of tillers per square meter, leaf area index and soil cover– for contrasted sowing dates and plant population densities under the climatic conditions of the Paris region.

Winter wheat Cv. 'Soissons' was grown for two growing seasons at two sowing dates (early and late) and three contrasted plant population densities (low, intermediate and high). The final number of leaves (N_{leaf}) of an axis varied between and within treatments: it was higher for lower density and early sowing. Moreover, 1 to 3 values of N_{leaf} could be found for a given axis within the same treatment. Patterns of blade, sheath and internode dimensions resembled to those usually found for winter wheat but varied between treatments. There was almost no difference in blade and sheath dimensions of juvenile phytomers –growing before the onset of stem elongation– between density treatments, but the low plant population density yielded longer adult leaf blades and sheaths during the adult phase (i.e., emerged during stem elongation). Besides, low plant population density resulted in higher number of tillers/plant but in lower rates of progress in leaf area index (LAI) and ground cover and finally less shoots/m². Earlier sowing led to an increase in the number of juvenile phytomers on the main stem, whereas the number of adult phytomers was almost identical; blade and sheath dimensions of adult phytomers were almost identical between the two sowings. Number of shoots/m² and rates of progress of LAI and ground cover were higher in the early sowing. Further there were little differences in the size of leaf blades, sheaths and internodes between the main stem and axillary tillers. Plants with higher main stem final leaf number produced blades, sheaths and internodes of adult phytomers with higher dimensions. Data presented here can be used to enlarge the understanding of wheat plasticity regarding the regulation of organ size and dynamic development of the wheat canopy and to simulate 3D wheat plant and canopy.

Key words: plasticity, wheat (Triticum aestivum L.), sowing date, plant population density, plant architecture, organ dimensions

Introduction

Plasticity of plant architecture is a major way by which plants respond to their environment. Such responses concern growth and development through regulation of tillering, leaf and stem extension, timing of phase change and modulation of the number of phytomers. These effects are mediated by the changes in environmental conditions that plant organs perceive. Agronomic practices such as date and density of sowing create interactions between different levels of environmental factors leading to various environments and thus to various responses of plant architecture.

On the one hand, many experimental and modelling studies have focused on the plastic response of cereals to sowing date and density regarding number of final leaves and rate of leaf appearance (Kirby et al., 1982, 1985), number of shoots per plant (Darwinkel, 1978, Spink et al., 2000, Lafarge et al., 2002) and phytomer dimensions (mainly blades, sheaths and internodes) (Hotsonyame and Hunt, 1997, Evers et al., 2005). Amongst these studies, many have investigated variations of organ dimensions according to phytomer position along the main shoot (Pararajasingham and Hunt, 1996, Hotsonyame and Hunt, 1997, Fournier et al., 2003) and in some cases attempted to describe organ profiles using simple descriptive functions e.g., the Lorentz peak distribution function to describe blade length profile in function of phytomer rank (Evers et al., 2005, Buck-Sorlin, 2002) or the model of Prévot et al. (1991) to describe leaf curvature (Fournier et al., 2003, Evers et al., 2005). Nevertheless, so far, only few studies have investigated the plasticity of organ dimensions on all tillers (Dornbusch et al. (2010a), Evers et al. (2005), Fournier et al. (2003) for wheat; Tivet et al. (2001); Jaffuel and Dauzat (2005) for rice; Lafarge and Hammer (2002) for sorghum). Dornbusch et al. (2010), Evers et al. (2005), Fournier et al. (2003) and Tivet et al. (2001) compared phytomer dimensions between main stem and axillary tillers using the concept of phytomer shift (Fournier et al., 2003) or summed leaf position (Bos and Neuteboom, 1998).

On the other hand, many authors tried to understand and quantify the underlying plant responses of development to environmental variables. Changes of leaf size with leaf position in cereals have been generally explained in terms of ontogeny (Abbe et al., 1941, Borrill, 1959). Abbe et al. (1941) proposed that the increase in relative width of the successive maize leaves is directly linked to the increasing size of the shoot apex. Borill (1959) suggested that the decline in leaf length for wheat from a given leaf position is linked to the time of formation of double ridge.

However, although ontogeny plays a role in leaf size, environmental factors strongly modify the overall pattern. Amongst these variables, temperature is a major factor affecting plant development. A positive correlation between temperature and leaf length have been repeatedly reported (Bos and Neuteboom, 1998, Equiza and Tognetti, 2002) and was explained by the increase in leaf elongation rate (LER) when temperatures increase (Dale, 1982, Kemp and Blacklow, 1982). Kemp and Blacklow (1982) pointed that leaf extension rate of winter wheat Cv. Gamenya showed a curvilinear response to temperature with an optimum at 28.4 °C. Besides, it was found that temperature affects organ size through its effect on both cell division (Francis and Barlow, 1988) and expansion (Woodward and Friend, 1988). Otherwise, some wheat varieties require a chilling treatment prior to the acquisition of the ability to flower i.e., vernalization. Therefore, together with photoperiod, cold temperatures influence the time of flowering and the final leaf number on the main stem (Miglietta, 1989, Miglietta, 1991, Kirby, 1990). Indeed, the longer the plant remains in the vegetative phase, the higher the number of initiated vegetative primordia and thus of final leaves. However, it is still not clear if plants respond immediately to photoperiod after emergence (Miglietta, 1991)

and that at this time the number of leaves on the main stem is fixed or there is a continuous effect of photoperiod during wheat development (Slafer et al., 1994). More recently, Brooking and Jamieson (2002) showed that there is an interaction between vernalization and daylength so that the rate of vernalization under short photoperiods was greater than under long photoperiods.

Analysis of light effect on wheat plasticity regarding tillering dynamics led to the hypothesis that the number of tillers per plant is related to the intensity of photosynthetically active radiation (PAR) (Bos, 1999) and the ratio between the intensities of red and far-red light (R:FR) (Evers et al., 2006). Bos (1999) found that the light quantity received by a parent leaf is decisive for the outgrowth of its bud into a tiller. In this view, outgrowth of a tiller is prevented if carbon resources are insufficient to sustain growth and functioning of parent plant organs. Furthermore, recent studies on light conditions inside wheat canopies agreed that bud tillers remain dormant below a specific threshold of R:FR ratio (Sparkes et al., 2006, Evers et al., 2006). This decline in R:FR ratio results from a differential reflection and transmission of red and far red light (Holmes, 1981) within the canopy. R:FR ratio is detected by phytochrome photoreceptors located in vertically oriented plant organs (Skinner and Simmons, 1993) which allow the plant to perceive early competition for light and to adapt its behaviour accordingly (Casal and Smith, 1989, Skinner and Simmons, 1993). In grasses, the length of the sheath tube formed by the lower leaves plays a role in determining the extension of the new leaves that grow inside (Casey et al., 1999). Artificial (Wilson, 1985) or natural (Andrieu et al., 2006) lengthening of the whorl results in larger lamina and sheath lengths. This effect was denoted as a size-mediated effect (Louarn et al., 2010).

Analyzing and modelling leaf canopy development in terms of its different components involves measurements of several processes often complex and interrelated and some of which are not fully understood. As a consequence, existing models of plant architecture are largely descriptive and rely on simple patterns of architectural variables according to their age or position within a plant as it is the case for maize (Fournier and Andrieu, 1999b) wheat (Fournier et al., 2003, Evers et al., 2005), barley (Buck-Sorlin, 2002), sorghum (Kaitaniemi et al., 1999), among others.

In the present study, a two-year field experiment was carried out with winter wheat at two sowing dates and three sowing densities. Measurements of organ dimensions on both main stem and axillary tillers were performed in order to investigate the plastic response of wheat and to provide a detailed dataset of architecture variables for canopy reconstruction with a virtual plant model. In a previous work, this two-year experiment was complemented by other studies with variable genotypes and fertilization treatments; this allowed giving a wider view on wheat plasticity (Dornbusch et al., 2010a). Thereby, the two studies share the same description of organ dimensions for sowing date and density treatments. In addition, in the current study, we put emphasis on the variability of final leaves for all tillers within and between treatments and on the subsequent effect on organ dimensions. Otherwise, here we present wheat variability both at the plant and the canopy scale and we discuss the results in the prospect to give an overall view for modelling purpose.

Materials and methods

1. Overview

A two-years field experiment was performed in Grignon in 2007/2008 and 2008/2009 with winter wheat Cv. 'Soissons' at two sowing dates and three contrasted densities. Detailed measurements of architecture variables on the main stem and axillary tillers were carried out along the growing season to characterize the wheat architecture.

2. Experimental design and treatments

The experiment was conducted in the INRA experimental fields at Thiverval-Grignon, France (48°51'N, 1°58'E) on a silty loam soil. *T. aestivum* Cv. 'Soissons' was grown in two seasons, 2007/2008 (Y1) and 2008/2009 (Y2). Six treatments were carried out. There was an early (S1, late September) and a late (S2, mid November) sowing date and three sowing densities: 77, 228, 514 plants m^{-2} referred to as respectively: low density (D1), intermediate density (D2) and high density (D3). In Y2, S1 was excluded because partridges damaged the crop: only the main stem final leaf number of plants from D1 and D3 were recorded. Each treatment was carried out in three parallel plots, at least 30 m in length and spaced 0.2 m from each other. Each plot consisted of nine rows of plants with an inter-row distance of e = 0.175 m. The space between plots was used as an access path, so the two external rows on each side of the plots were considered as borders and not used for measurements.

For both years of experiment, the previous crop was *Vicia faba*. The soil nitrogen (N) content was measured at the end of January, to adjust fertilization following recommendation for high yielding crops. The amount of N in soil was around 70 kg ha^{-1} at the end of January, thus depending on density, 130 to 200 kg ha^{-1} ammonium nitrate were provided overall, divided into two applications (Appendix II). An irrigation system was installed to complement natural rainfall when needed. Weeds were controlled by herbicide application at sowing and during the crop cycle. Recommended fungicides and insecticides were applied to prevent diseases and insect damage. Dates, doses and product names of the different applied chemicals are given in detail in Appendix II.

3. Measurements and sampling procedure

3.1. Plant population density and date of seedling emergence

For both years, in each treatment, the number of emerged plants was determined at seedling emergence as follows: plants located within a segment of length L (L = 3m, 1m and 0.5 m respectively for D1, D2 and D3) of the third row of each plot per treatment, were counted. This operation was repeated on the same segments, each 3 to 5 days, depending on temperature, from the moment leaf 1 of the first plants emerged from the soil, until the number of plants hold steady. The final number was used to compute the plant population density:

$$D = \frac{1}{r}\sum_{i=1}^{n}\left(\frac{p}{e \times L}\right) \quad (1)$$

where D is the plant population density , r the number of repetition (r = 3), p is the number of plants within a segment of length L and e is the inter-row distance.

Actual plant population densities were lower than targeted sowing densities especially for the late sowing where emergence occurred during the period of cold temperatures.

Therefore, actual plant populations were not identical between treatments over the two years (Table 1). Date of seedling emergence was defined as the time when 50% of seedlings emerged. In both years the first notation was done after this time, when there was 75%-80% of emerged seedling, so date of 50% emergence was estimated retrospectively and is likely with ± 2 days of confidence interval.

Table 1
Sowing and seedling emergence dates, and actual plant population densities for winter wheat Cv. 'Soissons' grown in Grignon during two growing seasons 2007/2008 (Y1) and 2008/2009 (Y2) at two sowing dates: early (S1) and late (S2) and three sowing densities D1, D2 and D3.

Season	Sowing date treatment	Date of sowing	Date of seedling emergence	Sowing density (plant. m^{-2})		Plant density
Y1	S1	25/09/2007	01/10/2007	D1	77	77
				D2	228	211
				D3	514	483
	S2	12/11/2007	01/12/2007	D1	77	53
				D2	228	168
				D3	514	394
Y2	S1	30/09/2008	08/10/2008	D1	77	55
				D2	228	180
				D3	514	374
	S2	17/11/2008	18/12/2008	D1	77	59
				D2	228	160
				D3	514	406

3.2. Organ dimensions

In all experiments, we aimed at a faithful estimation of the dimensions of leaf blades, sheaths and internodes. The main stem and the primary axillary tillers are denoted as T_k (k = 0, 1, 2…), T_0 being the main stem and T_1 being the tiller that emerges from the axil of the first true leaf. The coleoptile tiller rarely emerged and was thus not considered in data processing.

For both years, in all treatments (except Y2S1D2), final number of leaves on the main stem and primary tillers was monitored on 20 tagged plants in the field. Main stem and primary tillers were previously tagged to allow leaf rank identification. Number of final leaves on a given tiller is denoted as $N_{leaf}(k)$ with $N_{leaf}(0)$ being the final leaf number of the main stem. These plants were sampled at flowering, allowing to measure dimension of organs present at flowering on main stem and primary tillers, with an exact knowledge of the tiller and phytomer rank.

Depending on the treatment, at three to nine occasions during crop growth (Table 2), plants of the five-central rows were harvested over a length of 0.5 m, representing a subplot of area $S = 0.35$ m² (Fig. 1) with three repetitions per treatment. In each subplot a sample of five plants were dissected to measure the dimensions of all mature organs (blades, sheaths and internodes). In Y1, the subplots and the dissected plants were chosen randomly at the moment of the sampling. This procedure was efficient at the early stages of plant development but after full tillering, it was no longer possible to identify accurately the rank of the tillers and leaves, especially at the lower density D1, in which plants produced as much as 15 tillers. In Y2, the place of each subplot for destructive measurements was delimited by

placing takes at crop emergence. When plants had approximately five liguled leaves on the main stem, eight plants in each subplot were chosen randomly, their main stem and primary tillers were tagged with coloured rings to allow accurate identification of leaf and tiller rank. Tags were later moved to upper leaves as lower leaves were senescing. At each sampling date, five out of the eight tagged plants were randomly chosen and dissected to determine organ dimensions. In both years, lamina images were obtained with a flat-bed scanner and were processed using the program Lamina2Shape (Dornbusch and Andrieu, 2010) to compute blades length (l_{bl}), width (w_{bl}). Leaf blade area (A_{bl}) was calculated as $A_{bl} = l_{bl} \cdot w_{bl} \cdot f_t$ were mean values for the shape factor f_t for each leaf rank were taken from measured data on several genotypes given by Dornbusch et al. (2010b). Length of sheaths (l_{sh}) and internodes (l_{in}) were measured with a ruler. Distance to a leaf collar from the shoot base (h_{col}) was computed as the sum of l_{in} below a respective phytomer rank plus the l_{sh} of that phytomer.

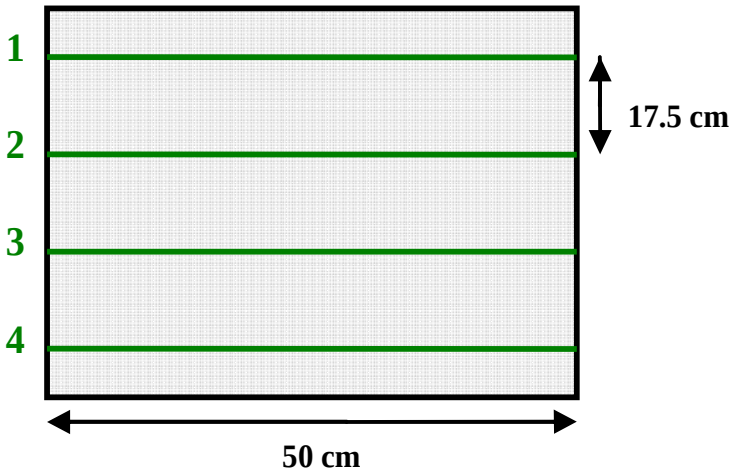

Figure 1. Scheme of the plot harvested periodically during wheat cycle for determination of organ dimensions and leaf area index. Green lines represent sowing lines.

Table 2
Number and dates of harvests of plants for winter wheat Cv. 'Soissons' grown in Grignon during two growing seasons 2007/2008 (Y1) and 2008/2009 (Y2) at two sowing dates: late september (S1) and mid november (S2) and three sowing densities D1: 77, D2: 228, D3: 514 plants.m^{-2}.

Harvest number	Y1		Y2
	S1	S2	S2
1	29/10/2007	25/03/2008	09/03/2009
2	28/11/2007	29/04/2008	08/04/2009
3	21/01/2008 (1)	26/05/2008	27/04/2009
4	28/01/2008(2)		18/05/2009
5	18/02/2008		08/06/2009
6	17/03/ 2008		
7	07/04/2008		
8	28/04/2008		
9	20/05/2008		

(1)only D3 was harvested, (2) only D1 and D2 were harvested.

In Y1, starting from the last measurements at flowering where the exact leaf rank was known, we built up the profile of main stem organ dimensions for different final number of leaves. Then, we went back harvest by harvest to match the profile of blades, sheaths and internodes according to the typical profile. Finally, organ dimensions with their accurate correspondence with phytomer rank were obtained for the main stem in all treatments and growing seasons and for tillers only in Y2S2 (Table 3).

3.3. Leaf senescence

Leaf senescence was estimated at each harvest date (cf. Table 2) by image processing of scans of the leaf laminae and this was supplemented in Y2 S2 by visual notation on tagged plants in the field.

a. Analysis of scans of leaves

Image processing allowed determining the total number of liguled main stem leaves (Haun stage) and the fraction of dead tissue for each leaf position. The decimal number of dead leaves on an axis is referred below as the Shoot Senescence Index (SSI); the difference between HS and SSI represents the decimal number of green leaves on the main stem. This was monitored until the date of flag leaf ligulation where harvests were stopped. The program used for image processing distinguishes only between green and no green areas. Therefore, senescence computed in this case includes not only apical necrotic area but all the necrotic and chlorotic tissues in the rest of the leaf.

b. Visual notations on tagged plants

Detailed measurements of leaf senescence in the field were performed only in Y2S2. When plants had three liguled leaves, 30 plants were chosen within the five central rows of the middle plot in each density treatment. Along a row, plants were spaced 80 cm and those on the adjacent row were shifted by 40 cm so that plants were placed in quincunx. Leaves of the main stem were tagged with coloured rings to allow identification of their rank. For each individual leaf of the main stem of the 30 tagged plants, we recorded the proportion of apical necrotic leaf area (including possible disease lesions). Measurements were performed every 80-100 °Cd starting from leaf 5 counted acropetally. These measurements were then used to compute the Shoot Senescence Index (SSI). Compared to the destructive method described above, the non destructive method allowed more frequent measurements and avoiding variability intrinsic to monitoring by destructive measurements.

3.4. Leaf area index

At each sampling date (Table 2), the leaf area index (LAI) was calculated as follows: the number (n) of plants in each subplot was counted. The 5 plants used for determining organ dimensions and the rest of the plants were placed separately in an oven during 48h to determine their dry mass (M). The LAI (m^2/m^2) was calculated as:

$$LAI = A_{bl}^{5} \times \frac{M^{n}}{M^{5}} \times \frac{D}{n} \qquad (2)$$

where A_{bl}^{5} is the total blade area of the 5 dissected plants, M^{5} is their dry mass, M^{n} is the total dry mass of the subplot, n the total number of plants and D the plant population density. In Y2, all plants of the harvested subplot were used whereas, in Y1 only 40 plants (including the processed plants) were considered, i.e., n = 40.

3.5. Ground cover

In both years, once every one or two weeks from seedling emergence until flag leaf ligulation, three photographs of the canopy were taken at constant locations in each treatment. We used a NIKON camera (D70, sensor size =23.6x15.8 mm) with a lens of focal length 50 mm. This defines a maximum view angle of ±13.5°. Photographs were taken at vertical from a 2.8 m height and covered an area of 1.32m x 0.88m. Thus, one pixel represented 0.4mm x 0.4mm. Ground cover, defined as the fraction of green area on the photo, was then determined by separating canopy from ground pixels based segmentation of the spectral space defined by the red and the green coordinates of the pixels. Boundaries for segmentation were defined interactively using the "Optimas" Software. The process is illustrated in Figure 2.

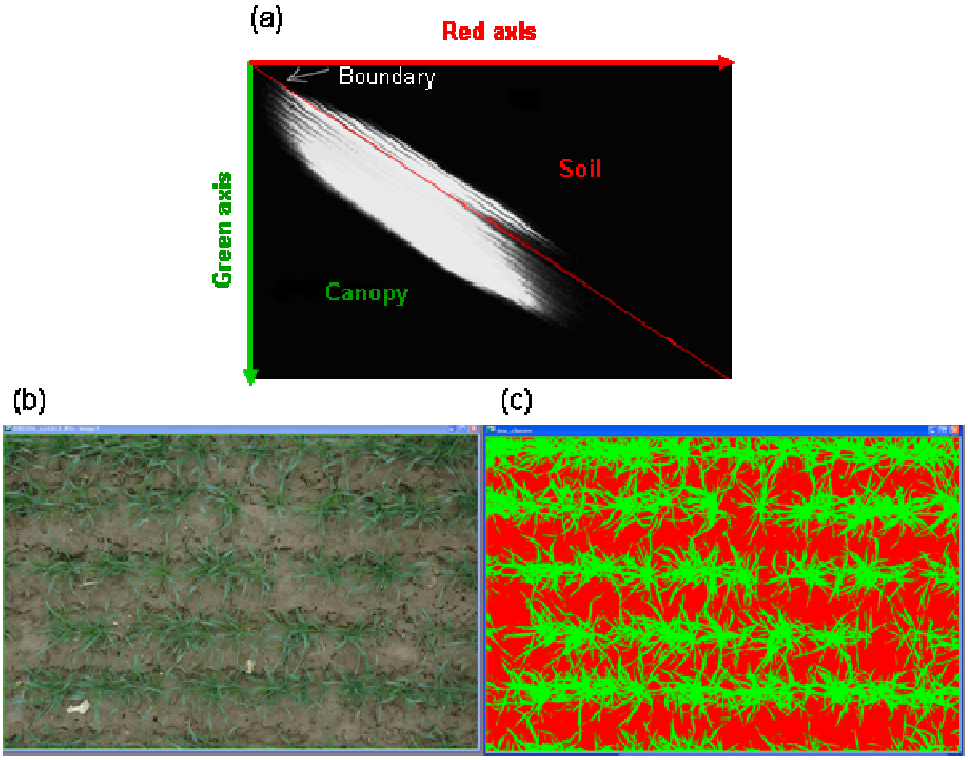

Figure 2. (a) Histogram of a photo processed with Optimas software. The red line corresponds to a manually drawn boundary separating soil and canopy pixels. Each point of the histogram (in white) represents the couple of coordinates of a given pixel from the photo expressed in red and green. Example of ground cover photo **(b)** before and **(c)** after image processing by Optimas software.

As a summary, Table 3 gives the detail of the measured variables in each treatment.

Table 3
Summary of the measured architecture variables for winter wheat Cv. 'Soissons' grown in Grignon during two growing seasons: 2007/2008 (Y1) and 2008/2009 (Y2) at two sowing dates: late September (S1) and mid November (S2). Gray cells indicate that the variable was measured for the corresponding treatment.

		Y1		Y2	
		S1	**S2**	**S1**	**S2**
Final leaf number	Main stem			D1, D2 only	
	Tillers			D1, D2 only	
Blade length	Main stem				
	Tillers				
Blade width	Main stem				
	Tillers				
Sheath length	Main stem				
	Tillers				
Internode length	Main stem				
	Tillers				
Collar height	Main stem				
	Tillers				
Senescence	Main stem				
	Tillers				
Leaf area index					
Ground cover					
Tillers number					

4. Data processing and presentation of results

To compare vertical profiles of architectural variables between different treatments and tillers, we used two methods of phytomer counting: phytomer rank N counted from the base (acropetally) that is $N = 1$ is the rank of the first true phytomer; and phytomer rank N' counted from the top (basipetally) (N' = -1, -2,…), where N' = -1 represents the rank of the flag leaf.

Confidence intervals (IC) were calculated for each phytomer, axis, final leaf number and treatment:

$$IC = \frac{se}{\sqrt{n}} \cdot t \tag{3}$$

$$se = \frac{1}{n-1}\sum_{i=1}^{n}\left(y_i - \bar{y}\right)^2 \tag{4}$$

where se is the standard error, y_i is the measured and $\bar{y}$ the mean value of a variable, n the number of measurements and t the value of the Student table at the risk α=0.05.

Confidence intervals were reported in the figures above and below the corresponding mean points. Most of the cases confidence intervals did not overlap meaning that at the risk α=0.05, means do not come from the same population. Otherwise no statistics were performed to test the significance or not of treatment differences.

As a measure for the deviation from an ideal 1:1 line we used the mean error (ME) and the mean squared error (RMSE):

$$\mathrm{ME} = \frac{1}{n}\sum_{i=1}^{n}\left(y'_i - y_i\right) \tag{5}$$

$$\mathrm{RMSE} = \sqrt{\frac{1}{n}\sum_{i=1}^{n}\left(y'_i - y_i\right)} \tag{6}$$

where y'_i represents the predicted and y_i the corresponding measured value.

Results

In this section, results of architecture variables are presented first at the plant scale then at the canopy scale. In the former part, comparisons between treatments are shown for the final number of leaves formed on an axis (N_{leaf}), organ dimensions, senescence and tillering dynamics. When available, data for the main stem are compared to data of primary tillers as for the final number of leaves and some organ dimensions. Concerning architecture variables at the canopy scale, we show results for number of axes par square meter, ground cover and leaf area index (LAI).

I. Architecture at plant scale

1. Final leaf number for main stem and tillers

Main stem final leaf number varied between density and sowing date treatments

Sowing date was the major source of variation of the total number of leaves formed on the main stem. Early sowing typically resulted in 12 to 14 main stem leaves whereas S2 typically resulted in 9 to 11 main stem leaves. Main stem final leaf number varied amongst plants of a same treatment: the most frequent $N_{leaf}(0)$ represented 50 to 90% of the plants and one or two other less frequent values could be found (Fig. 3, Table 4). The proportion of plants with high $N_{leaf}(0)$ decreased with increasing densities. On average, the most frequent N_{leaf} (0) was approximately one less at D3 compared to D1: in S1, N_{leaf} (0) was 14 and 13 respectively for D1 and D3 and in S2, it was 10 and 9. Interestingly, in Y1S2, all density treatments resulted in the same most frequent $N_{leaf}(0) = 10$ and there was also little variability between plants within a same density in this case ($N_{leaf}(0) = 10$ represented at least 80% of the plants). This result was not reproduced for S2 in the second growing season.

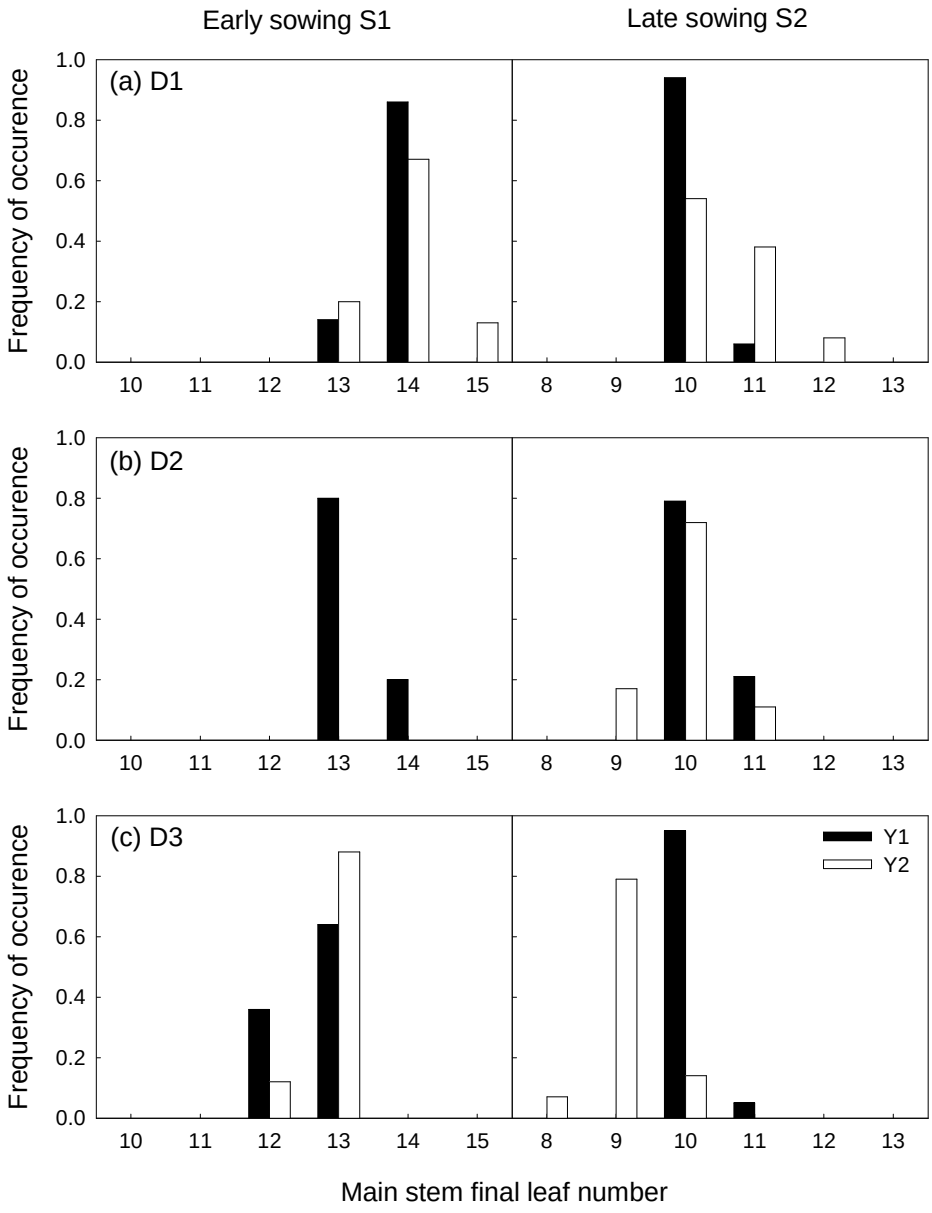

Figure 3. Frequency of occurrence *vs.* the number of final leaves (N_{leaf}) on the main stem of winter wheat Cv. 'Soissons' grown in Grignon in late September (S1: left) and mid November (S2: right) during two growing seasons: 2007/2008 (Y1, black bars) and 2008/2009 (Y2, empty bars) at three sowing densities **(a)** D1: 77, **(b)** D2: 228 and **(c)** D3: 514 plants.m^{-2}.

Table 4
Main stem final leaf number in 2007/2008 (Y1) and 2008/2009 (Y2), for 2 sowing dates (S1, S2) and 3 sowing densities (D1, D2, D3). D1: 77, D2: 228, D3: 514 plants.m^{-2}. S1: Late September, S2: Mid November. Numbers in bold correspond to the most frequent values for each density. Numbers between brackets correspond to the total number of used plants.

			N_{leaf} (0)							
Experiment	**Sowing**	**Density**	**8**	**9**	**10**	**11**	**12**	**13**	**14**	**15**
Y1	**S1**	**D1** (7)						0.14	**0.86**	
		D2 (15)						**0.80**	0.20	
		D3 (11)					0.36	**0.64**		
	S2	**D1** (17)			**0.94**	0.06				
		D2 (19)			**0.79**	0.21				
		D3 (20)			**0.95**	0.05				
Y2	**S1**	**D1** (15)						0.20	**0.67**	0.13
		D2 (-)								
		D3 (16)					0.12	**0.88**		
	S2	**D1** (13)			**0.54**	0.38	0.08			
		D2 (18)		0.17	**0.72**	0.11				
		D3 (14)	0.07	**0.79**	0.14					

Tillers final leaf number followed the same pattern as the main stem

Similarly to the main stem, final leaf number of primary tillers varied with sowing date and plant population density. For each treatment (sowing date*density) and N_{leaf} modality, N_{leaf} (k) of tillers T_1, T_2, T_3 varied (1 to 3 values) with the most frequent values representing 50 to 90%. Altogether, plants with the same N_{leaf} (0) showed the same pattern of variation in N_{leaf} (k) as shown in Figure 4. Thus, there was not a representative number of leaves for a given tiller rank and a given N_{leaf} modality.

When all plants from a given sowing date were pooled together (independently of the sowing density), a general pattern of decrease in the final leaf number of the three first primary tillers was found: both T_1 and T_2 produced 3 leaves less than the main stem and T_3 one leaf less than T_1 and T_2. The median value for N_{leaf} (k) for successively T_0, T_1, T_2 and T_3 was 13, 10, 10, 9 for S1 and 10, 7, 7, 6 for S2.

A cumulative number of leaves (N_{leaf}^{cum}) was computed for primary tillers T_k (for k= 1 to 3) as the sum of the mean N_{leaf} (k) and the HS of the main stem when T_k appeared. Thus, we added 3 for T_1, 4 for T_2, etc. For each sowing date a linear model was then adjusted to the cumulative number of leaves plotted against tiller rank (Fig. 5)

$$N_{leaf}^{cum} = N_{leaf}(0) + \alpha k \quad (7)$$

where $N_{leaf}(0)$ is the mean final leaf number of the main stem, k the tiller rank and α a fitted parameter that represents the difference of N_{leaf} between two successive tillers.

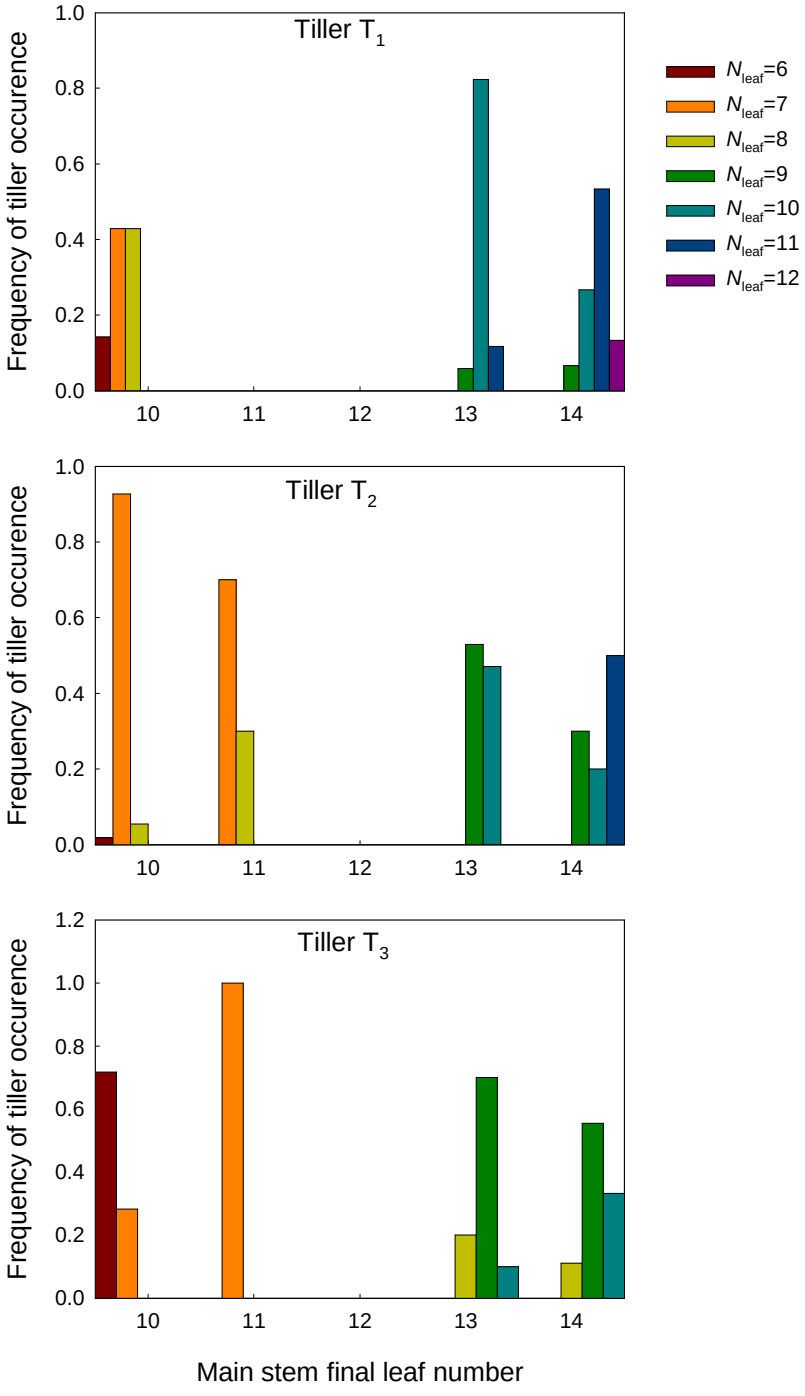

Figure 4. Frequency of occurrence of tillers T_1, T_2 and T_3 separated according to their final leaf number *vs.* the number of final leaves on the main stem for winter wheat Cv. 'Soissons' sown in late September 2007 (Y1S1) and in mid November 2008 (Y2S2) in Grignon at 3 sowing densities: D1: 77, D2: 228, D3: 514 plants.m^{-2}.

The linear model represented the change in cumulative leaf number *vs.* tiller rank with a high accuracy (Table 5) and the difference of N_{leaf} between two successive tillers was significantly different between the two sowing treatments: respectively 0.26±0.05 and 0.48±0.05 for S1 and S2.

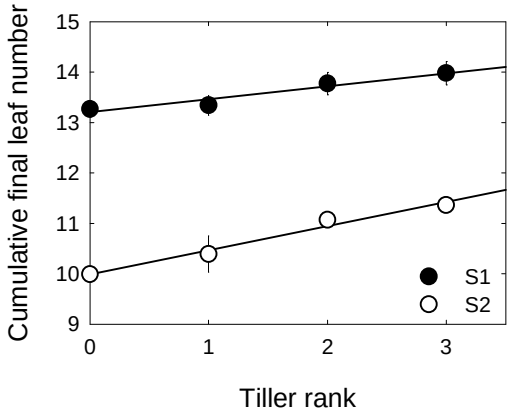

Figure 5. Cumulative final leaf number *vs.* tiller rank. Data correspond to mean values of final leaf number of a given tiller rank plus the HS of the main stem when that tiller appeared. Data are for winter wheat Cv. 'Soissons' grown in Grignon in 2007/2008 and 2008/2009 at two sowing dates: late September (S1,●) and mid November (S2,○). Lines correspond to linear regression for cumulative leaf number *vs.* tiller rank. Vertical bars show confidence intervals (α=0.05) when larger than the size of the symbol.

Table 5. Parameter values of the adjusted linear model to cumulative leaf number of tillers T_k (k = 0 to 3) *vs.* tiller rank for winter wheat Cv. 'Soissons' grown in Grignon in 2007/2008 and 2008/2009 at two sowing dates: late September (S1) and mid November (S2).

	$N_{leaf}(0)$	α	R^2
S1	13.2±0.09	0.26±0.05	0.94
S2	9.98±0.09	0.48±0.05	0.98

2. Organ dimensions

General pattern in the vertical profiles of length of blades, sheaths and internodes

Leaf blade, sheath and internode dimensions increased with increasing phytomer rank counted from the base of the shoot (Fig. 6), except for the flag leaf blade which was shorter than the previous leaf blade. These patterns are those usually found for winter wheat and have been reported in previous works. Sheath and internode dimensions of upper phytomers increase almost linearly with increasing phytomer rank whereas for lower phytomers, internode do not elongate and the length of sheaths increase only marginally with increasing phytomer rank. Following Poethig (2003), we will refer to the first basal phytomers (with non elongated internodes) as juvenile phytomers and to the last phytomers (with elongated internodes) as adult phytomers. When treatments resulted in differences in final leaf number, this always came from variations in the number of juvenile phytomers, whereas the number of adult phytomers was almost constant (4 or 5 adult phytomers).

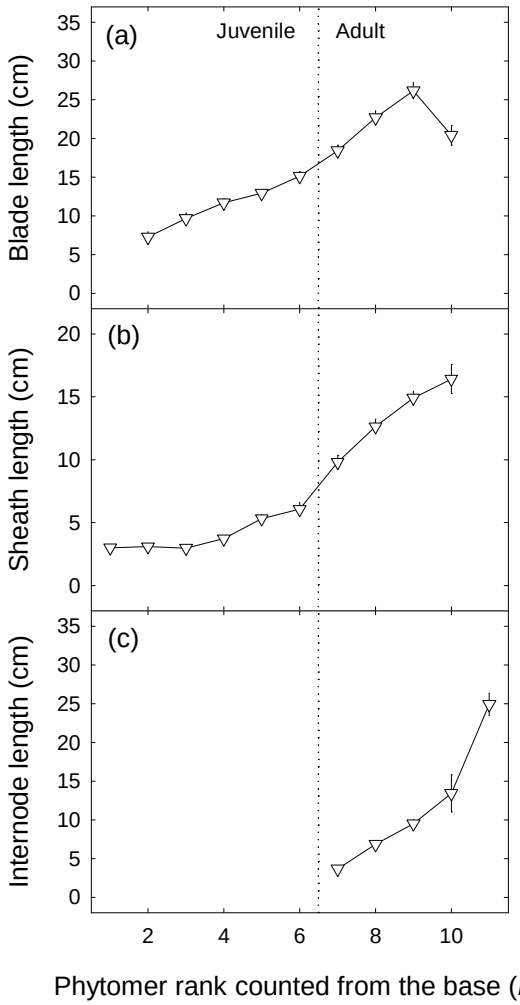

Figure 6. Length of **(a)** leaf blade, **(b)** sheath and **(c)** internode *vs.* leaf rank *N* counted acropetally for the median main stem of winter wheat Cv. 'Soissons' sown in mid November (S2) in 2008/2009 (Y2) in Grignon at sowing density 228 plants.m^{-2}.

For each experimental year, treatment, tiller rank, and N_{leaf} modality, the mean values of architectural traits were computed for each phytomer rank. To allow comparison between axes differing in N_{leaf} we referred to phytomer rank counted from the base (*N*) for juvenile phytomers and to phytomer rank counted from the top (*N'*) for adult phytomers.

While sharing the general pattern mentioned above, vertical profiles of organ dimensions differed between treatments. To allow accurate comparisons, plants were separated according to sowing date, density, and main stem final leaf number.

- We investigated the density effect by comparing groups of plants having produced the same $N_{leaf}(0)$ from different densities.
- Given that number of leaves differed substantially between sowing date treatments we used data representing plants having formed the most frequent final leaf number to compare organ profiles between early and late sowing.
- Within a same sowing and density treatment, profiles of organ dimensions were compared between N_{leaf} modalities.
- Within a same sowing and density treatment, profiles of organ dimensions were compared between main stem and axillary tillers. For this, we used only data of axes

having formed the most frequent final leaf number for the corresponding botanical position.

Within a same treatment, plants with higher leaf number had smaller juvenile leaves, but larger adult leaves and higher stature.

Vertical profiles of organ dimensions from plants differing in final leaf number are presented in Figure 7 and in Appendix III/A for all treatments where different N_{leaf} modalities were found: these are the intermediate density D2 in Y1S1 and all density treatments in Y2S2. For juvenile leaves, blade length, width and area were slightly lower for plants with a higher final leaf number, except for the first leaf ($N = 1$), that showed almost the same dimensions regardless of the final leaf number. Figure 8a shows the blade area of juvenile leaves from plants producing N final leaves, plotted against those of the corresponding phytomer rank from plants producing N+1 final leaves (data are for all treatments in Y2S2). Points fell below the 1:1 line (ME=-0.31 cm²) with a significant linear correlation (slope =0.77, R^2=0.96) showing that blade area was approximately 23 % smaller for plants with higher N_{leaf}.

On the contrary, for adult leaves, blade length, width and area were increased for higher $N_{leaf.}$ However, these differences vanished for the penultimate leaf and were reversed for the flag leaf: lower N_{leaf} resulted in higher leaf dimensions (Fig. 8b and 8c). Collar height of adult leaves was increased for higher N_{leaf} (Fig. 7 and 8d), with a constant difference between N_{leaf} modalities. This is further illustrated in Figure 8d where collar height of plants with N final leaves was plotted against those with N+1 final leaves. Points fell above the 1:1 line and a linear model could be fitted with a slope close to 1 (slope= 1.02, R^2=0.99). The difference of height at the level of the flag leaf collar was about 4-6 cm between the N_{leaf} modalities of the same density.

Lower sowing density resulted in longer blades and sheaths and higher area of adult leaves

Data from all treatments in Y1 and from S2 in Y2 were used to compare plants between density treatments (Figs. 9, 10 and Appendixes III/B and III/C). Plants were grouped according to N_{leaf}. Little differences between density and no clear trend were found for the dimensions of juvenile phytomers. For adult phytomers, all dimensions were higher for lower density. However, differences were very small for sheath and internode length in Y1S1. For the late sowing, differences between density treatments in vertical profiles of blade length, width and area and of sheath length were small for the first elongating phytomers and increased progressively with higher phytomer rank so that differences were largest at the penultimate and ultimate phytomers. This trend was not observed for the early sowing, where differences between density treatments were rather visible for the first elongating phytomers but were maintained or reduced at the ultimate leaf.

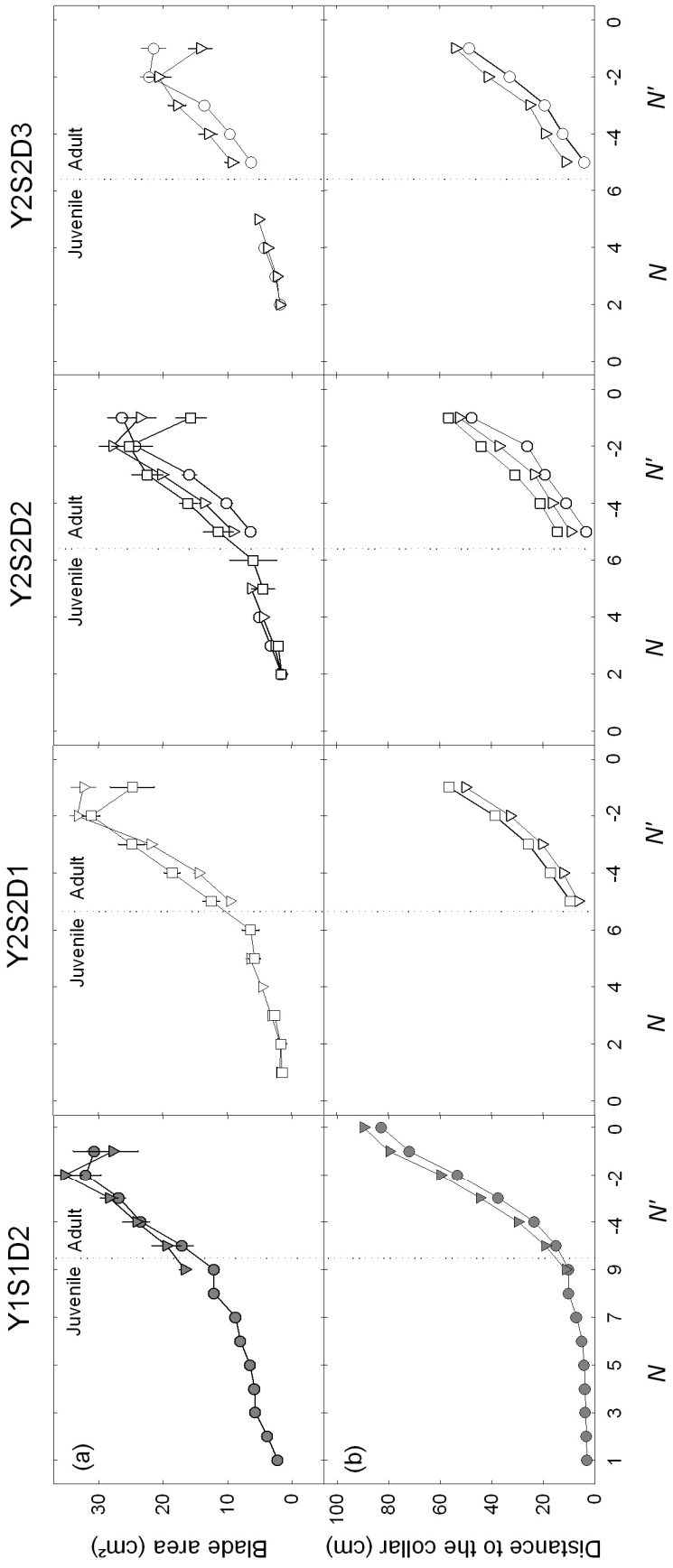

Figure 7. (a) Area of leaf blade, **(b)** distance to the collar from the shoot base, *vs.* leaf rank *N* counted acropetally for juvenile phytomers and *vs.* leaf rank *N'* counted basipetally for adult phytomers. Data are for the main stem of winter wheat Cv. 'Soissons' sown in late September 2007 (Y1S1) and in mid November 2008 (Y2S2) in Grignon at 3 sowing densities: D1, D2, D3. For each density treatment data are pooled by final leaf number N_{leaf} : 9 (○), 10 (▽), 11 (□), 13 (●), 14 (▶). D1: 77, D2: 228, D3: 514 plants.m^{-2}. Vertical bars show confidence intervals (α=0.05) when larger than the size of the symbol.

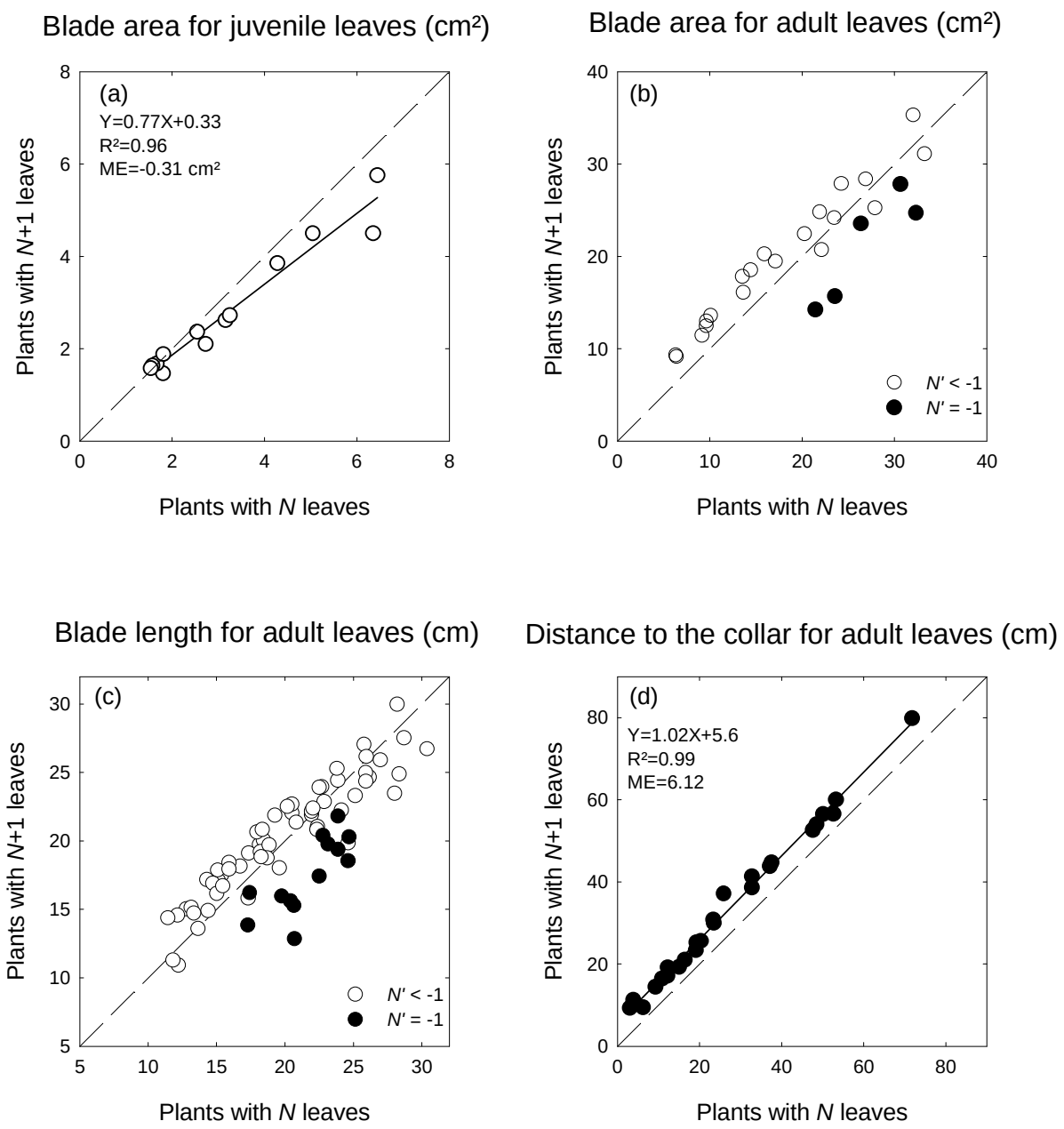

Figure 8. Dimensions of phytomer of plants having produced a total of *N*+1 main stem leaves *vs.* dimensions for the same phytomer rank for plants having produced a total of *N* main stem leaves. Each point represents the mean value for a given treatment and phytomer position. Rank is counted acropetally for juvenile leaves and basipetally for adult leaves. **(a)** blade area of juvenile leaves, **(b)** blade area of adult leaves **(c)** blade length of adult leaves and **(d)** collar height of adult leaves. Data are for winter wheat Cv. 'Soissons' sown in Grignon in late September 2007 (Y1S1) at sowing density 228 plants.m^{-2} and in mid November 2008 (Y2S2) at three sowing densities: 77, 228 and 514 plants.m^{-2}. The 1:1 line is shown; coefficients of determination (R^2) and mean error (ME) are given in (a) and (d).

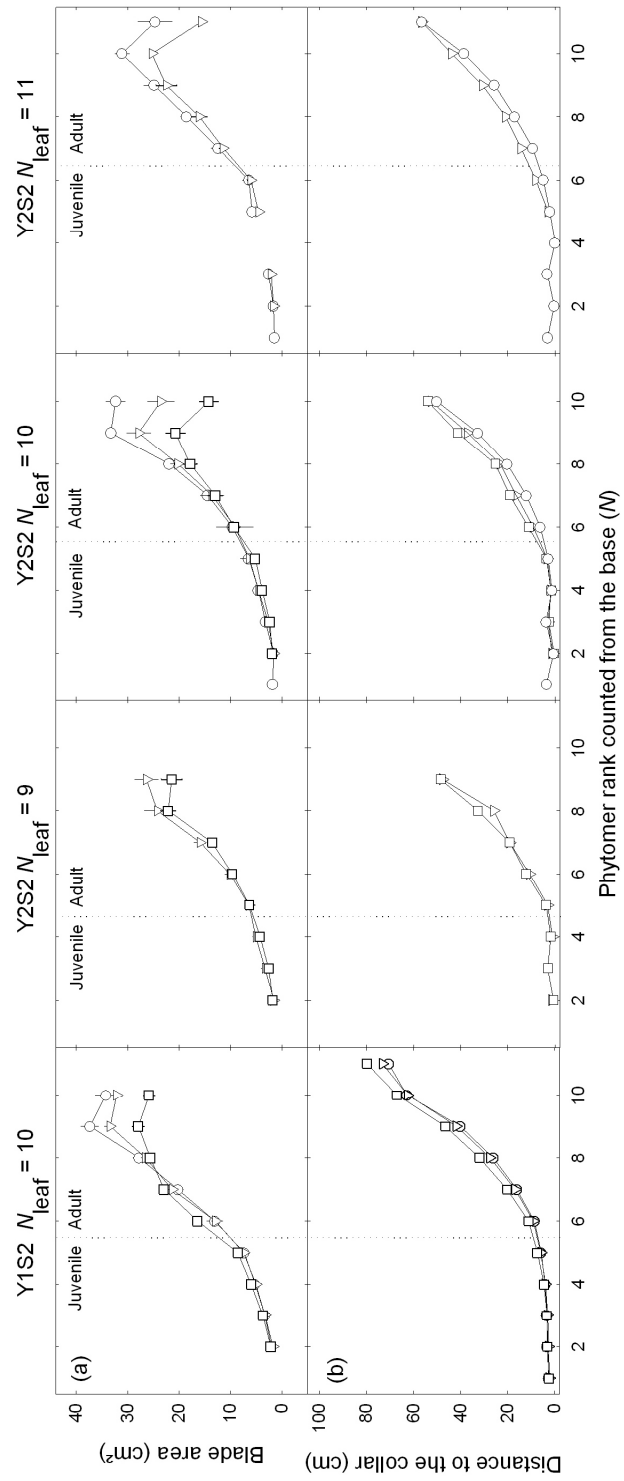

Figure 9. (a) Area of leaf blade and **(b)** distance to the collar from the shoot base *vs.* leaf rank *N* counted acropetally for the main stem of winter wheat Cv. 'Soissons' sown in mid November in 2007 (Y1S2) and in 2008 (Y2S2) in Grignon at 3 sowing densities: D1 (○), D2 (▽), D3 (□). Data are pooled by final leaf number. D1: 77, D2: 228, D3: 514 plants.m^{-2}. Vertical bars show confidence intervals (α=0.05) when larger than the size of the symbol.

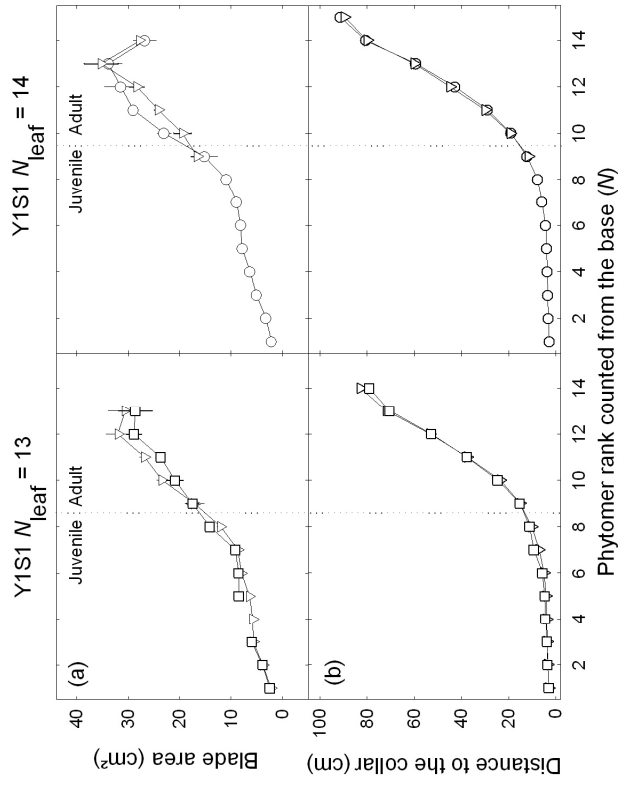

Figure 10. (a) Area of leaf blade and **(b)** distance to the collar from the shoot base *vs.* leaf rank *N* counted acropetally for the main stem of winter wheat Cv. 'Soissons' sown late September in 2007 (Y1S1) in Grignon at 3 sowing densities: D1 (○), D2 (▽), D3 (□). Data are pooled by final leaf number. D1: 77, D2: 228, D3: 514 plants.m^{-2}. Vertical bars show confidence intervals (α=0.05) when larger than the size of the symbol.

Main stem showed different profiles of length of blades, sheaths and internodes between the two sowing dates

Figure 11 shows the vertical profiles in organ dimensions of plants from D2 with the most frequent final leaf number for sowings S1 (N_{leaf} = 13) and S2 (N_{leaf} = 10) in Y1. Juvenile leaves had longer and wider blades at S1 compared to S2 whereas sheath lengths were similar. At S1, leaves growing during winter did not increase in blade length (Fig. 11a), whereas they did increase in blade width (Fig. 11b). Dimensions of the four uppermost leaf blades and sheaths were almost the same irrespective of the sowing date. Hence, dimensions of the leaves present at flowering were very similar for both sowing dates. The length of the uppermost internode (N' = -1) and the peduncle (N' = 0) were also very similar irrespective of the sowing date (Fig. 11e). However, the length of the lower internodes ($-5 \leq N' \leq -2$) was increased at earlier sowing leading to taller plants at flowering: final height of the peduncle was 82.9 cm for S1 and 73.2 cm for S2 (Fig. 11f).

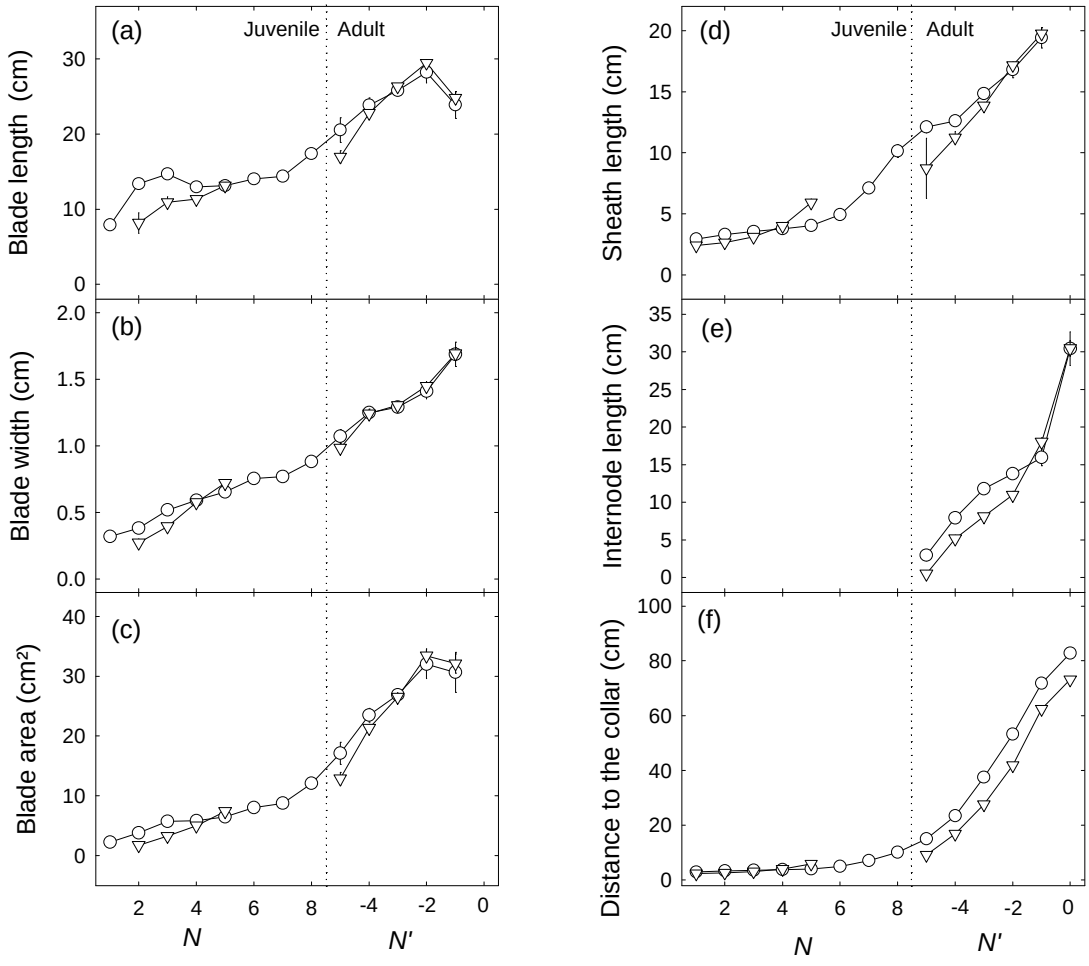

Figure 11. (a) Length of leaf blade, **(b)** width of leaf blade, **(c)** area of leaf blade, **(d)** length of sheath, **(e)** length of internode and **(f)** distance to the collar from the shoot base *vs.* leaf rank N counted acropetally for juvenile phytomers and *vs.* leaf rank *N'* counted basipetally for adult phytomers. Data are for the main stem with the most frequent N_{leaf} of winter wheat Cv. 'Soissons' sown in late September (Y1S1,○) and in mid November (Y1S2,▽) 2007 at sowing density D2= 228 plants.m^{-2}. Vertical bars show confidence intervals (α=0.05) when larger than the size of the symbol.

Length of adult leaf blades, sheaths and internodes was almost identical between the main stem and axillary tillers of the same rank counted from the shoot top

Vertical profiles of organ dimensions for the median main stem from the three density treatments in Y2S2 and their corresponding ones for the three axillary tillers: T_1, T_2, T_3 that appeared most frequently are shown in Figure 12. During the juvenile growing phase, leaf blades on T_1, T_2, T_3 were longer compared to the corresponding ones of the main stem with the same phytomer rank *N*. However, during the adult growing phase, vertical profiles of blade length for T_1, T_2, T_3 showed the same pattern as for the main stem and their values were very similar (Fig. 12a). Blade area on T_1, T_2, T_3 was smaller compared to main stem (Fig. 12b). For the sheath, internode and distance to the collar vertical profiles, there were very small differences between main stem and tillers. It was not clear if the decreasing in organ dimensions for axillary tillers is linked to tiller rank.

Considering data from all density treatments of the Y2S2 treatment, the length of the last four adult leaf blades, sheaths and internodes ($-4 \leq N' \leq -1$) of T_1, T_2, T_3 were plotted against the corresponding measured values of the main stem (Fig. 13a). Data points fell close to the 1:1 line, but blade, sheath and internode dimensions on T_1, T_2, T_3 were mostly smaller than the corresponding values for main stem (negative value for ME=-0.57 cm). The overall relationship was good (RMSE=1.75 cm). No trend in decreasing length of blade, sheath and internode with increasing tiller rank ($T_1 > T_2 > T_3$) compared to main stem was found. For blade area, a stronger deviation from the 1:1 line was obtained (RMSE=3.13 cm², Fig. 13b) and in most cases, tillers produced smaller leaves than the main stem (ME=-2.26 cm²). More generally, a good relationship was also found between blade length of axillary tillers and the corresponding ones of the main stem on plants monitored in the field (Fig. 13c), even if points deviated more from the 1:1 line (RMSE = 3.66 cm).

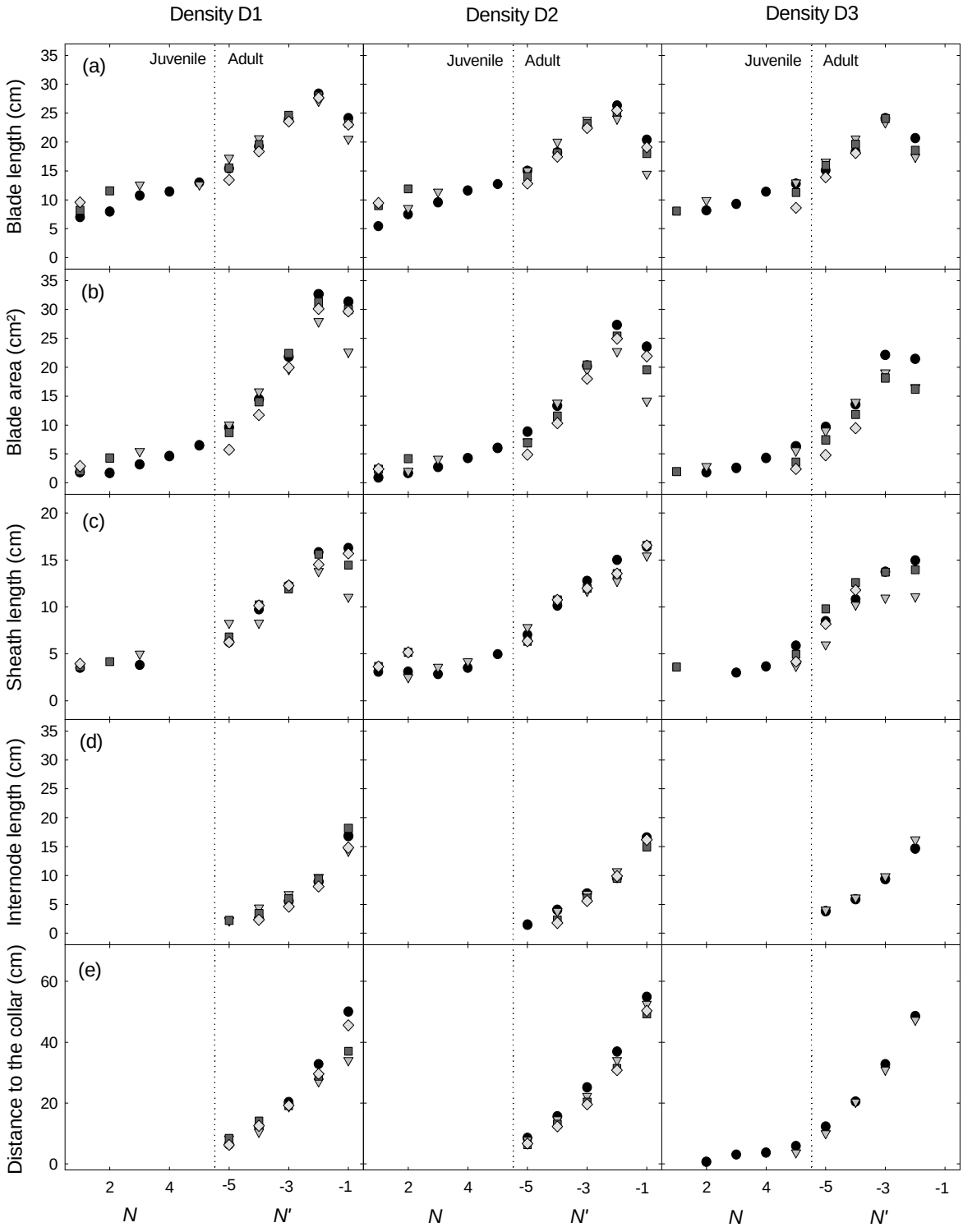

Figure 12. (a) Length of leaf blade, **(b)** area of leaf blade, **(c)** length of sheath, **(d)** length of internode and **(e)** distance to the collar from the shoot base *vs.* leaf rank *N* counted acropetally for juvenile phytomers and *vs.* leaf rank *N'* counted basipetally for adult phytomers. Data are for the main stem of winter wheat Cv. 'Soissons' sown in Grignon in mid November 2008 (Y2S2) at three sowing densities: D1 (left column), D2 (middle column) and D3 (right column). Symbols correspond to different tillers: T_0 (●), T_1 (▽), T_2 (■), T_3 (◊); symbols represent measured median values. D1: 77, D2: 228, D3: 514 plants.m^{-2}.

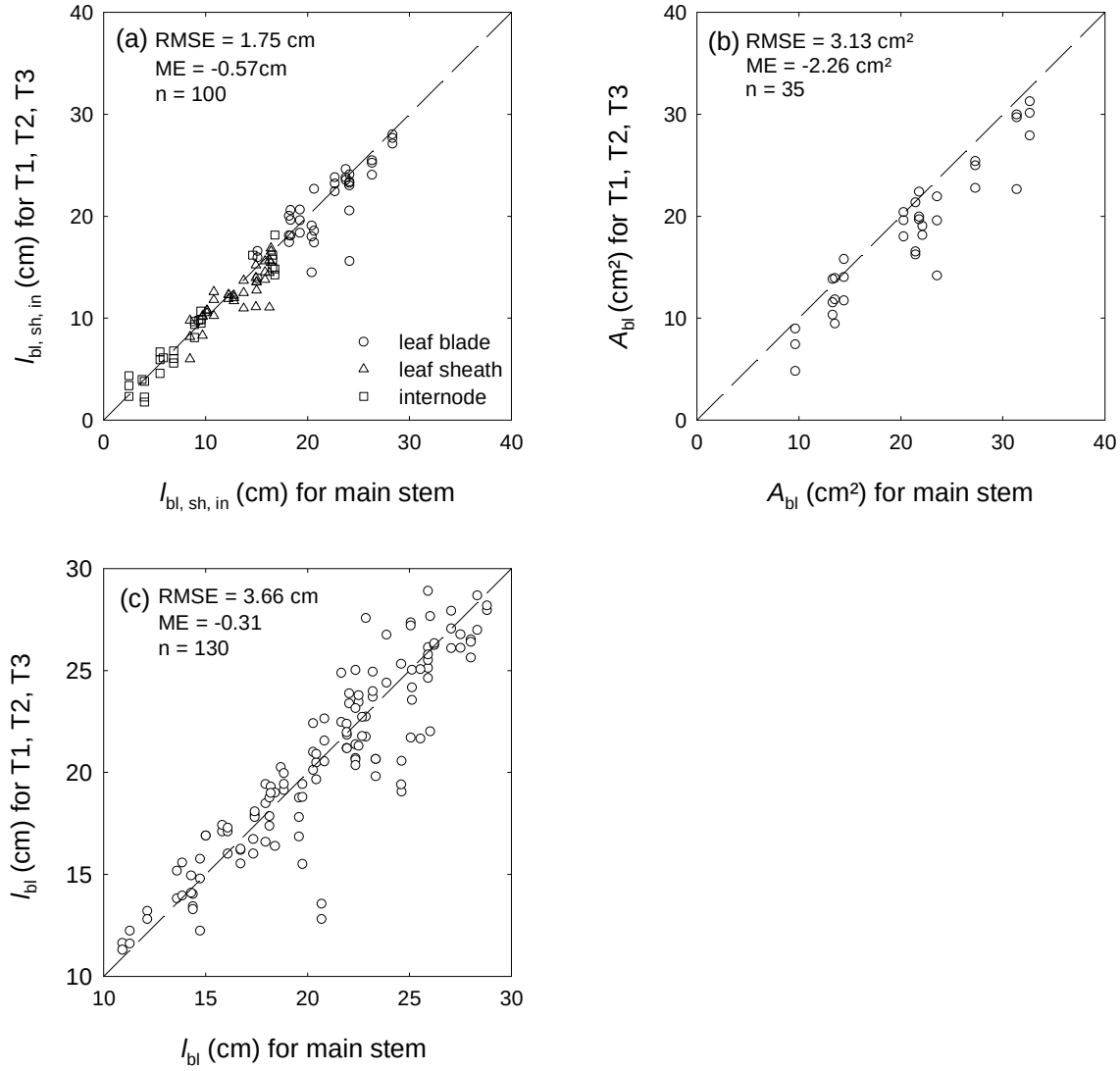

Figure 13. (a) Median length of blades (○), leaf sheaths (Δ) and internodes (□) of adult leaves of the main stem *vs.* median length of blades, sheaths and internodes of adult leaves of axillary tillers T_1, T_2, T_3 with the same phytomer rank *N'*; **(b)** Median blade area of adult leaves of the main stem *vs.* median blade area of adult leaves of axillary tillers T_1, T_2, T_3 with the same phytomer rank *N'*, **(c)** Median length of blade of adult leaves of the main stem *vs.* median blade length of adult leaves of axillary tillers T_1, T_2, T_3 with the same phytomer rank *N'* .1:1 line is shown; root mean squared error (RMSE), mean error (ME) and number of samples (n) are given.

3. Senescence

Senescence at leaf scale

Figure 14 shows the progress of total necrotic leaf area for the six upper leaves ($-6 \leq N' \leq -1$) of the main stem for the three density treatments in Y2S2. The total necrotic area within a leaf blade progressed at a low rate up to the time when 10-15% of blade area was necrotic, then at a fast rate, approximately constant up to total leaf death. Senescent tissues appeared on successive leaf layers according to an acropetal sequence, from lower to upper leaves. However, the time interval between necroses of successive leaves was much longer for lower leaves (170-270 °Cd) than for the upper leaves (70°Cd).

Overall, the pattern and the timing of senescence progress for a given leaf did not show much variability between the three densities. A small but not regular trend was found with higher density where senescence onset was slightly delayed (up to 100 °Cd for flag leaf between D1 and D3) for the three upper leaves.

Senescence at the shoot scale

The shoot senescence index followed the typical pattern described in Hillier et al. (2007): a regular increase with thermal time up to the end of stem extension (around 1600°Cd_{12}), followed by a quasi plateau around flowering, up to 1900°Cd_{12}, that is the onset of fast grain filling, then a linear increase corresponding to monocarpic senescence when leaf nitrogen is remobilized towards grain (Fig. 15). This general pattern differed for a given sowing density according to main stem final leaf number: from 1000 °Cd_{12} the rate of senescence progress increased for higher N_{leaf} reaching a difference of one leaf at some cases. The difference in senescence progress was not regular along the shoot development but was yet maintained until the end. Areas of overlap between the direct and indirect senescence measurements showed that there was an important difference and that indirect measurements overestimated senescence. These differences come most probably from the different methods of estimates of senesced tissues. In the direct method, only apical senescent area is considered whereas in the indirect method senesced area includes all non green tissues.

The effect of density was investigated by comparing plants with the same final leaf number (N_{leaf} (0) = 10) from the three density treatments (Fig. 16). Until senescence of leaf 6, the low density treatment showed a slightly higher rate of senescence, and at 1500°Cd_{12} there was approximately half of leaf less in D1 compared to D3. Later the difference decreased and starting from the onset of monocarpic senescence the progress of senescence was the same in all treatments.

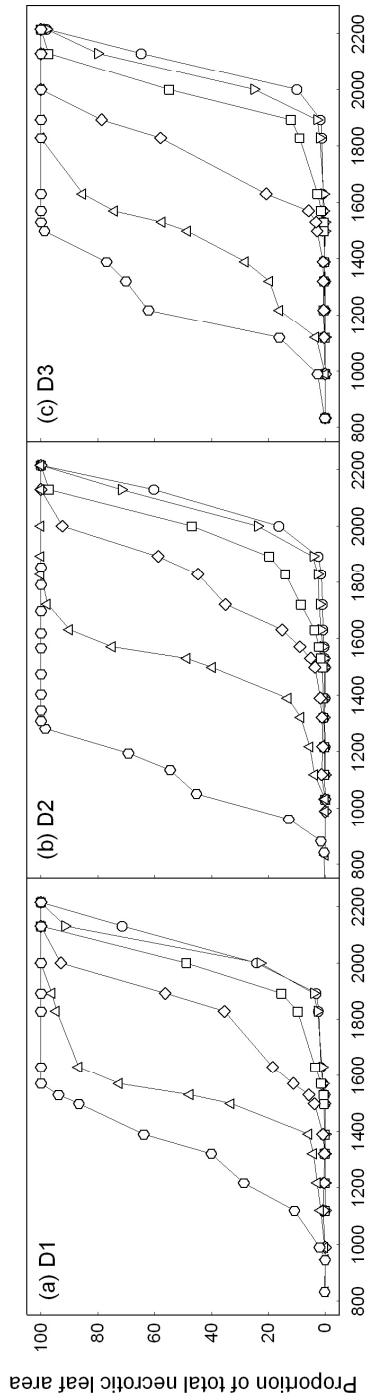

Figure 14. Proportion of total necrotic leaf area for the six upper leaves (*N'*=-1, ○), (*N'*=-2, ▽), (*N'*=-3, □), (*N'*=-4, ◊), (*N'*=-5, Δ) and (*N'*=-6, ⬡) on main stem of winter wheat Cv. 'Soissons' sown in mid November in 2008/2009 (Y2S2) at three sowing densities **(a)** D1: 77 **(b)** D2: 228 and **(c)** D3: 514 plants.m^{-2}.

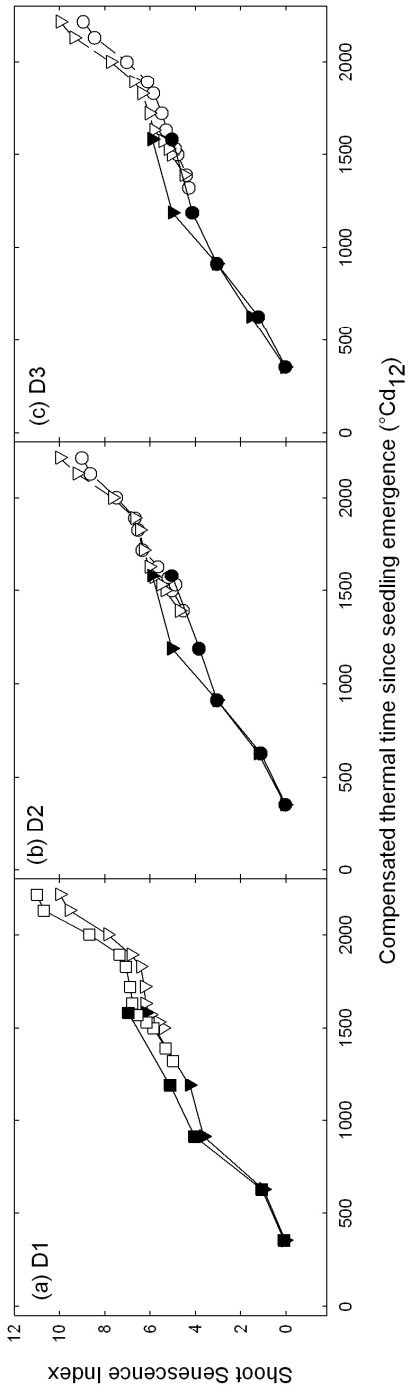

Figure 15. Fractional number of senesced leaves (SSI) *vs.* thermal time as of seedling emergence for main stem of winter wheat Cv. 'Soissons' grown at mid November in 2008/2009 (Y2S2) at three sowing densities: **(a)** D1: 77, **(b)** D2: 228 and **(c)** D3: 514 plants.m^{-2}. Data are pooled by final leaf number N_{leaf} = 9 (○, ●), N_{leaf} = 10 (▽, ▼) and N_{leaf} = 11 (□, ■). Empty symbols are for direct measurements performed on tagged plants in the field and filled symbols are for indirect measurements computed from main stem Haun Stage and fractional number of green leaves.

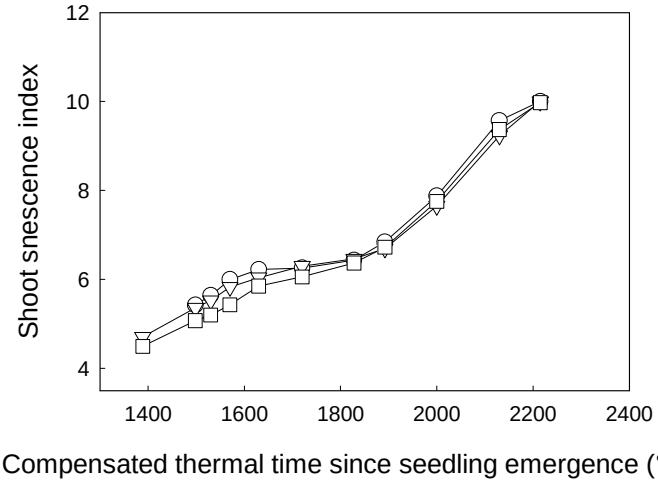

Figure 16. Fractional number of senesced leaves (SSI) *vs.* compensated thermal time since seedling emergence for main stem that had produced 10 final leaves of winter wheat Cv. 'Soissons' grown at mid November 2008 (Y2S2) at three sowing densities: D1 (○), D2 (▽) and D3 (□). D1: 77, D2: 228, D3: 514 plants.m^{-2}.

4. Tillering dynamics

Tillering was much more important in the early sowing treatments compared to the late one (Fig. 17 and Table 6). Indeed, plants of a given density treatment produced up to 3 times more tillers in S1 in comparison to S2. However, the final number of tillers bearing ears was almost the same irrespective of the sowing date (Table 5) which means that there was a high tiller regression in S1, whereas in S2 between 75% (D1) and 90% (D3) of emerged tillers survived until flowering.

At both sowing dates, the low density D1 resulted in the production of the highest number of tillers followed by D2 then D3; but a drastic tiller regression led to the reduction of a high proportion of these tillers. For D2 and D3, tiller regression was much less specially in S2 as mentioned previously.

Table 6
Number of tillers at full tillering (just before tiller regression) and number of tillers bearing ears for winter wheat Cv. 'Soissons' sown in late September in 2007 (Y1S1) and in mid November 2008 (Y2S2) at 3 sowing densities: D1: 77, D2: 228, D3: 514 plants.m^{-2}.

	Y1S1		**Y2S2**	
	Maximum number of tillers	**Final number of tillers bearing ears**	**Maximum number of tiller**	**Final number of tillers bearing ears**
D1	18±0.89	7.7±1.49	8.5±1.05	6.4±0.87
D2	10.8±0.72	3.7±0.59	3.9±0.76	3.4±0.97
D3	6.5±0.45	2.3±0.32	2.1±0.32	1.9±0.97

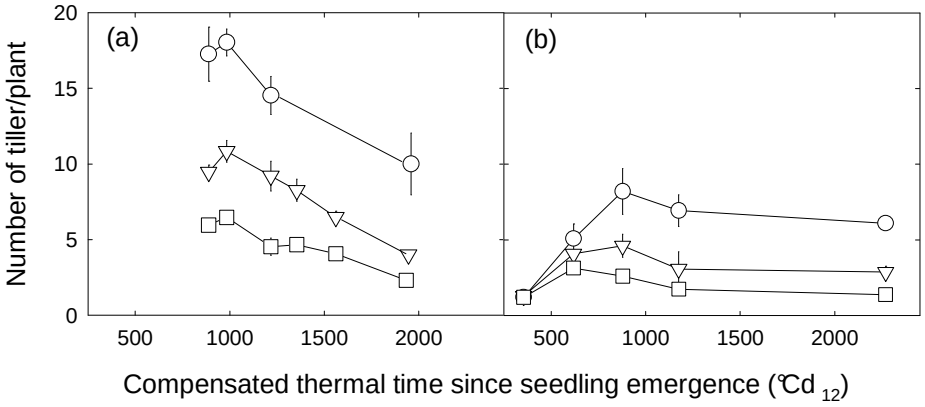

Figure 17. Number of tillers par plant *vs.* compensated thermal time since seedling emergence for winter wheat Cv. 'Soissons' grown at 3 sowing densities: D1 (○), D2 (▽), D3 (□) at **(a)** an early sowing date (S1: late September) in 2007/2008 (Y1) and **(b)** a late sowing (S2: mid November) in 2008/2009 (Y2). D1: 77, D2: 228, D3: 514 plants.m^{-2}. Vertical bars show confidence intervals (α=0.05) when larger than the size of the symbol.

II. Architecture at canopy scale

1. Number of tillers per square meter

For both Y1S1 and Y2S2, a higher number of axes/m² was produced by D3 followed by D2 then D1 (Figure 18A). The number of axes was much higher along the growing season for the three density treatments in the early sowing compared to the late sowing because both actual plant population and number of tillers produced by plant were higher in S1 (cf. section 1.4 and Table 1). In both sowings, there was a drastic tiller regression; thus, the final number of axes after flowering was two to three times (depending on density) smaller that the maximum number produced at end of tillering. However, for the same density, there was still more tillers at the early than at the late sowing (844 *vs.* 460 axes/m² for D2). At plant maturity, differences between density treatments were much reduced despite the persistent sequence following density treatment (D3 > D2 > D1).

2. Ground cover and leaf area index

Concerning the dynamic of ground cover, plants of the high density D3 covered more and faster the soil in a relatively short time compared to the two other densities (Fig. 18B). At the early sowing treatment (Y1S1), the pattern of the ground cover curve differed between densities: for D3, there was a rapid and linear increase of soil cover until 80% followed by a slower rate; whereas for D1, ground cover curve was almost linear all over the growth cycle with a constant slow slope. D2 showed an intermediate pattern between D1 and D3. Finally, shortly before flag leaf ligulation, ground cover reached almost 100% for D3 and D2 and only 66% for D1. However, at the late sowing treatment (Y1S2 and Y2S2), differences between densities were smaller and the pattern of ground cover curves was the same: differences between densities were established between seedling emergence and 500°Cd$_{12}$; thereafter, a linear and constant progress of ground cover was observed with almost the same rate independently of the density. Though, we noticed that this linear trend appeared shortly later for the low density treatment D1 (around 100 to 150 °Cd$_{12}$ after D2 and D3). Thus, to draw a

linear correlation between ground cover and thermal time, we used points measured after 500 °Cd12 for D2 and D3 and only points measured after 600 °Cd_{12} for D1 (Table 7). Indeed, it has been found that ground cover increased with a mean rate of 0.0012 for Y2S2 and 0.0014 for Y1S2. Yet, overall, the high density D3 covered more soil surface in comparisons to D2 and D1.

Table 7
Parameters (*a* and *b*), coefficient of determination (R^2) and number of points used for the linear correlation between ground cover data and compensated thermal time since seedling emergence ($y = ax + b$) of wheat canopy Cv. 'Soissons' grown at 3 sowing densities: D1, D2 and D3 at a late sowing date (S2: mid November) in 2007/2008 (Y1) and 2008/2009 (Y2). D1: 77, D2: 228, D3: 514 plants.m^{-2}.

Year	Sowing	Density	*n*	*a*	*b*	R^2
Y1	**S2**	**D1**	3	0.0016	-0.6386	0.99
		D2	3	0.0018	-0.8608	0.99
		D3	2	0.0014	-0.8497	1
Y2	**S2**	**D1**	4	0.0012	-0.4317	0.99
		D2	4	0.0013	-0.5592	0.98
		D3	3	0.012	-0.7271	0.99

Leaf area index (LAI) increased much faster for D3 in comparison with D2 and D1 (Fig. 18C). Thus, at flag leaf ligulation, the wheat leaf area per meter square was 9.40 and 12.36 for respectively D2 and D3 at S1 and 3.12, 3.71 and 4.69 for respectively D1, D2 and D3 at S2. At flag leaf ligulation, the LAI was higher for the early sowing treatment. The pattern in LAI increase was fairly described by an exponential curve as shown in Figure 18C and Table 5 (R^2>0.96, P>0.0001).

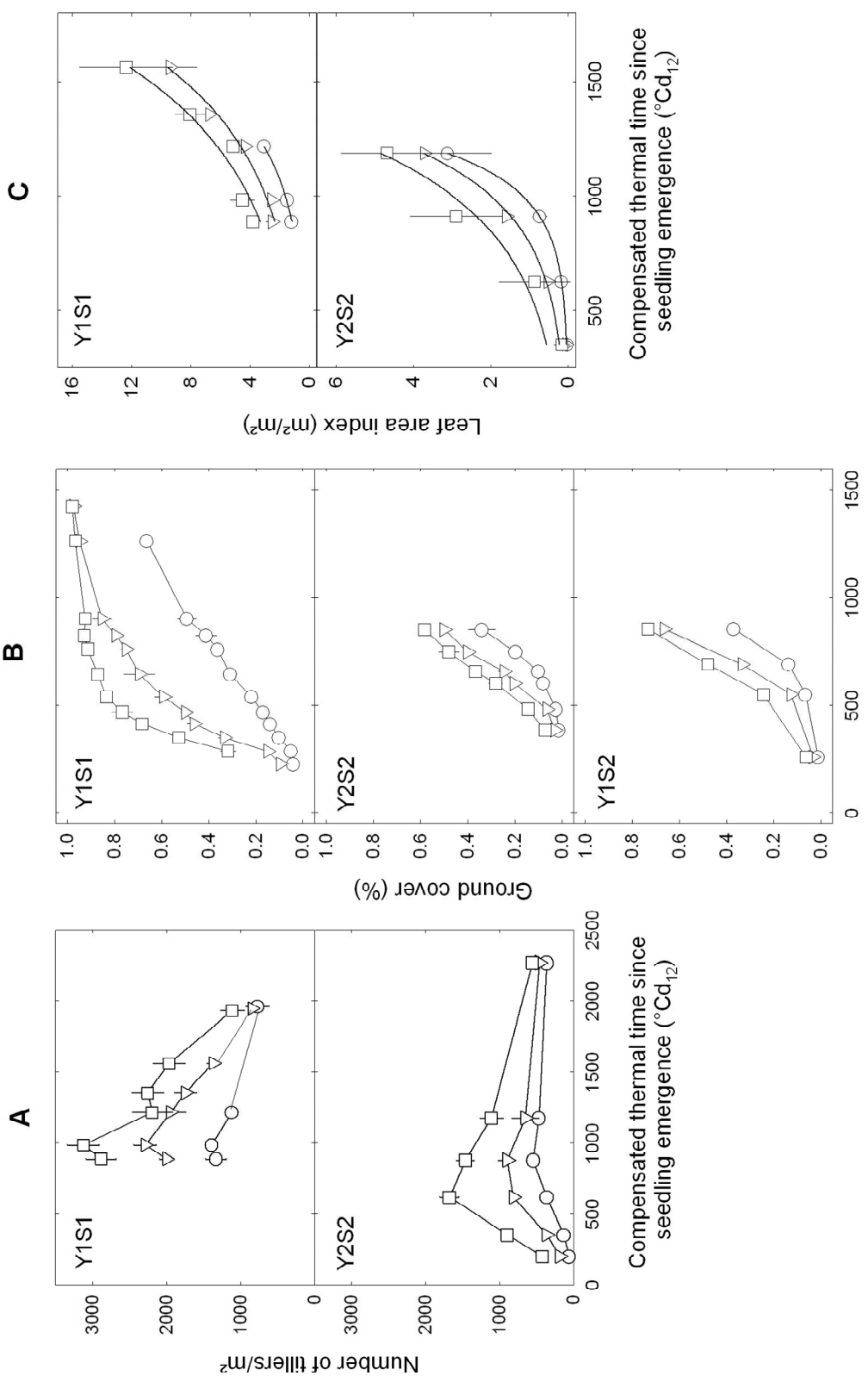

Figure 18. (A) Number of tillers per square meter, **(B)** proportion of ground cover and **(C)** leaf area index (LAI) *vs.* thermal time as of seedling emergence for winter wheat Cv. 'Soissons' sown during two growing seasons: 2007/2008 (Y1) and 2008/2009 (Y2) at two sowing dates: early (S1, late September) and late (S2, mid November) at 3 sowing densities: D1 (○), D2 (▽), D3 (□). D1: 77, D2: 228, D3: 514 plants.m^{-2}. Vertical bars show confidence intervals (α=0.05) when larger than the size of the symbol. Y axis scaling is not the same for leaf area index.

Discussion

This study aimed first at making a comprehensive description of architecture variables at the plant and the canopy scale with respect to different sowing and density treatments and second at producing a dataset of winter wheat architecture for these different treatments which will be used for 3D reconstruction using the model Septo3D (Robert et al., 2008). We studied the pattern of blade, sheath and internode dimensions of main stem (in all treatments) and axillary tillers (in Y2S2) in relation to their position on the stem. When data were available, patterns of organ dimensions were compared between main stems differing in their final number of leaves and between main stem and tillers. Otherwise, we examined the differences of architecture at the canopy level (i.e., number of shoots per square meter, leaf area index and ground cover). Below, results of this section will be discussed according to the two aims.

I. General pattern of organ dimensions and main differences between treatments, plants and tillers

A general pattern describes organ dimensions for a given cultivar and under similar conditions

Patterns of blade, sheath and internode dimensions resembled to those usually found for winter wheat and most broadly for cereals. Such data are mainly available for blade dimensions, whereas much less has been published regarding sheath and internodes. In this regard our dataset usefully contribute to complement existing data. For lower phytomers, sheath length increased only marginally with increasing phytomer rank whereas internodes did not elongate. Sheath and internode dimensions of upper phytomers increased almost linearly with increasing phytomer rank as reported in few previous studies that investigated sheath and internode length in wheat. The typical profile of blade length showed an increase with phytomer rank up to the penultimate leaf, then a decrease for the ultimate leaf.

Patterns of blade length similar to those observed here have been reported for various gramineous, e.g. wheat (Borrill, 1959, Gallagher, 1979, Fournier et al., 2003, Evers et al., 2005), maize (Fournier and Andrieu, 1999b), sorghum (Lafarge et al., 2002, Lafarge and Tardieu, 2002), barley (Buck-Sorlin, 2002) and rice (Tivet et al., 2001, Jaffuel and Dauzat, 2005). Our data do not bring additional understanding to this behaviour but is compatible with what was proposed by previous authors. Bos and Noteboom (1998) observed that leaf elongation rate (LER) increased with main stem leaf position and proposed that LER of a leaf depends on the LER of the previous leaf on the same tiller or of the parent tiller. Such size mediated effect was also proposed by Andrieu et al. (2006) for maize and could contribute to the progressive increase in size for successive leaves. Blade length is responsive to temperature but this would not explain the increase in size starting around leaf 6-7 as they elongate during winter, especially in early sowing. It is likely that the sharp linear increase that occurs here involve change in gibberellin production, in relation to change from vegetative to reproductive phase. Poethig (2003) reported that changes in leaf size and shape and internode elongation among other changes are part of the features that distinguish plant developmental phases which are: juvenile vegetative phase, adult vegetative phase and reproductive phase (Poethig, 1990). In wheat the peak of the blade profile is commonly situated at the penultimate leaf, as observed in our case, whereas in the other species the

decline starts at lower phytomers. Borill (1959) suggested that the decline in leaf length for wheat from a given leaf position is linked to the time of formation of double ridge.

Blade width showed a continuous increase with phytomer rank with the flag leaf being the widest, similar to reports by Pararajasingham and Hunt (1996), Hotsonyame and Hunt (1997), Bos and Noteboom (1998). Here there was no obvious break point that could be related to floral change. Abbe et al. (1941) proposed that the increase in relative width of the successive maize leaves is directly linked to the increasing size of the shoot apex. Light has been also involved in the determinism of leaf width (Friend et al., 1962) but this would not explain the increase in width of successive juvenile leaves as this occurs in autumn when available light is decreasing.

Architecture differences between sowing dates

Variability in the main stem final leaf number was one of the major differences found between sowing date treatments: for all densities, number of leaves was much lower in S2 compared to S1. The early sowing resulted in higher rate of plant emergence, higher number of tillers per plant and despite a higher rate of tiller mortality, a higher number of ear-bearing axes at flowering. Besides, blade and sheath dimensions of juvenile phytomers were significantly higher in early sowing whereas the size of adult phytomers were almost identical for both sowing dates (Fig. 11). Finally for a given density, S1 resulted in a faster rate of progress in ground cover and leaf area index, and finally a higher number of axes per m².

Similarly to many previous studies on wheat (Kirby et al., 1982, 1985, Miglietta, 1989, Brooking et al., 1995, Spink et al., 2000), the final number of leaves decreased with later sowing. In our experiment, early sowing (S1, late September) resulted in the production of 12 to 14 leaves on the main stem and the late sowing (S2, mid november) resulted in 9 to 11 leaves. The median number of leaves on axillary tillers decreased consequently. It has been well established that variations of final leaf number with sowing date are driven by differences of vernalization and photoperiod (Miglietta, 1989, 1991, Hay and Kirby, 1991, Kirby, 1992). The number of final leaves is determined when vernalization requirements of the plant are satisfied (Kirby et al., 1985, Kirby, 1992). In early sowing, mild autumn temperatures result in plants with a high rate of leaf initiation while vernalization proceeds slowly. In late sowing, the rate of leaf initiation is slower and the vernalization progresses more rapidly resulting in a consequent reduction in the number of leaves (Kirby et al., 1985). There is an interaction between vernalization and photoperiod in relation to number of leaves on the main stem but the Cv. 'Soissons' is know to have very little influence of photoperiod on leaf number (J. Legouis, pers comm.). In our experiment, difference in the total number of leaves came from variations in the number of juvenile leaves whereas the number of adult leaves was quasi stable (4 to 5). Similarly, Kirby (1990) found that plants sown increasingly later (i.e., with decreasing final number of leaves) produced less leaves before beginning of rapid stem elongation whereas they produced almost the same number of leaves after this time.

The typical pattern of organ dimensions varied between sowing dates especially for the juvenile phytomers. Early sown plants had longer and wider juvenile leaf blades while sheaths had almost the same length as in late-sown plants. Besides, for the early sowing, there were no or few changes in blade length for leaves up to leaf 7, similarly to what has been observed by Gallagher (1979) and Kirby et al. (1982), whereas for the late sowing there was a small increase of size for successive juvenile leaves. Temperature and photoperiod are the major factors invoked to explain differences of blade size. The lower juvenile leaves of the early sowing treatment emerged during long photoperiod and warm temperature days in

comparison to those from the late sowing. Later juvenile leaves in early sowing emerged in conditions of lower temperatures and shorter days.

Many authors agree upon the fact that low temperatures result in a reduction of wheat leaf size (Kirby, 1982; Hotsonyame and Hunt, 1997). Effects of photoperiod are though more controversial: some authors invoked that long days enhance leaf size (Friend et al., 1962, Pararajasingham and Hunt, 1996) while others found no effect of photoperiod (Hotsonyame and Hunt, 1997). These results may just represent each one part of the story as (i) the different studies did not explore the same range of photoperiods and (ii) different cultivars may have different responses (iii) Kirby et al. (1982) suggested that the temperature and daylength may interact so that the combination of short days (less than 12h) and low temperatures (less than 8°C) lead to the stagnation in leaf length which, according to the authors, adapt the plant to withstand hard environmental conditions.

On the contrary, for the adult phytomers, the dimensions of leaf blades, sheaths and the two uppermost internodes were almost identical for the two sowing treatments grown during the same season (Fig. 11). This could be fairly explained by the fact that adult phytomers grew approximately at the same time and under similar conditions in spring independently of the sowing date; the date of flowering also changed very little. However, lower elongated internodes were slightly longer in the early sowing which resulted in taller plants at flowering.

For a given sowing density, early-grown plants were more successful to emerge (Table 1) and produced more tillers per plant than late-grown plants which is probably linked to longer tillering period. Nonetheless, after flowering, number of tillers per plant was almost the same for S1 and S2 (Table 6) meaning that a much higher number of tillers regressed in S1. However, at the canopy scale, a higher number of axes was maintained at flowering for S1 compared to S2. These observations are similar to those by Spink et al. (2000): these authors observed a lower probability of seedling emergence in later sowing (such difference could probably originate from the cold temperatures experienced during plant emergence in the late-sown plants); further, they observed that the maximum number of shoots per plant increased linearly with main stem final leaf number and thermal time to full vernalization i.e., it was higher in early sowings. Finally they reported also a higher rate of tiller survival in late sowing date.

As a consequence to above-mentioned differences in tillering between S1 and S2, soil coverage and leaf area production progressed much faster in S1 than in S2, and at flowering earlier sowing had produced a higher number of axes of individual size similar to those in the late sowing.

Architecture differences between plant population densities

In our experiment, the median number of leaves on the main stem decreased slightly with increasing density. For the juvenile phytomers, no density effect on organ dimensions was observed. For the adult phytomers, density effect was marked for leaf blades which were longer and wider for lower density, whereas the effect was smaller on sheaths and was absent on internodes. At the canopy scale, the low density resulted in the production of the highest number of tillers per plant, but this by far did not compensate for the lower number of plants : any time during crop development the high density treatment resulted in a higher leaf area index and ground cover that lower density treatments.

A decrease of median number of leaves on the main stem with higher plant density was observed in all cases except in Y1S2 where all density treatments resulted in the same major final leaf number. Generally, a difference of one leaf was found in the median final leaf number between low (D1) and high (D3) density. This appears to follow a general trend, as a

similar decrease in the median number of leaves on the main stem with high density has been reported on barley (Kirby and Faris, 1972) and maize (Andrieu et al., 2004).

No difference was observed between density treatments on blade dimensions during the juvenile phase nor on sheath and internode during all the wheat development. It is widely reported that high densities result in an increase of leaf and sheath length on juvenile phytomers (Ballaré and Casal, 2000, Andrieu et al., 2006). These features among others are part of the "shade avoidance syndrome" defined as the set of responses to low R:FR that allow the plant to perceive early competition for light and to adapt its behaviour accordingly (Casal and Smith, 1989, Skinner and Simmons, 1993). While such responses likely exist in all species we did not find clear report of identifying them in field-grown wheat and we speculate they were not large enough to induce visible changes in organ dimensions.

Otherwise, in agreement with Andrieu et al. (2004) working on maize, a decrease of blade length and width was found for adult phytomers in high density. Similar behaviour was observed by Evers et al. (2005) on spring wheat. Some authors proposed that a reduction of leaf extension rate, following the lack of carbohydrate may be responsible for the shorter length of upper leaves. Andrieu et al. (2006) proposed an alternative view: although they reported for maize a similar decrease in final length for the upper leaves at high density, leaf extension rate was not lower but instead somewhat higher. They showed that the shorter length resulted of a shorter duration of extension, linked to a delay in the onset of leaf extension while the timing of development of leaf ligule was unaffected. In our case, leaf ligulation was not affected by density (cf. chapter 1) but we did not record the onset of leaf extension so that it is not possible to determine whether the process behind reduced leaf length is the same.

The number of tillers per plant was increased for the low density D1 compared to D2 and D3 as usually observed while reducing plant density (Kirby and Faris, 1972, Darwinkel, 1978, Spink et al., 2000, Whaley et al., 2000) and despite a high tiller regression for D1, the difference in tiller number was maintained until flowering. According to Whaley et al. (2000) and Spink et al. (2000), the higher shoot production comes from longer duration of tillering rather than enhanced tiller production rate. Darwinkel (1978) reported also that shoot survival increased as plant density was reduced. Besides, the number of tillers per plant is related to the intensity of photosynthetically active radiation (PAR) (Bos, 1999) and the ratio between the intensities of red and far-red light (R:FR) (Evers, 2006). Recent studies on light conditions inside wheat canopies (Sparkes et al., 2006, Evers et al., 2006) agreed that bud tillers remain dormant below a specific threshold of R:FR ratio, which explains thus the low number of tillers per plant in high density stands. However, high density treatments resulted in faster ground cover and higher leaf area index in comparison to the low one. Therefore, differences in tillering, number of leaves and leaf dimensions did not compensate for the differences in plant population density; differences in ground cover and LAI were maintained until the end of the wheat cycle.

Variability of architecture between plants differing in the final leaf number

Number of leaves produced on the main stem varied amongst plants of the same treatment and number of leaves on axillary tillers varied amongst plants with the same N_{leaf} (0). Besides, vertical profiles of main stem organs varied according to final leaf number: main stems with a higher number of leaves produced lower organ dimensions for the juvenile phytomers and higher organ dimensions for the adult phytomers.

In each sowing date*density treatment, a major final leaf number (50 to 90%) and one or two less frequent values were found for the main stem (Fig. 3) in agreement with results reported for wheat (Brooking et al., 1995, Hotsonyame and Hunt, 1997) and rice (Jaffuel and

Dauzat, 2005). The reason for the variation of final leaf number on an axis is unknown but one could speculate that variations in final leaf number between and within treatments arises from the same cause which may be local variations of plant density leading to an early effect of light quality. This hypothesis makes sense especially that in the case where no variation of leaf number was found between density treatments, there were also few variations within treatments (Y1S2).

Organ dimensions varied according to final leaf number. For juvenile leaves, the tendency was that plants that produced more leaves, have shorter and narrower leaf blades. For adult phytomers, on the contrary, blades, sheaths and internodes were longer for plants with higher final leaf number. It is possible that plants that produced a high number of leaves had a bigger shoot apex meristem which could explain their higher sizes. Indeed, several authors have reported an association between the diameter of the shoot apex meristem and the blade size (Abbe et al., 1941). However, this does not explain why leaf dimensions were lower for plants with high N_{leaf} for juvenile phytomers.

Differences between main stem and axillary tillers

Final leaf number of primary tillers varied for a given tiller rank. The mean value of final leaf number decreased linearly with increasing tiller rank. To investigate the similarity in leaf organ dimensions between tillers, we compared patterns of organ dimensions between tillers for the same phytomer rank counted basipetally Adult phytomers of main stem and tillers T_1, T_2, T_3 for the same phytomer rank had the same organ dimensions.

For a given N_{leaf} modality, final leaf number of a tiller *k* was variable. The number of leaves on primary tillers varied i.e., there was a major number with one or two other less frequent values (Fig. 4); N_{leaf} of tillers T_1, T_2, T_3 was linearly correlated to N_{leaf} of the main stem for a given sowing date treatment. The first axillary tiller produced mainly three leaves less than the main stem. The decrease in the mean final leaf number for successive tillers ─starting from T_1─ was less than one leaf differing thus from reports by Masle-Meynard and Sebillote (1981). The cumulative final leaf number (N_{leaf}^{Cum}) was linearly correlated to the tiller rank.

Adult phytomers of main stem and tillers T_1, T_2, T_3 for the same phytomer rank counted from the top had the same organ dimensions. This is similar to the approach applied by Fournier et al. (2003) and Evers et al. (2005) respectively for winter and spring wheat. However, these authors counted phytomers acropetelly and added a phytomer shift (a decimal number), characteristic for each tiller, to the actual rank so as to obtain a relative phytomer rank. Alternatively, Bos and Noteboom (1998) used a "summed phytomer number" which amounts to apply a phytomer shift that is an integer. This is nearly equivalent to the basipetal numbering used in our case, but not fully since the decrease in total leaf number for successive tillers is lower than one. We did not attempt to compare all these solutions. Given the variability of the number of leaves per axis between plants in our experiment our solution to count phytomers from the top of each axis, had the advantage to be easy to use and reasonably accurate.

Using this approach, a high degree of stability in the pattern of adult organ dimensions was found between tillers including the main stem. The length of the adult leaf blades, sheaths and internodes were almost the same regardless of tiller rank (Fig.11 and 12). The fact that adult phytomers of main stem and axillary tillers grew almost at the same time and thus under similar conditions may explain or at least contribute to this convergence. This was already reported for wheat (Bos and Noteboom, 1998; Evers et al., 2005) and rice (Tivet et al., 2001). Besides, the peak of blade length was found to occur at the same time for main stem and

tillers which suggest that the mechanism involved in this change of blade length is triggered at the level of the whole plant.

The virtue of the established relation in final number of leaves and the stability in organ size between main stem and tiller dimensions, outlined above, is that detailed measurements of number and dimensions of organ can be carried out on main stem only and the same properties can be modelled for all axes introducing the appropriate shift for each tiller rank. However, for juvenile leaves, blade length was higher for higher tiller rank similarly to what has been observed on rice (Jaffuel and Dauzat, 2005).

II. Ability to reproduce wheat architecture with a 3D model using the collected data

Because of non accuracy of phytomer rank identification in the first experimental year and architecture modification by bird damages in the early sowing of the second year, the most accurate and complete dataset of architecture corresponded to late sowing of the second experimental year. Data of plant architecture from this treatment were used for wheat reconstruction with the model Septo3D (cf. Chapter 3) and were given as input. For recall, input tables of the canopy model are (i) the rate of leaf appearance and senescence for each axis, (ii) the tillering dynamic of the plant, (iii) the dimensions of mature plant organs and, (iv) the geometry of leaves. Here, we discuss with respect to the organisation of the canopy model presented above, to which extent the collected data are representative of the wheat canopy for the different treatments and if they allow for a good parameterisation of the model.

The rate of leaf appearance and senescence for each axis

The rate of leaf appearance was monitored on main stem and primary tillers for almost all the treatments (except Y2S1D2). The measurements allowed proposing a descriptive model of phyllochron (cf. chapter 1). For sake of simplification and for time and technical constraints, in our experiment we chose to omit measuring the rate of leaf appearance for secondary tillers. So far, very few studies have performed this kind of measurements (Bos and Neuteboom, 1998; Evers et al., 2005), but not for field-grown wheat. In addition, detailed measurements of senescence were performed only for the main stem in Y2S2. To overcome this lack of information concerning secondary tillers, we adopted the principle of cohort advanced by Masle-Meynard and Sebillote (1981) for the coordination of tiller emergence assuming that tillers of the same cohort share the same properties of leaf appearance and senescence. At the moment, this approach has been implemented in the current model without specific validation.

The tillering dynamic of the plant

Punctual measurements of the total number of tillers and the frequency of occurrence of primary tillers were performed for all the treatments but these data were not enough to fully describe tiller dynamics. Thus a tillering dynamic model was used (Dornbusch, unpub. res.) following the assumption of coordination between leaf and tiller emergence (Masle-Meynard, 1981) and the Fibonacci sequence for the determination of the potential number of tillers produced in each cohort. Experimental data were used to estimate the fraction (actual/potential) of tillers that did emerge and to estimate the rate of tiller regression, supposed to take place at a constant rate between the onset of stem extension and flowering. Resulting tillering dynamics simulated by the model were close to observed data (cf. Fig 3b in Chapter 3). Finally, despite the limited number of available data on tillering, this approach allowed to adequately parameterize tiller dynamics. This means that for modelling purposes,

it is possible to alleviate measurements and that punctual data at specific period of the wheat development (e.g., flag leaf ligulation, flowering, etc.) are sufficient to reconstruct tiller dynamic when combined to simple behavioral rules. However, in our experiment, total number of tillers was determined at harvest times which were stopped at flag leaf ligulation, excepted for the final number of ears measured after flowering. Thus we lacked measurement to assess the accuracy of a constant rate of tiller regression.

Dimensions of mature organs

As for the rate of leaf appearance, measurements of leaf dimensions for the secondary tillers were not performed and again the principle of cohorts was applied i.e., we supposed that secondary tillers have the same organ dimensions of the primary tiller of the same cohort. This assumption represents a possible source of error as a secondary tiller of a given cohort can hardly show the same organ dimensions than the primary tiller from that cohort especially if, genealogically it is located far from the main stem. However, given that the reconstructed canopy corresponded to a late sowing and that few secondary tillers developed at this sowing treatment, this should not induce a substantial error in the simulated leaf area index.

Geometry of organs

Geometry for azimuth of leaves and curvature of leaf midribs were not measured in our experiment. Leaf curvature was therefore parameterized based on data from another experiment carried out with the same cultivar at the same location at density of 250 plant.m-2 (Ljutovac, 2002). Thus, leaf posture was parameterised similarly for all densities whereas it is known that density influences the plant posture in the sense that leaves on plants sown in dense stands are more erected than those on plants sown in sparse stands. Following results of Ledent (1977, 1978) on changes in leaf angle, in the current parameterisation, leaves are considered vertical before collar appearance; and from collar appearance until total senescence, leaf curvature changes at each phyllochron interval so that the leaf bends increasingly down until reaching its final position. This approach allowed giving a realistic and dynamic leaf and plant shape. In previous works of virtual wheat simulation (Fournier et al., 2003; Evers et al., 2005), this dynamic aspect of leaf geometry was not taken into consideration; it was rather assumed that shape and inclination of leaves did not change after ligulation. Nonetheless, this approach still needs to be improved by distinguishing the pattern of leaf curvature for juvenile and adult leaves. In fact, in reality, leaves on non-elongated internodes have a rosette habit and thus present a flattened posture compared to those on elongated internodes.

Detailed parameterization of leaf geometry is of high interest to investigate disease propagation (Lovell et al., 1997) movement of liquid water (Bassette and Bussière, 2008), light interception at the leaf and plant scale (Chelle et al., 2009).

Difficulties and improvements of the sampling protocol

More broadly, difficulties in producing complete and accurate data of architecture measurements in our experiment came mainly from the conditions of field-grown winter wheat and from the wheat morphology itself. In fact, field-grown wheat is subject to many biotic and abiotic factors likely to disturb its architecture. Hence, soil heterogeneity, differences of seed depth at sowing, heterogeneity of emergence, climate hazard as well as local nutrient shortage and pest and disease pressure, are all factors that could disrupt, or even destroy the plant and canopy architecture.

In comparison to monoculm cereals, wheat presents a relatively complex architecture due to the production of a more or less important number of tillers. Therefore, if we are to reconstruct accurately wheat plant architecture, we need to characterize and parametrise a

given number of supplementary parameters in relation to the tillering dynamic, frequency of occurrence of tillers and their dimensions. Subsequently, wheat architecture simulation in virtual plants appears to be more challenging than other cereals that do not make tillers such as maize widely studied and simulated in virtual plants (Fournier and Andrieu, 1999a, Fournier and Andrieu, 1999b).

With these difficulties in mind, one could better think future experiments aimed to collect data for wheat architecture simulation:

- It seems more interesting to study a reduced number of treatments which allow processing more plants per treatment and cover thus all the variability of plants in the field. In our experiment, six treatments (two sowing dates x three densities) were monitored. In order to handle all the treatments during a harvest, we reduced the number of processed plants to only 15 plants/treatment. In the case of the high density treatment (more than 400 plant/m²), this number is very small; there was thus a risk that the sampling plants could be not representative of the field canopy.
- Measurements at the plant scale can not be extrapolated at the canopy scale such as the leaf area. Indeed, a small bias for a subsample of 15 plants can create a big bias at the square meter. Therefore, it is necessary to distinguish plant measurements (e.g., dimensions) from canopy measurements (e.g., LAI) by using separate and appropriate samples for each purpose.

References

Abbe EC, Randolph LF, Einset J. 1941. The developmental relationship between shoot apex and growth pattern of leaf blade in diploid maize. *American Journal of Botany*, **28**: 778-784.

Andrieu B, Hillier J, Birch C. 2006. Onset of sheath extension and duration of lamina extension are major determinants of the response of maize lamina length to plant density. *Annals of Botany*, **98**: 1005-1016.

Andrieu B, Moulia B, Maddonni G, Birch C, Sonohat G, Sohbi Y, Fournier C, Allirand JM, Chartier M, Hillier J, Drouet J-L, Bonhomme R. 2004. Plasticity of plant architecture in response to density: using maize as a model. In: Godin C, Hanan J, Wingfried Kurth, Lacointe A, Takenaka A, Prusinkiewicz P, Dejong T, Beveridge C, Andrieu B eds. *4th International Workshop on Functional Structural Plant Models (FSMP04).* C. Godin et al ed. Montpellier (FRA), UMR Cirad-Cnrs-Ephe-Inra-Inria-Ird-Université de Montpellier II "Botanique et Bioinformatique de l'Architecture des Plantes" (AMAP).

Ballaré CL, Casal JJ. 2000. Light signals perceived by crop and weed plants. *Field Crops Research*, **67**: 149-160.

Bassette C, Bussière F. 2008. Partitioning of splash and storage during rainsdrop impacts on banana leaves. *Agricultural and Forest Meteorology*, **148**: 991-1004.

Borrill MART. 1959. Inflorescence initiation and leaf size in some *gramineae*. *Annals of Botany*, **23**: 217-227.

Bos HJ. 1999. *Plant morphology, environment, and leaf area growth in wheat and maize* PhD thesis, Wageningen University and Research Center. pp. 149, Wageningen, the Netherlands.

Bos HJ, Neuteboom JH. 1998. Growth of individual leaves of spring wheat (Triticum aestivum L.) as influenced by temperature and light intensity. *Annals of Botany*, **81**: 141-149.

Brooking IR, Jamieson PD. 2002. Temperature and photoperiod response of vernalization in near-isogenic lines of wheat. *Field Crops Research*, **79**: 21-38.

Brooking IR, Jamieson PD, Porter JR. 1995. The influence of daylength on final leaf number in spring wheat. *Field Crops Research*, **41**: 155-165.

Buck-Sorlin GH. 2002. L-system model of the vegetative growth of winter barley (*Hordeum vulgare* L.). In: Polani D KJ, Martinez T, eds ed. *Fifth German Workshop on Artificial Life.* Lubeck, Germany, Akademische Verlagsgesellschaft Aka GmbH.

Casal JJ, Smith H. 1989. The function, action, and adaptive significance of phytochrome in light-grown plants. *Plant, Cell and Environment*, **12**: 855-862.

Casey IA, Brereton AJ, Laidlaw AS, McGilloway DA. 1999. Effects of sheath tube length on leaf development in perennial ryegrass (Lolium perenne L.). *Annals of Applied Biology*, **134**: 251-257.

Chelle M, Liu S, Ney B. 2009. Which air temperature drives epidemiological processes of fungal foliar wheat diseases at leaf scale? *Association Francaise de Protection des Plantes, 9eme conference international sur les maladies des plantes, Tours, France, 8 et 9 Decembre 2009.*

Dale JE. 1982. Some effects of temperature and irradiance on growth of the first four leaves of wheat, *Triticum aestivum*. *Annals of Botany*, **50**: 851-858.

Darwinkel. 1978. Patterns of tillering and grain production of winter wheat at a wide range of plant densities. *Netherlands Journal of Agricultural Science,* **26**: 383-398.

Dornbusch T, Andrieu B. 2010. Lamina2Shape - an image processing tool for an explicit description of lamina shape tested on winter wheat (*Triticum aestivum* L.). *Computers and Electronics in Agriculture,* **70**: 217-224.

Dornbusch T, Baccar R, Watt J, Hillier J, Bertheloot J, Fournier C, Andrieu B. 2010a. Plasticity of winter wheat modulated by sowing date, plant population density and nitrogen fertilisation: Dimensions and size of leaf blades, sheaths and internodes in relation to their position on a stem. *Field Crops Research,* **(accepted for publication 2.12.2011)**.

Dornbusch T, Watt J, Baccar R, Fournier C, Andrieu B. 2010b. A comparative analysis of lef shape of wheat, barley and maize using an empirical shape model. *Annals of Botany*: Available online. doi: 10.1093/aob/mcq181.

Equiza MA, Tognetti JA. 2002. Morphological plasticity of spring and winter wheats in response to changing temperatures. *Functional Plant Biology,* **29**: 1427-1436.

Evers JB. 2006. Tillering in spring wheat: a 3D virtual plant modelling study. *Tillering in spring wheat: a 3D virtual plant modelling study.*

Evers JB, Vos J, Andrieu B, Struik PC. 2006. Cessation of tillering in spring wheat in relation to light interception and red:far-red ratio. *Annals of Botany,* **97**: 649-658.

Evers JB, Vos J, Fournier C, Andrieu B, Chelle M, Struik PC. 2005. Towards a generic architectural model of tillering in Gramineae, as exemplified by spring wheat (Triticum aestivum). *New Phytologist,* **166**: 801-812.

Fournier C, Andrieu B. 1999a. ADEL-Maize: a crop model based on L-Systems. Application to simulation of plant-to-plant competition. *XVI International Botanical Congress.* Saint Louis, Missouri (USA).

Fournier C, Andrieu B. 1999b. ADEL-maize: an L-system based model for the integration of growth processes from the organ to the canopy. Application to regulation of morphogenesis by light availability. *Agronomie,* **19**: 313-327.

Fournier C, Andrieu B, Ljutovac S, Saint-Jean S. 2003. ADEL-wheat: A 3D architectural model of wheat development. In: Hu B-G, Jaeger M eds. *Proceedings of International Symposium of Plant Growth Modeling and Applications.* Beijing, China. 2003 Tsinghua University Press - Springer Verlag.

Francis D, Barlow P. 1988. Temperature and the cell cycle. In: Long SP, Woodward FI eds. *Plants and Temperature.* Company of Biologists: Cambridge. pp. 181-202.

Friend DJC, Helson VA, Fisher JE. 1962. Leaf growth in Marquis wheat, as regulated by temperature, light intensity and daylength. *Canadian Journal of Botany,* **40**: 1299-1311.

Gallagher JN. 1979. Field studies of cereal leaf growth. I. Initiation and expansion in relation to temperature and ontogeny. *Journal of Experimental Botany,* **30**: 625-636.

Hay RKM, Kirby EJM. 1991. Convergence and synchrony-a review of the coordination of development in wheat. *Australian Journal of Agricultural Research,* **42**: 661-700.

Holmes MG. 1981. Spectral distribution of radiation within plant canopies. *Plants and the daylight spectrum (ed. H. Smith). Academic Press, London*: 147-158.

Hotsonyame GK, Hunt LA. 1997. Sowing date and photoperiod effects on leaf appearance in field-grown wheat. *Canadian Journal of Plant Science*, **77**: 23-31.

Jaffuel S, Dauzat J. 2005. Synchronism of leaf and tiller emergence relative to position and to main stem development stage in a rice cultivar. *Annals of Botany,* **95**: 401-412.

Kaitaniemi P, Room PM, Hanan JS. 1999. Architecture and morphogenesis of grain sorghum, Sorghum bicolor (L.) Moench. *Field Crops Research,* **61**: 51-60.

Kemp DR, Blacklow WM. 1982. The responsiveness to temperature of the extension rates of leaves of wheat growing in the field under different levels of nitrogen fertilizer. *Journal of Experimental Botany*, **33**: 29-36.

Kirby EJM. 1990. Co-ordination of leaf emergence and leaf and spikelet primordium initiation in wheat. *Field Crops Research,* **25**: 253-264.

Kirby EJM. 1992. A field study of the number of main shoot leaves in wheat in relation to vernalization and photoperiod. *Journal of Agricultural Science,* **118**: 271-278.

Kirby EJM, Appleyard M, Fellowes G. 1982. Effect of sowing date on the temperature response of leaf emergence and leaf size in barley. *Plant Cell and Environment,* **5**: 477-484.

Kirby EJM, Appleyard M, Fellowes G. 1985. Effect of sowing date and variety on main shoot leaf emergence and number of leaves of barley and wheat. *Agronomie,* **5**: 117-125.

Kirby EJM, Faris DG. 1972. The effect of plant density on tiller growth and morphology in barley. *Journal of Agricultural Science, Cambridge,* **78**: 281-288.

Lafarge T, Tardieu F. 2002. A model co-ordinating the elongation of all leaves of a sorghum cultivar was applied to both Mediterranean and Sahelian conditions. *Journal of Experimental Botany,* **53**: 715-725.

Lafarge TA, Broad IJ, Hammer GL. 2002. Tillering in grain sorghum over a wide range of population densities: Identification of a common hierarchy for tiller emergence, leaf area development and fertility. *Annals of Botany,* **90**: 87-98.

Ledent JF. 1977. Anatomical aspects of leaf angle changes during growth in wheat. *Phytomorphology,* **26**: 309-315.

Ledent JF. 1978. Changes in the angle and curvature of the uppermost leaves on winter wheat. *J. Agric. Sci., Camb.*, **90**: 319-323.

Ljutovac S. 2002. *Coordination dans l'extension des organes aériens et conséquences pour les relations entre les dimensions finales des organes chez le blé,* PhD thesis, Institut National Agronomique Paris-Grignon, Paris, France.

Louarn G, Andrieu B, Giauffret C. 2010. A size-mediated effect can compensate for transient chilling stress affecting maize (Zea mays) leaf extension. *New Phytologist,* **187**: 106-118.

Lovell DJ, Parker SR, Hunter T, Royle DJ, Coker RR. 1997. Influence of crop growth and structure on the risk of epidemics by Mycosphaerella graminicola (Septoria tritici) in winter wheat. *Plant Pathology,* **46**: 126-138.

Masle-Meynard J. 1981. Elaboration of ear number in a population of winter wheat subjected to competition for nitrogen. I. Evidence of a critical state for elongation of a tiller. *Agronomie,* **1**: 623-631.

Masle-Meynard J, Sebillotte M. 1981. Study of the heterogeneity of a winter wheat stand. II. Origin of the different sorts of individuals in the stand; factors allowing description of its structure. *Agronomie,* **1**: 217-223.

Miglietta F. 1989. Effect of photoperiod and temperature on leaf initiation rates in wheat (Triticum spp.). *Field Crops Research,* **21**: 121-130.

Miglietta F. 1991. Simulation of wheat ontogenesis. II. Predicting dates of ear emergence and main stem final leaf number. *Climate Research,* **1**: 151-160.

Pararajasingham S, Hunt LA. 1996. Effects of photoperiod on leaf appearance rate and leaf dimensions in winter and spring wheats. *Canadian Journal of Plant Science,* **76**: 43-50.

Poethig RS. 1990. Phase Change and the Regulation of Shoot Morphogenesis in Plants. *Science* **250**: 923-930.

Poethig RS. 2003. Phase change and the regulation of developmental timing in plants. *Science,* **301**: 334-336.

Prévot L, Aries F, Monestiez P. 1991. Modélisation de la structure géomètrique du maïs. *Agronomie,* **11**: 491-503.

Robert C, Fournier C, Andrieu B, Ney B. 2008. Coupling a 3D virtual wheat (Triticum aestivum) plant model with a Septoria tritici epidemic model (Septo3D): a new approach to investigate plant-pathogen interactions linked to canopy architecture. *Functional Plant Biology,* **35**: 997-1013.

Skinner RH, Simmons SR. 1993. Modulation of leaf elongation, tiller appearance and tiller senescence in spring barley by far-red light. *Plant, Cell and Environment,* **16**: 555-562.

Slafer GA, Connor DJ, Halloran GM. 1994. Rate of leaf appearance and final number of leaves in wheat: effects of duration and rate of change of photoperiod. *Annals of Botany,* **74**: 427-436.

Sparkes DL, Holmes SJ, Gaju O. 2006. Does light quality initiate tiller death in wheat? *European Journal of Agronomy,* **24**: 212-217.

Spink JH, Semere T, Sparkes DL, Whaley JM, Foulkes MJ, Clare RW, Scott RK. 2000. Effect of sowing date on the optimum plant density of winter wheat. *Annals of Applied Biology,* **137**: 179-188.

Tivet F, Pinheiro BdS, Raissac Md, Dingkuhn M. 2001. Leaf blade dimensions of rice (Oryza sativa L. and Oryza glaberrima Steud.). Relationships between tillers and the main stem. *Annals of Botany,* **88**: 507-511.

Whaley JM, Sparkes DL, Foulkes MJ, Spink JH, Semere T, Scott RK. 2000. The physiological response of winter wheat to reductions in plant density. *Annals of Applied Biology,* **137**: 165-177.

Wilson RE. 1985. The role of the sheath tube in the development of expanding leaves in perennial ryegrass. *Annals of Applied Biology,* **106**: 385-391.

Woodward FI, Friend AD. 1988. Controlled environment studies on the temperature responses of leaf extension in species of *Poa* with diverse altitudinal ranges. *Journal of Experimental Botany,* **39**: 411-420.

Chapter 3

Modelling the effect of wheat canopy architecture as affected by sowing density on *Septoria tritici* epidemics using a coupled epidemic-virtual plant model

Annals of botany (published)

Modelling the effect of wheat canopy architecture as affected by sowing density on *Septoria tritici* epidemics using a coupled epidemic-virtual plant model

Rim Baccar[1,2], Christian Fournier[3,4], Tino Dornbusch[1,2], Bruno Andrieu[1,2], David Gouache[5], Corinne Robert[1,2*]

[1] INRA, UMR 1091 EGC, F-78850 Thiverval-Grignon, France.
[2] AgroParisTech, UMR 1091 EGC, F-78850 Thiverval-Grignon, France.
[3] INRA, UMR 759 LEPSE, 2 Place Viala, F-34060 Montpellier, France
[4] SupAgro, UMR 759 LEPSE, 2 Place Viala, F-34060 Montpellier, France
[5]ARVALIS-Institut du végétal, Service Génétique et Protection des Plantes, IBP-Université Paris Sud, Rue de Noetzlin- Bat. 630, F-91405 ORSAY CEDEX, France

* *Corresponding author: Corinne.Robert@grignon.inra.fr*

Abstract

- *Background and Aims* The relationship between *Septoria tritici*, a splash-dispersed disease, and its host is complex because of the interactions between the dynamic plant architecture and the vertical progress of the disease. The aim of this study is to test the capacity of a coupled virtual wheat-*Septoria tritici* epidemic model (Septo3D) to simulate disease progress on the different leaf layers for contrasted sowing density treatments.

- *Methods* A field experiment was performed with winter wheat Cv. 'Soissons' grown at three contrasted densities. Plant architecture was characterized to parameterise the wheat model and disease dynamic was monitored to compare with simulations. We defined three simulation scenarios differing by the degree of detail with which plant variability of development was represented.

- *Key Results* Despite architectural differences between density treatments, few differences were found in disease progress; only the lower density treatment resulted in a slightly higher rate of lesion development. Model predictions were consistent with field measurements but did not reproduce the higher rate of lesion progress in the low density. The canopy reconstruction scenario in which inter-plant variability was taken into account yielded the best agreement between measured and simulated epidemics. Simulations performed with the canopy represented by a population of the same average plant deviated strongly from the observations.

- *Conclusions* It was possible to compare the predicted and measured epidemics on detailed variables, supporting our hypothesis that the approach is able to provide new insights into the processes and plant traits that contribute to the epidemics. On the other hand, the complex and dynamic responses to sowing density made it difficult to precisely test the model and to disentangle the various aspects involved. This could be overcome by comparing more contrasted and/or simpler canopy architectures such as those resulting from quasi-isogenic lines differing by single architectural traits.

Key words: crop architecture, modelling, *Septoria tritici*, wheat (*Triticum aestivum* L.), sowing density, 3D virtual plant model, plant-pathogen interaction.

Introduction

To limit pesticide use, one option is the use of crop architecture to promote disease escape. Several studies have shown that some architectural traits allow escape by either limiting pathogen contact with the host, or creating an unfavourable environment for pathogens, or limiting the ability of the pathogen to trigger the infection process (Ando et al., 2007). Indeed, architecture traits such as plant posture (Saindon et al., 1995), growth habit (Ando and Grumet, 2006) and plant height (Hilton et al., 1999) have been reported to be critical factors in determining disease incidence in several crops. Disease severity has also been shown to be influenced by the spatial distribution of leaf area in the canopy (Schwartz et al., 1978), the number of leaves (Jurke and Fernando, 2008), as well as leaf shape (Gan et al., 2007) and size (Ando et al., 2007).

For *Septoria tritici*, wheat architecture can play a key role. *Septoria tritici* is a foliar disease caused by *Mycosphaerella graminicola*, a splash-dispersed pathogen. It progresses from the base to the top of the canopy when spores are incorporated in droplets resulting from the impact of rain drops on sporulating tissues of the lower infected leaves. The relationship between *S. tritici* and its host is dynamically complex and is comparable to a race between the vertical progress of the pathogen and the production of new leaves. According to Shaw and Royle (1993), opportunities of escape exist due to the long latency period of the pathogen compared to the time needed for internode extension to move leaf blades of successive phytomers sufficiently away (a phytomer is the morphological building unit of plant axes, consisting of an internode, a node, a sheath and a leaf blade). Several studies reported that tall plants were less attacked by *S. tritici* (Tavella, 1978, Danon et al., 1982, Camacho-Casas et al., 1995, Simon et al., 2005). It has been suggested that this could result from unfavorable environmental and epidemiological factors due to plant height (Bahat et al., 1980, Scott et al., 1985, Simon et al., 2005), or from linkage between resistance and plant height (Scott et al., 1982). A modelling study of light leaf spot, a splash-dispersed disease (caused by *Pyrenopeziza brassicae*) has shown that differences in leaf area distribution resulted in differences in the vertical progress of the disease (Pielaat et al., 2002). The vertical transport of the pathogen is also tightly linked to the distance between healthy and infected organs. It has been shown that the position of the healthy newly emerging leaves relatively to the inoculum sources (soil or older diseased leaves) modulates *S. tritici* severity (Bahat et al., 1980, Eyal, 1981, Scott et al., 1985). Lovell et al. (1997) hypothesized that spore transfer to the upper leaves is affected by the rate of stem extension: during stem extension, the distance between young and old leaves becomes higher and thus the plant may outgrow the disease. Leaf posture also influences the proximity between sources and receptors of the pathogen. For instance, the tips of leaves that bend down are further from the emerging upper leaves than those with an erect position (Lovell et al., 1997).

Cropping practices (e.g., nitrogen fertilization, sowing density and date of sowing) influence disease development in many ways, including the modification of canopy architecture. However, these effects are irregular and interpretations may be controversial. Regarding the effect of sowing density, several authors have suggested that increasing density enhanced foliar disease (Ando and Grumet, 2006, Gan et al., 2007, Jurke and Fernando, 2008). The density effect was attributed either to the establishment of a favorable microclimate such as higher relative humidity (Tompkins et al., 1993) or to modifications of canopy architecture. Pielaat et al. (2002) reported that denser canopies increase the contacts between leaves and thus facilitate the progress of the disease through the canopy. According to Broscious et al. (1985), the significant increase in wheat tiller number with higher plant density could favor *M. graminicola* spore deposition. However, discrepancies concerning the

density effect are found in the literature. Pfleeger and Mundt (1998) found only very little effect of sowing density on disease development. Eyal (1981) reported that reduced plant densities resulted in sparser canopies, which increased the probability that raindrops impact on lower leaves, resulting in a faster disease progress by splashing in less dense plant stand. Ultimately, there are difficulties to identify and to understand the effects of cropping practices on disease development. First, effects are irregular between years in terms of intensity and direction. Second, the mechanisms that are likely involved are complex and difficult to disentangle. A modelling approach could thus be useful to better understand the role of crop architecture in the effect of cropping practices on epidemic development.

To study the effect of crop architecture on disease dynamics, one possible tool is the use of coupled epidemic-virtual plant models. "Virtual Plants" use morphogenesis rules and geometric information to simulate the time course of 3D position of botanical entities. Room (1996) proposed that by handling 3D information on the development and growth of individual plants and activities of the organisms which live on them, these models should allow representing in depth the interactions between the plant architecture and pathogen or herbivore dynamics. Since that time, plant models have progressed in realism and functionality (Godin and Sinoquet, 2005, Vos et al., 2010), however few examples exist where they have been used to investigate the interactions between plants and diseases or pests. Wilson and Chakraborty (1998) used a virtual plant model to quantify the impact of anthracnose on the branching of a pasture legume. Later, two plant models were proposed to simulate theoretical movement of insects at the individual plant and the field scales (Hanan et al., 2002, Skirvin, 2004). More recently, virtual plant models were applied to two pathosystems: grape-powdery mildew (Calonnec et al., 2008) and wheat-*S. tritici* (Robert et al., 2008). The model of wheat-*S. tritici* (Septo3D) has been used to assess the influence of architectural traits on *S. tritici* development by varying separately each trait. This supported the view that the rate of plant development is a major factor in determining disease severity. However, until now, the model has not been validated with detailed disease measurements.

In this study, we address the question whether coupled epidemic-virtual plant models can capture and help us to better understand the role of architecture in the effect of cropping practices on epidemics. Here we study the example of the pathosystem wheat-*S. tritici*, focusing on the effect of sowing density. We aim (i) to develop a method for increasing the realism of 3D wheat reconstruction, particularly by including plant-to-plant variability (ii) to test the model for its capacity to simulate *S. tritici* epidemics for different sowing densities and (iii) to define to which extent the level of architecture description influences disease simulations.

Materials and methods

1. Overview

A field experiment was performed in Grignon, France in 2008/2009 with winter wheat (*Triticum aestivum* Cv. 'Soissons') grown at three densities. Detailed architecture and disease measurements were performed along the growing season. Plant measurements were used to calibrate the plant model while disease measurements were used to evaluate the disease dynamics simulated by the model Septo3D. We compared three scenarios of simulation differing by the degree of detail with which the observed variability of architecture between plants was represented.

2. Modelling

2.1. Model description

The model Septo3D (Robert et al. 2008) combines a dynamic architectural model of wheat, ADEL-Wheat (Fournier et al., 2003) with a dynamic model of *S. tritici* epidemic based on Rapilly and Jolivet (1974). Starting from a given initial state of infection, the model simulates the lesion development and propagation from the infected lower leaves to the healthy upper leaves in a canopy. Epidemics result from repeated successions of lesion development resulting in spore production and spore dispersal. In the model, canopy architecture influences epidemics through the amount of tissue available for lesion development, which is driven by plant development, and through its effects on rain penetration and infectious droplet distribution. Model outputs are the dynamics of green (S_{green}), apical senescent (S_{sen}) and diseased leaf blade areas distinguishing between incubating (S_{inc}), chlorotic (S_{chlo}), sporulating (S_{spo}), and emptied lesion (S_{empty}) tissues on each leaf (Fig. 1a). To make the link with measured variables, we distinguished between sporulating and emptied lesions located in the apical senescent part of the leaf (S_{spo}^{Ap} and S_{empty}^{Ap}) from those located in the green part of the leaf (S_{spo}^{Green} and S_{empty}^{Green}). The model includes three modules, which deal respectively with canopy development, lesion development and spore dispersal. Here we describe main functioning of the three modules and changes with respect to Robert et al. (2008).

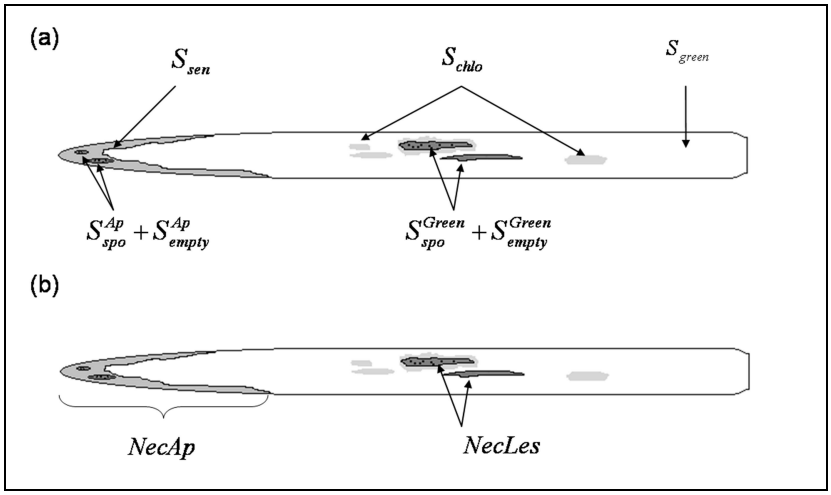

Figure 1. Scheme of **(a)** simulated disease variables by Septo3D and **(b)** measured disease variables on a wheat leaf. $NecLes_{Green}$ is calculated from model outputs as: $\left(S_{spo}^{Green} + S_{empty}^{Green}\right) / S_{green}$ where S_{spo}^{Green} and S_{empty}^{Green} are respectively the sporulating and emptied lesions located in the green part of the leaf S_{green}.

Canopy development

Canopy simulation is based on the model ADEL-Wheat which simulates in 3D the dynamics of appearance and extension of all vegetative organs of a wheat canopy. Several modifications have been made to the version described in Fournier et al. (2003): they allow for a more flexible and detailed parameterisation of plant development and its variability in the canopy. The present version of ADEL-Wheat takes as input parameterisations of (i) the rates of leaf appearance as a function of thermal time for several types of axes, (ii) the individual thermal time course of senescence progression on leaves on each axis, (iii) the

tillering dynamics, and (iv) the geometry and dimensions of mature plant organs. These parameterisations can be given in the form of numeric look-up tables so that no constrains exist in the patterns they follow. In ADEL-Wheat, the rate of leaf appearance is used to drive the extension of laminas, sheaths and internodes using coordination schemes (Fournier et al., 2005). The concept is extended after flag leaf appearance by assuming that all durations are stable fractions of the phyllochron value before flag leaf appearance (the phyllochron being the interval, expressed in thermal time, between appearance or ligulation of two successive leaves; (Wilhelm and McMaster, 1995). The measured senescence dynamic of leaves could be directly used as input. Alternatively, senescence progression could be given at the shoot level, using an index of progression: the Shoot Senescence Index (SSI) that represents the fractional number of leaves senesced on an axis. The progression of senescence within each leaf is then computed with stable functions of SSI. Tillering dynamics are simulated from measured probability of appearance and regression for primary tillers and using the principle of cohorts to extrapolate to secondary tillers. A cohort refers to the set of tillers that emerge on a plant at the same time. Tiller emergence is coordinated with the emergence of leaves on the main stem so that the potential number of tillers in each cohort follows precisely a Fibonacci series (Friend, 1965, Masle-Meynard and Sebillotte, 1981, Masle, 1985). These authors and others (Darwinkel, 1978) have reported that behaviour of a tiller is highly related to the time of emergence. In the model, it is assumed that tillers of a same cohort behave identically: they have the same properties of probability of emergence and disappearance, rate of growth, and dimensions.

Lesion development

This module simulates the development of a lesion after deposition of a spore-containing droplet on the leaf. Four stages are considered: infection (spore germination and penetration in the leaf), incubation, appearance and extension of chloroses, and maturation of chloroses into sporulating necrotic tissue (during the latency period). Infection and incubation are assumed to occur only on green tissue. In Septo3D, each leaf blade is divided into small regions called sectors in which we keep track of disease development. At each time step, the model computes in each leaf sector the area allocated to each stage of the infection cycle: incubating, chlorotic, and sporulating.

Spore dispersal

Dispersal occurs when drops with sufficient kinetic energy hit sporulating surfaces, and are splashed away into droplets carrying spores. In the model, splash occurs for rain events with intensity above 0.5 mm/h, and the kinetic energy of splashed droplets is considered too low to allow re-splashing. Sporulating lesions are considered empty after having being exposed to rain three times.

For the simulation of spore dispersal, the canopy is represented as a horizontally homogenous turbid medium and droplet transport is simulated between layers of the vegetation as a function of the distance to the source. The properties of the turbid medium are derived from the 3D representation of the canopy. Rain penetration is computed using an analogy with light penetration in a multi-layered turbid medium, and droplet transportation and interception in analogy to light scattering. The 3D representation of the canopy makes it possible to calculate the density and orientation of leaves in each layer and to assign, afterwards, the intercepted droplets of a layer to the appropriate leaf sector.

More precisely, taking into account the density and orientation of vegetation in each layer, the model first computes a global production of droplets per layer, proportional to the rain intercepted within that layer. The fraction of droplets that contains spores is calculated as the ratio between the sporulating area and the total area of that layer. A term of loss is subtracted, that represents the evaporation of too small droplets. Spore-containing droplets are

emitted in all directions above the leaf surface; they are assumed to move in straight line till a limited distance and then to fall down vertically. Along their trajectory, droplets may be intercepted according to density and orientation of vegetation elements. The output of the spore dispersal module is the number of spore-containing droplets that have reached green tissues and have not been washed away by the rain. Washing is calculated for each layer as a function of rain intensity and duration.

Sowing density changes the time course of vegetation density in each layer, which impacts (1) the amount of rain intercepted in each layer and thus droplet production (2) the interception of spore-containing droplets during their upward and downward movements; and (3) the loss by washing of intercepted spore-containing droplets. For example increasing the sowing density may reduce rain penetration resulting in fewer droplets produced in the lower leaf layers where active sporulating lesions are generally abundant; this is referred to as the "umbrella effect". However, for high density, once spore-containing droplets are produced, there is a higher probability of interception and thus of successful dispersal at shorter distance. At the same time, the umbrella effect could also mean less washing of the lower infected leaf layers. These processes have contradictory effects and their relative importance will depend on rain event intensity, on the vegetation profile and on the initial contamination.

2.2. Epidemic model parameterisation

Parameter values of the dispersal model and the lesion model were taken from Robert et al. (2008, Tables 1 and 2). Only the latency period was given a slightly lower value of 310 °Cd.

Initialisation of disease in the model was the only significant change compared to the version presented in Robert et al. (2008). Here, it is assumed that initial contamination on the first lower leaves results from spore-containing droplets splashed from the soil. This was represented using two parameters: $S_{sposoil}$ (m²/m²), the fraction of soil surface covered by infectious leaf debris and $T_{infsoil}$ (°Cd), the duration during which this soil surface bears spores. Therefore, the amount and the interception of spore-containing droplets from soil are determined by the canopy architecture and the interactions with rainfall. Parameters of the initial infection conditions were adjusted so that simulated infection of the three uppermost leaves were in best agreement with field measurements and that the ranking of density treatments for infection of the lowermost simulated leaf (here leaf 6 counted from the top) was as close as possible to the observed. Thereby, T_{infsol} was fixed to 1000 °Cd and S_{sposol} to $0.65\ 10^{-4}$ m²/m².

2.3. Reconstruction of individual plant architecture

The model was parameterised for simulating the architecture of wheat plants of three contrasted densities of a field experiment. Reconstructions were performed for each density and for each type of plants differing in final number of leaves (referred to N_{leaf} modality). Rates of appearance, growth and senescence of plant organs, tillering dynamics and dimensions of mature organs of the main stem and primary tillers were based on field measurements and those of secondary tillers were inherited from the primary tillers of the same cohort. Leaf curvature was not measured during our experiment. It was parameterised based on data from a previous field experiment carried out with the same cultivar. To compute the dates of leaf appearance on the main stem and on primary tillers, we fitted a linear model on the data of leaf collar appearance i.e., the Haun Stage (HS: decimal index for the number of liguled leaves; Haun, 1973) and considered a delay of 1.6 HS between leaf emergence and collar appearance (Fournier et al., 2005). The progression of senescence was estimated at the shoot level using the SSI and ADEL-Wheat default functions until leaf 4 (counted acropetally from the first true leaf), and using spline functions fitted to the measurements for upper leaves. The measurements of the number of active main stem tillers

were used to fit a tillering dynamic model using a set of approximations derived from literature. The Fibonacci sequence was used to calculate the potential number of secondary tillers, and their probability of appearance was given the value measured for the corresponding primary tiller. The calculation was validated for the maximum number of tillers. We assumed (and verified in our data for the first two primary tillers) that the emergence of a tiller n is synchronous with the emergence of leaf on phytomer n+3 (Masle-Meynard and Sebillotte, 1981). The senescence of tillers was simulated assuming that (i) the tiller regression takes place at a constant rate during stem extension and (ii) tillers regress by cohorts, in the reverse order compared to their appearance. When a tiller starts to regress, it is still represented in the model for 400°Cd_{12}, without producing any new leaf, then disappears.

2.4. Canopy reconstruction with different levels of plant variability

Three scenarios of canopy reconstruction (S_{ref}, S_1 and S_2) differing in the level of description of plant architecture variability were defined. In S_1, the canopy is represented by cloning a mean plant without considering any variability, whereas in S_2 and S_{ref} canopies are composed of two types of plants differing in their total number of leaves (N_{leaf}). In S_{ref}, the variability of timing of development between plants is also taken into account (all plants are unique). The latter scenario is the more realistic and is considered as the reference.

To get average values for S_1, organ dimensions, rate of organ appearance and senescence were computed for each phytomer as the mean of measurements for corresponding phytomers counted from the top of the canopy. The final number of leaves on a tiller axis was given the most frequent value for that type of tiller. In scenarios S_2 and S_{ref}, the architecture of the plant representing each N_{leaf} modality was computed from the average of measurements for all plants that produced N_{leaf} leaves. Each modality was represented in the proportions observed in the field. For S_{ref}, the plant-to-plant variability of development was represented by variability in the date of seedling emergence. It was represented as a normal distribution with standard deviation equal to that measured for Haun Stage. In the model, a population of 10 plants was created to capture this variability, each plant corresponding to a decimal quartile of the normal distribution. The simulated leaf area index of the three density treatments was similar between the three scenarios (Fig. 2). Scenarios are used to test how the level of detail in the description of plant-to-plant variability of development influences epidemic simulations.

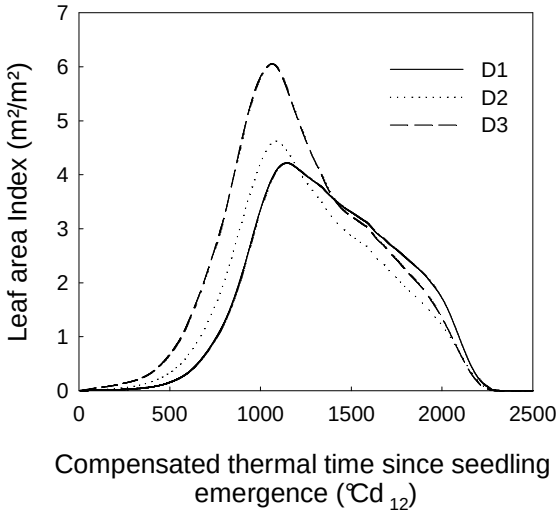

Figure 2. Simulated leaf area index (LAI) *vs.* compensated thermal time since seedling emergence for the canopy of winter wheat Cv. 'Soissons' grown at three densities. D1: 59, D2: 160, D3: 406 plants.m^{-2}. Simulations are for the scenario that takes into account plant-to-plant variability of development and number of final phytomers (S_{ref}).

3. Field experiment

3.1. Treatments and experimental design

The field experiment was carried out in 2008/2009 at the unit research of INRA at Thiverval-Grignon near Paris, France (48°51'N, 1°58'E) on a silty loam soil. The previous crop was *Vicia faba*. Winter wheat, *T. aestivum* Cv. 'Soissons' was sown on 17 Nov. 2008 at three sowing densities: low (D1: 77 plants.m^{-2}), standard (D2: 228 plants.m^{-2}) and high (D3: 514 plants.m^{-2}). At seedling emergence, actual plant densities were respectively: 60, 160 and 406 plants.m^{-2}. Each density treatment was sown in 3 parallel plots approximately 80 m length and spaced 0.2 m from each other. Each plot was further separated into two parts for fungicide treatments: treated (T) and non-treated (NT), separated by a 10 m distance. Each plot consisted of nine rows of plants with an inter-row distance of 0.175 m. The two external rows on each side of the plots were not used for measurements. The soil nitrogen content was measured to be 70 kg ha^{-1} at the end of January, and fertilization was adjusted following recommendations for high yielding crops (Table 1). An irrigation system was installed to complement natural rainfall when needed. Weeds were controlled by herbicide application (Table 1). Three fungicide treatments were performed on the treated part of the field 470, 860 and 1580 °Cd after seedling emergence, corresponding to Haun Stage HS = 4 and HS = 8 for the two first applications and to grain filling for the last.

Table 1
Dates, products, active agents and doses of different agronomic applications performed on winter wheat Cv 'Soissons' grown in Grignon in 2008/2009 at three densities. D1: 59, D2: 160, D3: 406 plants.m^{-2} under two fungicide treatments: treated (T) and non-treated (NT).

Treatment	Date	Product	Active agents	Dose
Herbicide	26 Aug. 2008	Roundup Max 480	Acid glyphosat	2.5 l.ha^{-1}
(on T and NT)	30 Apr. 2009	Bofix	Fluroxypyr Clopyralid	2.5 l.ha^{-1}
Fungicide	2 Apr. 2009	Input pack	Prothioconazol	0.8 l.ha^{-1}
(on T only)	5 May 2009	Opus team	Epoxiconazol Fenpropimorph	1.5 l.ha-1
	23 June 2009	Soleil	Bromuconazol	1.2 ha^{-1}
Fertilization	9 Apr. 2009	Ammonium nitrate (33.5%)		80 kg.ha^{-1}
(on T and NT)	6 May 2009	Ammonium nitrate (33.5%)		50 kg.ha^{-1} (D1) 120 kg.ha^{-1} (D2, D3)

3.2. Field measurements

Measurements for plant model calibration

Architectural measurements used to calibrate the plant model were performed on plants from the fungicide treatment (T). In each density treatment, 20 plants were tagged to monitor weekly the Haun Stage on the main stem and on primary tillers. At five occasions during crop growth, 15 plants previously tagged were dissected to measure the dimensions of all mature organs. Lamina images obtained with a flat-bed scanner were processed using the program Lamina2Shape (Dornbusch and Andrieu, 2010) to compute blade length (l_{bl}), width (w_{bl}), and area (A_{bl}). In addition, lengths of sheaths (l_{sh}) and internodes (l_{in}) were measured with a ruler. Distance from the shoot base to a leaf collar (h_{col}) was computed as the sum of l_{in} below the considered leaf plus the l_{sh} of that leaf. Final leaf number on the main stem (N_{leaf})

and number of tillers per plant were also recorded. In addition, all the tagged plants from treated and non-treated plots (60 plants per density) were used to determine the total number of leaves per axis in each density.

Some measurements were duplicated on non-treated plants to insure that they were consistent with those of treated plants. HS was measured both on T and NT plots on 20 plants on 3 Apr. 2009 and on 30 plants on 30 Apr. 2009 for each density treatment. Measurements of l_{sh} on 20 plants picked randomly from each density on NT plot were carried out at a single sampling date (11 May 2009).

Disease and senescence measurements

For both T and NT plots, 30 plants were tagged in each density treatment to monitor, on the true leaf rank, the dynamics of apical senescence and *S. tritici* necrotic lesions. Measurements began on 15 April 2009 and were performed once or twice each week, which corresponds to an interval of 80-100 °Cd. Starting with leaf 5 counted acropetally, each leaf was measured at least 4 times during its lifespan. For each leaf of the tagged plants, we recorded the proportion of total leaf area occupied by (1) apical necrosis (*NecAp*) (bearing pycnidia or not) and (2) by *S. tritici* necrotic lesions located in the green part of the leaf (*NecLes*) (Fig. 1b).

From these measurements, two variables were used to describe the *S. tritici* epidemic: the proportion of total necrotic leaf area and the proportion of lesions in the green part of the leaf ($NecLes_{Green}$). The total necrotic leaf blade area was computed as the sum of measured areas occupied by *S. tritici* lesions (*NecLes*) and of the apical necroses (*NecAp*). Lesion development was characterized as the proportion of lesion surface area in the green part of a leaf ($NecLes_{\mathrm{Green}}$). Assuming that the fraction of tissue occupied by lesions was the same in the apical region as in the rest of the leaf, the proportion of lesions in the green part of the leaf was calculated as:

$$NecLes_{Green} = NecLes \times \frac{1}{1 - NecAp} \quad (1)$$

where *NecLes* and *NecAp* are the fraction of the total leaf area occupied by necrotic lesions (assessed in the green part) and by apical necrosis respectively.

The green leaf area decreases when the leaf senesces, so that the proportion of lesions becomes increasingly difficult to estimate. The indicator $NecLes_{\mathrm{Green}}$ is reliable only as long as apical necrosis and necrotic lesions do not merge on the leaf. For that reason, only the first stage of lesion development was used to compare with simulations.

Meteorological measurements

Air temperature at 2 m height, amount of rainfall in millimetres and relative humidity were monitored hourly over the growing season at a weather station 500 m from the field. Soil temperature (T_{soil}) at 3 cm deep was measured within one row of the plots of density treatments D1 and D3 from sowing until starting of fast internode elongation. No differences were found between density treatments so measurements were averaged to represent soil temperature regardless of the density.

3.3. Data analysis

Calculation of thermal time

Linear thermal time (Γ,°Cd) based on air temperature was used to drive the dynamics of *S. tritici*. Linear thermal time is computed assuming a linear response to temperature above a base temperature T_b (taken 0°C here):

$$\Gamma = \frac{1}{24} \sum_i \max(0, T_{air} - T_b) \quad (2)$$

where *i* is the number of hours elapsed after seedling emergence and T_{air} is the hourly-averaged air temperature.

A non-linear thermal time (Γc) based on growing zone temperature was used to drive wheat development. The growing zone temperature (T_p) was assumed to be equal to T_{soil} before internode elongation then to T_{air}. Non-linear thermal time Γ_c was computed based on a modified Arrhenius equation that describes a non-linear response $F(T)$ of biological processes to temperature (Johnson and Lewin, 1946). Applicability of this equation to plant development was established in Parent et al. (2009) and calibration for wheat is presented in Baccar et al. (2010). Here the temperature sum is expressed in °Cd_{Tref} (T_{ref} is a reference temperature that can be chosen arbitrarily) and is calculated as:

$$\Gamma_c = \frac{T_{ref}}{24} \sum_{i=1} \frac{F(T_p)}{F(T_{ref})} \quad (3)$$

where *i* is the number of hours elapsed after seedling emergence, T_p is the average hourly plant temperature and T_{ref} is the reference temperature. We chose $T_{ref} = 12$°C, which is close to the average temperature during the wheat growing season.

Convention for leaf numbering

To express the kinetics of disease, we referred to leaf number counted from the top of the canopy, starting with 1 for the flag leaf.

Statistical analysis

Means and standard errors were calculated for all the measured and derived disease and architectural variables. The significance of differences in the stage of development and in sheath lengths between T and NT plants were tested using the non-parametric Mann and Whitney test for samples < 30 and the student t test for samples ≥ 30 (Georgin and Gouet, 2000).

4. Disease simulations and test of Septo3D

Simulations of lesion development were run with three scenarios of canopy reconstruction. The proportion of lesion in the green part of the leaves ($NecLes_{Green}$) was used to compare field measurements to model simulations. This indicator is an accurate estimate of disease in the early stage of leaf infection. As a measure for the deviation from a 1:1 line between measured and simulated disease variables we used the root mean squared error (RMSE).

Results

1. Effect of density on plant architecture and development

1.1 Comparison between treated and non-treated plants

The mean values of Haun Stage measured on 3 and 30 Apr. 2009 were found similar for treatments T and NT with no significant differences at the level of 0.1 (Table 2). For dimensions, the average length of sheaths 6, 7 and 8 (counted acropetally) was found lower by 0.5 to 1.5 cm for treated plants (Table 2). These differences were in the range of the standard deviation with each treatment, and in most of the cases were not significant at the level of 0.05. Thus, we considered that T and NT plants did not differ in their development or organ dimensions.

Table 2
Mean values and standard errors of Haun Stage (HS) measured at two dates (3 and 30 Apr. 2009) and sheath length (lsh) for main stems of winter wheat Cv. 'Soissons' grown in Grignon in 2008/09 at three densities. D1: 59, D2: 160, D3: 406 plants.m^{-2} under two fungicide treatments: treated (T) and non-treated (NT). Numbers between brackets following l_{sh} correspond to the phytomer rank counted from the base of the shoot. Numbers followed by the same letter are not statistically different at the level of α=10% across columns.

		D1	D2	D3
HS	**NT**	5.33±0.25 [a]	5.09±0.35 [a]	4.92±0.44 [a]
(3 Apr. 2009)	**T**	5.16±0.3 [a]	5.00±0.4 [a]	4.58±0.17 [b]
HS	**NT**	8.84±0.23 [a]	8.63±0.12 [a]	8.23±0.23 [a]
(30 Apr. 2009)	**T**	9.08±0.3 [a]	8.5±0.3 [a]	8.2±0.21 [a]
l_{sh} (6)	**NT**	10.42±1.18 [a]	10.56±0.72 [a]	7.97±0.49 [a]
	T	10.17±1.21 [a]	9.09±1.43 [b]	7.64±0.6 [a]
l_{sh} (7)	**NT**	13.03±1 [a]	13.37±1.43 [a]	10.61±0.77 [a]
	T	12.90±1.02 [a]	11.88±1.18 [a]	10.10±0.66 [b]
l_{sh} (8)	**NT**	-	-	13.70±0.94 [a]
	T	-	-	12.91±0.97 [b]

1.2. Final leaf number and phyllochron

The total number of leaves produced on the main stem (N_{leaf}) varied from 9 to 11 among plants at all densities. The proportion of plants with a given N_{leaf} varied between densities (Table 3): low density treatment D1 produced very few plants with 9 leaves and similar proportions of plants with 10 and 11 leaves, D2 had almost exclusively plants with 10 leaves and D3 produced a majority of plants with 9 leaves and a bit less than half with 10 leaves. Thus the mean value for N_{leaf} decreased with increasing density

The phyllochron of a plant was negatively correlated with N_{leaf} (Baccar et al., 2010). For a given N_{leaf}, phyllochron did not depend on plant density. However, as the proportion of plants with high N_{leaf} decreased with increasing densities, the average phyllochron increased accordingly, from 98 °Cd_{12} in D1 to 117 °Cd_{12} in D3 (Fig. 3a).

Table 3
Proportions of final leaf number on main stems of winter wheat Cv. 'Soissons' grown in Grignon in 2008/09 at three densities. D1: 59, D2: 160, D3: 406 plants.m^{-2} under two fungicide treatments: treated (T) and non-treated (NT). Total number of plants for each density = 60.

	D1	D2	D3
N_{leaf} = 8			0.05
N_{leaf} = 9	0.03	0.08	**0.63**
N_{leaf} = 10	**0.52**	**0.89**	0.32
N_{leaf} = 11	0.44	0.03	

1.3. Organ dimensions

A detailed description of organ dimensions measured in this experiment is presented in Dornbusch et al. (2010). Here we summarize these results through two synthetic variables that illustrate the differences in the shoot architecture between population density treatments: the leaf blade area (A_{bl}) and the height of leaf collar (h_{col}). Both A_{bl} and h_{col} varied between density treatments and between N_{leaf} modalities. Few or no differences were observed for lower phytomers whereas differences existed for the 4 upper phytomers, i.e., those with elongated internodes. For the same N_{leaf}, A_{bl} was higher for lower density whereas h_{col} was higher for high density (Fig. 3c, 3d). A_{bl} differed increasingly between density treatments with

lower leaf rank counted from the top. Hence, the difference of A_{bl} between D1 and D3 was respectively 3 % and 65 % for leaf 3 and leaf 1. Collar height h_{col} increased approximately linearly with decreasing leaf rank counted from the top and the difference between the densities was constant along the shoot (2-4 cm). For a given density, A_{bl} and h_{col} were increased at higher N_{leaf}. Only A_{bl} of the flag leaf was reduced at high N_{leaf} modality. Finally these effects resulted in slightly taller plants (53 *vs.* 50 cm for the height of flag leaf collar) with larger blade area (100 *vs.* 66 cm² for cumulated area of blades 1-4) in D1 compared to D3, with intermediate values for D2.

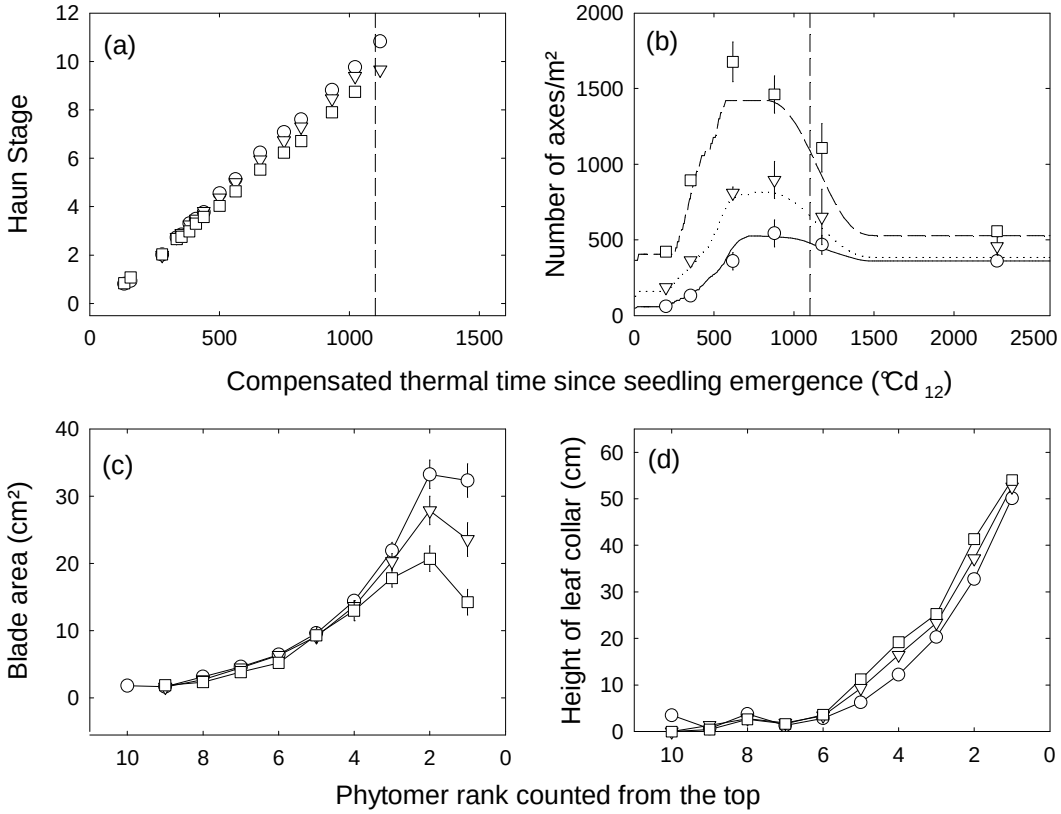

Figure 3. (a**)** Mean Haun stage of main stem and **(b)** number of axes per square meter *vs.* compensated thermal time since seedling emergence **(c)** Mean blade area and **(d)** height of leaf collar *vs.* phytomer rank counted from the top. Data are for main stems with 10 leaves of winter wheat Cv. 'Soissons' grown in Grignon in 2008/2009 at three densities: D1 (○), D2 (▽) and D3 (□). D1: 59, D2: 160, D3: 406 plants.m^{-2}. Error bars mark the 95% confidence intervals when larger than the size of the symbol. The vertical dashed line corresponds to the date of flag leaf ligulation.

1.4. Tillering dynamics

In wheat the number of actively growing tillers increases up to a maximum, then remains stable and finally decreases during stem elongation. The number of actively growing tillers at the very beginning of stem extension is a good estimate of the maximum reached. Here it was respectively 8.2, 4.2 and 3.1 axes/plant for D1, D2 and D3 which corresponds respectively to 542, 896 and 1461 axes/m² (measured 880 °Cd$_{12}$ after seedling emergence at HS = 7.5-8). The final number of axes was estimated at harvest (2270 °Cd$_{12}$) by counting the number of ears: there were 6.2, 2.5 and 1.3 axes/plant respectively for D1, D2 and D3 (Fig. 3b), corresponding respectively to 359 ±16, 458±60 and 557±33 axes per m².

2. Plant-to-plant variability of development

Measurements of Haun Stage performed 30 Apr. 2009 on 30 plants per density treatment were used to assess the plant-to-plant variability of development and parameterise it in scenario S_{ref}. We first pooled data by groups of plants that produced different N_{leaf}, and study the dispersion of HS around the mean of each group. Calculated standard deviations of HS were similar for all groups in all treatments (between 0.54 and 0.77). Therefore, a unique normal distribution of HS with a standard deviation of 0.65 was used in the parameterisation (Fig. 4).

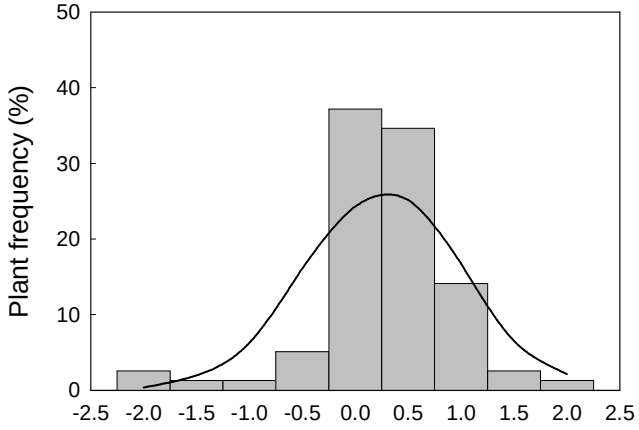

Figure 4. Frequency of classes of plant development. Each class is made of plants quasi-synchronous in development; the x axis represents the delay (in Haun stage) between a class and the mean calculated over all plants. Measurements were performed the 30 Apr. 2009 for winter wheat Cv. 'Soissons' grown in Grignon in 2008/2009; plants from three density treatments: D1, D2, D3 are pooled together. The line represents the normal distribution of the dispersion of Haun stage used in the parameterisation of the scenario S_{ref}. D1: 59, D2: 160, D3: 406 plants.m^{-2}.

3. Disease development

3.1. Pattern of total necrosis development

The total necrotic area within a leaf blade progressed at a low rate up to the time when 15-20% of blade area was necrotic, then at a fast rate, approximately constant up to total leaf death (Fig. 5a). Necrotic tissues appeared on successive leaf layers according to an acropetal sequence, from lower to upper leaves. However, the time interval between necroses of successive leaves was much longer for lower leaves (170-270 °Cd) than for the upper leaves (70°Cd). This pattern occurred similarly in treated and non-treated plots, but was hastened in the absence of fungicide treatment: starting from leaf layer 4 (counted from the top) in D1 and D3, and leaf layer 6 in D2, leaf life span was shortened by 50 to 170 °Cd in the absence of fungicide compared to treated plots (Fig. 5b). This reflects a moderate epidemic. Yield was high and similar in treated and non-treated plots (61±4, 72±2 and 74±4 q.ha^{-1} for respectively D1, D2 and D3).

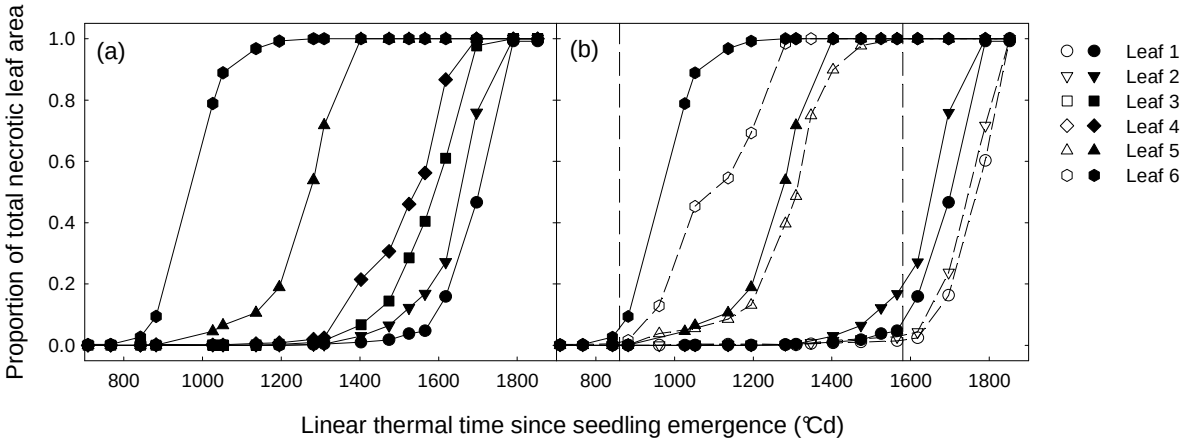

Figure 5. (a) Total necrotic leaf area *vs.* linear thermal time since seedling emergence, for leaves 1 (●), 2 (▼), 3 (■), 4 (♦), 5 (▲) and 6 (●) counted from the top of main stem of wheat plants non-treated with fungicide; **(b)** Total necrotic leaf area *vs.* linear thermal time for leaves 1, 2, 5 and 6 of main stem from wheat plants non-treated (solid line, filled symbols) and treated (dotted line, open symbols) with fungicide. Data are for winter wheat Cv. 'Soissons' grown in Grignon in 2008/2009 at an intermediate density D2 (160 plants.m^{-2}). Vertical dashed lines correspond to dates of fungicide treatment.

3.2. Effect of density treatment on lesion development

Lesion development was characterized as the proportion of lesions in the green tissue of a leaf blade. To compare between leaves of different ranks, or of same rank between plants that are not synchronous in development, we used as time origin the moment of leaf emergence. A leaf can be infected as soon as it emerges and the time interval between leaf emergence and lesion development reflects the timing of infections for that leaf. Comparison between density treatments are presented first at the plot level by averaging over all plants: in this case the average lesion development measured for each leaf rank was plotted against the thermal time since the average date of leaf emergence (Fig. 6). Second, we separated within each density treatment between plants with different final leaf number (N_{leaf}) (Fig. 7).

Figure 6 shows the pattern of lesion development for the six upper leaves (numbered from the top) for the three density treatments. In each leaf layer, lesions appeared almost simultaneously in all density treatments. For leaves 6 and 5, lesions appeared starting around 400°Cd after leaf emergence, suggesting favourable conditions of infection shortly after leaf emergence (latency period of *S. tritici* being around 300-400°Cd). Lesion appearance was delayed on upper leaves (between 600°Cd and 700°Cd). After appearance of the first lesion on a leaf, lesion area progressed similarly in treatments D2 and D3, while the rate of development was higher in D1. Lesion development was thus similar in the three density treatments, except for the faster rate of development in the low density treatment D1.

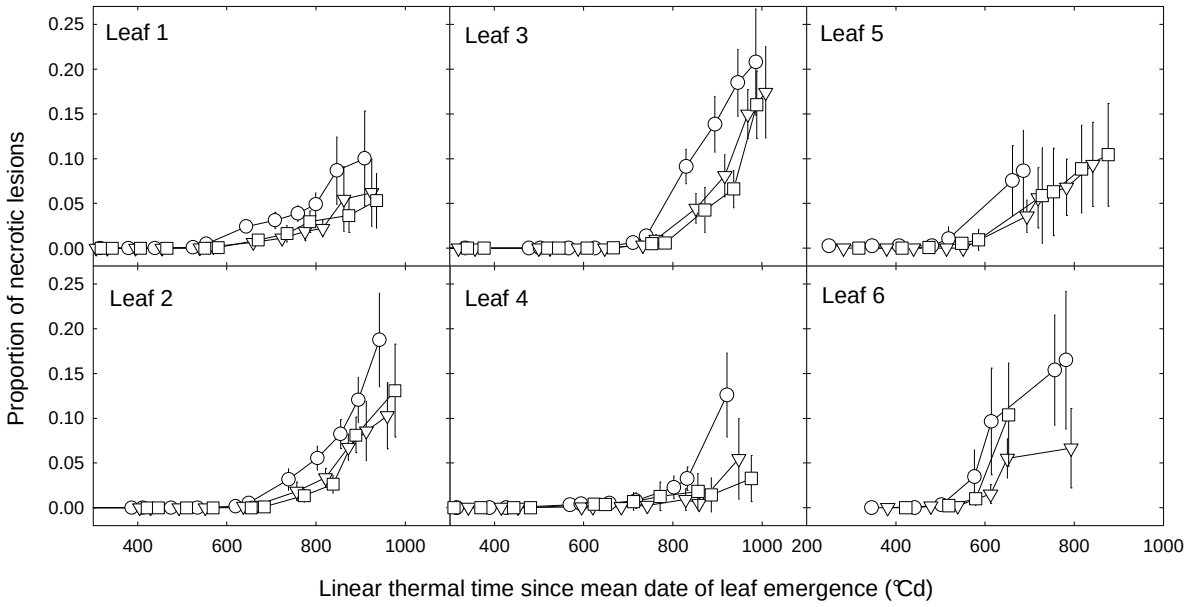

Figure 6. Dynamic of necrotic lesions of *Septoria tritici vs.* linear thermal time since the mean date of leaf emergence, for main stem leaves 1 to 6 (counted from the top) of winter wheat Cv. 'Soissons' grown in Grignon in 2008/2009 at three densities: D1 (○), D2 (▽) and D3 (□). D1: 59, D2: 160, D3: 406 plants.m^{-2}. Error bars mark the 95% confidence intervals.

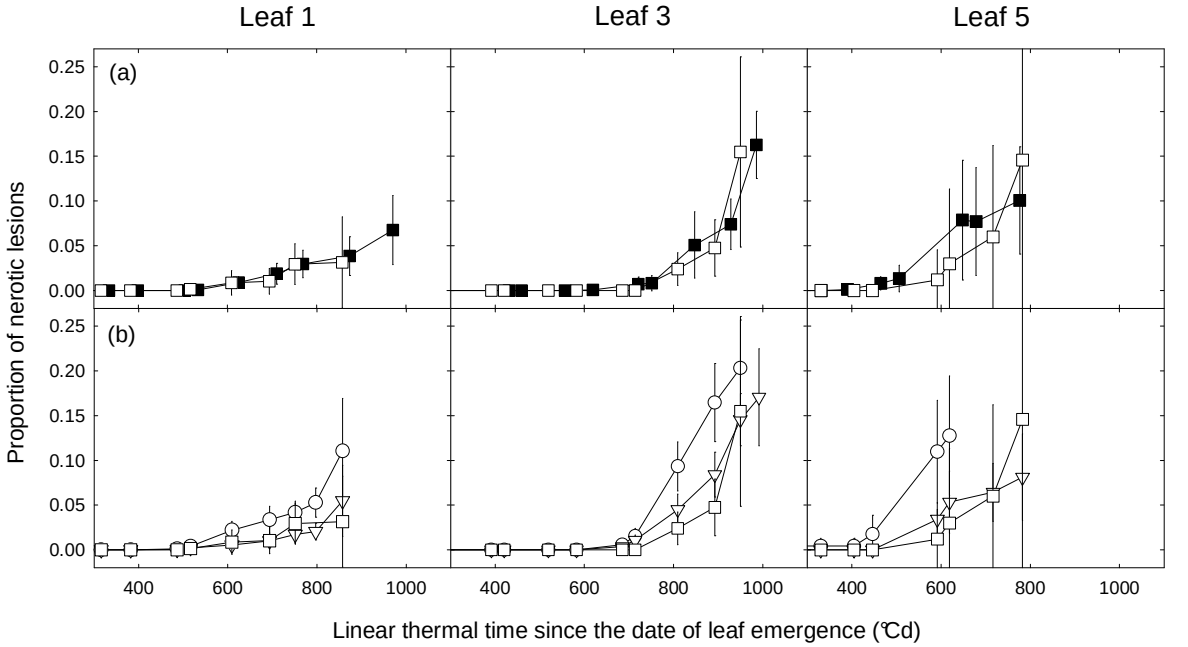

Figure 7. Dynamic of necrotic lesions of *Septoria tritici vs.* linear thermal time since the date of leaf emergence, for leaves 1, 3 and 5 (counted from the top) of main stem **(a)** for plants with N_{leaf} = 9 (□) and N_{leaf} = 10 (■) grown at a high density D3 (406 plants.m^{-2}) **(b)** for plants with N_{leaf} = 10 grown at three densities: D1 (○), D2 (▽) and D3 (□). D1: 59, D2: 160, D3: 406 plants.m^{-2}. Data are for winter wheat Cv. 'Soissons' grown in Grignon in 2008/2009. Error bars mark the 95% confidence intervals.

For each density treatment, we investigated lesion development separately for plants differing by the final leaf number on the main stem. Overall, within each density treatment, there was no noticeable difference in the pattern of lesion development between the groups of plants (Fig. 7a). Thus, differences in the date of leaf emergence, and the slightly shorter phyllochron for plants with higher number of leaves had no noticeable effect on disease progress. We also compared lesion development between densities considering only plants with the same number of leaves (N_{leaf} =10 that could be found in the three treatments) (Fig. 7b). The differences between density treatments were very similar to those found when all plants were considered.

Altogether these results indicate that (i) no strong difference in lesion development between the three density treatments was observed (ii) plants from the same treatment, but differing in final leaf number showed the same disease development in the upper leaves and (iii) the lowest density resulted in slightly stronger disease development compared to the two other densities but this did not result from the higher number of leaves in this treatment.

4. Disease simulations

4.1. Simulations of lesion development with the reference scenario Sref

Figure 8A shows measured and simulated kinetics of lesions ($NecLes_{Green}$) for leaves 1 to 6 with scenario of canopy reconstruction S_{ref}. Simulations were similar for the three density treatments. The onset of fast lesion development was predicted to take place nearly simultaneously in all treatments, consistent with observations. The simulated increase in lesion development was consistent with field observations for the intermediate (D2) and high (D3) density treatments. However, the model did not reproduce the higher rate at which lesions extended in treatment D1 compared to D2 and D3. Figure 9 illustrates how the model simulated the earliest detectable signal of lesion development (estimated as the time when $NecLes_{Green}$ = 0.5% of blade area). This was correctly predicted for leaves 1, 5 and 6, but was underestimated by approximately 250°Cd for leaves 2, 3 and 4. On leaves 2 and 3, the model predicted appearance of a small lesion area, starting 400°Cd after leaf appearance, but increasing with a low rate. Given the latency period (310°Cd in the model), this corresponds to a very limited infection predicted to have taken place shortly after leaf emergence. Field observations did not detect such small amount of early necrotic lesions. This could be either because they were too small to be seen or because model prediction of an early infection was not correct. In the case of leaf 4, the simulated onset of first lesions was followed by a significant development of the simulated lesions so that here model clearly deviated from what occurred in the field. Differences between field data and simulations were important for leaf 6; in this leaf, the timing of first lesion appearance was similar between simulations and field measurements (approximately after 500°Cd), but the rate of lesion development was underestimated in the simulation. This difference was quantitatively stronger for the low density treatment D1 with more than 10% difference at 620°Cd after leaf emergence. This was true also for leaf 7 (not shown since few measurements were available).

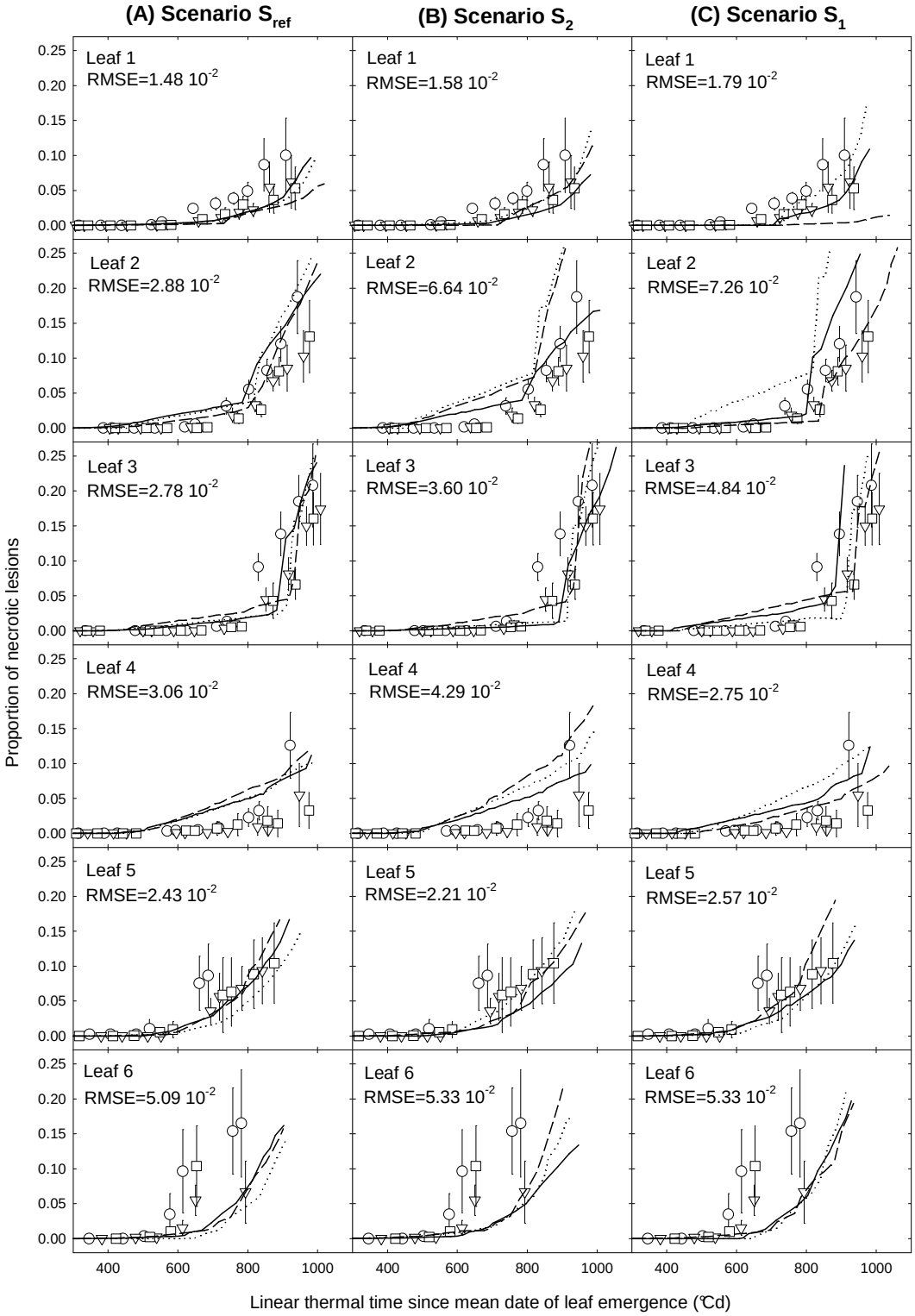

Figure 8. Predicted (lines) and measured (symbols) dynamic of necrotic lesions of *Septoria tritici vs.* linear thermal time since the average date of leaf emergence of leaves 1 to 6 (counted from the top) for wheat main stem for three scenarios of simulation differing in the degree of architecture description: (A) scenario S_{ref}, (B) scenario S_1 and (C) scenario S_2. Simulated canopy is represented by the mean plant in scenario S_1, by two mean plants differing in their final leaf number in S_2 and by plants differing in their final leaf number and stage of development in S_{ref}. Data are for winter wheat Cv. 'Soissons' grown in Grignon in 2008/2009 at three densities D1 (○, solid line), D2 (▽, dotted line) and D3 (□, long dashed line). D1: 59, D2: 160, D3: 406 plants.m^{-2}. Error bars mark the 95% confidence intervals.

To give an overall impression of the model fit, figure 10 shows the difference between simulated and observed lesions ($NecLes_{Green}$) for leaves 1 to 6, for the three density treatments, as a function of the leaf age. The RMSE values calculated for leaves 1-6 pooled are very similar and low for the three treatments (0.029, 0.028 and 0.027 for treatments D1, D2 and D3, respectively). However, simulation errors increased for higher leaf age. This could reflect that the decrease in the amount of green tissue (due to apical senescence) results in a lower accuracy in both the simulated and measured proportion of lesions ($NecLes_{Green}$) in these tissues. Moreover, during fast lesion development a small error in the predicted timing of development corresponds to a large difference in the amount of lesions at a given time. The comparison is most meaningful before 900°Cd, when there is more than 50% of green tissue. During this period, the points for treatments D2 and D3 are centred on zero, indicating that there is no overall bias, whereas for treatment D1 the model underestimates the disease.

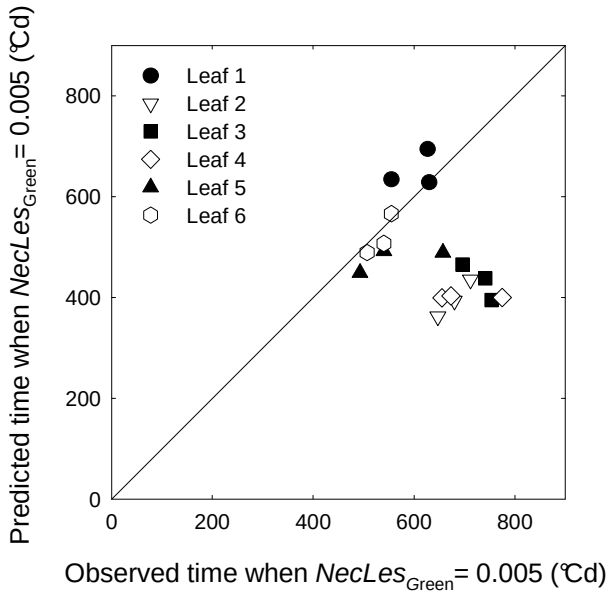

Figure 9. Predicted *vs.* observed time when $NecLes_{Green}$ = 0.005 for leaves 1 (●), 2 (▽), 3 (■), 4 (◊), 5 (▲) and 6 (⬡) counted from the top for main stem of winter wheat Cv. 'Soissons' grown in Grignon in 2008/2009 at three densities D1: 59, D2: 160, D3: 406 plants.m^{-2}. Time is expressed in linear thermal time (°Cd) since the average date of leaf emergence. Predictions are for the scenario that takes into account interplant variability of development (S_{ref}). Each point corresponds to a leaf of a density.

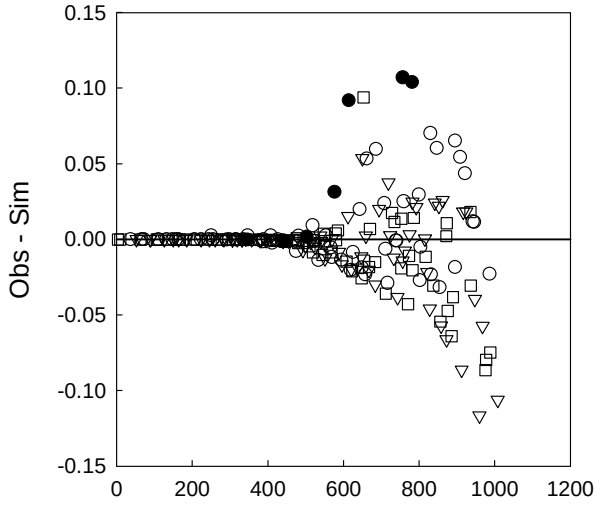

Figure 10. Differences between observed and predicted proportions of blade occupied by *Septoria tritici* necrotic lesions *vs.* linear thermal time since leaf emergence. Predictions are simulated with scenario S_{ref} (that takes into account interplant variability of development) for leaves 1 to 6 counted from the top for main stem of winter wheat Cv. 'Soissons' grown in Grignon in 2008/2009 at three densities D1 (○), D2 (▽) and D3 (□). Data for leaf 6 of the low density D1 are shown in (●). D1: 59, D2: 160, D3: 406 plants.m^{-2}.

4.2. Effect of the canopy reconstruction scenarios on the disease simulation

The model run with the three scenarios of canopy reconstruction S_{ref}, S_2 and S_1 (Fig. 8A, B and C) showed differences in simulated epidemics mostly on the two upper leaves and mostly between the two extremes S_{ref} and S_1 i.e., when comparing between taking into account the interplant variability of development and cloning a same mean plant without any variability. Besides, small differences in the timing of lesion appearance were observed between the three scenarios.

Simulations with S_2 did not show much change compared to S_{ref}. It is noticeable however that the ranking of the treatments with regards to the epidemics was changed: in S_{ref} the ranking of simulated necrotic development was D1≥D2≥D3 whereas in S_2, the model simulated a slightly higher level of necrotic development in D2, compared to D1 and D3.

More important differences were observed between S_{ref} and S_1. In S_1, differences between density treatments in the simulated lesion development increased and became large for leaves 1 and 2. For these leaves, S_1 resulted in a strong hierarchy of lesion development between density treatments, (D2>D1>D3) that did not match the field observations. It is noticeable that S_1 even predicted that the disease will not reach leaf 1 in the high density treatment D3. Scenario S_1 also yielded "stairs" shaped curves.

Discussion

In this study, we tested the capacity of a coupled virtual wheat-*Septoria tritici* epidemic model (Septo3D) to simulate *S. tritici* progress on the different leaf layers for three contrasted sowing density treatments. For this, we first experimentally characterised the plants to parameterise their description in the model. Then, we compared the simulated and observed epidemics. Despite the contrasted canopy structures, there were few differences in disease progress between treatments: only the low density treatment resulted in a higher rate of lesion development. Simulating lesion development using the canopy reconstruction that includes plant developmental variability (S_{ref}) yielded the best agreement with field measurements. In particular, the model predicted lesion onset on each layer to take place simultaneously on all treatments which was consistent with observations. However, simulations did not reproduce the higher rate at which lesions developed in the low density treatment.

Originalities of the field experimental design

One of the originalities of our experiment is the high level of detail with which both plant architecture and disease dynamics were measured. It resulted in the acquisition of an original dataset. Compared to the few existing similar studies (Evers et al., 2005), architecture characterisation here included two novel aspects: (i) the characterisation not only of axis development but also of tiller regression and leaf senescence and (ii) the characterisation of plant-to-plant variability in terms of seedling emergence, number of axes, number of phytomers and correlations with the size of mature phytomer components. We also monitored in detail the development of *S. tritici* on each leaf. It is not always possible to distinguish in the field necrosis due to the lesions (that show pycnidia) from those due to monocarpic senescence (Robert, 2003, Royle et al., 1986). In the literature, two types of assessments can be found: either based on the lesions containing pycnidia (Lovell et al., 2004b, Shaw and Royle, 1993), or based on the total area of necrotic tissues (Robert et al., 2004, Bancal et al., 2007). Here we use the area of necrotic lesions in the green part of the leaf blade, which allowed for an accurate characterisation of the early stage of infection of each layer.

Density effect on architecture

The three sowing densities resulted in varied architecture dynamics. The effects observed are in line with those described in previous studies on the effect of sowing density for wheat (Evers et al., 2005, Ljutovac, 2002). Changing sowing density was partially compensated by regulation in (i) the number of tillers, (ii) the dimensions of leaf blades in upper phytomers and (iii) the lower total number of leaves formed on an axis for higher densities. However, compensation took place progressively and was not complete even at flowering. At the onset of stem extension, the total number of axes per square meter was respectively 542 and 1461 for D1 and D3. At flowering, it was respectively 359 and 557. Thus, the environment of development of individual plants and pathogen differed between treatments.

Density effect on epidemics

Irregular intervals between kinetics of total necrotic lesions were observed for successive leaf layers for the three density treatments. Robert et al. (2004) reported that the death of successive wheat leaves infected by *S. tritici* occurred at regular intervals, corresponding to one phyllochron. This regularity results from very favourable climatic conditions that cause infection of leaves just after leaf emergence. In our experiment, the unfavourable environment could have resulted in irregular timing of infection of successive leaves.

Contrasted effects of sowing density on foliar diseases have been reported: increasing densities may enhance epidemics (Tompkins et al., 1993, Ando and Grumet, 2006, Gan et al., 2007, Jurke and Fernando, 2008); have little effect (Pfleeger and Mundt, 1998); or even reduce epidemics (Eyal, 1981). For *S. tritici*, increasing plant density was reported to enhance epidemics by several authors (Broscious et al., 1985, Tompkins et al., 1993, Ansar et al., 1996, Ansar and Leitch, 2009). However *S. tritici* increased only up to some threshold in plant density, above which either no further effect (Ansar et al., 1996), or a decrease in disease severity was observed, even to a level below that observed at the lowest density (Ansar and Leitch, 2009). In a field trial carried out by Broscious et al. (1985), only 5 out of 13 trials showed a significant sowing rate effect on *S. tritici* severity, one of which was a decrease. In our experiment, the different density treatments resulted in similar epidemics, except for a slightly higher rate of lesion development in the low density. This higher rate of development was observed from leaf 6, a rosette leaf, and persisted throughout the season on the upper leaves, suggesting that the density effect resulted partly from interaction between architecture and climate during the winter, i.e., the rosette stage. The potential importance of the winter period for the resulting epidemic may possibly be linked to two characteristics of our experiment: the late sowing date reduced the duration during which rosette leaves could be infected, and the rather unfavourable environmental conditions for *S. tritici* during the stem extension may have given a strong importance to differences established in the rosette leaves.

Two processes may have contributed to the higher disease development observed in the rosette leaves in the low density treatment. The sparser canopy may have (1) induced a higher rain penetration and thus a stronger contamination from the soil, and (2) resulted in a higher number of spores deposited per unit of leaf area. Assuming that during a rain event spores on the soil are splashed until they are deposited on a leaf, an equal amount of spores is then divided by a smaller leaf area for less dense vegetation. This is consistent with Eyal (1981) who reported that the raindrop-splashing effect was increased in less dense crops leading to earlier and faster pathogen progress.

Finally, it is also possible that the physiological status of the leaves and in particular the leaf nitrogen content played a role in the difference in disease development between the density treatments. This effect is suggested because on the one hand, leaf nitrogen dynamics

likely differed between density treatments, as the content of nitrogen usually decreases rapidly in leaves and shoots of seedlings grown at high density (Sasaki and Toriyama, 2006, Ansar and Leitch, 2009) and on the other hand, foliar lesion development has been found to be influenced by the leaf nitrogen content (Leitch and Jenkins, 1995, Lovell et al., 1997).

Within a density treatment, we did not observe difference in disease development on upper leaves between plants with different numbers of leaves. We checked this because differences in final leaf number implies differences in phyllochron and date of leaf emergence (Baccar et al., 2010), which is known to influence the leaf infection by *S. tritici* (Shaw and Royle, 1993, Moreau and Maraite, 1999). A possible hypothesis is that the variability in plant development in the field (in part due to variability in the date of seedling emergence) was strong enough to mitigate the effect of the variability between plants due to different leaf number.

Modelling canopy variability and its effect on epidemics

One of the originalities of the present architecture reconstruction is to address the modelling of interplant variability. Most of the time, a mean plant is reconstructed, and random variability is added on the top of this base (Evers et al., 2005, Fournier and Andrieu, 1999, Fournier et al., 2003). Here we quantified experimentally two sources of variability, and tested the impact of taking into account each of them on disease simulation. The first source of variability is that related to differences in total number of leaves produced on the main stem, which are linked to various architectural variables (dimensions, development, and senescence) on main stems and tillers. We took into account this variability by integrating separately in the model architectural variables of each group of plants with the same number of leaves and by representing the observed proportions of each group of plants in the reconstructed canopy. The second source of variability is linked to delays in date of plant emergence. We characterized the variability in development between plants at two dates and estimated from this variability in the date of emergence that was introduced in the simulation. The level of variability included in the canopy reconstruction influenced the simulated disease dynamics. Decreasing the variability of plant development increased the difference between the density treatments, leading to unrealistic differences when all plants were taken identical. In addition, taking into consideration the plant-to-plant variability of development (i.e., in scenario S_{ref}), resulted in realistic kinetics with smooth curves of lesion development. Scenarios S_2 and mostly S_1 yielded "stairs" shaped curves reflecting simultaneous response of the same type of plants to a single infection event. Simulating a canopy of identical plants introduces the risk of missing the infection of an entire leaf layer if the predicted leaf emergence happens to be just after a rare but important rain event.

New parameterisation of initial infection conditions improved triggering the disease

Septo3D requires an initialisation of disease. In the previous version of the model (Robert et al., 2008), initial infection was parameterised by infecting directly the three first rosette leaves. In the present version, the rosette leaves are infected by splashes from spores on the ground as in Audsley et al. (2005). The parameters for initial conditions are the period during which infection can occur, taken infinite here as in Audsley et al. (2005), and area of sporulating surface on the ground. Using this new parameterisation, the three densities responded differently to varying initial conditions, showing that the infection of the rosette leaves does now respond to architecture.

Capacity of the model to simulate S. tritici epidemics

For scenario S_{ref}, the most realistic architecture description, simulations of lesion development displayed little difference between the three density treatments. For the 5 upper leaves, the simulations were consistent with field data (within the 95% confidence intervals,

RMSE above 3.06 10^{-2} of the proportion of necrotic lesions) particularly for high and intermediate density treatments. The model simulated consistently the onset of lesion development in leaves 6, 5 and 1 (numbered from the top). Three main discrepancies were found between simulations and observed epidemics:

(i) the model underestimated disease progress on leaf 6, especially strongly for the low density. Two known mechanisms of infection: ascospore deposition (Shaw and Royle, 1989, Hunter et al., 1999) and contamination by direct contact between leaves (Lovell et al., 2004b) are currently lacking in Septo3D, which may explain the disease underestimation on the rosette leaves.

(ii) the model did not reproduce the higher rate at which lesion developed in the low density treatment compared to intermediate and high density treatments. The underestimation observed on leaf 6 for all densities, was subsequently observed on all upper leaves only for the low density. This suggests that the underestimation on rosette leaves did not affect the simulation of the higher leaves for intermediate and high density, whereas it did for the low density. In this treatment, the underestimation of the infection of rosette leaves may have resulted in a simulated inoculum sufficiently low to hamper the simulated disease progress and thus in the underestimation of the infection of higher layers.

(iii) on leaves 2 and 3 the model predicted appearance of small, slowly extending, lesions largely before the date we observed the first lesions. This also occurred for leaf 4 and in this case, it resulted later in a significant development of the simulated disease sooner than observed in the field. One possible explanation is that we used a fixed duration of the latency period (310°Cd) whereas the latency period may be much longer when conditions of temperature and humidity hamper fungus development (Shaw, 1990, Shaw, 1991, Lovell et al., 2004a).

Difficulties of validation of coupled architecture-epidemic models

Testing the model predictions appeared to be quite a challenge. *S. tritici* epidemics turned out to be low in our experiment: the assessed disease severity was below 20% for all leaves and yields were similar in the treated and non-treated plots. Therefore, density effects were less likely to be expressed or detectable. Moreover, lesions can only be identified in green tissue, meaning that in the case of a slow developing epidemic, such as here, the progress of monocarpic senescence hampers the completeness of the description of lesion extension.

Using sowing density treatments to vary canopy architecture and test the model was a complex task for two reasons: (i) despite using extreme ranges of densities, the plasticity of wheat resulted in the compensation of differences between the three densities at canopy level over time and introduced complex effects within a single density (ii) the phenotypic response of the plants to density is complex and rises important challenges for a realistic reconstruction of the canopy. To overcome these difficulties, a possible solution could be to test the model with field experiments using more contrasted and/or simpler canopy architectures such as monoculm wheat canopies avoiding thus compensation by tillering, different Rht-gene lines allowing strong differences in stem height, or modified plant architectures: e.g., clipping an entire leaf layer.

Acknowledgements

The authors gratefully acknowledge Fabrice Duhamel and Maxime Marques for their excellent technical assistance, and Valérie Bontemps for her high degree of commitment in the characterisation of *S. tritici* epidemics. The Unité Expérimentale of Centre INRA,

Versailles-Grignon, headed up the agronomic work. The work was funded by INRA, Department of Environnement et Agronomie and by ARVALIS, Institut du végétal.

References

Ando K, Grumet R. 2006. Evaluation of altered cucumber plant architecture as a means to reduce Phytophthora capsici disease incidence on cucumber fruit. *Journal of the American Society for Horticultural Science,* **131**: 491-498.

Ando K, Grumet R, Terpstra K, Kelly JD. 2007. Manipulation of plant architecture to enhance crop disease control. *CAB Reviews: Perspectives in Agriculture, Veterinary Science, Nutrition and Natural Resources,* **2**: 8 pp.

Ansar M, Leitch MH. 2009. The effect of agronomic practices on the development of Septoria Leaf Blotch and its subsequent affect on the yield and yield components of wheat. *American-Eurasian Journal of Sustainable Agriculture,* **3**: 57-67.

Ansar M, Leitch MH, Jenkins PD, Hayden NJ. 1996. Effect of nitrogen fertilizer, crop density and development of Septoria tritici on components of growth and yield of winter wheat in the UK. *Proceedings of the 5th International Wheat Conference.* June 10-14, 1996, Ankara, Turkey. 270-272.

Audsley E, Milne A, Paveley N. 2005. A foliar disease model for use in wheat disease management decision support systems. *Annals of Applied Biology,* **147**: 161-172.

Baccar R, Dornbusch T, Abichou M, Gate P, Andrieu B. 2010. Description of the effect of sowing date and density on the phyllochron of winter wheat (*Triticum aestivum* L.): a two-phase model determined by photoperiod and final leaf number. *submitted in European Journal of Agronomy*.

Bahat A, Gelernter I, Brown MB, Eyal Z. 1980. Factors affecting the vertical progression of Septoria leaf blotch in short-statured wheats. *Phytopathology*, **70**: 179-184.

Bancal MO, Robert C, Ney B. 2007. Modelling wheat growth and yield losses from late epidemics of foliar diseases using loss of green leaf area per layer and pre-anthesis reserves. *Annals of Botany*, **100**: 777-789.

Broscious SC, Frank JA, Frederick JR. 1985. Influence of winter wheat management practices on the severity of powdery mildew and Septoria blotch in Pennsylvania. *Phytopathology*, **75**: 538-542.

Calonnec A, Cartolaro P, Naulin JM, Bailey D, Langlais M. 2008. A host-pathogen simulation model: powdery mildew of grapevine. *Plant Pathology,* **57**: 493-508.

Camacho-Casas MA, Kronstad WE, Scharen AL. 1995. Septoria tritici resistance and associations with agronomic traits in a wheat cross. *Crop Science,* **35**: 971-976.

Danon T, Sacks JM, Eyal Z. 1982. The relationships among plant stature, maturity class, and susceptibility to Septoria leaf blotch of wheat. *Phytopathology,* **72**: 1037-1042.

Darwinkel. 1978. Patterns of tillering and grain production of winter wheat at a wide range of plant densities. *Netherlands Journal of Agricultural Science,* **26**: 383-398.

Dornbusch T, Andrieu B. 2010. Lamina2Shape - an image processing tool for an explicit description of lamina shape tested on winter wheat (*Triticum aestivum* L.). *Computers and Electronics in Agriculture,* **70**: 217-224.

Dornbusch T, Baccar R, Watt J, Hillier J, Bertheloot J, Fournier C, Andrieu B. 2010. Plasticity of winter wheat modulated by sowing date, plant population density and nitrogen fertilisation: Dimensions and size of leaf blades, sheaths and internodes in relation to their position on a stem. *Field Crops Research,* **(accepted for publication 2.12.2011)**.

Evers JB, Vos J, Fournier C, Andrieu B, Chelle M, Struik PC. 2005. Towards a generic architectural model of tillering in Gramineae, as exemplified by spring wheat (Triticum aestivum). *New Phytologist,* **166**: 801-812.

Eyal Z. 1981. Integrated control of Septoria diseases of wheat. *Plant Disease,* **65**: 763-768.

Fournier C, Andrieu B. 1999. ADEL-maize: an L-system based model for the integration of growth processes from the organ to the canopy. Application to regulation of morphogenesis by light availability. *Agronomie,* **19**: 313-327.

Fournier C, Andrieu B, Ljutovac S, Saint-Jean S. 2003. ADEL-wheat: A 3D architectural model of wheat development. In: Hu B-G, Jaeger M eds. *Proceedings of International Symposium of Plant Growth Modeling and Applications.* Beijing, China. 2003 Tsinghua University Press - Springer Verlag.

Fournier C, Durand JL, Ljutovac S, Schaufele R, Gastal F, Andrieu B. 2005. A functional-structural model of elongation of the grass leaf and its relationships with the phyllochron. *New Phytologist,* **166**: 881-894.

Friend DJC. 1965. Tillering and leaf production in wheat as affected by temperature and light intensity. *Canadian Journal of Botany,* **43**: 1063-1076.

Gan Y, Gossen BD, Li L, Ford G, Banniza S. 2007. Cultivar type, plant population, and ascochyta blight in chickpea. *Agronomy Journal,* **99**: 1463-1470.

Georgin P, Gouet M. 2000. *Statistiques avec Excel 2000,* Paris, Eyrolles.

Godin C, Sinoquet H. 2005. Functional-structural plant modelling. *New Phytologist,* **166**: 705-708.

Hanan J, Prusinkiewicz P, Zalucki M, Skirvin D. 2002. Simulation of insect movement with respect to plant architecture and morphogenesis. *Computers and Electronics in Agriculture,* **35**: 255-269.

Hilton AJ, Jenkinson P, Hollins TW, Parry DW. 1999. Relationship between cultivar height and severity of Fusarium ear blight in wheat. *Plant Pathology,* **48**: 202-208.

Hunter T, Coker RR, Royle DJ. 1999. The teleomorph stage, Mycosphaerella graminicola, in epidemics of Septoria tritici blotch on winter wheat in the UK. *Plant Pathology,* **48**: 51-57.

Johnson FH, Lewin I. 1946. The growth rate of *E.coli* in relation to temperature, quinine, and coenzyme. *Journal of Cellular and Comparative Physiology,* **28**: 239 - 251.

Jurke CJ, Fernando WGD. 2008. Effects of seeding rate and plant density on sclerotinia stem rot incidence in canola. *Archives of Phytopathology and Plant Protection,* **41**: 142-155.

Leitch MH, Jenkins PD. 1995. Influence of nitrogen on the development of Septoria epidemics in winter wheat. *Journal of Agricultural Science,* **124**: 361-368.

Ljutovac S. 2002. *Coordination dans l'extension des organes aériens et conséquences pour les relations entre les dimensions finales des organes chez le blé,* PhD thesis, Institut National Agronomique Paris-Grignon, Paris, France.

Lovell DJ, Hunter T, Powers SJ, Parker SR, Bosch Fvd. 2004a. Effect of temperature on latent period of septoria leaf blotch on winter wheat under outdoor conditions. *Plant Pathology,* **53**: 170-181.

Lovell DJ, Parker SR, Hunter T, Royle DJ, Coker RR. 1997. Influence of crop growth and structure on the risk of epidemics by Mycosphaerella graminicola (Septoria tritici) in winter wheat. *Plant Pathology,* **46**: 126-138.

Lovell DJ, Parker SR, Hunter T, Welham SJ, Nichols AR. 2004b. Position of inoculum in the canopy affects the risk of septoria tritici blotch epidemics in winter wheat. *Plant Pathology,* **53**: 11-21.

Masle-Meynard J, Sebillotte M. 1981. Study of the heterogeneity of a winter wheat stand. II. Origin of the different sorts of individuals in the stand; factors allowing description of its structure. *Agronomie*, **1**: 217-223.

Masle J. 1985. Competition among tillers in winter wheat : Consequences for growth and development of the crop. In: Day W, Atkin RK eds. *Wheat Growth and Modelling.* New-York and London, Plenum Press. 33-44.

Moreau JM, Maraite H. 1999. Integration of knowledge on wheat phenology and Septoria tritici epidemiology into a disease risk simulation model validated in Belgium. *Information technology for crop protection, 23 September 1999, Harpenden, UK.*

Parent B. 2009. *Leaf development in rice and maize: framework of analysis, compared responses to temperature and growth regulation under water deficit.*, PhD degree, Montpellier Supagro, Montpellier, France.

Pfleeger TG, Mundt CC. 1998. Wheat leaf rust severity as affected by plant density and species proportion in simple communities of wheat and wild oats. *Phytopathology*, **88**: 708-714.

Pielaat A, Bosch Fvd, Fitt. BDL, Jeger MJ. 2002. Simulation of vertical spread of plant diseases in a crop canopy by stem extension and splash dispersal. *Ecological Modelling*, **151**: 195-212.

Rapilly F, Jolivet E. 1974. Construction d'un modèle (episept) permettant la simulation d'une épidémie de Septoria nodorum BERK sur blé. *Revue de statistiques appliquées*, **3**: 31-60.

Robert C. 2003. *Etude et modélisation du fonctionnement d'un couvert de blé attaqué par le complexe parasitaire Puccinia triticina - Mycosphaerella graminicola,* PhD thesis, Institut National Agronomique de Paris-Grignon, Paris, France.

Robert C, Bancal MO, Nicolas P, Lannou C, Ney B. 2004. Analysis and modelling of effects of leaf rust and Septoria tritici blotch on wheat growth. *Journal of Experimental Botany*, **55**: 1079-1094.

Robert C, Fournier C, Andrieu B, Ney B. 2008. Coupling a 3D virtual wheat (Triticum aestivum) plant model with a Septoria tritici epidemic model (Septo3D): a new approach to investigate plant-pathogen interactions linked to canopy architecture. *Functional Plant Biology*, **35**: 997-1013.

Room P, Hanan J, Prusinkiewicz P. 1996. Virtual plants: new perspectives for ecologists, pathologists and agricultural scientists. *Trends in Plant Science*, **1**: 33-39.

Royle DJ, Shaw MW, Cook RJ. 1986. Patterns of development of Septoria nodorum and S. tritici in some winter wheat crops in Western Europe, 1981-83. *Plant Pathology*, **35**: 466-476.

Saindon G, Huang HC, Kozub GC. 1995. White-mold avoidance and agronomic attributes of upright common beans grown at multiple planting densities in narrow rows. *Journal of the American Society for Horticultural Science*, **120**: 843-847.

Sasaki R, Toriyama K. 2006. Nitrogen content of leaves affects the nodal position of the last visible primary tiller on main stems of rice plants grown at various plant densities. *Plant Production Science*, **9**: 242-248.

Schwartz HF, Steadman JR, Coyne DP. 1978. Influence of *Phaseolus-vulgaris* blossoming characteristics and canopy structure upon reaction to *Sclerotinia Sclerotiorum Phytopathology*, **68**: 465-470.

Scott PR, Benedikz PW, Cox CJ. 1982. A genetic study of the relationship between height, time of ear emergence and resistance to Septoria nodorum in wheat. *Plant Pathology*, **31**: 45-60.

Scott PR, Benedikz PW, Jones HG, Ford MA. 1985. Some effects of canopy structure and microclimate on infection of tall and short wheats by Septoria nodorum. *Plant Pathology*, **34**: 578-593.

Shaw MW. 1990. Effects of temperature, leaf wetness and cultivar on the latent period of Mycosphaerella graminicola on winter wheat. *Plant Pathology*, **39**: 255-268.

Shaw MW. 1991. Interacting effects of interrupted humid periods and light on infection of wheat leaves by Mycosphaerella graminicola (Septoria tritici). *Plant Pathology,* **40**: 595-607.

Shaw MW, Royle DJ. 1989. Airborne inoculum as a major source of Septoria tritici (Mycosphaerella graminicola) infections in winter wheat crops in the UK. *Plant Pathology*, **38**: 35-43.

Shaw MW, Royle DJ. 1993. Factors determining the severity of epidemics of *Mycosphaerella graminicola* (*Septoria tritici*) on winter wheat in the UK *Plant Pathology*, **42**: 882-899.

Simon MR, Perello AE, Cordo CA, Larran S, Putten PELvd, Struik PC. 2005. Association between Septoria tritici blotch, plant height, and heading date in wheat. *Agronomy Journal*, **97**: 1072-1081.

Skirvin DJ. 2004. Virtual plant models of predatory mite movement in complex plant canopies. *Ecological Modelling*, **171**: 301-313.

Tavella CM. 1978. Date of heading and plant height of wheat varieties, as related to Septoria leaf blotch damage. *Euphytica,* **27**: 577-580.

Tompkins DK, Fowler DB, Wright AT. 1993. Influence of agronomic practices on canopy microclimate and Septoria development in no-till winter wheat produced in the Parkland region of Saskatchewan. *Canadian Journal of Plant Science,* **73**: 331-344.

Vos J, Evers JB, Buck-Sorlin GH, Andrieu B, Chelle M, de Visser PHB. 2010. Functional-structural plant modelling: a new versatile tool in crop science. *Journal of Experimental Botany*, **61**: 2101-2115.

Wilhelm WW, McMaster GS. 1995. Importance of the phyllochron in studying development and growth in grasses. *Crop Science,* **35**: 1-3.

Wilson PA, Chakraborty S. 1998. The virtual plant: a new tool for the study and management of plant diseases. *Crop Protection*, **17**: 231-239.

Chapter 4

General discussion

I. Summary of main results

Our work addressed plasticity of winter wheat in response to sowing date and density and the effect of architecture variations with density on disease measured and simulated with the model Septo3D. Here, we summarize the main results of each chapter.

Chapter 1: Variations of phyllochron in response to sowing date and density

Phyllochron is an important parameter in crop models and has been reported to play a crucial role on *Septoria* disease propagation (Lovell et al., 1997, Robert et al., 2008). We investigated the variation of phyllochron during the wheat growth and differences between sowing date and density treatments. The use of non-linear response to temperature to compute thermal time was addressed. The relation between the phyllochron on main stem and primary tillers was also investigated.

The use of compensated thermal time assuming a non-linear response to temperature allowed for a high reproducibility of the rate of leaf emergence between years and treatments. When expressed in compensated thermal time, the phyllochron of a wheat tiller could be described with a two-phase descriptive model. Rate in Phase I depended on sowing date and rate in phase II depended on both sowing date and final leaf number. Phyllochron in phase II could be up to 15% longer in high density compared to low density and 30% longer for early sowing compared to late sowing for plants from the same density. The time of shift in phyllochron between the two phases coincided with the timing of flag leaf initiation suggesting that it is linked to plant ontogeny. The phyllochron of primary tillers showed the same pattern of that of the main stem. Finally, much of the variation in the phyllochron of a wheat tiller with density and sowing date could be ascribed to the photoperiod at seedling emergence and to the final leaf number.

The fitted model allowed an accurate estimation of phyllochron of each phase and the quantification of its variation with sowing date and density. Further, the model parameters were implemented in the model Septo3D to compute dates of leaf emergence and rate of stem extension. The quantification of the variations in phyllochron between treatments could help predicting the amplitude and direction of the possible effect on disease development. Robert et al. (2008), reported that a reduction by 30% in phyllochron resulted in a drastic reduction in Septoria epidemics.

Chapter 2: Plasticity of wheat architecture with sowing date and density

Agronomic practices such as sowing date and plant population density are known to lead to modulation of plant architecture. We aimed both at making a comprehensive description of architecture variability at the plant and the canopy scale and at producing a dataset of winter wheat architecture for the investigated treatments with intent to use it for 3D reconstruction. This required intensive characterisation of architectural variables at phytomer level, for main stem and axillary tillers. Vertical profiles of organs dimensions were compared between sowing date and density treatments and between plants of a same treatment that differed in their final leaf number. Characterisation of canopy variables such as leaf area index and ground cover were also performed.

Patterns of blade, sheath and internode dimensions resembled to those usually found for winter wheat but varied between treatments. There was almost no difference between density treatments in organ dimensions of juvenile phytomers (growing before the onset of stem elongation), but there were differences for adult phytomers (borne on elongated internodes): organ dimensions were higher for the low plant population density. At the canopy

scale, although the low density resulted in higher number of tillers/plant, it showed a lower rate of progress in leaf area index (LAI) and ground cover than the high density. On the other hand, there were differences in the number and dimensions of juvenile phytomers between sowing date treatments. Early sowing led to a higher number of juvenile phytomers and larger leaves of these phytomers compared to late sowing. For adult phytomers, the number and dimensions of organs were almost identical between sowing date treatments, probably because plants experienced the same environmental conditions during stem extension. Number of shoots/m² and rates of increase in LAI and ground cover were higher in the early sowing.

The final number of leaves was higher for low density and early sowing. Moreover, 1 to 3 values of final leaf number could be found for a given axis within the same treatment. There were differences of main stem organ dimensions between plants with different final leaf number: plants with a higher number of leaves produced lower organ dimensions for the juvenile phytomers (counted acropetally) and higher organ dimensions for the adult phytomers (counted basipetally). Local variations of density and thus on light quantity and quality could be behind the observed variation of final leaf number and organ dimensions.

Our findings confirm that the similarity in the pattern of organ dimensions between main stem and tillers was maintained when considering a range of densities. The similarities in the vertical profiles of organ dimensions could be simply expressed by considering phytomer position counted from the top.

Ability to reproduce wheat architecture with a 3D model using measured architectural variables

Because of non accuracy of phytomer rank identification in the first experimental year and damages caused by birds in the early sowing of the second year, an accurate and comprehensive dataset of architecture could be obtained only for late sowing of the second experimental year. In this case, organ dimensions with their accurate correspondence with phytomer rank were obtained for the main stem and primary tillers at the three densities. These data were used to parameterise the canopy model in Septo3D and were given as input variables.

Model parameterisation required supplemental variables to fill the inputs. Indeed, the canopy model takes as input parameterisation of (i) the rate of leaf appearance and senescence for each axis, (ii) the tillering dynamic of the plant, (iii) the dimensions of mature plant organs and, (iv) the geometry of leaves. This was done either by using additional data from other experiment, or by applying theoretical assumptions. Here, we remind the main assumptions used to provide these informations and the adequacy of these assumptions for the model parameterisation:

- The rate of leaf appearance as well as organ dimensions were measured on main stem and primary tillers but not on secondary tillers. A general scheme of coordination in tiller emergence has been proposed by Masle-Meynard and Sebillote (1981). This approach supports that tillers emerge by cohorts and that tillers of the same cohort share the same properties. Thus, considering this concept, we assumed that secondary tillers have the same rate and organ dimensions as primary tillers of the same cohort. As it was not checked before, this assumption may be a possible source of error. However, given that the reconstructed canopy corresponded to a late sowing and that few secondary tillers developed at this sowing, this should not induce a substantial error in the simulated leaf area index.

- Punctual measurements of tiller occurrence frequency and total number of tillers were not sufficient to describe tillering dynamic. A tillering model was thus developed based on the

Fibonacci sequence and the cohort principle and fitted to these measurements. Resulting tillering dynamics simulated by the model were close to observed data which proved that this approach was appropriate to parameterise tillering and, that using a limited number of measurements combined to adequate behavioural rules was sufficient to reconstruct tiller dynamics.

- Geometry for azimuth of leaves and curvature of leaf midribs were not measured in our experiment. Leaf curvature was therefore parameterized based on data from another experiment carried out with the same cultivar at the same location. Thus, leaf posture was parameterized similarly for all densities which is not fully realistic as density is known to influence the leaf posture. On the other hand, parameterisation of leaf geometry was improved in the current version of the model by including a dynamic change in leaf angle with time course.

Chapter 3: Simulation of the effect of differences in wheat canopy architecture between sowing densities on Septoria tritici epidemics

The dataset of wheat architecture corresponding to three densities at a late sowing date were used to parameterise the model Septo3D. Simulated epidemics were compared to observed ones for model validation. This required detailed and frequent measurements of disease dynamics at the level of individual leaves. Moreover, simulations were run with three simulation scenarios differing by the degree of detail in the description of plant variability which was derived from field measurement.

The model predictions were consistent with field measurements and simulations revealed that despite the contrasted canopy structures, there were few differences in disease progress between densities Simulations performed with the different scenarios showed that the canopy reconstruction scenario in which inter-plant variability was taken into account yielded the best agreement between measured and simulated epidemics, whereas simulations performed with the canopy represented by a population of a same average plant deviated strongly from field observations. The main findings of this chapter are discussed further in the discussion.

II. Effect of differences in architectural variables due to sowing date and sowing density on disease development

1. *Septoria* epidemic and possible interactions with canopy architecture

1.1. Epidemic parameters influenced by canopy architecture

In this paragraph we present the internal variables of *S. tritici* likely to be influenced by architectural variables. We distinguish between variables linked to the disease propagation from those linked to the infection cycle.

Disease propagation

1. *Quantity of droplet produced* (infectious and non-infectious): this depends on the rain intensity and interception by the canopy vegetation. It thus depends on the leaf area profile and cover.
2. *Quantity of dispersal units* (DU) *produced*: depends on the vegetation profile, the fraction and location of sporulating lesions in the different leaf layers of the canopy (only raindrops that hit sporulating lesions will contain spores).
3. *Quantity of DU intercepted*: the quantity of DU intercepted by green tissue depends on the distance travelled by the droplet, and on the fraction and location of green tissue around the leaf source. It thus depends on vegetation density and distribution of green tissue.
4. *Efficiency of DU washing*: the fraction of spores that may be removed by subsequent rains (washing) depends on rain frequency and intensity after DU deposit and also in the vegetation profile and density which determine the capacity of a raindrop to reach a leaf layer.

Infection cycle

1. Efficiency of spore germination: spores germinate if microclimatic conditions of temperature and humidity are met. This depends on the vegetation density and the climate.
2. Ability to complete the infection cycle: pathogen incubation (biotrophic phase) needs green tissue to be completed; this depends on the rate and timing of monocarpic senescence. The physiological status of leaves may also contribute to enhance natural leaf senescence.
3. Duration of infection cycle: the latency period of *M. graminicola* can vary according to environmental conditions (Lovell et al., 2004a, Shaw, 1990). Hence, by influencing the microclimate, the vegetation density can vary the duration of the infection cycle and thus the potential number of cycles likely to occur on a leaf.

1.2. Architectural variables that could influence Septoria epidemic development

Authors who investigated the effect of architecture of *Septoria* development (cf. Introduction, section IV.4) have accounted for the effect of architecture by invoking variables either at the plant or at the canopy scale. However, many of these variables are correlated and a general overview is needed to clarify their interdependency on one side and their correlation with epidemic variables on the other side. The scheme presented in Figure 1, aims at giving this overview.

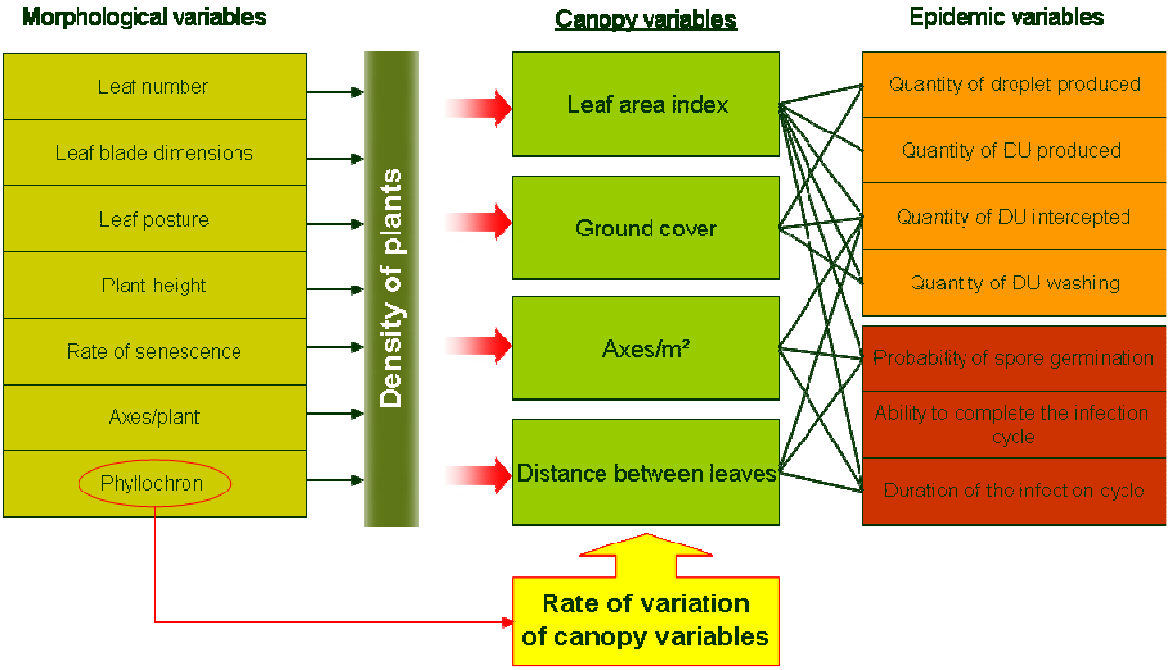

Figure 1. Scheme representing the relations between architectural variables (morphological and canopy) and epidemic variables.

In Figure 1, variables that are measurable at the plant scale and which are often determined by GxE interactions are referred to as **morphological variables**; whereas variables that are measurable at the canopy scale and that characterize the field structure are referred to as **canopy variables**. Phyllochron is a particular variable because by defining the rate of organ development at the plant scale, it also determines the rate of development of the whole canopy.

Despite the dependency relationships shown between morphological and canopy variables, we yet believe that it is necessary to report the effect on epidemic parameters of both type of variables. Indeed, morphological variables are easily identifiable and measurable whereas canopy variables are more abstract. Wheat architecture changes during the season and the spatial location of the disease as well. It is therefore difficult to understand the effect of architectural variables without considering the dynamic changes during the season and the associated mechanisms. For this reason, we defined a grid of architecture-pathogen interactions considering the dynamics in time of disease and wheat architecture (Table 1).

2. A grid of architecture-epidemic interactions during wheat growth cycle

Considering the cycle of wheat development and the development of *S. tritici* during this cycle, we distinguish three phases to analyse the possible architecture-disease interactions (Table 1). Both wheat and *Septoria* development have specific characteristics during these phases that may lead to different hierarchies in these interactions.

- **Phase 1:** from seedling emergence to the stage of three fully emerged leaves (beginning of tillering);
- **Phase 2:** from four fully emerged leaves to the beginning of stem extension (tillering phase);
- **Phase 3:** from the beginning of stem extension to flowering.

During phase 1, the three first leaves can be infected only by external inoculum i.e. air-borne ascospores (Shaw and Royle, 1989) or pycnidiospores from the soil. Indeed, considering that the latency period lasts on average 300°Cd and the mean phyllochron around 100 °Cd, the first sporulating lesions appear on leaf 1 when leaves 2 and 3 have already developed and most probably have been infected. During this phase, the wheat, in its rosette form, is characterised by a low ground cover and low leaf area index. The soil has higher chance to intercept rain drops resulting in the production of a high quantity of infectious droplets.

During phase 2, we consider that the first lesions have appeared on the first leaves; thus infection of new emerging leaves by pycnidiospores produced on these leaves is possible. However, as the vegetation develops, the soil becomes more difficult to reach by raindrops and lesions become more important in the first leaves. Consequently, we can hypothesise that, during this phase, infections due to splashing from leaf to leaf increases progressively, whereas infections from external inoculum decrease. During phase 2, wheat is still at the rosette stage; thus, distances between leaves are short which facilitate contamination by splashes. In this phase, the ground cover and the leaf area index increase faster than during phase 1 because of tiller development.

Phase 3 is characterised by an important change in wheat architecture: the stem extension. While the stem elongates, the disease continues to propagate through splashing which creates possibilities of escape. Indeed, a leaf that is farther from older infected leaves cannot be easily reached by infectious droplets. Hence, the stem elongation creates a dynamical relation, comparable to a race, between the plant and the disease. At this phase, canopy closure is almost complete.

Table 1 summarizes the expected effects on *Septoria* development of both morphological and canopy variables during the three identified phases.

Table 1
Summary of main architectural variables modified by density and sowing date and their interactions with *S. tritici* epidemic development through three stages of wheat cycle. DU=Dispersal Units.

			Phase 1 *From seedling emergence to 3 emerged leaves*	Phase 2 *From leaf 4 emergence to beginning of stem extension*	Phase 3 *From beginning of stem extension to flowering (5 upper leaves)*
Canopy variables	**Ground cover**		⊕ increased rain interception and droplet production	⊕ increased rain interception and droplet production	⊖ decreased rain penetration and droplet production (umbrella effect) ⊕ less washing in low and intermediate layers of the canopy
	Leaf area index		⊕ more green leaf area to intercept DU ⊖ less intercepted DU per unit of green area	⊕ more green leaf area to intercept DU	⊕ more green leaf area to intercept DU
	Horizontal distance between leaves			⊕ short distance to travel, high probability of DU interception	⊕ short distance to travel, high probability of DU interception ⊕ spore propagation by contact between leaves
Morphological variables	**Phyllochron**	**Rate of leaf appearance**		⊕ increase the number of leaves and tillers, thus more green leaf area	
		Rate of senescence		⊖ decrease probability of hitting green tissue ⊖ kill incubating lesions	⊖ decrease probability of hitting green tissue ⊖ kill incubating lesions
		Rate of stem extension			⊖ decrease duration and possibilities of overlap between infected and emerging leaves ⊖ increase distance to travel, so low probability of DU interception
	Leaf	**Number**		⊕ more green tissue to intercept DU	
		Dimensions	⊕ more green leaf area to intercept DU	⊕ more green tissue to intercept DU	⊕ more green tissue to intercept DU
		Posture (erect)	⊖ more splash on the soil ⊖ higher distance from the soil to the leaf	⊖ more splash on the soil ⊖ higher distance to travel for the splash	⊕ increase possibilities of overlap ⊕ shorter distance to travel for splash, high probability of DU interception

This table illustrates that:

- The effect of some architectural variables is not expressed during the whole wheat cycle (e.g., phyllochron, number of leaves) or at least their importance varies along the cycle. This suggests that variables do not have the same weight and action according to the wheat developmental phase, and according to their value and interaction with climate.
- The effect of some variables on *S. tritici* epidemic can change over time. On the one hand, the effect of a given variable can be positive for disease development at a given phase and become negative at another phase (e.g., for leaf posture). On the other hand, during one phase, a same variable can act on different processes which effects are opposite on disease epidemic (e.g., LAI and ground cover).
- Some of these variables can act on disease propagation simultaneously or at different moments of the wheat cycle. Often, variables have opposite effects on disease and the effect of one can counteract the effect of another. Thus, the severity and the rate of epidemic development is the result of the temporal and spatial interactions of multiple architectural variables.
- The effect of a given variable can be modulated depending on its interaction with climate conditions. This makes more complex the interpretation and the prediction of architecture effect on the disease. For instance, if the climate shows low rainfalls, all the variables supposed to enhance or prevent contamination by splash become less efficient and those that promote propagation by contact can become crucial.

3. Expected effects of architecture modified by density and sowing date on *Septoria tritici* development

Based on architectural differences found in our experiment, we attempt to analyse how density and sowing date could have influenced the disease via modifications of the canopy architecture; we will present these effects for the successive phases described in the previous section.

Phase 1

Given that the main way of disease propagation during this phase is external inoculum (pycnidiospores and/or ascospores), the ground cover and the LAI are the main architectural variables that may influence the disease onset in interaction with the climate.

At this stage, the canopy is much denser and the ground cover is much higher for higher density which results in a higher surface of interception for spores and ascospores. Therefore, we would have expected that plants of the high density treatment would be more exposed to contamination. However, both simulations and the first measurements of lower leaves suggested that disease severity was higher in the low density. One possible explanation is that in the particular conditions of our experiment (late sowing, unfavourable climate conditions), the primary inoculum was limiting which could have been favourable for disease development in D1 than in D3. Indeed, assuming that during a rain event, a limited number of spores on the soil is splashed continuously by droplets until being deposited on a green tissue, an equal amount of spores would then be divided by a smaller green area for the low than the high density. Unfortunately, the lack of disease measurements of the first three leaves does not allow checking this hypothesis.

The main differences between the early and the late sowings were: the period during which phase 1 occurred and the dimensions of the emerged leaves. For S1, phase 1 coincided with autumn period whereas for S2 it coincided with winter period. For S1, the first three leaves had more chance to experience warm temperatures, optimal for *S. tritici* development than for S2. Autumn is the peak time of ascospore release and dispersal by the wind (Shaw

and Royle, 1989) which makes plants of S1 more exposed to contamination by ascospores. In addition, because of the reduction in temperature, the first three leaves of late-sown plants had lower size and area and thus less green surface to intercept spores and ascospores than the same leaves grown at the early sowing. Hence, differences in architecture and in climate between S1 and S2 were likely to promote disease development in the early sowing during phase 1.

Phase 2

During this phase, ground cover is still a factor enhancing rain interception and DU production but this time from lower infected leaves rather than from the soil.

Although plants from the low density produced leaves with high area and a high number of tillers compared to the high density, this was not enough to compensate for the differences of density. During this phase, differences in ground cover and LAI were still important between densities. For instance at HS = 5, the ground cover was respectively 0.2, 0.6 and 0.8 for D1, D2 and D3 in S1 and 0.1, 0.2 and 0.3 in S2. Hence, the high density appears to be the most favourable for DU production and interception because spores that reach the upper leaves have more surface area available which may result in faster disease progress (Pielaat et al., 2002). The significantly higher number of tillers produced in D3 could also favour spore deposition (Broscious et al., 1985) by promoting the proximity and the horizontal contact between leaves or by enabling short distances between leaves which further facilitate disease propagation by splash without a high kinetic energy (Lovell et al., 1997).

Regarding the effect of sowing date, the duration of phase 2, was longer for S1 (600 $°Cd_{12}$) than for S2 (200 $°Cd_{12}$) which allowed plants in S1 to produce a higher number of leaves and tillers. Indeed, during this phase, the main stem produced 5-6 leaves in S1, whereas it produced only 2-3 leaves in S2. Therefore, most leaves in the early sowing emerged and developed lower in the canopy and were therefore closer to basal inoculum sources; this place them at a greater risk to disease progression (Lovell et al., 1997). In addition, the higher number of axes produced in S1 compared to S2 led to higher LAI (0.6 for S1 *vs.* 0.2 for S2 at HS = 5 for D2) and thus to more green leaf area likely to intercept dispersal units.

Phase 3

The new change in architectural features during this phase is the stem extension, which brings a new dynamical relation between the plant and the pathogen while the pathogen continues to spread by splashing. The effects of ground cover and leaf area index become though more complex.

On the one hand, the higher rate of ground cover leads to an earlier closure of the canopy for the high density. For instance, at the beginning of stem extension in the early sowing, soil cover exceeded 80% in D3 whereas it was only 50% in D1. The canopy closure for the high density represents a barrier that prevents raindrops from reaching the low and intermediate layers of the canopy where infected leaves are located. This effect referred to as "umbrella effect" may lead to a reduction in the amount of splashed dispersal units in comparison to a sparser canopy. This was proposed by Eyal (1981) who reported that the rain-drop splashing effect was increased in less dense crops leading to earlier and faster pathogen progress. On the other hand, when fewer raindrops penetrate within the canopy, there is less washing of the deposited spores which conversely increase the proportion of spores that will germinate in the dense crop. Therefore, it is difficult to conclude which of the low or high density would induce more disease propagation regarding the production and interception of infectious droplets. It is known that the top three leaves of winter wheat commonly emerge at a height below leaves that are fully developed (Lovell et al., 1997). Therefore, the erected

posture of leaves in the high density may facilitate the transmission of inoculum by allowing new emerging leaves to overlap with older infected leaves.

During phase 3, the main architectural difference between the two sowing dates was the phyllochron. The rate of stem extension was up to 30% slower in S1. With a low rate of stem extension, leaves stay longer at short distances from lower infected leaves and thus they can be contaminated by simple contact or by splashes with a low kinetic energy (Lovell et al., 1997). Otherwise, at flowering, the peduncle height of plants from D2 was about 10 cm higher in S1 than in S2 which might reduce the chances of contamination by splash. Indeed, Shaw (1987) calculated that there is a fivefold reduction in the number of spores transported vertically by splash with each increase in height of 10 cm. This means that the effect of plant height could thwart or diminish the effect of the rate of stem extension.

The complexity of the processes influencing epidemic parameters and their interaction with climate conditions, the dependency relationships between the different variables, the dynamic evolution of these interactions and the spatial and temporal changes of the plant and the canopy architecture; all these are factors that make disentangling and quantifying the effect of individual architectural variables on *Septoria* epidemics a challenging task. For these reasons, the use of coupled virtual plant-disease model appears as an appropriate means that can provide new insight into the processes involved in the architecture-disease interaction.

III. Improvements brought to Septo3D

Two main changes have been performed during this work to the model Septo3D (Robert et al., 2008). First, we included a more realistic parameterisation of the initialisation of the disease; second, we included interplant variability in the canopy representation.

1. Initialisation of the disease

A significant change in the model concerned the disease initialisation. In the previous version, epidemics were initiated by infecting the first three leaves similarly (Robert et al., 2008). Two parameters were used for the initial contamination: the date at which the leaf sectors were contaminated and the level of contamination. For instance in Robert et al. (2008), simulations were run with infections occurring when 20% of the total leaf surface had emerged. Their version did not take into account the effect of climate on the initial infections and neither the possible effects of plant architecture. Here, we needed more realistic initialisation of the disease, possibly depending on climate and canopy architecture. Indeed, it has been shown that initial infection can influence subsequent vertical disease progress (Pielaat et al., 2002, Calonnec et al., 2008).

In the current version of the model, initial contamination is caused by rain splashes that, by hitting an infected soil surface produce dispersal units which propagate spores to green leaves. Two new parameters are used to determine the level of initial infection: S_{sposoil} (m^2/m^2), the fraction of soil surface covered by sporulating plant debris and T_{infsoil} (°Cd), the duration during which this surface bears spores. The simulation of rain interception by the soil and splash of droplets is similar to that for dispersal of dispersal units from leaf to leaf. The amount of dispersal units produced during a rain event is determined by the amount of sporulating surface on the soil and the interception and intensity of the raindrops. The fraction of dispersal units intercepted by a green tissue depends on the leaf area and its distribution. Therefore, in the current version of the model, infection of the rosette leaves results from the interaction between the canopy architecture and the rain. Yet, we don't consider infections by the ascospores, the sexual form of the pathogen, which have been shown to contribute

considerably in the primary infection of winter wheat (Shaw and Royle, 1989, Hunter et al., 1999).

For the climate of 2008/2009 and for the three density treatments grown at a late sowing, we found that the two parameters ($S_{sposoil}$ and $T_{infsoil}$) had different effects on epidemic simulations. Simulations were not sensitive to $T_{infsoil}$, whereas a small variation of $S_{sposoil}$ could substantially modify the later disease development and more interestingly could even change the ranking of the densities. However, the effect of initial conditions was examined only for a single scenario in this study. Therefore, a further model analysis under variable values and climate conditions is required to investigate the sensitivity of the model to the initial conditions.

2. Modelling canopy variability and its effect on epidemic simulations

One new aspect in the plant module was the parameterisation of interplant variability, meaning that the simulated canopy included different types of plants. Variability was taken into account in terms of final leaf number and plant development and was based on field measurements. Generally, plant variability is simulated by reconstructing a mean plant and applying a random variability on this base (Evers et al., 2005, Fournier and Andrieu, 1999, Fournier et al., 2003). The first source of variability observed in the field was related to differences in total number of leaves produced on the main stem, which in turn affected various architectural variables (dimensions, development, and senescence) on main stems and tillers. This variability was addressed in the model by integrating separately architectural variables for groups of plants with the same number of leaves and by representing the observed proportions of each group of plants in the reconstructed canopy. The second source of variability was linked to delays in date of plant emergence. We characterized the variability in development between plants at two dates and estimated from this the variability in date of emergence that was introduced in the simulation. However, this new parameterisation of the plant architecture variability raises new challenges linked to both modelling and experimental measurements:

- Modelling interplant variability in three-dimensional simulations brought constraints in terms of computer memory and time consumption. The computer memory was a limiting factor for simulations involving a high number of axes. This was the case when running simulations with the scenario that takes into account interplant variability for the low density. Besides, increasing plant variability and the number of simulated axes increased the time of running the model.
- In our modelling study, we tried to include plant variability in the canopy model as observed in the field. This increased the realism of reconstructed canopies, but still there are some weaknesses. First, we chose to model only variability of the number of final leaves and that of plant development, considering that they are the main variables that influence *Septoria* epidemics. However, one could include variability of other variables (e.g., organ dimensions) known to influence diseases. Second, we did not take into account possible correlations between variables when we varied one of them. Finally, measurement and parameterisation of interplant variability of development could be questioned. Here, we assumed that deviations of the HS of plants from the mean HS measured at a single date reflect the interplant variability through the growth cycle. Nonetheless, it is possible that plant variability in development was different according to N_{leaf} modality, density and stage of development.

IV. Critical assessment of Septo3D

Comparison between simulated (by Septo3D) and observed disease data was performed for three sowing densities grown during one season. This revealed that disease simulations were consistent with field measurements (reflected by RMSE below 0.029 for leaves 1-6 pooled for a given density). In particular, despite architectural differences, simulations showed few differences in disease development between densities in agreement with field observations. However, the model failed to simulate correctly the rate or the onset of disease on some leaves, underestimated disease development on the rosette leaves and did not reproduce the slightly higher rate of lesion development for the low density.

More generally, this modelling study allowed to address three issues related *Septoria* disease simulations. First, this study pinpointed the steps or criteria to which we need to pay particular attention to insure simulating successfully the disease. Second, it allowed identifying lacking processes that should be addressed in the model. Finally, simulations revealed the importance of the choice of comparative variables and treatments for the model validation.

Steps or criteria important to succeed disease simulation

The first aspect concerned the importance of taking into account variability of plant development for disease simulations. The comparison between simulations run with scenarios differing in the level of architecture description showed that the scenario in which interplant variability is considered yielded the best agreement between measured and simulated epidemics. Decreasing the variability of plant development increased the difference between densities and between simulated and observed disease levels. Simulations run with the scenario that represents only a mean plant showed unrealistic stairs shaped curves. Therefore, if we do not consider variability between plants, simulations may deviate considerably from the reality.

The second aspect concerned the importance of disease level simulated on the rosette leaves on the outcome of the disease on upper leaves. Under the conditions of simulation used here (i.e., unfavourable climate and late sowing date), the level of disease on the lower leaves was determinant. Indeed, an underestimation of *Septoria* level on rosette leaves had important repercussions on the upper leaves as for the low density treatment. Our hypothesis is that in this treatment, the underestimation of the infection of rosette leaves may have resulted in a limiting quantity of inoculum which hampered the disease progress for upper layers.

Lacking processes in the model

Pathogen propagation in the model is simulated only by spore dispersal during rain events whereas there are two other known mechanisms for *S. tritici* propagation: ascospores dispersed by wind (Shaw and Royle, 1989, Hunter et al., 1999) and contamination by direct contact between leaves (Lovell et al., 2004b). The lower rate of *Septoria* development on the rosette leaves support the hypothesis that these two missing mechanisms in the model are probably the cause.

The latency period of *S. tritici* is fixed in the model (here 310 °Cd) whereas it may vary between 270 and 500 °Cd depending on temperature and relative humidity (Lovell et al., 2004a). The early development of small lesions after a duration equal to one latency period from leaf emergence and which are not observed in the field denote that using a fixed latency period leads in some conditions to errors of simulations.

Choice of variable and treatments for disease assessment and model validation

This study allowed questioning the choice of the comparison variable and the used approach to validate the model. In *Septoria* disease assessment, one major difficulty was the

choice of the variable for comparison between treatments. Indeed, it is not always possible to distinguish in the field necrosis due to the lesions (that show pycnidia) from those due to monocarpic senescence (Robert, 2003, Royle et al., 1986). In the literature, two types of assessments can be found: either based on the lesions containing pycnidia (Lovell et al., 2004b, Shaw and Royle, 1993), or based on the total area of necrotic tissues (Robert et al., 2004, Bancal et al., 2007). Here we used the area of necrotic lesions in the green part of the leaf blade, referred to as $NecLes_{Green}$. However, this derived variable was computed from measurements of the fraction of total leaf area occupied by apical necrosis and by necrotic lesions. At higher leaf age (900-950 °Cd after leaf emergence), $NecLes_{Green}$ became less accurate because of the decrease in the amount of green tissue due to monocarpic senescence. Consequently, the accuracy of $NecLes_{Green}$ was limited to the early stages of leaf development, i.e., before rapid increase of senescence. Other variables have been proposed to assess necrotic lesion development such as the number of distinct lesions in the green tissue of leaves with less than 50% of die-back (Royle et al., 1986); the disadvantage of such method is yet that it underestimates lesions at higher levels as each new sample include small lesions and exclude larger, older ones previously included. Another used variable is the area under the disease progress curve (AUDPC) which takes into account precocity and intensity of disease development (Paveley et al., 2000, Simon et al., 2005, Robert et al., 2008).

Using realistic canopy architecture of contrasted sowing densities appeared to be a challenge task. Although important architecture differences were observed, there was much less differences in disease development between densities. One possible explanation is that the unfavourable climate conditions and the complex and opposite processes influencing disease development helped to mitigate the effect of architecture variability. This suggests that simpler canopies are probably more appropriate for model validation; for instance architectures that differ by a small number of variables but which differences are important enough to cause a visible effect on disease development (e.g., monoculm wheat, different Rht-genes or artificially modified plant architectures).

V. Perspectives and possible applications of the approach of coupled virtual plant-disease models

1. Possible applications of the approach using Septo3D

We identified two interesting perspectives for continuing using Septo3D in the analysis of the effects of sowing date and sowing density on *Septoria* epidemics. First, the model can be run for a large range of climatic conditions, with the characterized architectures of different sowing dates and densities. This allows identifying the interactions between climate and field treatments, and quantifying the chances to increase/decrease disease development when considering a long term simulation. Second, in a more mechanistic view, simulations can be run to better understand the interactions between the architectures obtained for different sowing dates and densities and the disease, and to identify some key architectural features influencing the disease severity.

1.1. Quantification of the effects of density and sowing date on disease development for different climate scenarios

In order to determine which density treatment and sowing date have the greatest probability of resulting in a lower disease development, a first step is to run Septo3D for a large range of climatic conditions with the architecture resulting from varied sowing dates and densities. As a preliminary analysis, we run Septo3D for 11 climatic seasons recorded in Grignon from 1998/99 to 2008/09, with three architectures corresponding to three density treatments (2008/09, late sowing date Simulations for three climate seasons resulting in different epidemics: very severe (1998/99), severe (2001/02) and medium (2004/05) were chosen to illustrate this analysis (Fig. 2). Preliminary analysis of *S. tritici* development in terms of proportions of lesion development for the different climatic seasons showed that:

- Septo3D responded quite strongly to the climatic scenarios. Three years (1998/99, 1999/00 and, 2007/08) resulted in a very severe lesion development for the upper leaves (until 80% of lesion development). The simulated epidemic was severe for the season 2001/02, and was low to moderate for seasons 2000/01, 2003/04, 2004/05, 2006/07 and 2008/09 (lesions did not exceed 30% of the leaf area). For two seasons (2002/03 and 2005/06), Septo3D simulated no or extremely few lesion development.
- Simulations suggest that for late sowing in the region of Grignon, the 11 last years were very variable in terms of *Septoria* development with years with strong development and years with very low pressure.
- Climate appears as the primary factor for disease simulation (it determines the overall level of the disease development) and density treatment is a secondary factor. Yet, during some years, a strong difference between density treatments could be observed. Differences in maximal lesion development between density treatments D1 and D3 reached 20% in some simulations (1998/99 and 2007/08).
- Density ranking for the climatic seasons: for the 9 climatic seasons that resulted in nonzero simulated epidemics, the lesion development was most often strongest in the high density treatment. When averaging over the three upper leaves, we find that in around half of the simulations, the high density results in more severe simulated disease than in the intermediate and low density (D3 > D2 > D1); in around a quarter of the simulations, disease is similar for high and intermediate density and is less severe in the low density (D3 = D2 > D1); and finally in around a quarter of the simulations there were no or few

differences between the three density treatments (D3 = D2 = D1). This trend was observed in each of the three upper leaves, but with some differences. For instance, in only a quarter of the simulations disease is more severe in the high compared to the medium density for leaf layer 2, whereas it is more than half of the simulations for leaves 1 and 3.

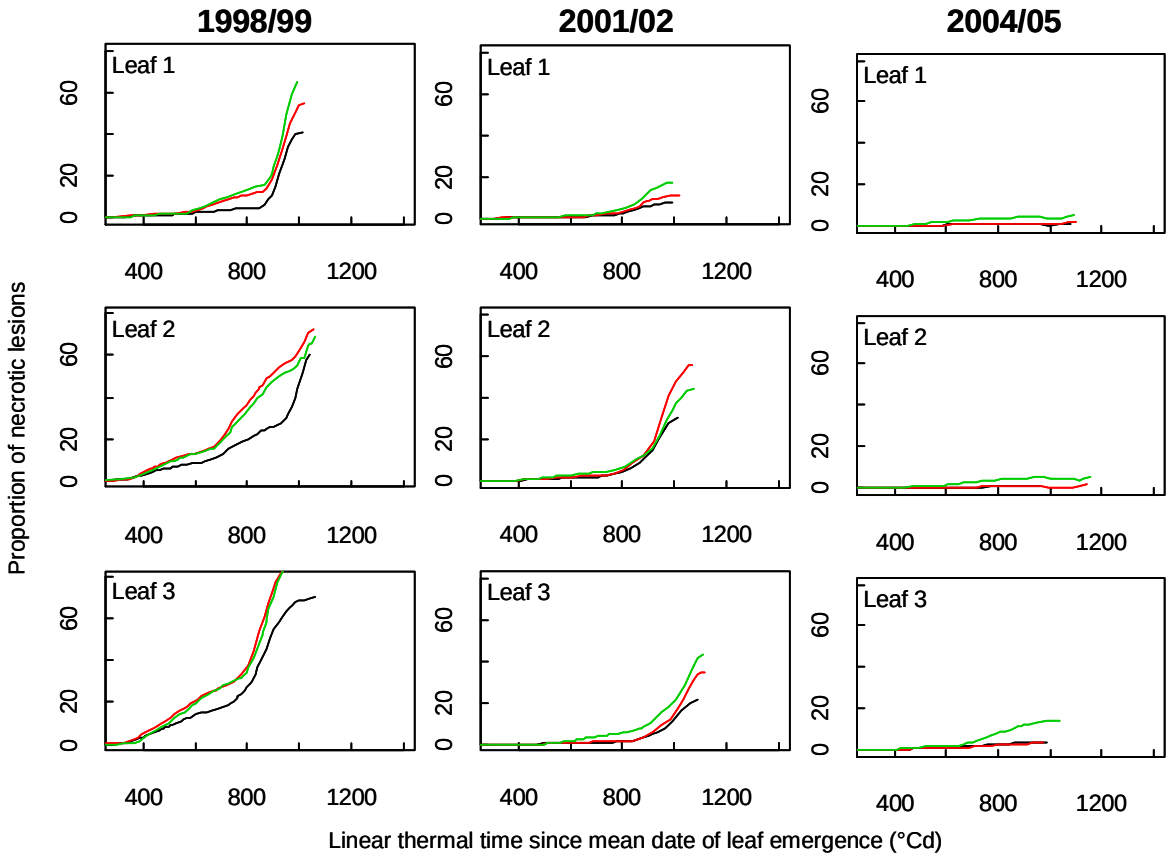

Figure 2. Predicted dynamic of total necrotic lesions of *Septoria tritici vs.* linear thermal time since the mean date of leaf emergence of leaves 1 to 3 (counted from the top) for wheat main stem for three growing seasons: 1998/99 (very severe epidemic), 201/02 (severe dynamic) and 2004/05 (medium dynamic). Architecture data are for winter wheat Cv. 'Soissons' grown in Grignon in 2008/2009 at three densities D1 (black line), D2 (red line) and D3 (green line). D1: 59, D2: 160, D3: 406 plants.m^{-2}.

This ranking of density treatments is quite consistent with the published literature where high density stands are often reported to show more disease pressure (Broscious et al., 1985, Tompkins et al., 1993, Ansar et al., 1996). Moreover, the similarity of disease level between the intermediate and high densities observed in many simulated climate seasons remind the study of Ansar et al. (2009) who found that increased plant density increase *Septoria* disease severity until a given threshold, but further increase has no effect.

This analysis is very preliminary. The differences between the simulations could be further quantified by analysing in more detail the disease development. It also needs to be complemented by using a more complete climatic dataset (including different locations) and enlarging the architecture treatments considered. One strong limit of this analysis is that we consider a similar architecture for the different climatic seasons (here, only the temperature-dependence of development is taken into account). Actually, architecture is modified by environmental factors; for instance, increased temperatures lead to higher leaf length (Bos and Neuteboom, 1998, Equiza and Tognetti, 2002) and higher rate of leaf appearance (Baker et

al., 1986, Cao and Moss, 1989, 1994). Therefore, the approach could be improved by changing also architecture for the different seasons. We think this analysis could help defining sowing dates and sowing densities that could reduce significantly the risk of disease development over a large range of climatic conditions and for different locations.

1.2. Identification of the key architectural features for disease propagation

Septo3D can serve as a tool to create artificial architectures which allow to pinpoint the specific role played by an architectural variable. For instance, starting from the realistic architectures corresponding to the two sowing dates and three densities investigated in this study, we could choose to keep the architecture of a treatment except for one variable (e.g., phyllochron, leaf size, tiller number) to which we can assign values of another treatment. Thus we can see the effect of a specific variable on the disease independently of all the other variables.

A risk analysis could also be performed on such an artificial architecture to check the impact of the variable of interest under different climate conditions and, the direction and the amplitude of its effect on disease development. Therefore, this approach could be a mean to classify architectural variables according to the importance and the stability of their effect on septoria development.

2. Potential improvements and applications of the model Septo3D

We consider that Septo3D is a relevant tool to simulate and understand the interactions between architecture and *S. tritici* epidemics. However some weaknesses of the model still need to be improved in the *short term*:

- To include a module that allows calculating a variable latency period as a function of temperature and relative humidity. This can be drawn from studies that investigated the effect of environmental factors on the duration of the latency period of *S. tritici* (Shaw, 1990, Lovell et al., 2004a).
- To include the other ways of *S. tritici* propagation i.e., ascospores and direct contact between leaves. For instance, it would be interesting to couple the model Septo3D with a module of spore transport by wind. This would allow computing the quantity and the flux of ascospores deposited in a green surface area.
- To couple Septo3D with a more realistic model of spore dispersal as that developed by Saint-Jean et al. (2004) which model splash of water droplets in a 3D plant canopy.

For the moment, the model deals only with the effects of architecture on the disease epidemic. However, other changes that are caused by agronomic practices and that are known to influence the disease (mainly the physiological status of leaves and the microclimate within a canopy) are not taken into account in the model. Therefore, the possible improvements of the model in the *long term* would be:

- To include a module for calculation of microclimatic conditions at the level of the canopy and the leaf layer. Indeed, the infectious cycle of S. tritici is highly sensitive to the prevailing conditions particularly temperature and relative humidity. For instance it has been shown that there are correlations between the amount of disease and the duration of surface wetness (Scott et al., 1985) which is a factor enhanced by high density.
- To take into account the physiological status of leaves, in particular the nitrogen status, this also influences Septoria development (Lovell et al., 1997; Ansar et al., 2009). One alternative would be to couple the model Septo3D with the process-based model developed by Bertheloot et al. (2008) and that simulate nitrogen distribution within a wheat culm during grain filling. Coupling these two models makes sense for at least two reasons: first, the fact that the base unit in the nitrogen model is the phytomer would facilitate its integration in

Septo3D in which plant architecture is presented by a modular approach. Second, regarding the functioning of the nitrogen model, the pathogen could be assimilated to a supplementary sink of nitrogen at the scale of leaf.

The model Septo3D is currently being implemented on the platform OpenAlea (Pradal et al., 2008) which is designed to facilitate the integration of heterogeneous models. The implementation of the model under the platform would open the way to new applications such as (i) the design of new agronomic practices that allow disease escape by running the model with various climates, varieties and architectures, (ii) the evaluation of the effect of fungicide strategies by coupling the model to fungicide application models. This would allow studying interactions between plant, pathogen and fungicide.

References

Ansar M, Leitch MH. 2009. The effect of agronomic practices on the development of Septoria Leaf Blotch and its subsequent affect on the yield and yield components of wheat. *American-Eurasian Journal of Sustainable Agriculture,* **3**: 57-67.

Ansar M, Leitch MH, Jenkins PD, Hayden NJ. 1996. Effect of nitrogen fertilizer, crop density and development of Septoria tritici on components of growth and yield of winter wheat in the UK. *Proceedings of the 5th International Wheat Conference.* June 10-14, 1996, Ankara, Turkey. 270-272.

Baker JT, Pinter PJ, Jr., Reginato RJ, Kanemasu ET. 1986. Effects of temperature on leaf appearance in spring and winter wheat cultivars. *Agronomy Journal,* **78**: 605-613.

Bancal MO, Robert C, Ney B. 2007. Modelling wheat growth and yield losses from late epidemics of foliar diseases using loss of green leaf area per layer and pre-anthesis reserves. *Annals of Botany*, **100**: 777-789.

Bertheloot J, Andrieu B, Fournier C, Martre P. 2008. A process-based model to simulate nitrogen distribution in wheat (Triticum aestivum) during grain-filling. *Functional Plant Biology*, **35**: 781-796.

Bos HJ, Neuteboom JH. 1998. Growth of individual leaves of spring wheat (Triticum aestivum L.) as influenced by temperature and light intensity. *Annals of Botany,* **81**: 141-149.

Broscious SC, Frank JA, Frederick JR. 1985. Influence of winter wheat management practices on the severity of powdery mildew and Septoria blotch in Pennsylvania. *Phytopathology*, **75**: 538-542.

Calonnec A, Cartolaro P, Naulin JM, Bailey D, Langlais M. 2008. A host-pathogen simulation model: powdery mildew of grapevine. *Plant Pathology*, **57**: 493-508.

Cao WX, Moss DN. 1989. Temperature effect on leaf emergence and phyllochron in wheat and barley. *Crop Science,* **29**: 1018-1021.

Cao WX, Moss DN. 1994. Sensitivity of winter wheat phyllochron to environmental changes. *Agronomy Journal,* **86**: 63-66.

Equiza MA, Tognetti JA. 2002. Morphological plasticity of spring and winter wheats in response to changing temperatures. *Functional Plant Biology*, **29**: 1427-1436.

Evers JB, Vos J, Fournier C, Andrieu B, Chelle M, Struik PC. 2005. Towards a generic architectural model of tillering in Gramineae, as exemplified by spring wheat (Triticum aestivum). *New Phytologist,* **166**: 801-812.

Eyal Z. 1981. Research on Septoria leaf blotch: recent advances. *EPPO Bulletin,* **11**: 53-57.

Fournier C, Andrieu B. 1999. ADEL-maize: an L-system based model for the integration of growth processes from the organ to the canopy. Application to regulation of morphogenesis by light availability. *Agronomie,* **19**: 313-327.

Fournier C, Andrieu B, Ljutovac S, Saint-Jean S. 2003. ADEL-wheat: A 3D architectural model of wheat development. In: Hu B-G, Jaeger M eds. *Proceedings of International Symposium of Plant Growth Modeling and Applications.* Beijing, China. 2003 Tsinghua University Press - Springer Verlag.

Hunter T, Coker RR, Royle DJ. 1999. The teleomorph stage, Mycosphaerella graminicola, in epidemics of Septoria tritici blotch on winter wheat in the UK. *Plant Pathology*, **48**: 51-57.

Lovell DJ, Hunter T, Powers SJ, Parker SR, Bosch Fvd. 2004a. Effect of temperature on latent period of septoria leaf blotch on winter wheat under outdoor conditions. *Plant Pathology*, **53**: 170-181.

Lovell DJ, Parker SR, Hunter T, Royle DJ, Coker RR. 1997. Influence of crop growth and structure on the risk of epidemics by Mycosphaerella graminicola (Septoria tritici) in winter wheat. *Plant Pathology*, **46**: 126-138.

Lovell DJ, Parker SR, Hunter T, Welham SJ, Nichols AR. 2004b. Position of inoculum in the canopy affects the risk of septoria tritici blotch epidemics in winter wheat. *Plant Pathology*, **53**: 11-21.

Masle-Meynard J, Sebillotte M. 1981. Study of the heterogeneity of a winter wheat stand. II. Origin of the different sorts of individuals in the stand; factors allowing description of its structure. *Agronomie*, **1**: 217-223.

Paveley ND, Lockley D, Vaughan TB, Thomas J, Schmidt K. 2000. Predicting effective fungicide doses through observation of leaf emergence. *Plant Pathology*, **49**: 748-766.

Pielaat A, Bosch Fvd, Fitt. BDL, Jeger MJ. 2002. Simulation of vertical spread of plant diseases in a crop canopy by stem extension and splash dispersal. *Ecological Modelling*, **151**: 195-212.

Pradal C, Dufour-Kowalski S, Boudon F, Fournier C, Godin C. 2008. OpenAlea: a visual programming and component-based software platform for plant modelling. *Functional Plant Biology*, **35**: 751-760.

Robert C. 2003. *Etude et modélisation du fonctionnement d'un couvert de blé attaqué par le complexe parasitaire Puccinia triticina - Mycosphaerella graminicola*, PhD thesis, Institut National Agronomique de Paris-Grignon, Paris, France.

Robert C, Bancal MO, Nicolas P, Lannou C, Ney B. 2004. Analysis and modelling of effects of leaf rust and Septoria tritici blotch on wheat growth. *Journal of Experimental Botany*, **55**: 1079-1094.

Robert C, Fournier C, Andrieu B, Ney B. 2008. Coupling a 3D virtual wheat (Triticum aestivum) plant model with a Septoria tritici epidemic model (Septo3D): a new approach to investigate plant-pathogen interactions linked to canopy architecture. *Functional Plant Biology*, **35**: 997-1013.

Royle DJ, Shaw MW, Cook RJ. 1986. Patterns of development of Septoria nodorum and S. tritici in some winter wheat crops in Western Europe, 1981-83. *Plant Pathology*, **35**: 466-476.

Saint-Jean S, Chelle M, Huber L. 2004. Modelling water transfer by rain-splash in 3D canopy using *Monte Carlo* integration. *Agricultural and Forest Meteorology*, **121**: 183-196.

Scott PR, Benedikz PW, Jones HG, Ford MA. 1985. Some effects of canopy structure and microclimate on infection of tall and short wheats by Septoria nodorum. *Plant Pathology*, **34**: 578-593.

Shaw MW. 1987. Assessment of upward movement of rain splash using a fluorescent tracer method and its application to the epidemiology of cereal pathogens. *Plant Pathology*, **36**: 201-213.

Shaw MW. 1990. Effects of temperature, leaf wetness and cultivar on the latent period of Mycosphaerella graminicola on winter wheat. *Plant Pathology*, **39**: 255-268.

Shaw MW, Royle DJ. 1989. Airborne inoculum as a major source of Septoria tritici (Mycosphaerella graminicola) infections in winter wheat crops in the UK. *Plant Pathology*, **38**: 35-43.

Simon MR, Perello AE, Cordo CA, Larran S, Putten PELvd, Struik PC. 2005. Association between Septoria tritici blotch, plant height, and heading date in wheat. *Agronomy Journal*, **97**: 1072-1081.

Tompkins DK, Fowler DB, Wright AT. 1993. Influence of agronomic practices on canopy microclimate and Septoria development in no-till winter wheat produced in the Parkland region of Saskatchewan. *Canadian Journal of Plant Science,* **73**: 331-344.

Appendixes

Appendix I

This appendix is divided in three fold:

- Appendixes I/A and I/B provide data of plant and air temperatures and of global radiation recorded during the growing seasons 2007/2008 (Y1) and 2008/2009 (Y2). Data of plant temperature are for winter wheat Cv. Soissons sown in Grignon at two sowing dates: early (S1, late September) and late (S2, mid November). Plant temperature was calculated using soil temperature measured at 3 cm deep from sowing until the start of fast internode elongation (estimated at the date of apex emergence from the soil), then using air temperature measured at 2m height. Air temperature (Tair) and global radiation (Rg) were measured at a weather station 500 m from the field. Figures presented in this appendix allow appraising the difference between plant and air temperatures at the first stages of wheat plant development for the investigated treatments.
- Appendix I/C represents the change in daylength as a function of Julian days in the Grignon region. The daylength was calculated as the duration between sunrise and sunset, using the classical astronomical formulas.
- Appendix I/D represents the quantity of daily rain and rainfall events with rain intensity above 0.5 mm/h since the date of seedling emergence for winter wheat grown at a late sowing date during the growing season 2008/2009, which correspond to the data used to run the model Septo3D in our study. In the model, splash occurs for rain events with intensity above the threshold of 0.5 mm/h.

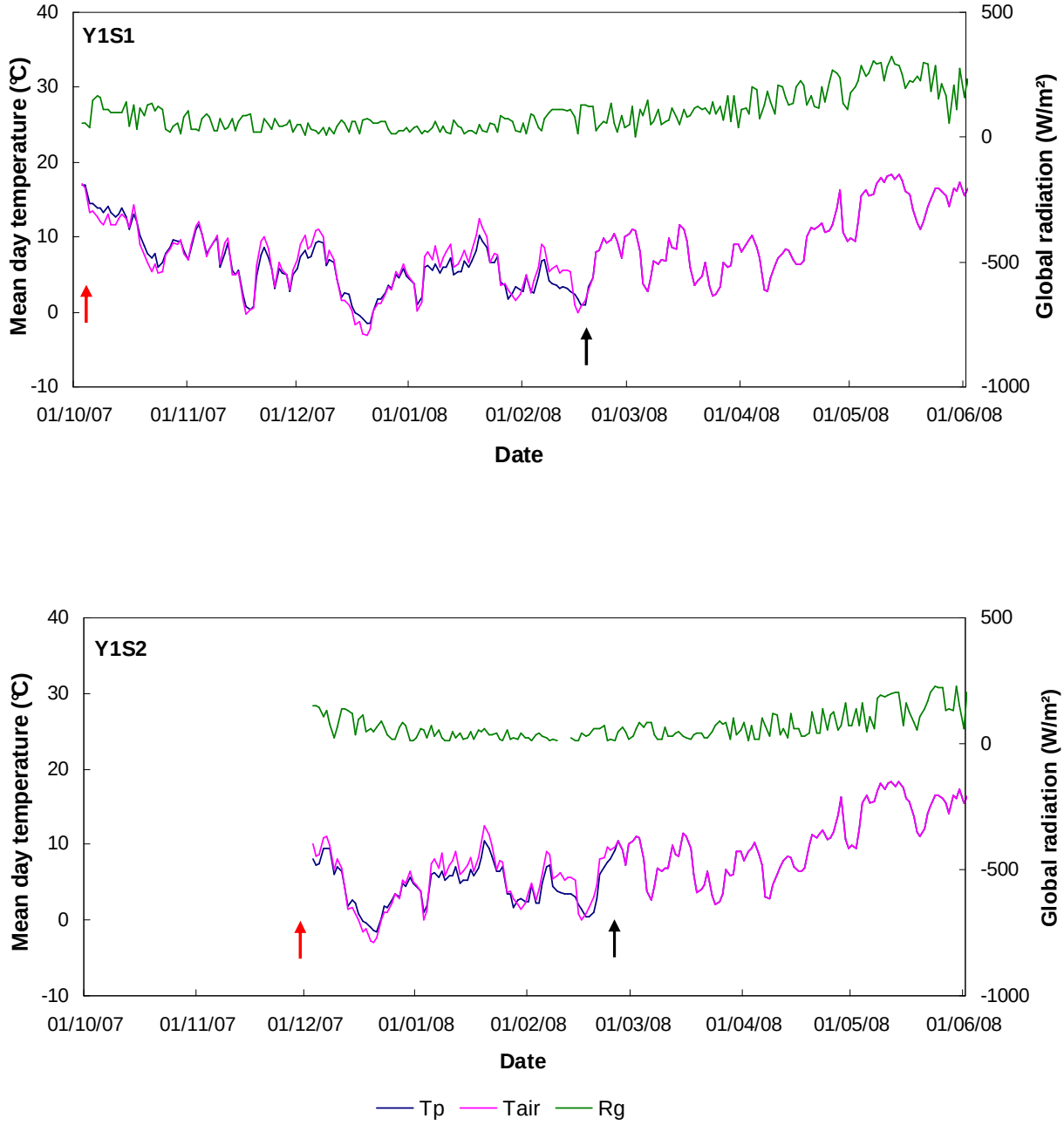

Appendix I/A. Mean daily temperatures measured around the plant apex (Tp, blue line) and at 2m height (Tair, pink line) and global radiation (Rg, green line) intercepted during the wheat growing cycle. Data are for winter wheat Cv. Soissons sown in Grignon during 2007/2008 (Y1) at two sowing dates: early (S1, late September) and late (S2, mid November). Red and black vertical arrows indicate respectively the date of seedling emergence and the date of apex emergence from the soil.

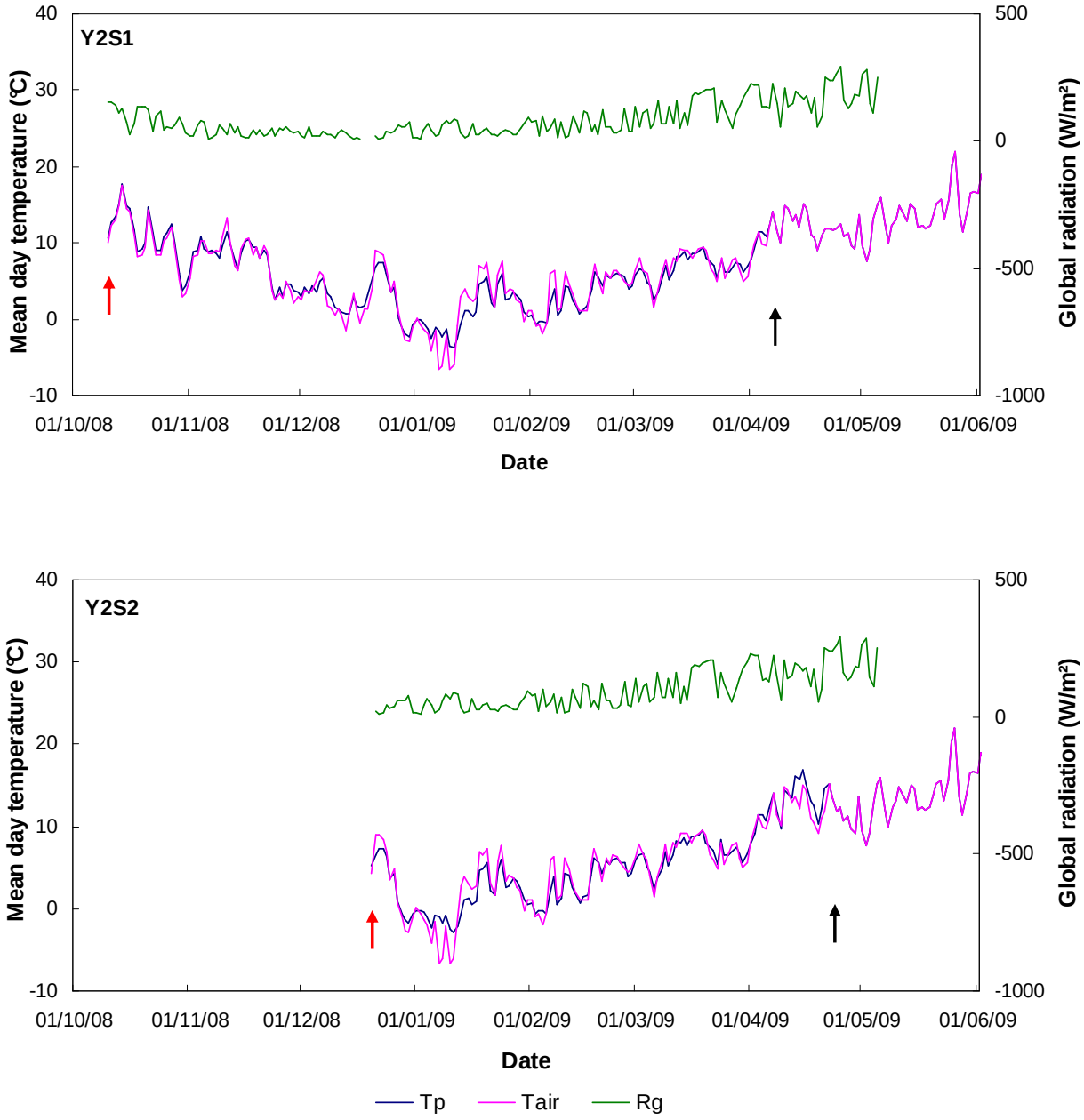

Appendix I/B. Mean daily temperatures measured around the plant apex (Tp, blue line) and at 2m height (Tair, pink line) and global radiation (Rg, green line) intercepted during the wheat growing cycle. Data are for winter wheat Cv. Soissons sown in Grignon during 2008/2009 (Y2) at two sowing dates: early (S1, late September) and late (S2, mid November). Red and black vertical arrows indicate respectively the date of seedling emergence and the date of apex emergence from the soil.

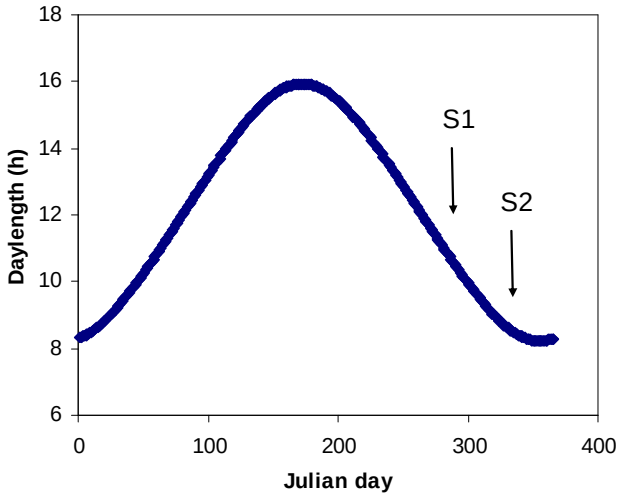

Appendix I/C. Daylength as a function of Julian day at Thiverval-Grignon, France (48°51N, 1°58E). Arrows indicate the date of seedling emergence for early (S1, late September) and late (S2, mid November) sowings in our experiments.

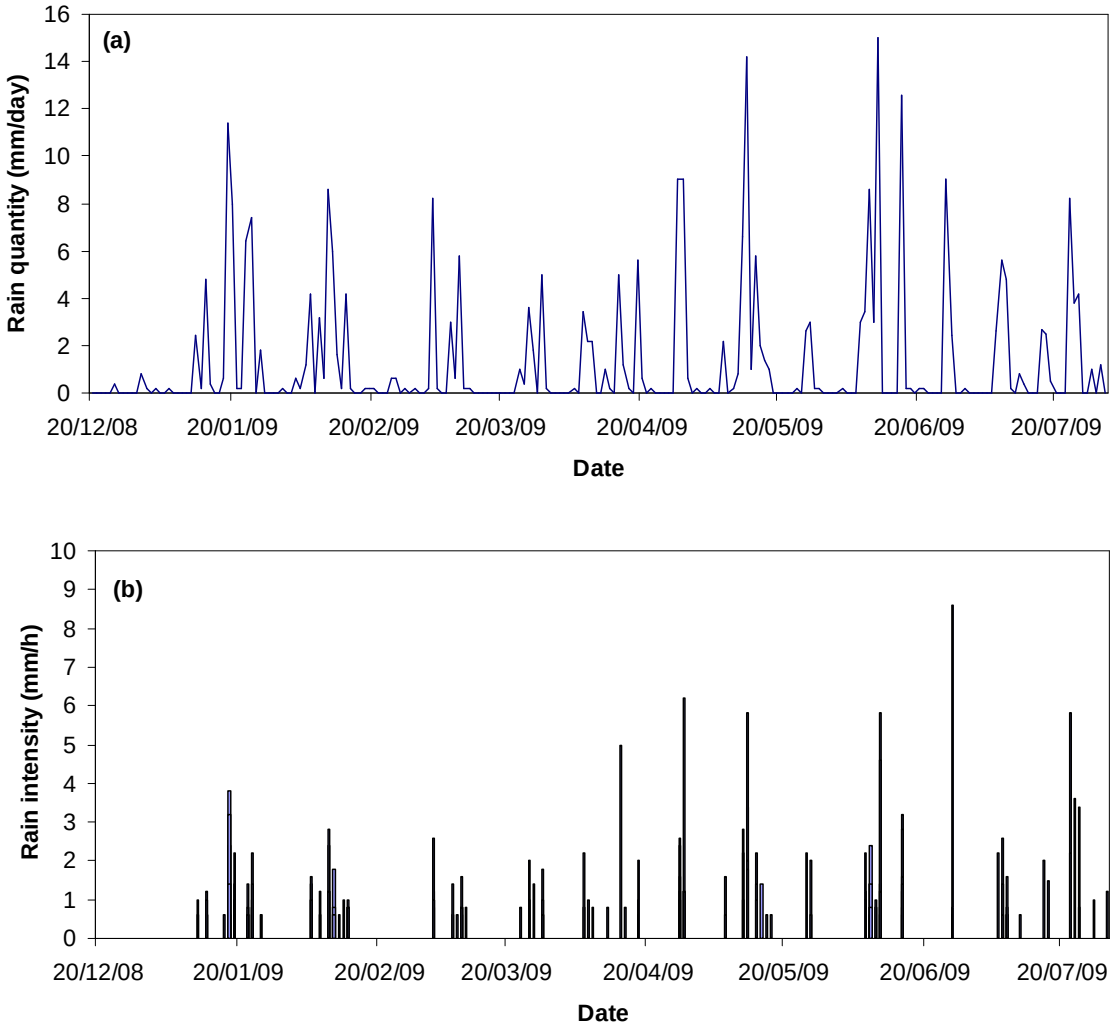

Appendix I/D. (a) Quantity of daily rain and **(b)** rainfall events with rain intensity above 0.5 mm/h since the date of seedling emergence (18/12/2008) for winter wheat Cv. Soissons sown in Grignon at 30/09/2008.

Appendix II

Appendix II/A. Summary of the dates, products and doses of different agronomic applications for the growing seasons 2007/2008.

Winter wheat Cv. 'Soissons'		Plot : BIOCLIM4 (0.75 ha)		Growing season : 2007/2008	
Date	**Sowing**	**Application**	**Material**	**Product**	**Dose**
31/07/2007	S1 - S2	Déchaumage	Chisel		
14/09/2007	S1 - S2	Déchaumage	Cover crop		
24/09/2007	S1	Travail du sol : labour			
24/09/2007	S1	Travail du sol animé	Horse rotative amazone		
25/09/2007	S1	Semis	Herriau	Cultivar Soissons	
03/10/2007	S1	Molluscicide		Mesurol pro	3 kg/ha
09/10/2007	S1	Molluscicide		Mesurol pro	3 kg/ha
30/10/2007	S1	Molluscicide		Mesurol pro	3 kg/ha
08/11/2007	S2	Fongicide		Opus team	1.5 kg/ha
12/11/2007	S1 - S2	Herbicide		Legacy duo	2.4 l/ha
12/11/2007	S2	Travail du sol : labour			
12/11/2007	S2	Travail du sol animé	Herse rotative amazone		
12/11/2007	S2	Semis	Herriau	Cultivar Soissons	
07/12/2007	S2	Molluscicide		Mesurol pro	3 kg/ha
11/01/2008	S2	Molluscicide		Mesurol pro	3 kg/ha
25/02/2008	S1 - S2	Fertilisation	aero	Ammonitre 27%	50 U/densité
07/03/2008	S1	Fertilisation	src	Ammonitrate 33.5%	150 U (D3) 80 U (D2) 0 U (D1)
04/04/2008	S1 - S2	Fongicide		Input pack	0.8 l/ha
23/04/2008	S2	Fertilisation	src	Ammonitrate 33.5%	150 U (D3) 80 U (D2) 80 U (D1)
02/05/2008	S1 - S2	Fongicide		Opus team Bravo	1.5 l/ha 1.3 kg/ha
22/05/2008	S1 - S2	Fongicide		Soleil	1.2 l/ha
28/07/2008	S1 - S2	Récolte			

Appendix II/B. Summary of the dates, products and doses of different agronomic applications for the growing seasons 2008/2009.

Winter wheat Cv. 'Soissons'		**Plot : Pointe Sud 49 (0.8 ha)**		**Growing season : 2008/2009**	
Date	**Sowing**	**Application**	**Material**	**Product**	**Dose**
26/08/2008	S1 - S2	Herbicide		Roundup max 480	2.5 l/ha
11/09/2008		Déchaumage	Rabe bluebird		
28/09/2008	S1	Travail du sol : labour			
28/09/2008	S1	Travail su sol animé	Herse rotative amazone		
29/09/2008	S1	Semis	Herriau	Cultivar Soissons	
17/10/2008	S1	Insecticide (Cicadelle, pucerons)		Judoka	0.125 l/ha
04/11/2008	S1	Fongicide (parcelle traitée)		Opus team	1.5 l/ha
10/11/2008	S1	Molluscicide	Manuel	Mesurol pro	3 kg/ha
17/11/2008	S2	Travail du sol : labour			
17/11/2008	S2	Travail du sol animé	Herse rotative amazone		
17/11/2008	S2	Semis	Herriau	Cultivar Soissons	
02/04/2009	S1 - S2	Fongicide (parcelle traitée)		Input pack	0.8 l/ha
09/04/2009	S1 - S2	Fertilisation	aero	Ammonitrate 33.5%	80 U/densité
16/04/2009	S1	Régulateur		Moddus	0.5 l/ha
30/04/2009	S1 - S2	Herbicide (anti dicotylédone)		Bofix	2.5 l/ha
30/04/2009	S1 - S2	Insecticide		Clameur	0.07 kg/ha
05/05/2009	S2	Régulateur		Moddus	0.5 l/ha
05/05/2009	S1 - S2	Fongicide (parcelle traitée)		Opus team	1.5 l/ha
06/05/2009	S1	Fertilisation		Ammonitrate 33.5%	50 U/densité
06/05/2009	S2	Fertilisation		Ammonitrate 33.5%	50 U (D1) 120 U (D2) 120 U (D3)
	S1 - S2	Récolte			

Appendix III

Appendix III/A. (a) Length of leaf blade, **(b)** width of leaf blade, **(c)** area of leaf blade, **(d)** length of sheath, **(e)** length of internode and **(f)** distance to the collar from the shoot base, *vs.* leaf rank *N* counted acropetally for juvenile phytomers and *vs.* leaf rank *N'* counted basipetally for adult phytomers. Data are for the main stem of winter wheat Cv. 'Soissons' sown in late September 2007 (Y1S1) and in mid November 2008 (Y2S2) in Grignon at 3 sowing densities: D1, D2, D3. For each density treatment data are pooled by final leaf number N_{leaf} : 9 (○), 10 (▽), 11 (□), 13 (●), 14 (▼). D1: 77, D2: 228, D3: 514 plants.m^{-2}. Vertical bars show confidence intervals (α=0.05) when larger than the size of the symbol.

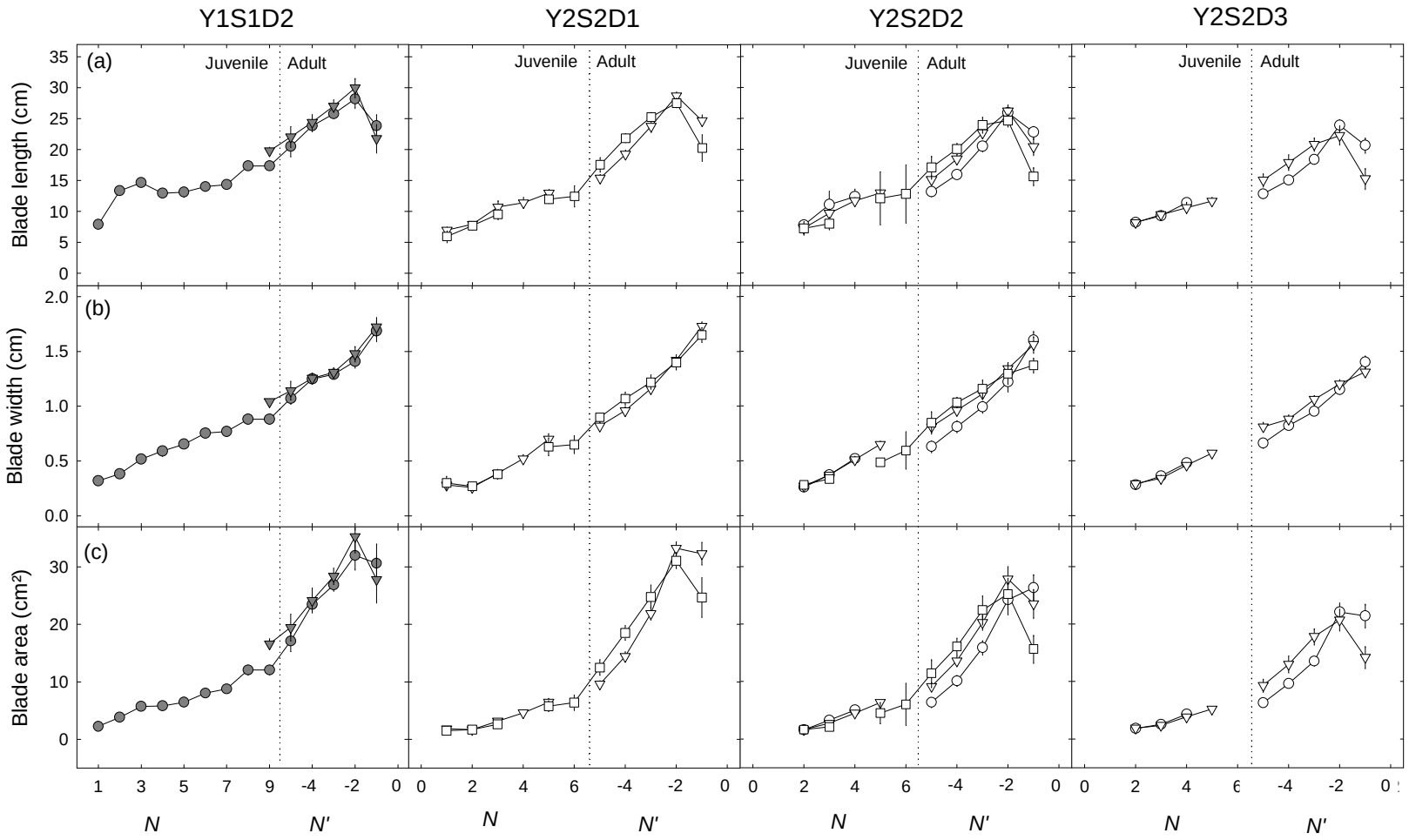

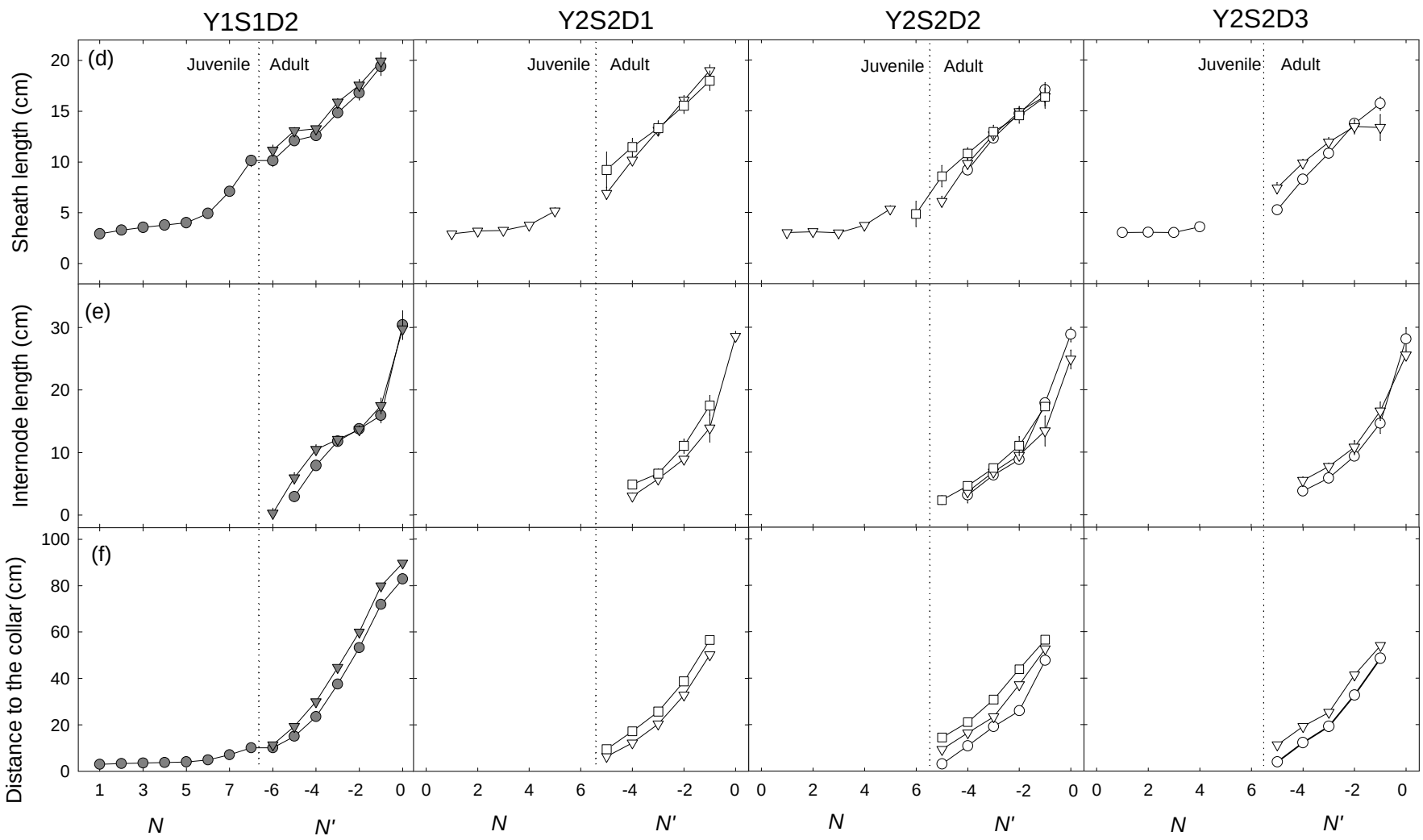
Y1S1D2
Y2S2D1
Y2S2D2
Y2S2D3
(d)
(e)
(f)
Juvenile
Adult
Sheath length (cm)
Internode length (cm)
Distance to the collar (cm)
N
N′

Appendix III/B. (a) Length of leaf blade, **(b)** width of leaf blade, **(c)** area of leaf blade, **(d)** length of sheath, **(e)** length of internode and **(f)** distance to the collar from the shoot base *vs.* leaf rank *N'* counted from the top for the main stem of winter wheat Cv. 'Soissons' sown in late September (S1) and mid November (S2) in 2007/2008 (Y1) in Grignon at 3 sowing densities: D1 (○), D2 (▽), D3 (□). Data are pooled by final leaf number N_{leaf} = 13 (left column), N_{leaf} =14 (middle column) for sowing S1 and N_{leaf} =10 (right column) for sowing S2. D1: 77, D2: 228, D3: 514 plants.m^{-2}. Vertical bars show confidence intervals (α=0.05) when larger than the size of the symbol.

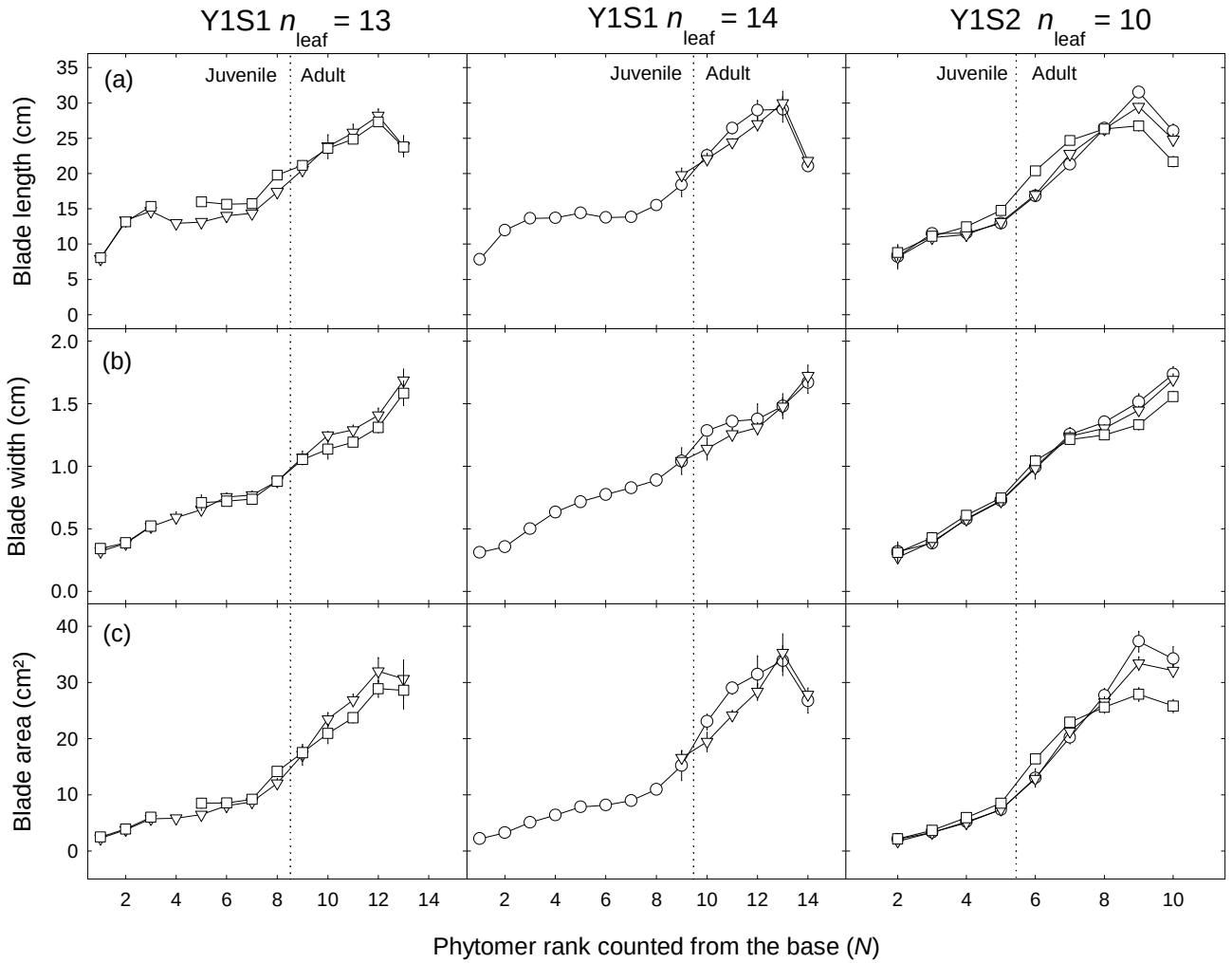

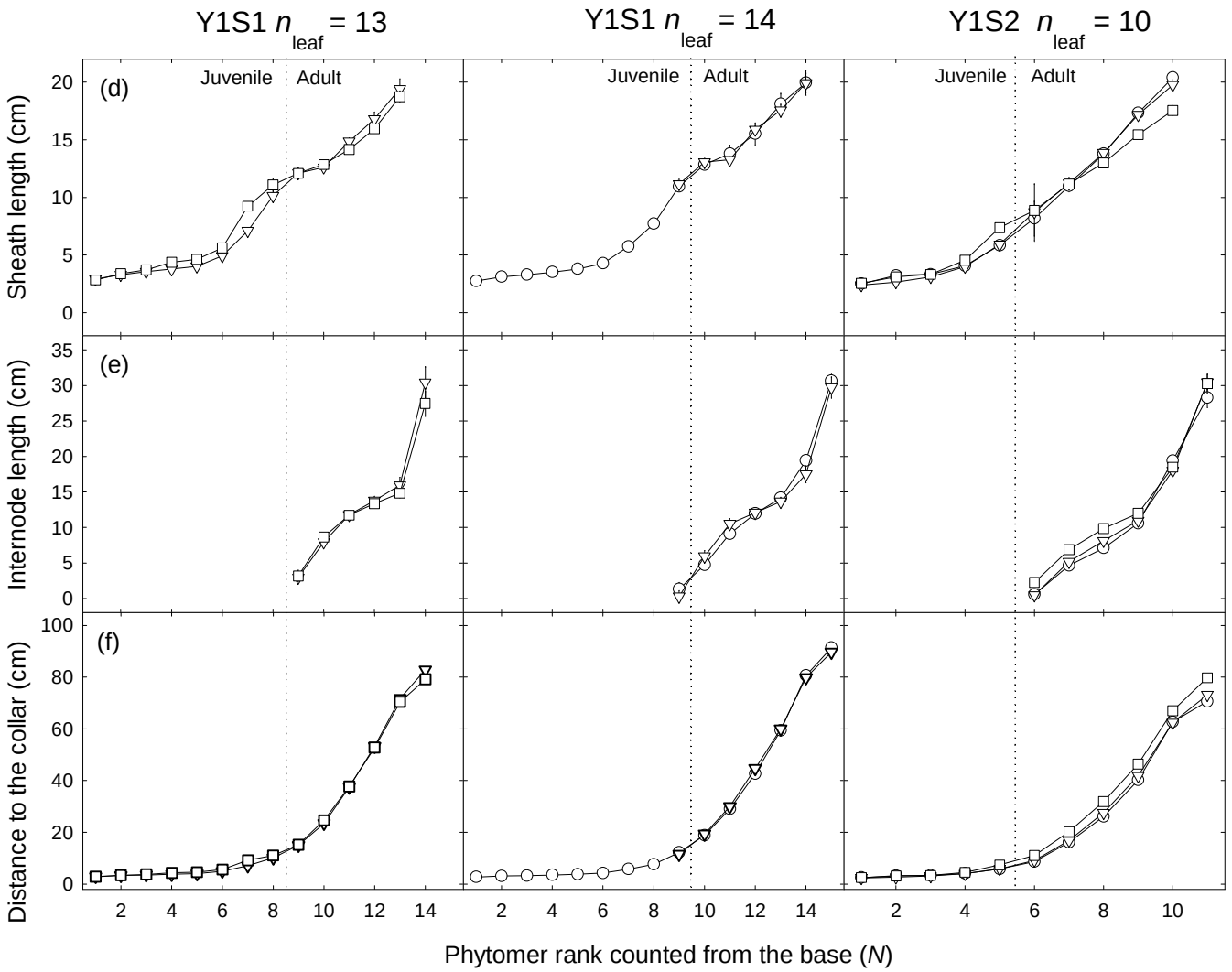
Y1S1 n_{leaf} = 13
Y1S1 n_{leaf} = 14
Y1S2 n_{leaf} = 10
(d)
(e)
(f)
Juvenile
Adult
Sheath length (cm)
Internode length (cm)
Distance to the collar (cm)
Phytomer rank counted from the base (N)

Appendix III/C. (a) Length of leaf blade, **(b)** width of leaf blade, **(c)** area of leaf blade, **(d)** length of sheath, **(e)** length of internode and **(f)** distance to the collar from the shoot base *vs.* leaf rank *N* counted acropetally for the main stem of winter wheat Cv. 'Soissons' sown in mid November 2008 (Y2S2) in Grignon at 3 sowing densities: D1 (○), D2 (▽), D3 (□). Data are pooled by final leaf number n_{leaf} = 9 (left column), n_{leaf} =10 (middle column) and n_{leaf} =11 (right column). D1: 77, D2: 228, D3: 514 plants.m^{-2}. Vertical bars show confidence intervals (α=0.05) when larger than the size of the symbol.

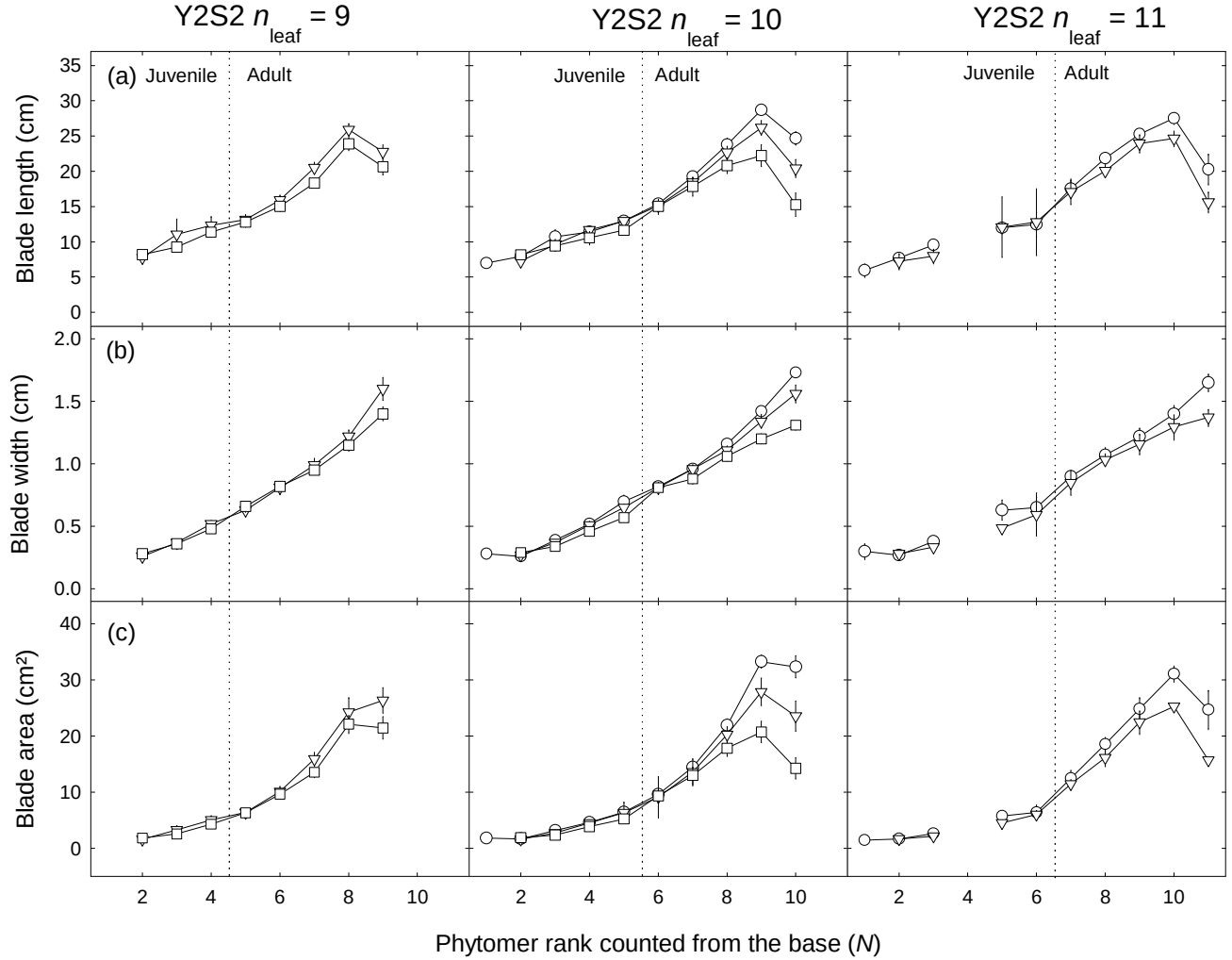

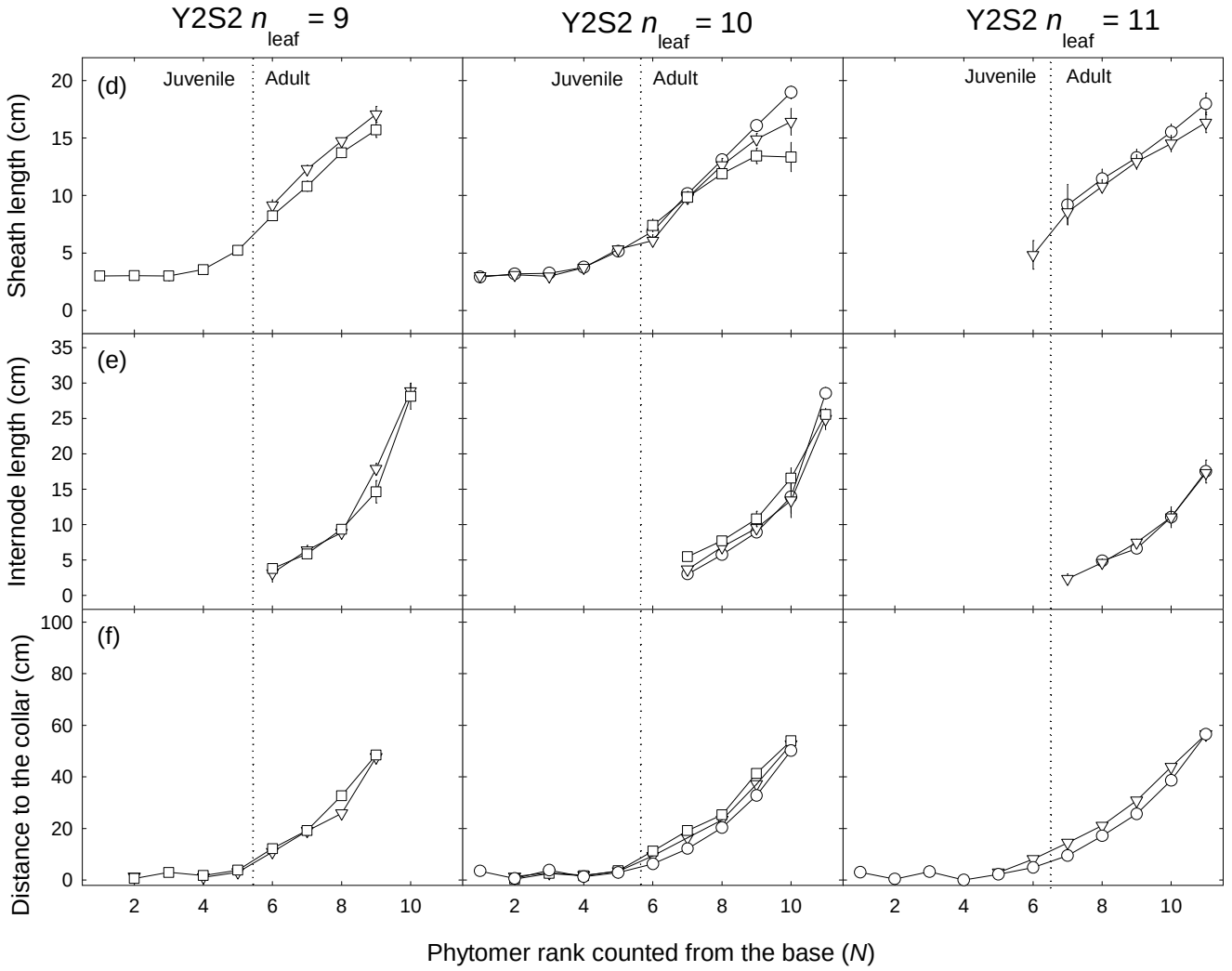
Y2S2 n_{leaf} = 9
Y2S2 n_{leaf} = 10
Y2S2 n_{leaf} = 11
(d)
(e)
(f)
Juvenile
Adult
Sheath length (cm)
Internode length (cm)
Distance to the collar (cm)
Phytomer rank counted from the base (*N*)

Appendix IV

Plasticity of winter wheat modulated by sowing date, density and nitrogen fertilisation: Dimensions and size of leaf blades, sheaths and internodes in relation to their position on a stem.

DORNBUSCH, T., BACCAR, R., WATT, J., HILLIER, J., BERTHELOOT, J., FOURNIER, C. AND ANDRIEU, B. 2011.

*Field Crops Research.*Vol:121.116-124.

Field Crops Research 121 (2011) 116–124

Contents lists available at ScienceDirect

Field Crops Research

journal homepage: www.elsevier.com/locate/fcr

Plasticity of winter wheat modulated by sowing date, plant population density and nitrogen fertilisation: Dimensions and size of leaf blades, sheaths and internodes in relation to their position on a stem

Tino Dornbusch[a,b], Rim Baccar[a,b], Jillian Watt[c], Jonathan Hillier[d], Jessica Bertheloot[e], Christian Fournier[f,g], Bruno Andrieu[a,b,*]

[a] INRA, UMR 1091 EGC, F-78850 Thiverval-Grignon, France
[b] AgroParisTech, UMR 1091 EGC, F-78850 Thiverval-Grignon, France
[c] University College London, Department of Geography, London WC1E 6BT, UK
[d] University of Aberdeen, School of Biological Sciences, Aberdeen, AB24 3UU Scotland, UK
[e] INRA, UMR 462 SAGAH, IFR 149 QUASAV, F-49071 Beaucouzé, France
[f] INRA, UMR 759 LEPSE, F-34060 Montpellier, France
[g] SupAgro, UMR 759 LEPSE, F-34060 Montpellier, France

ARTICLE INFO

Article history:
Received 29 July 2010
Received in revised form
26 November 2010
Accepted 1 December 2010

Keywords:
Plasticity
Wheat
Sowing date
Plant population density
Triticum aestivum
Leaf blade
Sheath
Internode
Stem height

ABSTRACT

Mathematical models to describe crop–environment interaction on organ scale need to take crop or plant architecture into account. Up to now, architectural plant models are largely descriptive and parameters need to be estimated for each species, cultivar and environment. Required measurements are extensive and time-consuming. Hence investigating morphological patterns and their modulation as a response to environmental conditions may help to reduce measurement efforts and to predict plant architecture in crop models. In this paper, we describe the plasticity of winter wheat – expressed as the dimensions and sizes of leaf blades, sheaths and internodes in relation to their position on a stem – under the climatic conditions of the Paris region. Results are discussed with respect to: (i) genotypic variability, (ii) inter-annual variability, (iii) sowing date and plant population density, (iv) Nitrogen fertilisation and (v) tiller rank.

Eight wheat cultivars grown in the same season showed similar patterns of leaf and internodes dimensions in relation to their position on the stem. For the cultivar 'Soissons', main stem architecture at flowering was remarkably stable when similar growth conditions were reproduced in the different seasons. Increased plant population density yielded longer juvenile, but shorter adult leaf blades and sheaths. Earlier sowing led to an increase in the number of juvenile phytomers – growing before the onset of stem elongation – on the main stem, whereas the number of adult phytomers was almost identical. Further there were little differences in the size of leaf blades, sheaths and internodes between the main stem and axillary tillers. We found remarkable differences in the size of adult leaf blades and sheaths in different growing seasons, with different timing of nitrogen fertilisation and we discuss decreased availability of nitrogen in the soil in spring as a likely cause.

Data presented here can be used to enlarge the understanding of wheat plasticity regarding the regulation of organ size by temperature, light, plant-available nitrogen and size-mediated effects towards a mechanistic modelling of these responses.

1. Introduction

The structure of crop canopies is an essential component to describe the interactions between crops and their environment with mathematical models. A simple description of structure is used in classical crop models taking only a small number of compartments – typically roots, stems and leaves – into account. Detailed representation of plant architecture at organ scale allows to investigate, e.g. radiation transfer (Chelle and Andrieu, 1998), movement of liquid water (Bassette and Bussière, 2008), or interception of pesticides (Dorr et al., 2008) by individual plants and organs. Development of functional–structural plant models and the use of descriptive architectural models to simulate physical trans-

* Corresponding author at: INRA, UMR 1091 EGC, F-78850 Thiverval-Grignon, France.
E-mail address: bruno.andrieu@grignon.inra.fr (B. Andrieu).

0378-4290/$ – see front matter © 2010 Elsevier B.V. All rights reserved.
doi:10.1016/j.fcr.2010.12.004

fers aim at addressing new questions such as competition of plants with weeds, analysis of epidemics, and design of new ideotypes (for review see Vos et al., 2010).

The plasticity of architecture in response to environmental conditions, which is an essential component of plant fitness and productivity, is however not fully understood. This arises from the number of processes involved in the regulation of the amount of plant modules (organs) produced, their size, geometry and lifespan. Leaf size, for example, is regulated by the availability of water, carbon (C) and nitrogen (N), physical factors (e.g. temperature, water vapour pressure deficit), phytohormons and other metabolites mediating responses to developmental (e.g. floral transition) and environmental signals (e.g. red: far red light).

In cereals, few quantitative studies on plasticity have been carried out so far, which take dimensions of phytomers (mainly: leaf blades, sheaths and internodes) on all tillers into account. Evers et al. (2005), Fournier et al. (2003) and Tivet et al. (2001) presented relationships of phytomer dimensions between main stem and axillary tillers for one cultivar. Other work encompass only data for the first juvenile leaves or for the main stem alone (Equiza and Tognetti, 2002; Kirby et al., 1982; Friend, 1965; Gallagher, 1979). Assuming non-limiting nutrient and water supply, temperature and incoming photosynthetically active radiation were identified as the most relevant external environmental factors to influence leaf dimensions. Further, Abbe et al. (1941) and Kirby (1977) proposed a direct relationship between size of the shoot apical meristem (SAM) and leaf blade width. Casey et al. (1999) pointed out that the length of the sheath tube a leaf blade grows in, largely determines its final length. In other words, the length of a cereal leaf (more precisely the whorl) influences the length of the consecutive one. This phenomenon was denoted as a size-mediated effect by Louarn et al. (2010). Size-mediated effects interplay with growth responses to environmental conditions. Hence a range of sometimes interconnected regulatory mechanisms – some of which have been indicated above – need to be taken into account to develop mechanistic models that are able to describe cereal plasticity.

As a consequence, existing models of plant architecture are largely descriptive. To a large extent they rely on the identification and formalisation of patterns found in the architectural traits of organs according to their age and topological position within a plant. The regulatory mechanisms that lead to the observed patterns are not fully understood, so that identifying these patterns – as stable relationships of organ dimensions with topological position that are conserved in a range of environments – is essential to build and parameterise architectural models. More generally, this would provide the framework for an efficient description of plasticity as a genotype–environment interaction (G × E).

Wheat (*Triticum aestivum* L.) is one cereal species for which architectural models are actively being developed and applied. For instance ADEL-wheat has been parameterised to model winter wheat architecture for one set of environmental conditions (Fournier et al., 2003). The model parameterisation has further been adapted for spring wheat and a different set of environmental conditions including various plant population densities (Evers et al., 2005). ADEL-wheat coupled to process-based models was used to investigate the conditions of axillary tiller bud outgrowth (Evers et al., 2007a) and disease epidemics (Robert et al., 2008). Recent works have partly elucidated functional aspects such as the translocation of nitrogen (Bertheloot et al., 2008) or the role of source–sink relationships in bud outgrowth (Evers et al., 2010), but modelling of organ size still remain empirical and hence dimensions need to be measured for each genotype and environment.

As a substitute for the lack of the availability of mechanistic models to predict organ size and as a step towards developing such models, this study explores the plasticity of the dimensions and size of winter wheat leaf blades, sheaths and internodes in relation to their position on the stem. Here we present the impact of: (i) genotypic variability, (ii) inter-annual variability, (iii) sowing date and plant population density, (iv) N fertilisation and (v) tiller rank, on the dimensions and size of leaf blades, sheaths and internodes based on datasets obtained during five years of field experiments.

2. Materials and methods

2.1. Field experiments

Experiments were located at the INRA research unit of Thiverval-Grignon, near Paris (48°51′N, 1°58′E, 70 m) with a maritime influenced climate (Köppen climate classification Cfb; Köppen, 1931) that permits high yields for winter annual crops. Winter wheat (*Triticum aestivum* L.) was grown on a deep loamy soil (typic *Eutrochrept*; US soil taxonomy) under non-limiting availability of water (irrigation when needed) and nutrients. The standard regional agronomic practices for winter wheat are: (i) sowing at mid to late October (ii) plant population density of 200–300 plants per m^2, (iii) N fertilisation of 150–200 kg ha^{-1} split into two doses, the first usually given late February to early March and the second at the onset of stem elongation, early to mid April and (iv) fungicide, herbicide and growth retardant applications if required. Our experiments comprised eight wheat cultivars (Y03/04), three plant population densities ('Soissons' in Y98/99, Y07/08, Y08/09), three sowing dates ('Soissons' in different seasons) and two N fertilisation treatments ('Soissons' in Y05/06). Plots consisted of nine planting rows with an inter-row distance of 0.175 m. Plant population density is referred to as low density (D_1), normal density (D_2), and high density (D_3). Sowing dates are divided into early sowing late September (S_1), normal sowing mid to late October (S_2) and late sowing mid November (S_3). N fertilisation followed the standard scheme (two doses) except in the N_0 treatment in Y05/06, where no N was supplied during the whole season. Major experimental conditions for the different growing seasons (abbreviated as e.g. Y08/09) are summarised in Table 1.

2.2. Sampling procedures and measurements

In all experiments, we aimed at a faithful estimation of the dimensions and size of mature (fully extended) leaf blades, sheaths and internodes using median plants, thus avoiding consideration of the plant-to-plant variability at crop level. To select median plants, we used two simple criteria: (i) similar number of tillers per plant, (ii) similar developmental stage of the main stem using the Haun stage (H; after Haun, 1973). Based on these criteria, leaf blades of tillers were regularly tagged during growth. The main stem is denoted as MS and the axillary tillers as Tk (k = 0, 1, 2, . . .) T1 being the tiller that emerges from the axil of the first true leaf blade. The coleoptile tiller T0 rarely emerged and was not considered in data processing.

In Y98/99, Y03/04, Y05/06, the architectural traits length (l_{bl}) and width (w_{bl}) of leaf blades, and length of sheaths (l_{sh}) and of internodes (l_{in}) were measured with a ruler. The distance of the leaf collar from the shoot base (in short: collar height h_{col}) was measured for each phytomer. The distance of the ear collar (sum of internodes + peduncle) is referred to as stem height. Leaf blade area (A_{bl}) was derived as $A_{bl} = l_{bl} \cdot w_{bl} \cdot f_t$, where mean values for the shape factor f_t for each phytomer rank were taken from measured data given by Dornbusch et al. (2011).

In Y07/08 and Y08/09, at two to eight occasions during crop growth depending on the experiment, 15–45 tagged median plants were collected and l_{bl}, w_{bl} and A_{bl} were computed from images obtained with a flat-bed scanner that were processed using the program Lamina2Shape (Dornbusch and Andrieu, 2010). In addi-

Table 1
Major agronomic details specific for: (i) different growing seasons; (ii) *T. aestivum* cultivars; (iii) sowing date: S_1 late September, S_2 mid to late October, S_3 mid November; (iv) nominal plant population density at sowing: D_1 low, D_2, normal, D_3 high (number of plants per m^{-2} in brackets); (v) specific agronomic treatments (agronomic treatments not specified were kept optimal) and further experimental details published in literature by the author group.

Season	Cultivars	Sowing date	Plant population density	Specific agronomic treatments
Y98/99	'Soissons'	S_2	D_1 (70) D_2 (250)	See also Ljutovac (2002)
Y03/04	'Soissons' 'Caphorn' 'Apache' 'Arminda' 'Isengrain' 'Thésée' 'Oratorio' 'Recital'	S_2	D_2 (250)	Growth retardants: 18/03/04 – 1.5 l ha^{-1} Cycocel C5 (BASF Agro); 15/04/04 – 0.4 l ha^{-1} Medax Top (BASF Agro)
Y05/06	'Soissons'	S_2	D_2 (250)	Growth retardants: 04/04/06 – 2.0 l ha^{-1} Cycocel C3 (BASF Agro); N-fertilisation: N_+ (optimal) N_0 (no N given)
Y07/08 and Y08/09	'Soissons'	S_1 S_3 Both seasons	D_1 (77) D_2 (228) D_3 (514) Both seasons	Growth retardants: 16/04/09 0.5 l ha^{-1} Moddus (Syngenta Agro GmbH) only in Y08/09 S_3D_3. See also Baccar *et al.* (2010)

tion l_{sh} and l_{in} were measured with a ruler and h_{col} was measured as described above. More details about the measurement protocols were described in previous papers (Baccar et al., submitted for publication; Dornbusch et al., 2011).

2.3. Data processing statistical tests and presentation of results

Measured architectural traits (e.g. l_{bl}) are usually displayed as a function of phytomer rank N (vertical profile) counted from the base, where $N = 1$ is the rank of the first true leaf. However, to better compare data of various tillers – which differ in final leaf number (n_{leaf}) – we use the phytomer rank N' counted from the top ($N' = -1, -2, \ldots$), where $N' = -1$ represents the rank of the flag leaf and $N' = 0$ the rank of the peduncle. The vertical profile of leaf blade length is for instance abbreviated as $l_{bl}(N')$.

For each experimental year, treatment and tiller rank, mean values of architectural traits (see above) were computed for each phytomer rank, for tillers with the same final number of leaves. The MS in the various treatments differed in final leaf number making direct comparison of specific phytomer ranks between treatments difficult. Therefore we looked separately at the first four to five basal phytomers (growing before stem elongation) and at the last six phytomers (growing after the onset of stem elongation). Following Poethig (2003), we will refer to these two categories as juvenile and adult phytomers, respectively. We used N to compare juvenile phytomers and N' to compare adult phytomers.

The non-parametric Wilcoxon Rank-Sum Test was applied to test statistical significant differences between measured traits of the same phytomer rank. P-values computed with the test are given as Supplemental material. Note that for Y98/99 only mean data on leaf dimensions and size were available. Therefore statistical analysis could not be performed for this treatment. As a measure for the deviation from an ideal 1:1 line between measured and model-predicted values, we used the mean error (ME) and the mean squared error (RSME):

$$\mathrm{ME} = \frac{1}{n}\sum_{i=1}^{n}(f_i - y_i) \quad (1)$$

$$\mathrm{RMSE} = \sqrt{\frac{1}{n}\sum_{i=1}^{n}(f_i - y_i)^2} \quad (2)$$

where here f_i represents the model-predicted and y_i the corresponding measured values.

3. Results

3.1. Differences in leaf blade area and stem height between cultivars were observed in the adult phase

The eight wheat cultivars grown in Y03/04 (names given in Table 1) showed a pattern of leaf blade, sheath and internode dimensions in relation to their position on a stem (vertical profiles) resembling those obtained under standard agronomic practices in the area and described below for Soissons (S_2 in Fig. 2). To discuss the differences between cultivars we present only the vertical profiles of blade area $A_{bl}(N')$ and collar height $h_{col}(N')$ of the main stem (MS) in Fig. 1. These two characteristics – along with leaf angle – strongly influence the vertical distribution of leaf area in the

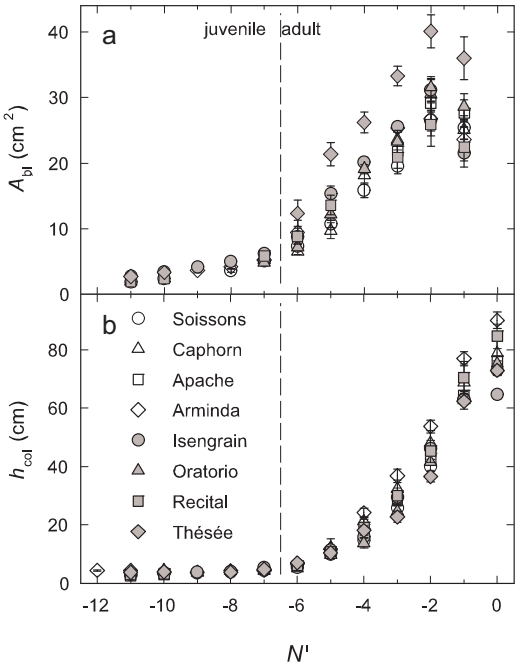

Fig. 1. (a) Area of leaf blades A_{bl}; (b) distance of the collar from the shoot base h_{col} vs. phytomer rank counted from the flag leaf N' for eight cultivars of *T. aestivum* (main stem) sown at normal density (D_2) in mid October (S_2) Y03/04; $N' = -1$: rank of flag leaf; $N' = 0$: rank of peduncle; the dashed line separates phytomers grown before (juvenile phase) and after the onset rapid internode elongation (adult phase). Error bars mark the 95% confidence interval of mean estimate. Data are given in Appendix I (Supplemental material).

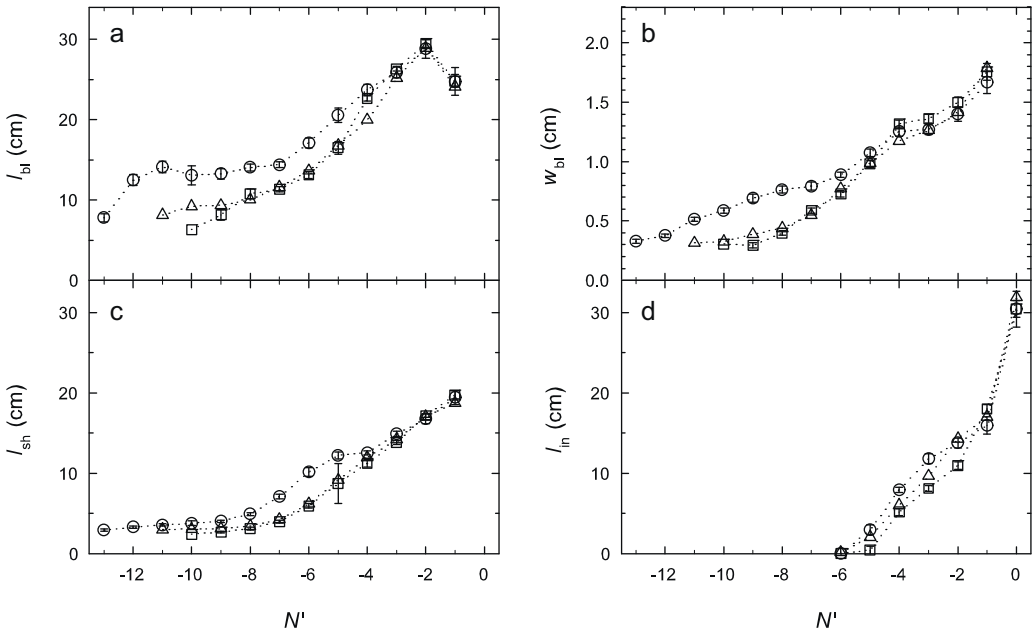

Fig. 2. (a) Length of leaf blades l_{bl}, (b) width of leaf blades w_{bl}, (c) length of leaf sheaths l_{sh}; (d) length of internodes l_{in} ($N'=0$ rank of peduncle); vs. phytomer rank counted from the flag leaf N' for *T. aestivum* 'Soissons' (main stem) at three different sowing dates: late September S_1 Y07/08 (○), late October S_2 Y98/99 (△), mid November S_3 Y07/08 (□); values represent measured mean values at normal plant population densities D_2; error bars mark the 95% confidence interval of mean estimate. Data are given in Appendix II (Supplemental material).

canopy. Leaf blade, sheath and internode dimensions are shown in Supplemental Fig. 1, and corresponding data in Appendix VI.

Leaf blades growing during autumn and winter in the juvenile growth phase increased in area A_{bl} with increasing phytomer rank, but only little in h_{col}. During this phase h_{col} represents only sheath length, leading to a 'rosette growth habit' of wheat. In the adult growth phase – which starts after the onset of rapid internode extension – both, A_{bl} and h_{col} of fully extended phytomers increased quasi linearly with increasing phytomer rank, except for the flag leaf blade which was smaller than the previous leaf blade.

Very little or no differences were found for the lower juvenile leaf blades (see Appendix I). Differences were observed starting from the first adult leaf blade ($N'=-6$). The largest leaf blades were found in 'Thésée' ($P<0.01$; see Appendix I). For 'Thésée', the flag leaf $A_{bl}(-1)$ was 36.0 cm^2 compared to 21.5 cm^2 for 'Isengrain' and 22.5 cm^2 for 'Recital', which had the smallest flag leaf blade (Fig. 1a).

Differences in $h_{col}(N')$ between cultivars were observed with the second elongated internode ($N'=-4$). 'Arminda' had the tallest ($h_{col}(0)=90.1$ cm; $P<0.001$; see Appendix I) and 'Isengrain' the shortest MS ($h_{col}(0)=64.6$; $P<0.001$). No systematic association between stem height and leaf blade area was found. The large-leaved 'Thésée' was amongst the shortest cultivars, while the tallest cultivar 'Arminda' was close to the mean in term of blade area.

3.2. Leaf blade, sheath and internode dimensions for the varying sowing dates

Experiments with varying sowing date were carried out using the cultivar 'Soissons'. Fig. 2 shows the vertical profiles $l_{bl}(N')$, $w_{bl}(N')$, $l_{sh}(N')$ and $l_{in}(N')$ for early (S_1), normal (S_2) and late sowing (S_3) treatments grown at normal plant population density (D_2; Fig. 2). The median n_{leaf} on MS was decreased in the later sowing dates; S_1: $n_{leaf}=13$, S_2: $n_{leaf}=11$ and S_3: $n_{leaf}=10$.

There were no clear differences in leaf blade and sheath dimensions between S_2 and S_3, except for the length of the first two emerged leaf blades. In contrast, early sowing S_1 resulted in longer and wider leaf blades (Fig. 2a and b) and longer sheaths (Fig. 2c) in the juvenile growth phase. At S_1 leaf blade $N=2$ was much longer than the ones at S_2 or S_3, but leaf width was almost the same. During winter, the length of successive leaf blades increased either little or not for all sowing dates (Fig. 2a). Differences for adult leaf blades were much less and vanished completely for the uppermost three phytomers: comparing S_1 and S_3, the length of the uppermost three adult leaf blades ($-3\le N'\le -1$) and the uppermost two sheaths ($-2\le N'\le -1$) were not different ($P>0.4$; see Appendix II) in Y07/08.

The width of adult leaf blades ($-4\le N'\le -1$) tended to be greater at S_3 compared to S_1 but differences were not significant ($P<0.14$; see Appendix II). The most frequent number of elongated MS internodes (including peduncle) was six for all treatments, but at S_1 and S_2 there were either six or seven elongated internodes, whereas at S_3 there were either five or six. As shown in Fig. 2d, internodes on MS were longer at S_1 than S_3 ($P<0.05$; see Appendix II), whereas the MS peduncle did not differ in length ($P>0.4$; see Appendix II). This led to taller plants at flowering for S_1 and S_2 ($h_{col}(0)=80.3$ cm and 81.0 cm, respectively) than S_3 ($h_{col}(0)=73.2$ cm).

3.3. Leaf blade, sheath and internode dimensions for contrasted plant population densities

In the juvenile growth phase, there were little changes associated with plant population density for the normal and late sowing dates, but at S_1, leaf blades and sheaths ($2\le N\le 5$) were longer at D_3 than D_1 (Fig. 3a; $P<0.05$; see Appendix III), whereas differences in A_{bl} were not significant for all phytomer ranks (see Appendix III).

In the adult growth phase, l_{bl} and A_{bl} were smaller at higher plant population density. The uppermost two leaf blades were significantly smaller at D_3 compare to D_1, both in S_1 and S_3. At lower phytomer ranks, differences in l_{bl} and h_{col} were not always significant (Fig. 3a and c; Appendix III). Further, h_{col} in the adult growth phase ($-5\le N'\le -1$) was significantly different between plant population density treatments (Fig. 3c; $P<0.01$; Appendix III), but effects differed according to sowing date: in early sowing plants were taller at low density (D_1: $h_{col}(0)=90.0$ cm and D_3:

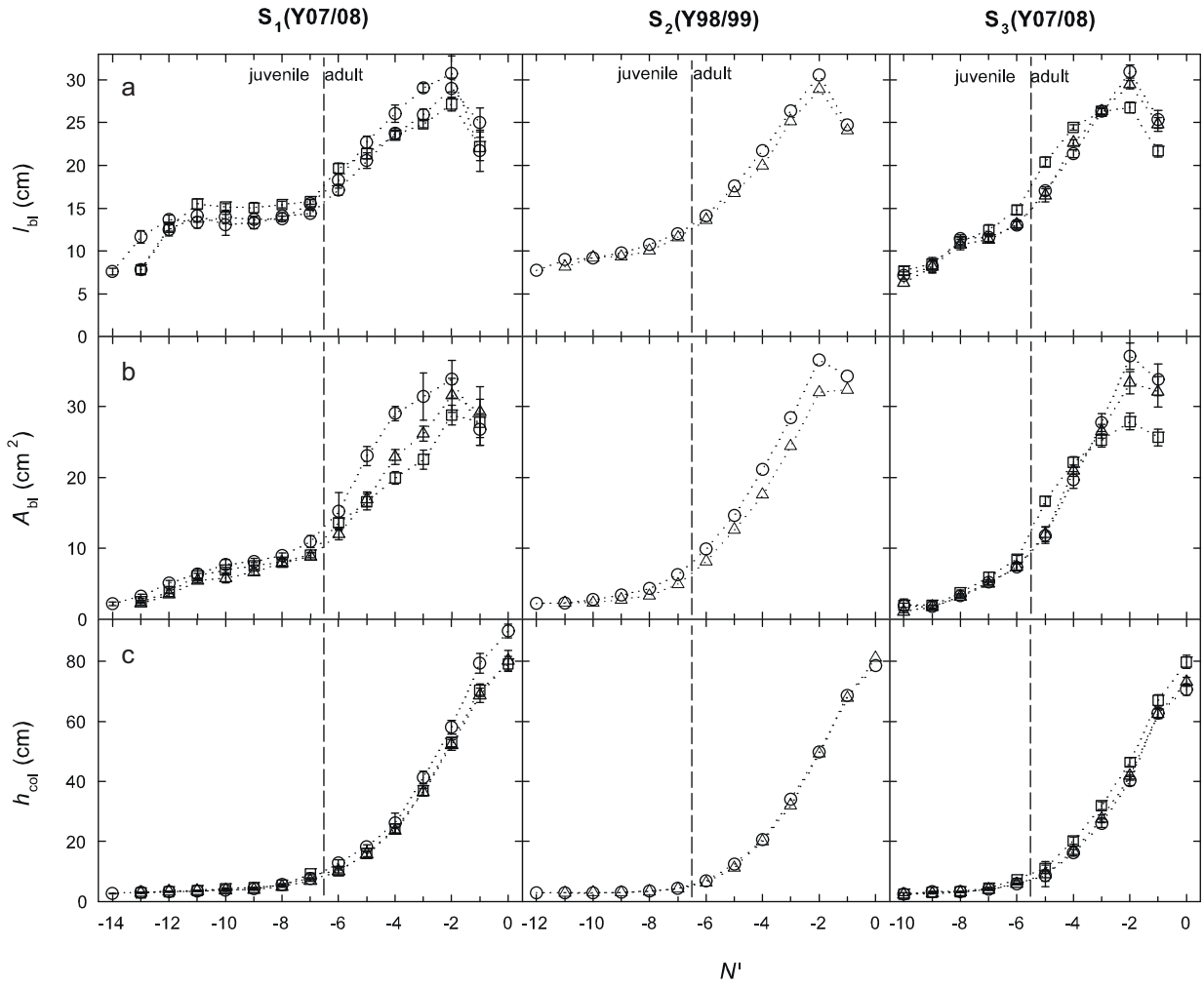

Fig. 3. (a) Length of leaf blades l_{bl}; (b) Area of leaf blades A_{bl}; (c) distance of the collar from the shoot base h_{col}; vs. phytomer rank counted from the flag leaf N' for *T. aestivum* 'Soissons' (main stem) sown in late September S_1 Y07/08 (left column), late October S_2 Y98/99 (middle column) and mid November S_3 Y07/08 (right column) and at three different plant population densities D: low density D_1 (○), normal density D_2 (△), high density D_3 (□); values represent measured mean values; the dashed line separates phytomers grown before (juvenile phase) and after the onset of rapid internode elongation (adult phase); $N' = -1$: rank of flag leaf; $N' = 0$: rank of peduncle. Error bars mark the 95% confidence interval of mean estimate. Data are given in Appendix III (Supplemental material).

$h_{col}(0) = 79.1$ cm), whereas in late sowing plants were taller at high density (D_1: $h_{col}(0) = 70.6$ cm and D_3: $h_{col}(0) = 79.7$ cm).

3.4. Lack of available nitrogen in early spring led to smaller leaf blades in the adult growth phase

Data from in the experimental year Y07/08 were obtained under growth conditions with optimal N fertilisation regarding timing and dosage as described in Section 2. In Y05/06 and Y08/09, the application of the first N dose in early spring was delayed by approximately three weeks compared to the usual time, so that at the time of the first N application, the MS had approximately two more leaves in Y05/06 and Y08/09 compared to Y07/08 (see Fig. 4). The first two leaves were longer and larger in Y05/06 than Y07/08 due to the earlier sowing date. However, during winter l_{bl} decreased in Y05/06, whereas A_{bl} was in the same magnitude as observed in Y07/08 and Y08/09. In the adult growth phase, the uppermost leaf blades ($-4 \le N' \le -1$) were shorter and smaller in Y05/06 and in Y08/09 compared to Y07/08 (Fig. 4; $P < 0.001$; Appendix IV). Further, in Y05/06, l_{bl} and A_{bl} was decreased in the N_0 treatment compared to N_+ (Fig. 4; $P < 0.001$; Appendix IV), but n_{leaf} on the MS was the same.

3.5. Differences in leaf dimensions, size and collar height between main stem and axillary tillers

At all sowing dates, the first three leaf blades appeared on T1, T2 and T3 were shorter than the corresponding leaf blades on the MS with the same rank N' (Fig. 5; $P < 0.001$; see Appendix V). With increasing phytomer rank N', differences in l_{bl} between MS, T1, T2 and T3 became smaller and the uppermost four adult phytomers were not different in length ($P > 0.15$; see Appendix V). The same trend was observed at S_2, but statistical confirmation of results was not possible, since only mean data values were available. At S_3, differences in l_{bl} between MS, T1, T2 and T3 were less significant compared to S_1 (see Appendix V), but the observed pattern was the same as for S_1 and S_2.

Further, values for w_{bl} and A_{bl} for the T1, T2, T3 were smaller than values for the MS (Fig. 5b and c). Differences were maintained for all phytomers up to the flag leaf at S_2, but became smaller starting from phytomer rank $N' = -5$ to the flag leaf at S_3 (see Appendix V). At any given position N', $w_{bl}(N')$ and $A_{bl}(N')$ were usually smaller for tillers of higher rank (MS > T1 > T2 > T3). An exception to this occurred for S_3 (Y08/09; right column), in which $w_{bl}(N')$ $A_{bl}(N')$ of T1 were smaller compared to T2 and T3, because of a frost period in winter that impeded and inhibited outgrowth of T1 on many plants.

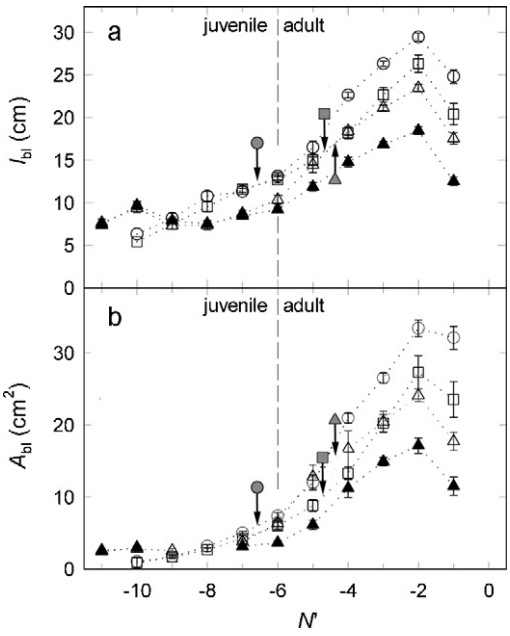

Fig. 4. (a) Length of leaf blades l_{bl}; (b) area of leaf blades A_{bl} vs. phytomer rank counted from the flag leaf N' for *T. aestivum* 'Soissons' (main stem) in three different experimental years at normal plant population density: Y05/06 sown late October (S_2) (△), Y07/08 (○) and Y08/09 (□) both sown mid November (S_3), data represents measured mean values; Y05/06 with two nitrogen (N) fertilisation treatments: optimal N_+ (△) and no nitrogen given N_0 (▲); the arrows with the filled symbol of the corresponding dataset mark the developmental stage where the first nitrogen dose was applied at the onset of the vegetation period in early spring. Error bars represent the 95% confidence interval of mean estimate. Data are given in Appendix IV (Supplemental material).

At S_3, we observed small differences in $h_{col}(N')$ between axillary tillers and MS. In tendency, the MS was taller than axillary tillers, but differences were not statistically significant (Appendix V).

To test for similarity in architectural traits between T1, T2, T3 and MS we selected data from all experimental years described in Section 2 and plotted the mean length of the last four adult leaf blades, sheaths and internodes ($-4 \leq N' \leq -1$) of T1, T2 and T3 against the corresponding measured values of the MS (Fig. 6a). Data points fell close to the 1:1 line. In tendency, values for l_{bl}, l_{sh}, and l_{in} for the T1, T2, T3 were smaller than the corresponding values for the MS (ME = −0.66 cm). This difference did not show a trend with tiller rank (data not shown). Thus, the length of the blade, sheath or internode of tillers could be estimated from the corresponding one of main stem with a low RSME (1.81 cm).

For A_{bl}, we obtained a stronger deviation from the 1:1 line (RSME = 3.85 cm^2) and A_{bl} for tillers was in most cases lower than for MS (ME = −2.86 cm^2). Looking at data from different genotypes and experimental years, no clear trend in decreasing A_{bl} with increasing tiller rank (T1 > T2 > T3) compared to MS was found (data not shown here).

4. Discussion

We investigated the pattern of organ dimensions and size in relation to the position on the main stem for different growing seasons and cultivars, and compared it to axillary tillers with respect to analysing whether a simple comprehensive description of the observed patterns could be proposed. In field-grown wheat, the typical profile of leaf blade length shows an increase in length with phytomer rank up to the penultimate leaf blade, with the flag leaf blade being shorter. Similar patterns have been reported in several studies (Evers et al., 2007b; Lock, 2003; Gallagher, 1979; Hotsonyame and Hunt, 1997). There was little or no change with phytomer rank in leaf blade length during the juvenile phase (in winter) as also observed in our experiments. Kirby et al. (1982) suggested that temperatures below 8 °C combined with a daylength shorter that 12 h, lead to stagnation in leaf length for successive phytomer ranks. The pattern of organ size was found to be quite stable for the eight wheat cultivars investigated here (Fig. 1a). It seems that a small number of typical profiles of organ size can be defined to represent winter wheat cultivars with similar genetic background grown under similar growth conditions. In our experiments we observed a very high degree of repeatability of the pattern of organ size between growing seasons for 'Soissons'. Under comparable growth conditions – optimal N fertilisation and no application of growth retardants – the size of adult leaf blades was not different in experiments performed in two different growing seasons. Even if growth retardants(gibbellerin biosynthesis inhibitors in our experiments) were applied in some experimental years the general pattern of leaf blade, sheath and internode length was very similar to the other years (see Supplemental Fig. 1). The impact of these growth retardants on winter wheat are mainly a reduction of internode elongation under very favourable (wet) conditions yielding to shorter stems and reduced lodging (for review see Rademacher, 2000).

The typical pattern of organ size is highly related to winter growth conditions and several authors reported that profiles of leaf blade length deviate strongly from the usual ones when juvenile growth occurs under conditions of long photoperiod and/or high temperature (Borrill, 1959; Gómez-Macpherson et al., 1998; Kirby et al., 1982; Ljutovac, 2002). Such atypical growth conditions occur in growth chambers, greenhouses or in early autumn sowings. They reported that, for several grass species – including winter wheat – leaf blade length increased with phytomer rank in the juvenile growth phase up to a maximum length at the time of floral initiation, and then decreased in the adult growth phase towards the flag leaf. In our experiments, early sown plants had longer and wider juvenile leaf blades compared to late sown plants. On the contrary, very little variation in the size of the last three to four adult phytomers was observed (Fig. 2); the date of flowering also changed only very little so that adult phytomer leaves grew approximately at the same time and under similar conditions in spring independently of sowing date. Consequently, size mediated effects (the length of leaf blade $N+1$ is related to the sheath tube length of the preceding leaf N) did not appear to be able to propagate the larger size of the juvenile leaves to adult leaves. That further supports the coherence of the pattern of organ size between years with similar growth conditions.

For 'Soissons' at high plant population density, we observed increased blade length – compared to the low density – for juvenile leaves starting from phytomer rank $N' = -11$ in S_1 and $N' = -6$ in S_3 (Fig. 3a). There – in contrast – the length and width of the four (S_1) and the two (S_3) topmost adult leaf blades were reduced at high density. Comparable effects were observed by Kirby and Faris (1970) who investigated a range of plant population densities from 50 to 1600 plants m^{-2} on barley. An increase in blade length for juvenile leaves and a decrease in length and width for adult leaves as a response to high plant population density has also been reported for maize (e.g. Andrieu et al., 2006). Contrary to wheat, tillering cannot compensate for the effect of decreased plant population density in maize, so that the effects of plant population density are more pronounced.

In our experiments, mild nitrogen stress occurred at a relatively late developmental stage and did not impact the dimensions of juvenile leaves, due to a low demand of N during winter. The number of leaves on the main stem was not affected by N stress, but the dimensions of adult leaf blades were largely reduced (Fig. 4). We observed a twofold reduction in individual leaf area between optimal and no further N supply. Apparently, tiller abortion occur-

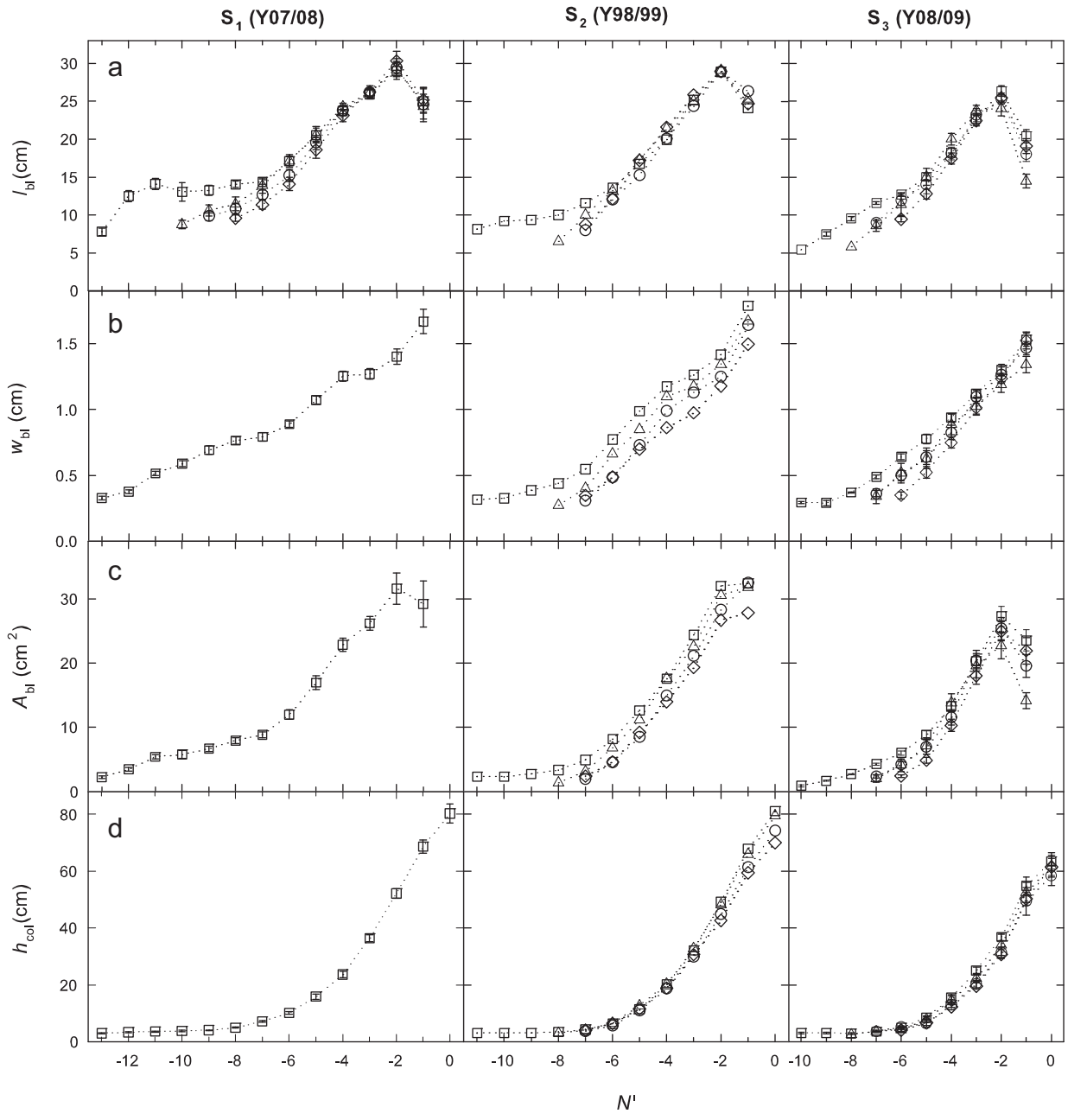

Fig. 5. (a) Length of leaf blades l_{bl}; (b) width of leaf blades w_{bl}; (c) area of leaf blades A_{bl}; (d) distance of the collar from the shoot base h_{col} vs. phytomer rank counted from the flag leaf N' for *T. aestivum* 'Soissons' sown in late September S_1 Y07/08 (left column), late October S_2 Y98/99 (middle column) and mid November S_3 Y08/09 (right column) all grown at normal plant population density D_2; symbols correspond to different tillers: MS (□), T1 (△), T2 (○), T3 (◊); the subscript for axillary tillers mark the phytomer rank where it originates from; symbols represent measured mean values. Data for A_{bl}, w_{bl}, h_{col} were not measured for axillary tillers at S_1 in Y07/08. Error bars mark the 95% confidence interval of mean estimate. Data are given in Appendix V (Supplemental material).

ring under N stress – leading to more N for the surviving tillers – did not fully compensate for the lack of available N so that the surviving tillers were impaired in their growth. Delayed application of N in spring also led to a reduction in adult leaf blade dimensions (Fig. 4), even if N application occurred before the growth of these leaf blades. The observed reduction in leaf blade size by N stress shares similarity with that observed for cold stress in maize (Louarn et al., 2008, 2010). A cold event at an early developmental stage resulted in a decreased size of all following leaf blades. Size mediated effects or a smaller shoot apical meristem (SAM) size may be the reason for such long-term propagation of growth response to a constraint in early plant development (Andrieu et al., 2006; Louarn et al., 2010).

Comparing axillary tillers to the main stem, the lengths of the uppermost adult leaf blades, sheaths and internodes were almost the same. This effect was also reported for wheat (Evers et al., 2005; Kemp, 1981) and rice (Jaffuel and Dauzat, 2005; Tivet et al., 2001). Due to the synchronisation of floral transition between tillers, adult phytomers grew almost at the same time and under similar growth conditions. However, regarding leaf blade width, we observed narrower leaf blades for axillary tillers following the tendency MS > T1 > T2 > T3. The observed difference tended to become smaller with increasing phytomer rank, so that in some treatments the flag leaf blades were of the same size for all tillers. The reason for the decreased leaf width is not known, but one may speculate that it arises from a smaller size of the SAM, since the SAM of axillary tillers

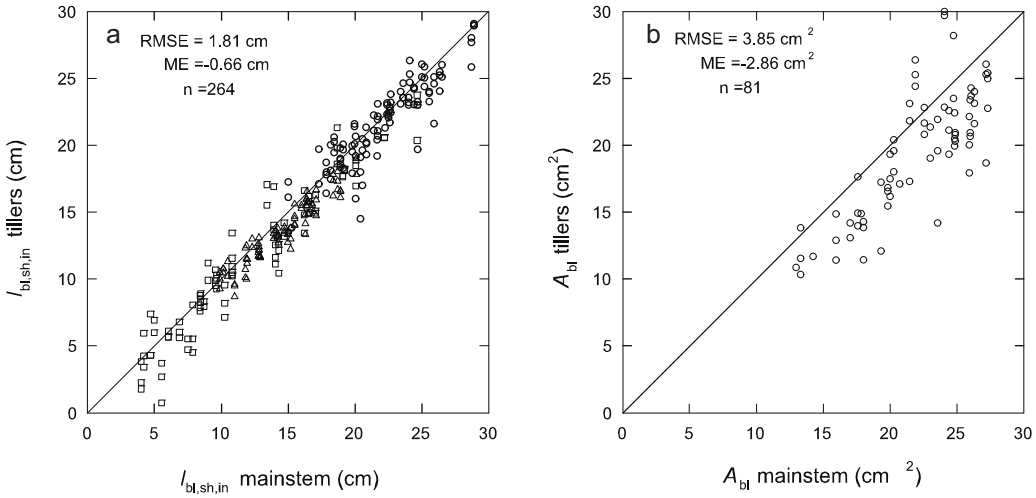

Fig. 6. (a) Median length of the uppermost four leaf blades l_{bl} (○), leaf sheath l_{sh} (△) and internodes l_{in} (□) of axillary tillers (T1–T3) vs. l_{bl}, l_{sh} and l_{in} of the main stem with the same phytomer rank N'; (b) Median area A_{bl} of the uppermost four leaf blades of the axillary tillers (T1–T3) vs. A_{bl} of the main stem with the same phytomer rank N'; 1:1 line, root mean squared error (RMSE), mean error (ME) and number of samples (n) are given.

is younger than the one of the main stem. Several authors have reported an increase in the diameter of the SAM with increasing age and associated that with an increase in width in barley (Kirby, 1977), rice (Yamazaki, 1963) and maize (Abbe et al., 1941). As adult leaf blades are narrower on axillary tillers while length is almost the same, this results in a moderate hierarchy in resources acquisition between main stem and axillary tillers; and we propose that this may be the reason for the hierarchy in grain production (e.g. reported by Wood and Thorne, 1985).

Winter wheat shows different plastic responses in the juvenile and the adult growth phase. Sowing date and density impacts the number of juvenile and adult leaves. Hence, to predict leaf dimensions and size for winter wheat, simple global equations, such as proposed by Dwyer and Steward (1986) for maize would be of limited use. At least, a higher number of parameters would be required, or sub-models (response functions) to include the regulation of leaf dimensions and size by temperature, light and nitrogen should be incorporated. Unfortunately, such response functions are not known at this point in time. Therefore measurements are still required to describe wheat architecture with architectural models. In this work, we observed that the size of adult leaves was weakly related to the size of lower juvenile leaves, thus measurements should include at least two sampling dates to assess dimensions and size of: (i) juvenile phytomers before the onset of stem elongation, and (ii) adult phytomers at flowering. Because of the high similarity in leaf blade, sheath and internode dimensions between tillers, identical patterns could be used for all tillers, just taking some decrease in leaf blade width higher tiller rank into account. Consequently, it would be of little importance to precisely identify the tillers rank when characterizing organ dimension at flowering.

Acknowledgements

We thank the Ministère des Affaires Etrangères [Dossier 2008453] and the German Research Foundation [DFG Do 1408/2-1] for granting the post doctoral fellowship for T. Dornbusch. Support in our experiments from F. Duhamel, E. Fovart and M. Marques is gratefully acknowledged.

Appendix A. Supplementary data

Online we have provided the results of the statistical analysis using the Wilcoxon Rank-Sum Test. The number of each Appendix is related to the corresponding Figure in the text.

Supplementary data associated with this article can be found, in the online version, at doi:10.1016/j.fcr.2010.12.004.

References

Abbe, E.C., Randolph, L.F., Einset, J., 1941. The developmental relationship between shoot apex and growth pattern of leaf blade in diploid maize. Am. J. Bot. 28, 778–784.
Andrieu, B., Hillier, J., Birch, C., 2006. Onset of sheath extension and duration of lamina extension are major determinants of the response of maize lamina length to plant density. Ann. Bot. 98, 1005–1016.
Baccar, R., Dornbusch, T., Abichou, M., Gate, P., Andrieu, B. Description of the effect of sowing date and density on the phyllochron of winter wheat (*Triticum aestivum* L.): a two-phase model determined by photoperiod and final leaf number. Eur. J. Agron. Submitted for publication.
Bassette, C., Bussière, F., 2008. Partitioning of splash and storage during raindrop impacts on banana leaves. Agric. Forest Meterol. 148, 991–1004.
Bertheloot, J., Andrieu, B., Fournier, C., Martre, P., 2008. A process-based model to simulate nitrogen distribution in wheat (*Triticum aestivum*) during grain-filling. Funct. Plant Biol. 35, 781–796.
Borrill, M.A.R.T., 1959. Inflorescence initiation and leaf size in some *Gramineae*. Ann. Bot. 23, 217–227.
Casey, I.A., Brereton, A.J., Laidlaw, A.S., McGilloway, D.A., 1999. Effects of sheath tube length on leaf development in perennial ryegrass (*Lolium perenne* L.). Ann. Appl. Biol. 134, 251–257.
Chelle, M., Andrieu, B., 1998. The nested radiosity model for the distribution of light within plant canopies. Ecol. Model. 111, 75–91.
Dornbusch, T., Andrieu, B., 2010. Lamina2Shape – an image processing tool for an explicit description of lamina shape tested on winter wheat (*Triticum aestivum* L.). Comput. Electron. Agric. 70, 217–224.
Dornbusch, T., Watt, J., Baccar, R., Fournier, C., Andrieu, B., 2011. A comparative analysis of leaf shape of wheat, barley and maize using an empirical shape model. Ann. Bot. in press, doi:10.1093/aob/mcq181.
Dorr, G., Hanan, J., Adkins, S., Hewitt, A., O'Donnell, C., Noller, B., 2008. Spray deposition on plant surfaces: a modelling approach. Funct. Plant Biol. 35, 988–996.
Dwyer, L.M., Steward, D.W., 1986. Leaf area development in field-grown maize. Agron. J. 78, 334–343.
Equiza, M.A., Tognetti, J.A., 2002. Morphological plasticity of spring and winter wheat in response to changing temperatures. Funct. Plant Biol. 29, 1427–1436.
Evers, J.B., Vos, J., Chelle, M., Andrieu, B., Fournier, C., Struik, P.C., 2007a. Simulating the effects of localized red:far-red ratio on tillering in spring wheat (*Triticum aestivum*) using a three-dimensional virtual plant model. New Phytol. 176, 325–336.
Evers, J.B., Vos, J., Fournier, C., Andrieu, B., Chelle, M., Struik, P.C., 2005. Towards a generic architectural model of tillering in *Gramineae*, as exemplified by spring wheat (*Triticum aestivum*). New Phytol. 166, 801–812.
Evers, J.B., Vos, J., Fournier, C., Andrieu, B., Chelle, M., Struik, P.C., 2007b. An architectural model of spring wheat: evaluation of the effects of population density and shading on model parameterization and performance. Ecol. Model. 200, 308–320.
Evers, J.B., Vos, J., Yin, X., Romero, P., van der Putten, P.E.L., Struik, P.C., 2010. Simulation of wheat growth and development based on organ-level photosynthesis and assimilate allocation. J. Exp. Bot. 61, 2203–2216.
Fournier, C., Andrieu, B., Ljutovac, S., Saint-Jean, S., 2003. ADEL-wheat: a 3D architectural model of wheat development. In: Hu, B.G., Jaeger, M. (Eds.), 2003' International Symposium on Plant Growth Modeling, Simulation, Visualization,

and their Applications. Tsinghua University Press/Springer, Beijing, PR China, pp. 54–63.
Friend, D.J.C., 1965. The effects of light and temperature on the growth of cereals. In: Milthorpe, F.L., Ivins, J.D. (Eds.), The Growth of Cereals and Grasses. Butterworths, London, pp. 181–199.
Gallagher, J.N., 1979. Field studies of cereal leaf growth. I. Initiation and expansion in relation to temperature and ontogeny. J. Exp. Bot. 30, 625–636.
Gómez-Macpherson, H., Richards, R.A., Masle, J., 1998. Growth of near-isogenic wheat lines differing in development – spaced plants. Ann. Bot. 82, 315–322.
Haun, J., 1973. Visual quantification of wheat development. Agron. J. 65, 116–119.
Hotsonyame, G.K., Hunt, L.A., 1997. Effects of sowing date, photoperiod and nitrogen on variation in main culm leaf dimensions in field-grown wheat. Can. J. Plant Sci. 78, 35–49.
Jaffuel, S., Dauzat, J., 2005. Synchronism of leaf and tiller emergence relative to position and to main stem development stage in a rice cultivar. Ann. Bot. 95, 401–412.
Kemp, D.R., 1981. Comparison of growth rates and sugar and protein concentrations of the extension zone of main shoots and tiller leaves of wheat. J. Exp. Bot. 32, 151–158.
Kirby, E.J.M., 1977. The growth of the shoot apex and the apical dome of barley during ear initiation. Ann. Bot. 41, 1308.
Kirby, E.J.M., Appleyard, M., Fellowes, G., 1982. Effect of sowing date on the temperature response of leaf emergence and leaf size in barley. Plant Cell Environ. 5, 477–484.
Kirby, E.J.M., Faris, D.G., 1970. Plant population induced growth correlations in the barley plant main shoot and possible hormonal mechanisms. J. Exp. Bot. 21, 787–798.
Köppen, W.P., 1931. Grundriss der Klimakunde, 2nd ed. Walter de Gruyter, Berlin.
Ljutovac, S., 2002. Coordination dans l'extension des organes aériens et conséquences pour les relations entre les dimensions finales des organes chez le blé. Ph.D. thesis. Institut National Agronomique Paris-Grignon, Paris, France.
Lock, A.A., 2003. The origin and significance of an indent on wheat leaves. J. Agric. Sci. 141, 179–190.
Louarn, G., Andrieu, B., Giauffret, C., 2010. A size-mediated effect can compensate for transient chilling stress affecting maize (*Zea mays*) leaf extension. New Phytol. 187, 106–118.
Louarn, G., Chenu, K., Fournier, C., Andrieu, B., Giauffret, C., 2008. Relative contributions of light interception and radiation use efficiency to the reduction of maize productivity under cold temperatures. Funct. Plant Biol. 35, 885–899.
Poethig, R.S., 2003. Phase change and the regulation of developmental timing in plants. Science 301, 334–336.
Rademacher, W., 2000. Growth retardants: effects on gibberellin biosynthesis and other metabolic pathways. Annu. Rev. Plant Physiol. Plant Mol. Biol. 51, 501–531.
Robert, C., Fournier, C., Andrieu, B., Ney, B., 2008. Coupling a 3D virtual wheat plant model with a *Septoria tritici* epidemic model: a new approach to investigate plant-pathogen interactions linked to canopy architecture. Funct. Plant Biol. 35, 997–1013.
Tivet, F.B., Silveira Pinheiro, D.A., Raissac, D.E., Dingkuhn, M.M., 2001. Leaf blade dimensions of rice (*Oryza sativa* L. and *Oryza glaberrima* Steud.). Relationships between tillers and the main stem. Ann. Bot. 88, 507–511.
Vos, J., Evers, J.B., Buck-Sorlin, G.H., Andrieu, B., Chelle, M., de Visser, P.H.B., 2010. Functional–structural plant modelling: a new versatile tool in crop science. J. Exp. Bot. 61, 2101–2115.
Wood, D., Thorne, G., 1985. A study of the relations between growth, development and tiller survival in winter wheat. In: Day, W., Atkin, R.K. (Eds.), Wheat Growth and Modelling. Plenum Press, New York, pp. 55–58.
Yamazaki, K., 1963. Studies on the leaf formation in rice plants. II. The development of leaves in relation to their position on a stem. Proc. Crop Sci. Soc. Jpn. 32, 81–88.

List of Publications

PEER REVIEWED JOURNALS

- **BACCAR, R.**, DORNBUSCH, T., ABICHOU, M., GATE, P. AND ANDRIEU, B., 2011 Description of the effect of sowing date and density on the phyllochron of winter wheat (*Triticum aestivum* L.): a two-phase model determined by photoperiod and final leaf number. *European Journal of Agronomy*. (to be submitted)
- **BACCAR, R.**, FOURNIER, C., DORNBUSCH, T., ANDRIEU, B. AND ROBERT, C. 2011 Modelling the effect of wheat canopy architecture as affected by sowing density on *Septoria tritici* epidemics using a coupled epidemic-virtual plant model . *Annals of botany*. (in press)
- DORNBUSCH, T., **BACCAR, R.**, WATT, J., HILLIER, J., BERTHELOOT, J., FOURNIER, C. AND ANDRIEU, B. 2011. Plasticity of winter wheat modulated by sowing date, density and nitrogen fertilisation: Dimensions and size of leaf blades, sheaths and internodes in relation to their position on a stem. *Field Crops Research*, 121: 116-124.
- DORNBUSCH, T., WATT, J., **BACCAR, R.**, FOURNIER, C. AND ANDRIEU, B., 2010. A comparative analysis of leaf shape of wheat, barley and maize using an empirical shape model. *Annals of botany*. doi:10.1093/aob/mcq181

CONFERENCE PROCEEDINGS

- **BACCAR, R.**, FOURNIER, C., DORNBUSCH, T., ANDRIEU, B. AND ROBERT, C. 2010. Assessing the effect of canopy architecture as affected by sowing density on epidemics using a virtual wheat plant model coupled with a *Septoria tritici* epidemic model. Oral presentation. In: Functional Structural Plant Modelling. Davis, USA.
- **BACCAR, R.**, ABICHOU, M., DORNBUSCH, T., GATE, P. AND ANDRIEU, B., 2009. Factors affecting leaf emergence rate in winter wheat (Triticum aestivum). Poster. In: Society of Experimental Biology Conference. Glasgow, UK.
- DORNBUSCH, T., **BACCAR, R.**, ABICHOU, A., FOURNIER, C. AND ANDRIEU, B., 2010. Plasticity of wheat architecture in response to sowing date and plant population density described with the 3D plant model ADEL wheat. Poster. In: European Society for Agronomy. Montpellier, France.

Résumé

Les pratiques culturales modifient l'architecture des couverts de manière à augmenter ou diminuer le développement des épidémies mais les processus mis en jeu sont complexes ; des modèles mécanistes simulant l'interaction entre plante et pathogène devraient aider à les clarifier. Les modèles de Plantes Virtuelles, qui permettent de décrire explicitement la structure tridimensionnelle de la plante, semblent particulièrement prometteurs pour exprimer les effets de l'architecture de la plante sur le développement des épidémies. L'objectif de cette étude est d'examiner la possibilité de simuler l'effet de l'architecture des plantes sur le développement de la maladie en utilisant un modèle Plante Virtuelle.

Dans ce travail, nous nous intéressons au pathosystème blé-*Septoria tritici*, dans lequel l'architecture joue un rôle important. En effet, les spores de *Septoria tritici* sont propagées par les éclaboussures de pluie depuis les feuilles infectées du bas du couvert vers les nouvelles feuilles saines. Notre travail s'est appuyé sur un modèle pré-existant d'épidémie de la septoriose, Septo3D. L'architecture du blé a été étudiée pour une gamme de densités et de date de semis. Les différences de phyllochrone entre traitements ont été dans une gamme susceptible de modifier le développement de la septoriose. Ces variations ont été représentées par un modèle descriptif qui tient compte du nombre de feuilles final et de la photopériode. Une description détaillée des variables d'architecture à l'échelle des organes et du couvert a fourni une documentation originale et complète sur la plasticité de l'architecture du blé. Ces données ont été utilisées pour paramétrer la description du blé dans Septo3D. Globalement, les traitements étudiés ont conduit à de fortes différences de la densité de végétation au cours du temps. Les dynamiques de développement de la septoriose ont été suivies pour trois traitements de densités contrastées. Les cinétiques de la maladie simulées par le modèle étaient conformes aux mesures expérimentales. Bien que, l'approche nécessite davantage de validation, les résultats confirment que l'approche Plante Virtuelle apporte un nouvel éclairage sur les processus et les caractéristiques des plantes qui impactent les épidémies. En conclusion, nous proposons quelques perspectives en vue de nouvelles applications et améliorations de l'approche.

Mots clés : blé d'hiver (*Triticum aestivum* L.), *Septoria tritici*, plasticité de l'architecture du blé, date de semis, densité de plantes, interaction plante-pathogène, modèle de Plante Virtuelle.

Abstract

Agronomic practices modify crop architecture in ways that may facilitate or hamper disease development. The processes involved are complex and mechanistic models simulating plant-pathogen interaction should help clarifying them. Virtual Plants, i.e. models in which the three-dimensional structure of the plant is explicitly described, appear specially promising to express the effects of the plant architecture on the epidemic development. The objective of this study is to examine the ability to simulate the effect of plant architecture on disease development using a Virtual Plant model.

The work focuses on the pathosystem wheat-*Septoria tritici*, in which architecture plays an important role because spores of *Septoria* are propagated from infected leaves to upper healthy leaves by rain splash. We build on a pre-existing model of *Septoria* epidemics, Septo3D. Wheat architecture was examined for a range of sowing date and density treatments. Differences of phyllochron between treatments were in a range sufficient to likely modify epidemic development; they were well represented by a descriptive model depending on photoperiod and final leaf number. A detailed description of architectural variables at the organ and canopy scale provided an original and comprehensive documentation of the plastic response of wheat, which was used for parameterising the wheat description in Septo3D. Overall, the investigated treatments resulted in strong differences in the time course of vegetation density. *Septoria* dynamics were monitored in a subset of three treatments of contrasted densities. Simulated disease kinetics were consistent with field measurements. Although, the approach needs further validation, results support that virtual plant modelling provides new insights into the processes and plant traits that impact epidemics. We conclude with prospects for further improvements and applications.

Key words: winter wheat (*Triticum aestivum* L.), *Septoria tritici*, plasticity of wheat architecture, sowing date, plant population density, plant-pathogen interaction, Virtual Plant models.